

Doctoral theses at NTNU, 2010:74

Martin Ludvigsen

An ROV toolbox for optical and acoustical seabed investigations

ISBN 978-82-471-2108-5
ISBN 978-82-471-2109-2 (electronic ver.)
ISSN 1503-818

Doctoral theses at NTNU, 2010:74



NTNU
Norwegian University of Science and Technology
Thesis for the degree of philosophiae doctor
Faculty of Engineering Science and Technology
Department of Marine Technology



NTNU – Trondheim
Norwegian University of
Science and Technology



NTNU – Trondheim
Norwegian University of
Science and Technology

Martin Ludvigsen

An ROV toolbox for optical and acoustical seabed investigations

Thesis for the degree of philosophiae doctor

Trondheim, April 2010

Norwegian University of Science and Technology
Faculty of Engineering Science and Technology
Department of Marine Technology



NTNU – Trondheim
Norwegian University of
Science and Technology

NTNU

Norwegian University of Science and Technology

Thesis for the degree of philosophiae doctor

Faculty of Engineering Science and Technology
Department of Marine Technology

© Martin Ludvigsen

ISBN 978-82-471-2108-5

ISBN 978-82-471-2109-2 (electronic ver.)

ISSN 1503-8181

ITK Report IMT-2010-57

Doctoral Theses at NTNU, 2010:74



Printed by Skipnes Kommunikasjon as

Abstract

This thesis describes a set of optical and acoustical methods for documenting a research site using underwater vehicles. The need for observations in cold-water coral research has formed the design problem in this work. A common survey protocol template is developed to describe video-, bathymetry-, photo mosaic- and photogrammetry surveys. For photogrammetry, the body of knowledge is small, and it was necessary to develop a new method rather than adapting existing methods. Axiomatic design methodology is applied to create the protocol template. Functional requirements for documenting these biological communities have been established and matched with solutions found in academic literature, industry standards and established best practice from hydrography, offshore subsea sector and related research disciplines.

The protocols provide guidelines for design of all phases of scientific surveys from planning to survey reporting. The first step in the survey design is to evaluate the practical constraints, the purpose of the operation and to establish requirements for the desired data products. Step two is to choose and configure the survey instruments using the information from step one. To create a plan for the operation containing a description of central parameters like survey lines, line spacing and necessary vehicle velocity the results from step one and two are applied. Step four is the final step in the survey design process where the data processing pipeline is compiled based on the previous design steps. The survey protocols presented are followed by data examples collected by the candidate to show their relevance and application.

The survey methods presented are complimentary with different levels of coverage and data resolution to cover a range of scales to address subjects like target confirmation, search, coral reef mapping and detailed documentation of individual specimen. Sonar surveys represent high coverage and low data resolution, while photogrammetry on the contrary provides high data resolution and low coverage.

This thesis may contribute to the establishment of a common practise for marine science using ROV for data acquisition. This can enhance the value of ROV-based surveys. The efficiency in data acquisition operations will increase and the value of the collected data increases if one succeeds standardizing operations.

Preface

Apart from the knowledge presented here my work has been enriched with extraordinary experiences from the bottom of the Bahamas Straits to the arctic ice at 81°N. These adventurous “side effects” of my work have given me the motivation I have needed to complete this work.

I would like to thank my advisor associate professor Bjørn Sortland and my co-advisor professor Geir Johnsen for their contributions and the time they have spent on my behalf. Bjørn’s enduring patience and Geir’s infectious enthusiasm have been a great help in completing this thesis. At the Department of Marine Technology I have received eager support from fellow PhD student Øyvind Tangen Ødegaard, principal engineer Knut Arne Hegstad, sectional engineer Oddvar Paulsen and professor Ludvig Karlsen. From the Department of Biology Johanna Järnegren and professor emeritus Jon-Arne Sneli have been friendly field company and teachers for an engineer entering the science of cold-water corals. I would also like to thank adjunct professor Fredrik Søreide for involving me in underwater archaeology challenges at the Ormen Lange excavation project. Large parts of my field work would have been impossible without the stable assistance from the crew on RV Gunnerus. This work has been funded by *NTNU Strategic research area of marine and maritime research* to which I am grateful.

This work has also relied on supporters outside NTNU who all deserve appreciation. A special gratitude goes to Hanumant Singh at Woods Hole Oceanographic Institution for inviting me to the Deep Submergence Laboratory, and for opening the field of photo mosaic and photogrammetry to me. GeoAcoustics Inc has made appreciated efforts on my behalf, setting equipment, software and personnel at my disposal. Kongsberg Seatex, FFI and Kongsberg Maritime have provided me with both software and equipment at no cost helping me out of difficult situations. My friends Bo Krogh, Robert Staven and Jan Henrik Borch also deserve to be mentioned for spending time and resources to support my work.

This work could not have been completed without the patience of my family and they owe my gratitude. My wife Kristine Bruun has encouraged and inspired me continuously. The help from my parents, Eva Lill and Rolf, and parents-in-law, Berit and Thorleif was crucial in the final stages of my project. They took care of our daughter Lill Synnøve when I needed silence to write.

Table of contents

ABSTRACT	I
PREFACE	III
TABLE OF CONTENTS	V
LIST OF ABBREVIATIONS	VII
1 INTRODUCTION	1
1.1 BACKGROUND	1
1.2 MOTIVATION	2
1.3 METHOD	2
1.4 ROV SYSTEMS IN SCIENTIFIC SERVICE	8
1.5 PROCEDURES FOR MARINE RESEARCH	9
1.6 NTNU ROV OPERATIONS	10
1.7 MAIN CONTRIBUTION OF THIS THESIS	10
1.8 SHORT DESCRIPTION OF THE THESIS	11
2 SYSTEM DESIGN	13
2.1 CUSTOMER DOMAIN	13
2.2 FUNCTIONAL REQUIREMENTS FOR ROV-BASED HABITAT MAPPING	15
2.3 SOLUTION CONCEPTS	17
3 VESSEL AND VEHICLE	19
3.1 RV GUNNERUS	19
3.2 ROV MINERVA	20
4 UNDERWATER NAVIGATION	27
4.1 PRINCIPLES OF ROV NAVIGATION	27
4.2 NAVIGATION SETUP SPECIFICATION	37
4.3 POSITION ACCURACY STANDARDS	39
4.4 PROCESSING	40
4.5 QUALITY ASSURANCE AND CONTROL	41
5 VIDEO SURVEY	45
5.1 INTRODUCTION	45
5.2 THE UNDERWATER IMAGING PROCESS	46
5.3 VIDEO SURVEY DESIGN	47
5.4 VIDEO SURVEY STANDARDS	58
5.5 QUALITY ASSURANCE AND CONTROL	63
5.6 REPORTING	63
6 VIDEO SURVEY FOR <i>LOPHELIA PERTUSA</i> AT THE TAUTRA RIDGE	65
6.1 BACKGROUND	65
6.2 METHOD	66
6.3 VIDEO RESULTS	68
6.4 DISCUSSION	73
7 BATHYMETRY SONAR SURVEY	75

7.1	INTRODUCTION	75
7.2	THE BATHYMETRY SURVEY PROCESS	75
7.3	SURVEY DESIGN.....	77
7.4	STANDARDS.....	86
7.5	QUALITY ASSURANCE AND CONTROL	87
7.6	REPORTING AND DATA PRODUCTS	88
8	BATHYMETRY DATA FROM THE TAUTRA RIDGE	89
8.1	INTRODUCTION	89
8.2	METHOD	90
8.3	RESULTS.....	94
8.4	DISCUSSION	96
9	PHOTO MOSAIC.....	99
9.1	INTRODUCTION	99
9.2	THE PHOTO MOSAIC PROCESS.....	100
9.3	SURVEY DESIGN.....	103
9.4	QUALITY ASSURANCE AND CONTROL	106
9.5	REPORTING	108
10	PHOTO MOSAIC FROM THE TAUTRA RIDGE.....	109
10.1	SURVEY MOTIVATION AND SITE.....	109
10.2	METHOD.....	110
10.3	RESULTS.....	111
10.4	DISCUSSION.....	114
11	PHOTOGRAMMETRY	117
11.1	INTRODUCTION	117
11.2	THE PHOTOGRAMMETRY PROCESS	118
11.3	SURVEY DESIGN.....	121
11.4	APPLICABLE STANDARDS	124
11.5	QUALITY ASSURANCE AND CONTROL	124
11.6	REPORTING.....	125
12	CLOSURE	127
12.1	PROTOCOL TEMPLATE STRUCTURE	127
12.2	ROV SURVEY STRATEGY	129
12.3	DESIGN FRAMEWORK APPLIED.....	133
12.4	FUTURE WORK:.....	134
13	REFERENCES.....	137
A	ARTICLE 1.....	147
B	ARTICLE 2.....	161
C	ARTICLE 3.....	169

List of abbreviations

APOS	Acoustic Positioning Operating System trademark of Kongsberg Maritime
AUV	Autonomous Underwater Vehicle
CCD	Charge-Coupled Device
CD	Compact Disc
CMOS	Complimentary Metal-Oxide Semiconductor
CODEC	COder/DECoder
CTD	Conductivity Temperature Depth
dGPS	differential GPS, see GPS
DLT	Digital Linear Tape
DOP	Dilution Of Precision
DP	Design Parameter or Dynamic Positioning
DSL	Deep Submergence Laboratory (Woods Hole Oceanographic Institution)
DTM	Digital Terrain Model
DV	Digital Video
DVCAM	Professional variant of DV format
DVD	Digital Versatile Disc
DVL	Doppler Velocity Log
EGNOS	European Geostationary Navigation Overlay Service
EUNIS	EUropean Nature Information System
FOG	Fibre Optic Gyro
FR	Functional Requirement
Gb	Giga Byte
GIS	Geographical Information System
GPS	Global Positioning System
HAIN	Hydroacoustic Aided Inertial Navigation
HD	High Definition and Hard Drive
HDOP	Horizontal Dilution of Precision
HDTV	High Definition Television
HID	High Intensity Discharge
LAT	Lowest astronomical tide
LBL	Long BaseLine
LED	Light Emitting Diode
LIDAR	LIght Detection and Ranging
MBARI	Monterey Bay Aquarium Research Institute
MBES	Multi Beam Echosounder
MESH	Mapping European Seabed Habitats
MTF	Modular Transfer Function
NAS	Network Attached Storage
NOAA	National Oceanic and Atmospheric Administration
NMR	Nuclear Magnetic Resonance
NS	Norsk Standard (Norwegian for: Norwegian Standard)
NTSC	National Television Steering Committee

IALA	International Association of Lighthouse Authorities
IFREMER	Institut Français d'Exploitation de la Mer
IHO	International Hydrographic Organization
IMU	Inertial Measurement Unit
IMCA	International Marine Contractor Association
ISE	International Submarine Engineering
HiPAP	High Precision Acoustic Positioning, trade mark of Kongsberg Maritime
JNCC	Joint Nature Conservation Committee
INS	Inertial Navigation System
QA	Quality Assurance
QC	Quality Control
PAL	Phase Alternating Line
pH	Measure of the acidity or basicity of a solution
PV	Process Variable
ROG	Recommended Operation Guidelines
ROV	Remotely Operated Vehicle
RLG	Ring Laser Gyro
RTK	Real Time Kinematic
SD	Standard Definition
SIFT	Scale Invariant Feature Transform
SLAM	Simultaneous Localization And Mapping
SUP	Strategic University Programme
SVHS	Super VHS, see VHS
TTL	Through The Lens metering
VHS	Video Home System
VRU	Vessel/Vehicle Reference Unit
UNESCO	United Nations Educational Scientific and Cultural Organization
USB	Universal Serial Bus
USBL	Ultra Short BaseLine
WAAS	Wide Area Augmentation System
WHOI	Woods Hole Oceanographic Institution
WROV	Work class ROV, see ROV

1 Introduction

This thesis aims to accommodate and expand the use of ROV (Remotely Operated Vehicles) in research. The opportunities ROV technology offers the scientific communities are underrated, mostly because potential users do not have the knowledge about ROV as an underwater platform and tool. The thesis work is a design task where ROV technology is applied to address seabed investigations in marine research. Seabed documentation methods are adapted from digital image processing, hydrography and the commercial offshore sector to fit applications in marine biology and archaeology. The research has been conducted in collaboration primarily with biologists, but archaeologists and geologists have also contributed.

1.1 Background

Underwater technology as an engineering discipline has been defined in different ways. Yet the term is attractive and therefore adopted by various engineering groups. In this work underwater technology refers to the engineering knowledge associated with operations under water and in particular the application of underwater vehicles. The curriculum of underwater technology is compiled from engineering subjects of hydroacoustics, hydrodynamics, oceanography, hydrography, control engineering, mechanical engineering and marine design.

Both technology and science has reached a level of complexity where it is difficult to manage both, and research questions should often be approached from different angles. The MODTEQ (Model-based development of advanced marine equipment) project (Odegaard, Sortland et al. 2001) was a five year strategic university programme (SUP) funded by the Norwegian Research Council in 1999. The aim was to facilitate communication and cooperation over the borders of marine scientific disciplines of engineering and science at NTNU and SINTEF. The goals of this project were:

- To develop an interdisciplinary research group that works at the interface between marine science and technology, focusing on marine model-based development and testing of advanced scientific and industrial equipment.
- To aid in future industrial development by "sharpening and refining" the tools used in marine research, thus improving marine data bases of importance to managing the marine environment and exploitation of marine resources.

This collaboration was the start of a long term collaboration between engineers from the Department of Marine Technology and marine biologists from Trondhjem Biological Station (Department of Biology, NTNU). A few years later NTNU

established a strategic research area for marine and maritime research where “Ocean space” research is defined as a priority area. Both the MODTEQ SUP and the mentioned strategic research area have contributed to make the multidisciplinary work in this thesis possible.

1.2 Motivation

The ocean is practically inaccessible to divers at depths below 30 meters and science relies on remotely operated tools or manned submersibles to access deep waters. The majority of marine research is conducted by wire-operated samplers and sensors or by hull-mounted sonars. Using an ROV presence on the seafloor and in the water column is achieved. ROV-based imagery provides an understanding of the seabed conditions unattainable with samplers or sonars alone. Underwater vehicles are advantageous for sampling and data acquisition since the vehicle can come close to the subject. To fully exploit the ROV in research there are two important areas of improvement; 1) standardization of procedures for established ROV services and 2) development of new methods and sensors. Standardised cold-water coral surveys could make data sets from different projects comparable. The solutions proposed in this work will not cover all possible situations in research, but covers the main concepts of seabed documentation. ROV have a large potential doing sampling of objects of interest. However, sampling is not included in the scope of work of this thesis.

1.3 Method

A large fraction of the present science and engineering projects imply multidisciplinary work. Researchers have miscellaneous motivations to seek collaboration with people with different specialities than themselves. The magnitude and diversity of the present science is continuously increasing and to face this development, multidisciplinary teamwork is endeavoured. Examples of multidisciplinary co-operation are found in most technological companies where specialists with different backgrounds work in concert. Collaboration across the scientific specialities leads to transfer of concepts and ideas. Methods for analysis in e.g. medical science have been adopted into marine biology. An example is the application of NMR (Nuclear Magnetic Resonance) analysis in marine biology i.e. (Chautón 2005) and (Størseth 2006). Science is often limited by the capabilities of the tools available for experiments and data acquisition in general. For engineers such limitations represent challenges and possibilities for development. An example of such “tools-limitation-engineering” collaboration is the research performed on the hydro thermal vents where biologists rely on new technology developed by the Deep Submergence Laboratory at WHOI (Woods Hole Oceanographic Institution) (Jakuba, Yoerger et al. 2004). Some research questions are broad and are approached from different angles to obtain progress and knowledge. An example of a wide research question attacked from various points of origin is the climate research and the possible global warming.

This multi-disciplinary research started by familiarization with the customer domain. Using design terminology, the biologists and the archaeologists are defined as customers and problem owner. Part of the customer domain familiarization process was participating in biology classes, biology conferences, archaeology cruises, biology cruises and lab work. Special emphasis was put on the challenges connected to cold-water corals. A mutual understanding of the challenges we were facing emerged, and we were able to produce joint publications.

1.3.1 Marine design

Marine design methods were the glue necessary to connect the special interest of the intended users and the engineering specialities used in the building blocks forming the system. At times it was useful to structure the situation with a design tool, and the axiomatic design paradigm established by Dr. Nam Pyo Suh was applied (Rinderie and Suh 1982).

Axiomatic design

The traditional design process like the design wheel proposed by Allmendinger (Allmendinger 1990) is an iterative process. In contrast, the axiomatic design process is linear. The first phase is to step into the situation of the problem-owner. In axiomatic design terminology this is termed the customer domain. The design proceeds as the designer proceeds from the customer domain to the process domain, see Figure 1.1.

There are 7 central concepts in axiomatic design (Suh 2001):

- *Axiom*: Self-evident truth or fundamental truth for which there are no counterexamples or exceptions. An axiom cannot be derived from other laws or principles of nature.
- *Colloray*: Inference derived from axioms or from propositions that follow from axioms or other propositions that have been proven.
- *Theorem*: A proposition that is not self-evident but that can be proved from accepted premises or axioms and so is established as a law or principle.
- *Functional requirement*: A minimum set of independent requirements that completely characterize the functional needs of the product expressed in the functional domain. By definition each FR is independent of every other FR at the time the FR was formulated.
- *Constraints*: They are bounds for the acceptable solution. There are two kinds of constraints; input constraints and system constraints. Input constraints are imposed by as a part of the design specification, while system constraints are imposed by the design choices made underway during the design process. Constant parameters or parameters inaccessible for the designer are often categorized as constraints. When

designing scientific marine surveys constraints can be cost, available vessels, vehicles and personnel.

- *Design parameter:* DP are the key physical variables in the physical domain that characterize the design that satisfies the specified FR's. There should be one DP for each FR.
- *Process variable:* PV's are the key variables in the process domain that characterize the process that generate the specified DP's.

The corollaries and theorems of axiomatic design are intended as design guidelines, but will not be pursued further in this text. Axiomatic design is based on two axioms. From these axioms a number of theorems and corollaries are derived and form the base for axiomatic design.

1. Maintain the independence of functional requirements
2. Minimize information content

The first axiom presented by Suh prescribes to maintain independence of the functional requirements. It is common to arrange FR and DP in a matrix, as shown in Table 1.1.

When the system is configured with minimum dependence, each design parameter should address only one functional requirement, see Table 1.1.A. A system like that is termed an uncoupled system. In a truly uncoupled system there are only correlations between the defined FR's and DP's along the diagonal as showed in the table. The advantage of an uncoupled system is that it possible to change one FR without affecting other FR's in the system.

Table 1.1 Relation between FR's and DP's in an uncoupled system, a decoupled system and a coupled system.

	DP 1	DP 2	DP 3
FR 1	X		
FR 2		X	
FR 3			X

A

	DP 1	DP 2	DP 3
FR 1	X		
FR 2	X	X	
FR 3	X	X	X

B

	DP 1	DP 2	DP 3
FR 1	X	X	X
FR 2	X	X	X
FR 3	X	X	X

C

In some situations it is difficult to find uncoupled FR's and a decoupled system can be defined. In a decoupled system there can only be correspondences along the diagonal in Table 1.1.B. and below the diagonal. In the design process one will start adapting "DP 1" to satisfy "FR 1", "FR 2", and "FR 3" for the general case in Table 1.1.B. The design for "DP2" can then be chosen without interfering with the previous design choices.

The design matrixes shown in Table 1.1 can be established at multiple levels. The design for “DP 1” and “FR 1” can be detailed in a sublevel for design choices. The functional requirements in “FR 1” will then be broken down to new functional requirements, FR 1.1, FR 1.2 and FR 1.3 with corresponding DP’s. When the designer wants to proceed from the physical domain to the process domain, similar tables and matrixes are constructed and the same preference for diagonal or triangular tables or matrices applies.

The relation between the FR’s and DP’s can be expressed mathematically, see (1.1). In the case where a_{ij} are defined mathematically, normal matrix operations can be used in the design. When A is constant, the system can be defined linear, while when A is a function of DP , the system is non-linear.

$$\begin{aligned} [FR] &= [A][DP] \\ [A] &= \begin{bmatrix} a_{11} & a_{12} \\ a_{21} & a_{22} \end{bmatrix} \end{aligned} \quad (1.1)$$

It has been mention subsequently that the design process is to map from one domain to the next, i.e. from the functional domain to the physical domain, see Figure 1.3.

The second axiom prescribes to reduce the information content in the design. In Suh 2001 the information content I_i is mathematical related to the probability P_i of satisfying FR_i through (1.2).

$$I_i = \log_2 \frac{1}{P_i} \quad (1.2)$$

The second axiom is applied when several designs are equally acceptable from a functional point of view. The design with the lowest information content is the superior design. An uncoupled design has always lower information content than a decoupled system (Suh 2001).

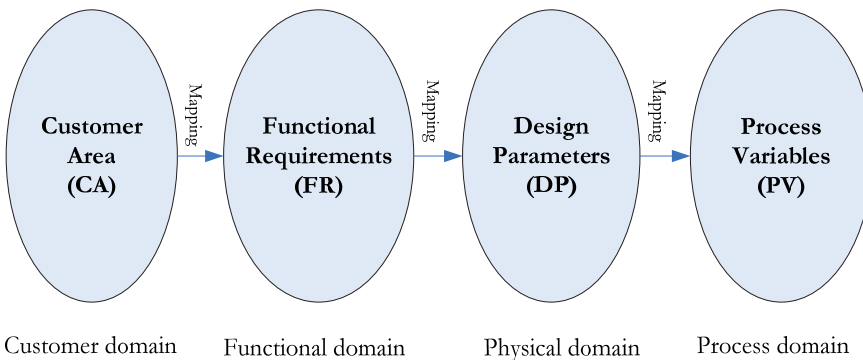


Figure 1.1 The stages of axiomatic design according to Suh.

Even though axiomatic design is a linear design method, the design can collapse at any point before the design is complete. The design collapses when functional

requirements cannot be kept independent or be met by design parameters. Then the design process has to start from the beginning and a different configuration of constraints, FR's and DP's must be attempted. A complete description of the axiomatic design system is given in (Suh 2001).

Example – design of a passive filter network

An example originally given by Rinderle (Rinderle 1982) will be given to illustrate the concept of axiomatic design. In this example there is a well defined mathematical relationship between the functional requirements and the design parameters. Mathematical relationship of this type is rare, and unfortunately not present in the thesis work presented.

A simple instrumentation system is to be designed to measure the mechanical displacement of a mechanical system. A displacement sensor is producing a measurement signal at 0 – 2 Hz. The measurement signal is then added to a carrier signal of 50 Hz before it is transmitted to a galvanometer in a light beam oscillograph. The light beam oscillograph is used to display the measured displacement to the user. Before the light beam oscillograph can interpret the signal from the displacement sensor, the carrier frequency has to be suppressed and the signal has to be amplified to the correct scale. The functional requirements for the passive filter are thus:

- FR1: Suppress the carrier without distorting the displacement signal
- FR2: Attenuate the signal to obtain the proper scale

Three proposals for a passive filter are presented in Figure 1.2:

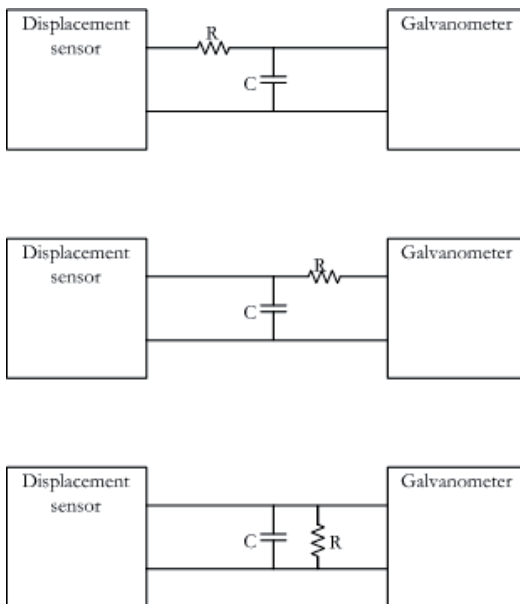


Figure 1.2 The 3 alternative networks for the passive filter.

The design starts by choosing an appropriate capacitor to achieve the desired low pass behaviour of the system. The desired cut-off frequency is 6.94 Hz and capacitor is found to be 246 μ F. The next step is to introduce a resistor to scale the signal. There are three alternative locations for the resistor to be inserted, see Figure 1.2. Alternative 1 reduces the cut off frequency 5 %, alternative 2 reduces the cut off frequency 95 % while alternative 3 increases the cut off frequency with 11300 %. The change in cut off frequency shows how FR 1 and FR 2 are coupled.

Rinderle defines the function domain and the physical domain with n dimension for a system with n FR's. The mapping from the function domain to the physical domain is then mathematically using (1.1). The angle between the axes of the functional domain and physical domain in Figure 1.3.B. is given by:

$$\beta_1 = \tan^{-1}\left(\frac{a_{12}}{a_{11}}\right)$$

$$\beta_2 = \tan^{-1}\left(-\frac{a_{21}}{a_{22}}\right)$$
(1.3)

β_1 denotes the angle between the 2. axis of the functional domain and the 2. axis of the physical domain shown in Figure 1.3.B. Correspondingly β_2 denotes the angle between the 1. axes. For an uncoupled design both β_1 and β_2 are zero, the functional domain will not be rotated or skewed entering the physical domain. The uncoupled design is sometimes referred to as orthogonal designs. The angles β are then used to enumerate the coupling between the FR's in case of a coupled or decoupled design.

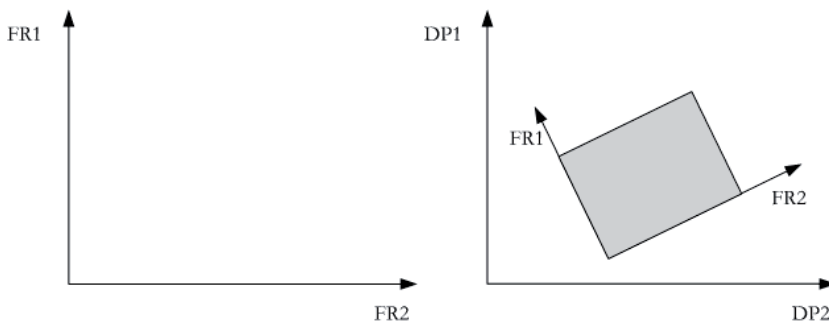


Figure 1.3 Two-dimensional functional domain and two dimensional physical domain

If the resistor had been change first, the choice of capacitor would not modify the resulting attenuation from the system. This emphasise the importance of sequence of FR's. However, the three alternative results in different levels of coupling between the FR's, alternative 1 have almost noe coupling, while alternative gives a strong coupling between the FR's. Due to the numerical nature of this design, this coupling can be quantified. Nevertheless, the design issues presented in this thesis work are not of a mathematical nature.

The strict mathematical structure of axiomatic design will in some situation require the same level of design detail at all levels if the decomposed FR's should be

compiled back in a larger matrix to reveal sub-level interdependence. Sometimes this leads to an unnecessary complicated design process.

1.4 ROV systems in scientific service

Some research groups that have successfully implemented ROV technology into research are WHOI (USA), IFREMER (France), ROPOS (Canada), MBARI (USA), and Southampton Oceanography Centre (UK). Research teams leading in specific sub areas of underwater technology e.g. navigation, bathymetry, image processing, and marine design are presented in the subsequent chapters.

1.4.1 Norwegian research underwater vehicles

The first science ROV in Norway was the Aglantha vehicle built by Argus Remote Systems¹ in Bergen in the late 1990's. NTNU achieved the Minerva ROV in 2003, a SUB-Fighter 7500 built by Sperre AS². In 2004 Sperre AS built an electric work class ROV (SUB-Fighter 30k) for archaeological exploration. This vehicle was financed by Norsk Hydro³ and operated by NTNU. The Bathysaurus ROV system was also built by Argus Remote Systems and designed to 5000 m depth. The vehicle was delivered to the University of Bergen and Institute of Marine Research⁴ in 2004 (de L. Wenneck, Falkenhaus et al. 2008). In addition to the mentioned systems, offshore ROV systems have been used for research from time to time and Hovland, Fosså and Mortensen have conducted a substantial amount of research using offshore work class vehicles (Hovland, Vasshus et al. 2002), (Mortensen 2000), (Fossa, Mortensen et al. 2002), (Fossa, Lindberg et al. 2005).

1.4.2 Woods Hole Oceanographic Institution

The most known scientific ROV team is the Deep Submergence Lab (DSL) at WHOI. DSL constructed the Jason ROV which was put into operation in 1988 (Ballard 1993). In 2002 the vehicle was replaced with the Jason II. The weight of the vehicle is approximately 3.7 tons and the dimensions are 3.4 by 2.4 by 2.2 meters. The vehicle is included in the National Deep Submergence Facility in the US and is also available to researchers outside the WHOI. The institution also has several AUV's (Autonomous Underwater Vehicle) in scientific service. Among the most famous applications of the Jason vehicles are the investigations of the antique Greek shipwrecks and the documentation of hydrothermal vents on the seabed (Ballard, McCann et al. 2000). From early on WHOI have been exploiting the advantages of multidisciplinary team work. The Deep Submergence Lab is organized under the Applied Ocean Physics and Engineering and consists mainly of engineers and technicians.

¹ Argus Remote Systems, Bergen, Norway

² Sperre AS, Notodden, Norway

³ Now Statoil, Lysaker, Norway

⁴ Institute of Marine Research, Bergen, Norway

Their multi-disciplinary structure appears in their project organizations. Engineers are looking for scientists having challenging and interesting problems, likewise scientists seek engineers holding technology to solve their problems. This type of multi-disciplinary collaboration forms the basis for many projects.

1.4.3 IFREMER

IFREMER (Institut Français d'Exploitation de la Mer) is a marine research organization run by the French government and was founded in 1984. The ROV Victor 6000 was put into regular operation in 1999. The vehicle weighs 4.6 tons and is 3.1 x 1.8 x 2.1 meters. All systems including ROV, LARS (Launch And Recovery System), power supply and containers have a total deck weight of 100 tons. There is a variety of sampling equipment available for the vehicle with water sampler and a carousel for fauna samples among other units. The design is modular and there is a sampling module under the vehicle (Soltwedel, Klages et al. 2000). Observation and monitoring of deep water benthic eco system has been the main research objective for the users of the system (Sarradin, Leroy et al. 2002). The system is operated by Genavir which is an offshore contractor partly owned by IFREMER. The ROV is operated from various ocean going research vessels, e.g. RV Polarstern, RV L'Atalante and RV Thalassa.

1.4.4 Other projects

In California the MBARI (Monterey Bay Aquarium Research Institute) research group operates two hydraulic ROVs and an AUV (Kirkwood 2000). ROPOS is a Canadian research ROV operated by an independent institution and the vehicle is used by various research groups from North America and Germany (Shepherd and Juniper 1997). The vehicle is hydraulic and was initially constructed by ISE (International Submarine Engineering) in Vancouver. In 2003 the University of Bremen purchased a Quest electric WROV (Work class ROV) from Schilling (Ratmeyer and Gross 2003). This vehicle is used 2-5 times a year for ocean-going research cruises. The UK SoC (Southampton Oceanography Centre) have a sister vehicle of the Jason II ROV (German 2004).

1.5 Procedures for marine research

Standards Norway⁵ has developed several standards for biological investigations for marine resource management purposes (Standards-Norway 2009). The most relevant standard for scientific ROV applications is NS 9435 (Norsk Standard) on visual seabed inspection for biological mapping purposes. Procedures for marine research are described in the Marine monitoring handbook published in 2001 by JNCC (Joint Natural Conservation Committee) (Davies, Baxter et al. 2001). MESH (Mapping European Seabed Habitats) is a European research project started in 2004, and the project has published recommended operating guidelines for several

⁵ Standards Norway, Lysaker, Norway

methods of biological seabed mapping like side scan sonar, LIDAR (LIght Detection And Ranging) surveys, video and swath sonars (Coggan, Populus et al. 2007). The MESH publications have several recommendations to ROV surveys regarding operational procedures and data processing. In spite of these efforts, there are still no common “best practice” for ROV-based research surveys.

1.6 NTNU ROV operations

During my project (2003 - 2008), the premises for experimental marine research at NTNU have changed considerably. As previously mentioned, the university purchased an observation ROV in 2003 and an electric work class ROV in 2004. The collaborations established in the MODTEQ project were used to set up a team of engineers and biologists for the observation ROV. In 2006 the university, lead by the *NTNU Strategic area for marine and maritime research*, acquired a state-of-the-art research vessel. The research vessel, RV Gunnerus, have expanded the possibilities for ROV operations considerably by offering an integrated USBL (Ultra Short BaseLine) system and DP-capabilities (Dynamic Positioning).

This significant equipment upgrade had to be followed by increased knowledge and improved methods at the university. The multi-disciplinary teams initiated under the MODTEQ project and the *NTNU strategic area for marine and maritime research* have strongly contributed. Students have benefited from the enhanced opportunities both through master project field work and cruises associated with courses. The possibilities offered have resulted in publications by international researchers besides the involved NTNU scientists ((Neulinger, Jarnegren et al. 2008), (Neulinger, Gartner et al. 2009), (More 2005), (Neyts and Sunde 2007), (Brooke, Jarnegren et al. 2005)). Today ROV surveys are regularly carried out both for research and education. Examples of NTNU ROV operations are the localization and recovery of a Blackburn Skua war plane (Tvedten 2008), (Dalheim 2008), (Gjølmesli and Koch 2007) and the search for victims of World War II at the Falstad (Tønset 2008).

1.7 Main contribution of this thesis

The main contributions of this thesis are protocols for ROV underwater positioning, video surveys, bathymetry surveys, photo mosaics and photogrammetry. The protocols are presented to support and guide marine scientists planning seabed investigations. Common practice for research surveys would increase the value of both the acquired data and the ROV as a research tool. A wider range of researchers could take advantage of the benefits of underwater vehicles if the methodology was more developed. Position determination of the ROV is fundamental for all seabed investigation operations, and the first protocol is on underwater positioning. The video survey protocol shows how the information content can be increased by proper planning and processing and how quantitative information can be obtained. Special requirements for bathymetry surveys related to ROV-based coral investigations are described in the bathymetry survey protocol. To achieve more detailed information of a site, the protocol for photo mosaic provides

procedures for this technique. Photo mosaic surveys for marine research are described in article 1 and 3 in the appendix. To effectively obtain underwater photogrammetry models a new method is developed and given a proper protocol. Underwater photogrammetry is also described in article 2 in the appendix. For the survey methods for video, bathymetry and photo mosaic data examples to clarify and verify the relevance of the protocols are presented. Data acquired by the candidate during cold-water coral investigations and archaeological surveys is used in the examples.

The new method for photogrammetric modelling of smaller sites is proven as valuable tool for underwater archaeology. For underwater archaeology there is a need to establish the dimensions of an underwater scene. In terrestrial archaeology photogrammetry is commonly used, but this method is challenging to adapt for underwater applications. By automatically recognising common points in overlapping images, and using information about the position and orientation of the camera for each image, a model for the overlapping area is established (local model). Local models are created for all overlaps in the data set. In the final step the local model is joined to a global model.

1.8 Short description of the thesis

The scientific ROV survey protocols in this thesis have the same structure. The protocol structure starts with a general description of the processes relevant to consider when planning the survey. Then the planning of the data acquisition commences with sensor selection and configuration. The next factor in the planning is designing the ROV-trajectory. Processing, interpretation and management of data are discussed along with relevant standards. A quality management scheme is proposed to increase the data integrity. Each survey protocol is closed with recommendations and suggestions for data reporting. The individual protocols are not independent and rely on cross references to avoid repetitions. The data examples are suited to illustrate the given protocols. However, they do not represent survey reports.

At the end of this thesis three articles are enclosed. The first is published in the scientific journal *Oceanography* in December 2007 and treats the application of underwater photo mosaics. The next article is published in the proceedings of the *Oceans 2006* and discusses photogrammetric measurements on an archaeology site. The last article is also published in the proceedings of the *Oceans 2006* and shows how different tools for seabed documentation are combined to enhance the information content.

These articles present data examples for the methodology. Article one represents a data set and a scheme of interpretation different from the one used in the example data set given in section 10 of the thesis and are in certain ways complementary to section 10. Article two elaborates the development of the photogrammetry method presented in section 11. Article three presents a larger data set than the data set

shown in the thesis. It is shown how the different data types and data set can strengthen each other when they are compared.

2 System design

This chapter aims to categorize ROV-observation tasks connected to cold-water coral investigations and propose solutions. Starting in the customer domain the information wanted is examined and mapped to functions for the system to complete. In the next design stage concepts executing the functions are found.

2.1 Customer domain

Cold-water coral research is a diverse field of science and is composed of biology, geology and technology. Some important research areas are:

- Coral mapping and distribution
- Geological investigations
- Physiology
- Ecology
- Environmental issues

Cold-water coral investigation occurs on many scales and levels of detail to achieve information addressing the research areas indicated above. Mapping and distribution of cold-water coral reefs can be performed by proving or disproving indications of coral occurrence based on reports from fishermen or sonar observations. Survey operations are evidently necessary to describe the coral distribution, and maps of the coral colonies are important for geological investigations. Focus on coral reef ecology is necessary to be able to distinguish different taxa, their behaviour and interactions. Coral physiology is challenging to address *in-situ* using an ROV, and any attempt would require detailed and scalable imagery besides sampling. To monitor the development and analyse possible trends, it is necessary to revisit certain specimen. Also for observation of environmental impact on the biological community, it is necessary to follow a set of specimen in detail over a period of time to monitor changes.

2.1.1 Customer motivation

Better understanding of the coral communities may increase our ability to perform effective marine resource management (Davies, Roberts et al. 2007). The coral colonies are threatened on several fronts. They are vulnerable to bottom trawling as the trawl breaks down the coral structure and buries the living corals with sediments (Fossa, Mortensen et al. 2002). A coral structure created over thousands of years can be terminated within minutes. The calcium carbonate structure is also sensitive to

variations in pH. Hence, the reefs may be threatened by the increased levels of carbon dioxide in the atmosphere. The carbon dioxide dissolves in seawater, lowering the pH (Sinclair D.J. 2006).

The calcium carbonate structures of the coral reefs are old. In Norwegian waters it has been shown that some reef structures are approximately 8000 years old (Hovland, Mortensen et al. 1998), and they may hold information about the conditions in the sea through earlier times. The reefs can also be used as markers for present environmental changes, due to their vulnerability to pH changes in the sea (Guinotte, Orr et al. 2006).

The coral reefs appear to be biological hot spots (high species diversity and abundance) in the deep water, below the photic zone. On the coral reefs the species diversity is measured to be considerably higher than the surrounding areas ((Burdon-Jones and Tambs-Lyche 1960) (Mortensen, Mortensen et al. 2008)), and a special biological community is often found around the corals. The calcium carbonate structures provide shelter for many species and the reefs are assumed to be important breeding areas to many species of fish.

Considering the important role of coral communities in the deep-water ecology and the threats from climate changes and fisheries (Fossa, Mortensen et al. 2002), the need for knowledge and research of these communities is urgent. To limit the destruction of the cold-water corals mapping of coral reef occurrence is necessary to be able to protect them. We need to know more about the role of the coral communities to be able to improve marine resource management. The large number of species present on the coral communities makes them interesting for bio prospecting. Methods for deposition of carbon dioxide in the ground below the seabed is being developed by the major oil companies, and the cold-water coral may be a useful biological indicator of a potential leakage from these deposits.

2.1.2 Cold-water corals reefs

In the North-Atlantic, the major reef forming cold-water coral is *Lophelia pertusa*, belonging to the stony corals. The reef structure of this species consists of the external calcium carbonate (aragonite) skeleton, see Figure 2.1. The aragonite skeleton of the coral can form large structures, up to 35 meters high several square kilometres in horizontal extent. The coral reefs are slow growing with a linear growth rate of 15-17 mm·yr⁻¹ (Orejas, Gori et al. 2008). The aragonite structure frequently collapses from its own weight which reduces the growth rate of the reef to approximately 1 mm·yr⁻¹ (Freiwald 1998). The calcium carbonate skeleton of the living corals is covered with mucus and often form cauliflower shaped structures.



Figure 2.1 *Lophelia pertusa* on the Tautra ridge with a rockfish and some sponges.

The *Lophelia pertusa* is found in waters 39 m to 2000 m deep. The coral seem to prefer cold water, and are found in temperatures between 4°C and 13°C with salinity ranging from 32‰ to 35‰ (Freiwald 1998). The coral thrives in deep waters with current (0.3 – 0.5 m/s) (Jonsson and Lundalv 2005). In Norwegian waters these environmental limits mean that the coral are found in the North Atlantic water masses (Sakshaug 1991). On the continental shelf the stony corals are hence found from 200 m to 400 m depth. On the continental shelf corals are found on edges of ice plough marks or on pock marks. In the fjords the preferred water type are found both deeper and shallower than on the shelf, and the corals are often located on elevations of the underwater terrain like thresholds and vertical walls.

The occurrence of cold-water coral reefs is also strongly connected to geological issues. It is believed that the corals are more likely to be found where there are hydrocarbon gases seeping from the ground (Hovland and Risk 2003). Considerable amounts of research remain for many basic physiological aspects of stony corals, e.g. their feeding patterns and reproduction mechanisms (Rapp and Snæli 1999), (Brooke, Järnegren et al. 2005).

2.2 Functional requirements for ROV-based habitat mapping

An ROV working on cold-water coral reefs must be able to handle the depth and current usually found on such reefs. It must be sufficiently large to carry the necessary equipment. All ROV data require some level of geo-referencing to enable the end-user to relate the observation to existing data and to be able to relocate targets.

From the main directions in coral research (ecology, physiology, mapping, geology and environmental research) four categories for documenting operations can be established:

1. Coral reef confirmation
2. Searching and mapping
3. Condition and fauna/taxa documentation
4. Development monitoring

Coral reef confirmation

One important work task for researchers working with mapping and distribution is to confirm possible coral occurrences. To obtain 100% confidence of a coral occurrence optical images (video or still image) are required. Considering the depths where stony cold-water corals are found, artificial light is necessary to obtain optical images. The quality of the imagery must be sufficient to distinguish dead and living coral, silt and gravel. To register different morphological versions of the corals colour images are necessary.

Search & mapping

To map the coral distribution the ROV-system must be able to run systematic lines and acquire data for production of a map indicating the coral reef ground area or the borders of the coral area. A description of a typical search operation is seen in (Yoerger and Kinsey 2009). The coverage efficiency is directly proportional to the speed of the ROV and the obtainable search width. The cold-water corals are often found on edges and underwater hills, search set-ups must hence be able to detect such terrain characteristics. Seabed covered with cold-water coral reefs is easy recognised by the high surface roughness, with its cauliflower features 20 cm and larger in diameter. The sensor used for the search should be able to detect this roughness. The topology of the reef can reveal information about the development of the reef area and should be documented. The thickness of the reef should be measured. For thickness investigations of coral colonies, the ranges to investigate are relatively narrow (0 – 35 meters).

Conditions and fauna/taxa documentation

Factors like sedimentation, human traces, portion of living and dead coral and the state of the biota are characteristic for the condition of the coral community. Damages to the reef due to human activities like trawl scars, garbage, etc. should be observable in the sensor data.

To reveal knowledge of the ecologic mechanisms in the coral community, the present species, their distribution, behaviour and interactions should be examined. In a coral fauna survey the distribution of live and dead stony coral, soft corals and sponges should be documented. It is also important to be able to scale the individuals observed. Detailed imagery is essential for documenting the present fauna, human traces and biological activity on the coral community.

Development monitoring

To be able to detect changes and development on a coral community there are at least four natural markers to monitor: the distribution of living and dead corals, changes in the fauna, coral growth and traces of human activities. To measure coral growth, the capability to measure a coral individual with millimetre precision and then relocate the coral individual after a period of time and repeat the measurement is needed.

2.3 Solution concepts

When the problems are defined, a concept for solution is chosen. Based on the technological solution concept, the functional requirements are further developed to more detailed levels.

Table 2.1 sums up the correspondence between technology concepts and categories of documentation operations. The categories are listed with the most used and most important operation first, and the less used, more detailed and advanced category of operation later.

Table 2.1 Functional requirements (FR) and design parameters (DP) for ROV surveys aimed at biology.

FR \ DP	Video	Sonar	Photo-mosaic	Photo-grammetry
Coral reef confirmation	X			
Search & dimension	X	X		
Condition and fauna/taxa documentation	X		X	
Development monitoring	X		X	X

According to the terminology on axiomatic design introduced in section 1.3, the system presented on Table 2.1 is a decoupled system. From an axiomatic design point of view this is sub-optimal but acceptable. The off-diagonal elements in Table 2.1 are tolerated. The fact that the video can be used for all the operation defined as FR's in Table 2.1 does not make video a poorer choice for e.g. *coral reef confirmation*. However, it is more challenging to configure a video system to satisfy all requirements associated with all four FR's, than it is to configure a video system for only one type of operation.

To avoid the situation in Table 2.1, where video appears as a complicated sensor with coupling to all functional requirements, the video functionality could have been broken down to sub system. We would gain a system that comply better to the axiomatic design, however that would complicate our design process and is not necessary as the complexity can be handled without further dissection.

2.3.1 Video

The four investigation categories established all rely on video. However, the type of video requirements varies. For confirmation of coral reefs and mapping and

distribution operations, the most important feature of the video system is the viewing range to increase efficiency in the operations. When documenting the fauna and conditions on a reef, detailed images are more important. The ability to get close-up images of different specimens, both colour rendition and image contrast are all important video features for documenting the condition on a cold-water coral reef and the present fauna. In projects aiming at documenting the development, the geometrical correctness of the images and the ability to determine scale of the objects observed is important. A protocol for video surveys is given in chapter 5.

2.3.2 Sonar

Four types of sonars are common on ROV's; 1) scanning sonar, 2) side scan sonar, 3) multibeam echosounder, and 4) sub bottom profiler. The scanning sonar is standard equipment for most ROV's. It has a mechanically rotation sonar transducer and outputs a circular sonogram as the head rotates. It is useful in search for corals when the intention is to confirm coral occurrences. Most available scanning sonars operate at high frequencies and are capable of detecting the coral surface. When the objective is to search over a larger area for corals, side scan sonar is better suited than the scanning sonar. Data acquisition is carried out along survey lines. During side scan surveys, the ROV should fly lower than ten meters above the seabed to achieve good quality data. Multibeam echosounders are used to measure the shape of the underwater terrain (bathymetry). From high resolution bathymetry data it is possible to perceive the seabed roughness of coral reefs. In situations where the seabed roughness cannot be detected, the bathymetry can be used to identify terrain features where cold-water coral reefs are likely to be found. Examples of such terrain features are pockmarks, plough marks, slopes, local tops and edges. Sub bottom profilers are used to document the vertical composition of the ground, and hence determine the type of seabed. Thus the thickness of the coral structure can be mapped. A bathymetry survey protocol for ROV surveys is presented in chapter 7.

2.3.3 Photo mosaic

Photo mosaics are used to document the fauna and the development of the reef by compiling a series of images to an image larger than the individual image frames. The data resolution offered by photo mosaics is high and the data are intuitive to interpret. The data acquisition efficiency is however low and photo mosaics are best suited for small areas as described in the survey protocol is found in chapter 9.

2.3.4 Photogrammetry

The resolution of the spatial models created using photogrammetry is high and the technique is attractive for detailed documentation. It can be used to measure how a limited area develops over time, and how certain specimen change dimension. The data coverage is limited in the same way as for photo mosaics, and the method is only applicable for small sites and is described in the protocol in chapter 11.

3 Vessel and vehicle

3.1 RV Gunnerus

NTNU's research vessel RV Gunnerus, see Figure 3.1, was put into operation in 2006. The length is 31.25 m and the beam is 9.60 m. A diesel electric propulsion system is installed on the vessel and three generators, a bow thruster and two fixed pitch variable speed propellers aft provide the propulsion. For ROV operations the most important feature is the DP-system which enables the vessel to automatically maintain the position to either absolute coordinates or relative to the ROV. RV Gunnerus has generous deck space allowing the ROV system a dedicated control container.

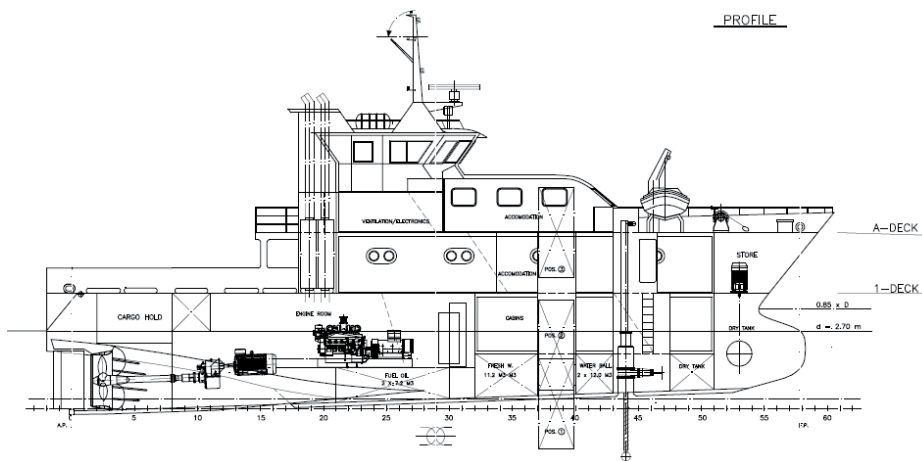


Figure 3.1 Arrangement for RV Gunnerus. Drawing by Polarconsult⁶.

3.1.1 Vessel instrument description

On RV Gunnerus a Kongsberg Seatex⁷ DPS 116 dGPS is installed. The unit applies a IALA and Fugro⁸ Starfix correction signals. A HiPAP 500 (High Precision Acoustic Positioning) USBL system is mounted on the vessel and is used to position the vehicle. The heading is measured to true north with a Simrad GC-80-S gyro. A Kongsberg Seatex MRU-5 is also installed on RV Gunnerus.

⁶ Polarkonsult, Harstad, Norway

⁷ Kongsberg Seatex, Trondheim, Norway

⁸ Fugro, Leidschendam, Netherlands

Table 3.1 Navigation instruments onboard RV Gunnerus.

Instrument type	Manufacturer	Model	Uncertainty
GPS	Kongsberg Seatex	DPS 116	3 [m]
Gyro	Simrad	GC-80-S	0.1 [°]
VRU	Kongsberg Seatex	MRU4	0.1 [°]
USBL	Kongsberg Maritime	HiPAP 500	0.18 [°] @ 10dB s/N 0.2 m range

3.2 ROV Minerva

The Minerva ROV is an observation class ROV, see Figure 3.2. The vehicle has five 1500 W frequency controlled AC thrusters. The dimensions are 140 by 80 by 81 cm and the ROV weighs 405 kg. The depth rating is 700 meters. Fibre optic multiplexers are installed for data communication and two simultaneous video lines. There are a total of four video cameras, three of which are connected to a common video line and a selector switch. Sonar and altimeter from Kongsberg Maritime are installed. To measure vehicle speed a Workhorse 600 kHz DVL from Teledyne RDI⁹ is fitted. A hydraulic five function manipulator from Hydro-lek¹⁰ is installed on the ROV. A control container is setup for the vehicle where the ROV pilot operates the vehicle. The navigator/surveyor is also placed in the control container.



Figure 3.2 The Minerva ROV and its main components. An electric manipulator has been mounted after this picture was taken.

3.2.1 ROV speed capabilities

The hydrodynamic drag forces on the ROV and the cable and the ROV thrust level limit the maximum speed the ROV and is hence important working on places like the Tautra ridge.

⁹ Teledyne RDI, San Diego, California, USA

¹⁰ Hydrolek, Berkshire, UK

$$F = \frac{1}{2} \rho U^2 (C_{D_{ROV}} A_{ROV} + C_{D_{Cable}} A_{Cable}) \quad (3.1)$$

To estimate the combined drag force on the vehicle and umbilical, F , eq. (3.1) can be used. This equation is a simplification giving reasonable results when one can assume that the current is constant over the water depth and the ROV and the surface vessel move with similar velocity and direction, see Figure 3.3. This is a typical set up running survey lines with the ROV on a few hundred meters of water depth. This is the most ROV-thrust demanding situation seen in our operations. The equation contains the quadratic damping terms of the Morrison's equation. The density of seawater is ρ , A_{ROV} is the projected front area of ROV and cable, C_D is the drag coefficient and U is the linear velocity. If the ROV is directly underneath the surface vessel, the vessel and the vehicle will share the umbilical forces equally.

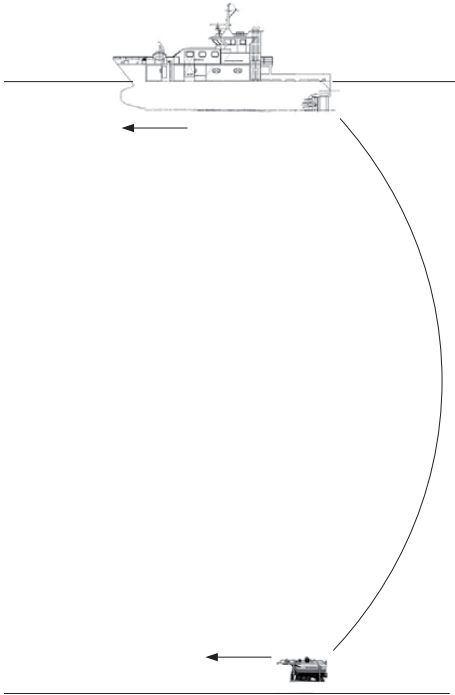


Figure 3.3 Situation where ROV and surface vessel is moving along a straight line with neutral umbilical and similar speed.

If the assumptions mention above is not valid, equation (3.1) will not hold and a more advanced calculation will be necessary. The applicable equation system is based on the catenary equations.

$$f_0 = \sum_{i=1}^N w_i (s_i - s_{i-1}) + \sum_{i=1}^N f_i \quad (3.2)$$

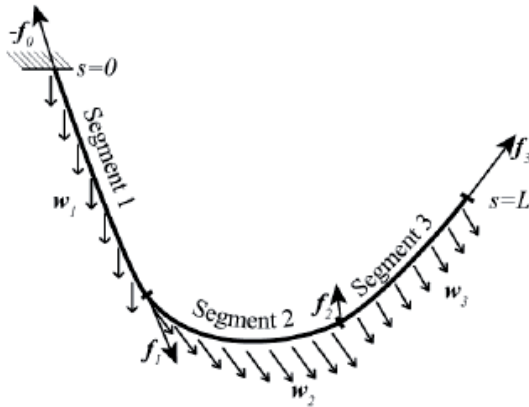


Figure 3.4 Figure illustration the catenary equations (Sortland and Vartdal 1990).

There are a variety of alternative formulation of the catenary equations, on variant the could be suitable for neutral ROV umbilical is found in (Johansen 2007) or (Sortland and Vartdal 1990)

To investigate the Minerva's capabilities in current hydrodynamic testing has been performed in laboratories. A 1:5 scale model, see Figure 3.7.A, was built and tow tests were performed. The tow tests showed that the vehicle had a drag coefficient in forward motion of 0.83. The drag force was measured for angle of attacks from $0^\circ - 360^\circ$, see Figure 3.5.

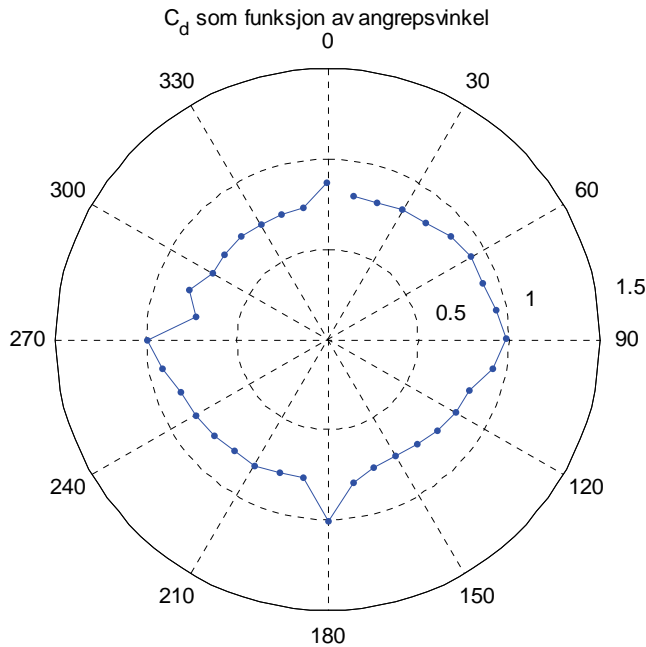


Figure 3.5 The drag coefficient C_d plotted for angle of attack of drag force.

Using eq.(3.1), the ROV velocity, U , can be calculated. In Figure 3.6 the bollard pull for the vehicle varying over angle of attack is plotted. The bollard pull forward, backward and sideways was measured, while the remaining angles were calculated by vector summation. Bollard pull tests were also executed with the vehicle, and the bollard pull was found to be approximately 500 N, Table 3.2.

Table 3.2 Results of full scale tests of Minerva for bollard pull and velocity.

	Forwards	Backwards	Sideways	Vertically
Bollard pull [N]	478	219	195	389
Velocity (m/s)	1.03	0.55	0.50	-

Eq. (3.1) can be used to calculate the theoretical velocity of the ROV. $C_{d-cable}$ can be estimated to 1.2, \emptyset is 22 mm. Using depth information to create an estimate for A_{cable} , eq. (3.1) can be solved for U . The $C_{d-cable}$ equal to 1.2 is found in Hoerner (Hoerner 1965).

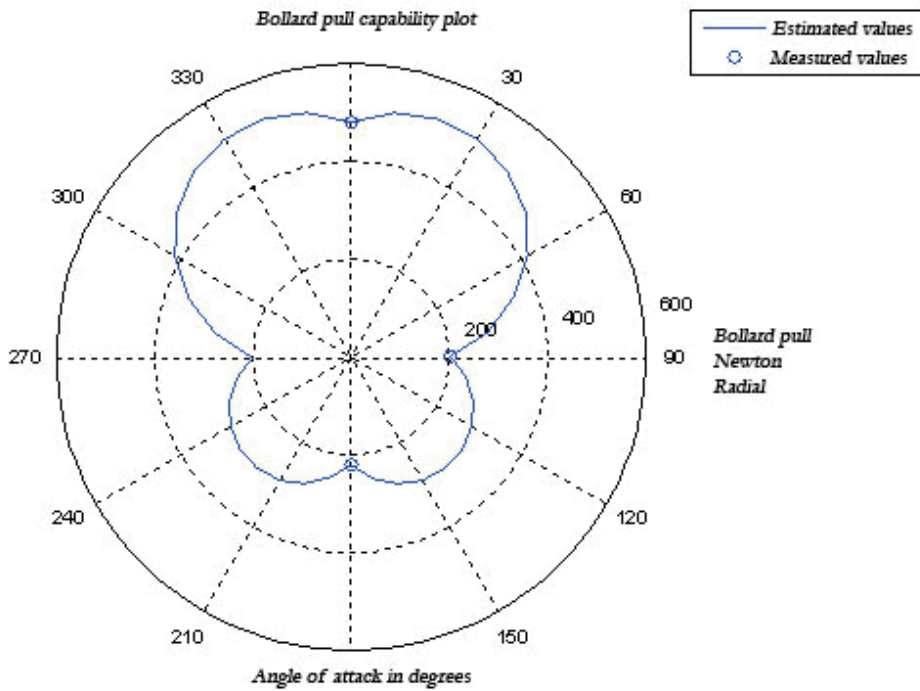
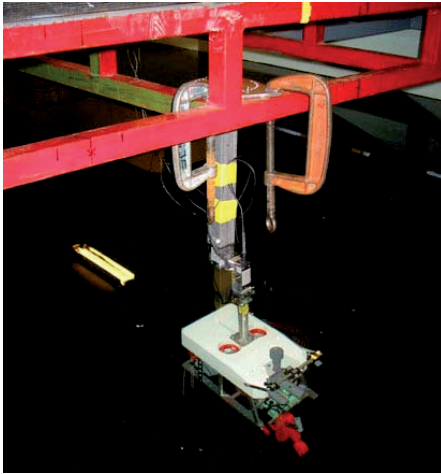
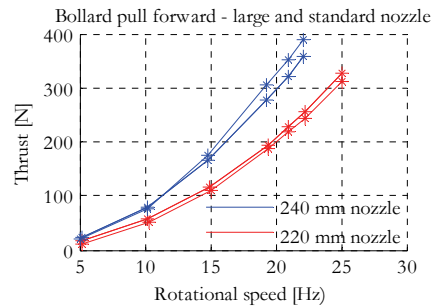


Figure 3.6 Capability plot showing the bollard pull varying over angle of attack for the vehicle

To be able to estimate the force, the thrusters were tested in the cavitation tunnel at NTNU. In Figure 3.7.B bollard pull for individual thrusters are plotted for the standard 220 mm nozzle and propeller and a modified 240 mm nozzle and propeller. The rotation speed of the thrusters on Minerva is around 24 Hz, corresponding to 250 – 300 N in Figure 3.7.



A)



B)

Figure 3.7 A) 1:5 scale model of Minerva during towing experiments. B) Bollard pull curve for a single thruster tested in cavitation tunnel. Two nozzles and propellers were tested, 240 mm and 220 mm. Minerva is fitted with 220 mm thrusters.

An automatic control system is desired to enhance performance in grid surveys. The most important function of the control system would be to manoeuvre the vehicle along a predefined survey line keeping velocity, heading and seabed altitude constant while minimizing the cross track error to the survey line. A secondary useful feature is the ability for the ROV to automatically maintain position, so-called auto positioning capability.

To achieve this functionality a digital processor needs to take control of the thrusters of the vehicle and there must be measurements of ROV heading, velocity, altitude and cross track error. An IMU and a DVL were mounted on the ROV to provide these inputs. Control algorithms were developed by the Department of Cybernetics, NTNU (Svendby 2007). The system was however never implemented on Minerva except for prototype testing. If it is not possible to continue this work in the future, there are commercial systems that could be attempted (SeeByte 2007). An alternative implementation of automatic control system for ROV's is also shown for the WHOI vehicle Jason (Whitcomb, Howland et al. 2003).

4 Underwater navigation

The purpose of ROV navigation is two-folded, the first is practical considerations, as it is necessary to know the location of the vehicle at all times for operational safety and to find the research targets. The second motivation is geo-referencing of collected data. As important as the data themselves is the knowledge of where the data are collected. The precision requirement for the survey data position tag determines navigation equipment and survey procedures. Certain sensors require that each data sample (e.g. acoustic ping) are compiled with previous samples to form the data set. For such surveys the position accuracy should ideally match survey sensor resolution to maximize the value of the survey data. On video surveys the relation between instrument resolution and navigation accuracy is less significant.

Table 4.1 Examples of survey sensors resolution typically deployed on ROVs.

	Unit	Data resolution	Sensor
Bathymetry sonar	[m]	0.3	Imagenex ¹¹ Delta T
Side scan sonar	[m]	0.2	GeoAcoustics ¹² GS500+
Photography	[mm]	2 – 4	Uniq Vision ¹³ UC 1830CL – 12B

4.1 Principles of ROV navigation

Positioning is the term used for direct position measurement, opposed to navigation which is a broader term. There are two dominating methods for measuring the ROV position: USBL and LBL (Long BaseLine), see (Milne 1983) for thorough explanations of the positioning principles. To achieve a global ROV position using a USBL system one need: 1) a ship mounted transceiver 2) a ship mounted heading-, roll- and pitch sensor, 3) a dGPS (Differential GPS) and 4) a transponder mounted on the ROV, see Figure 4.1 and Figure 4.2. A LBL positioning system consists of an array of transponders placed on the seabed and a transceiver mounted on the ROV. The position can hence be obtained independently of the vessel sensors, shown in Figure 4.3.

¹¹ Imagenex, Port Coquitlam, British Colombia, Canada

¹² GeoAcoustics, Great Yarmouth, England

¹³ Uniq Vision, Santa Clara, California, USA

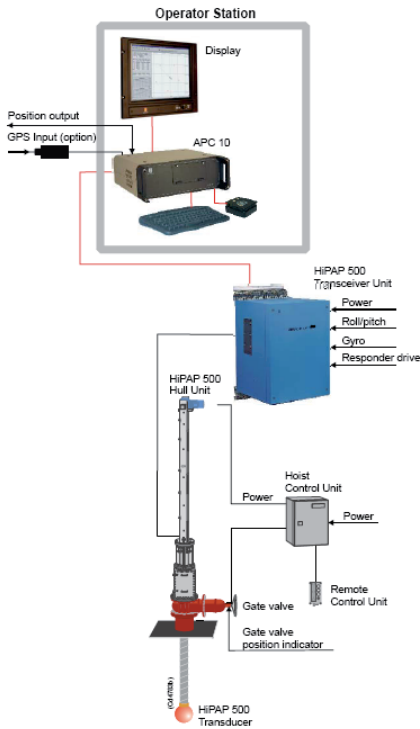


Figure 4.1 Kongsberg Maritime's¹⁴ HiPAP system (Source HiPAP brochure) like it is installed on the NTNU research vessel Gunnerus (Kongsberg 2004).

4.1.1 Surface positioning

GPS

GPS-positioning (Global Positioning System) is based on satellites in orbit around the Earth. On the surface of the Earth each GPS receiver calculates the ranges to a set of satellites by measuring the time of flight from the signal leaves the satellite till it arrives the receiver. The positions of the satellites are sent from the satellites to the receiver units. Using the satellite positions and ranges, the position of the GPS receiver unit on the ground can be calculated. Four satellites are necessary to solve a three dimensional position for the receiver unit. For conventional GPS navigation, 15 meters horizontal standard deviation is normal. The main error sources are: atmospheric distortions to the signal path, inaccuracies of the indication of the satellite orbits, satellite clock errors and numerical errors.

Differential GPS

To increase the position accuracy on a given platform, ground based reference stations broadcast the system error. The error is determined by measuring the

¹⁴ Kongsberg Maritime, Horten, Norway

difference between known positions of the reference stations and positions estimated by GPS receiver units on the reference stations. The broadcasted difference between known position and the measured position is often termed differential correction. There are several systems available, both freely available (e.g. WAAS (Wide Area Augmentation System) EGNOS (European Geostationary Navigation Overlay Service) and IALA (International Association of Lighthouse Authorities)) and subscription services (e.g. Omnistar, Veripos). Most modern GPS systems have incorporated some variant of differential correction like the EGNOS. dGPS (Differential GPS) receivers typically offer position estimates with standard deviations varying from 5 m to 0.1 m depending on the quality of the differential correction service.

Real Time Kinematic GPS

The signal containing the information used for conventional GPS position estimation is encoded on a signal carrier wave. RTK (Real Time Kinematic) GPS position estimation measures the carrier wave itself. In the signal processing of conventional GPS units the system aligns the received signal to a pseudo random code. In RTK processing the carrier phase itself is aligned. The phase of the carrier is considerably faster than the phase of the signal and here is the potential for improvement of position accuracy. Due to the wave length of the carrier frequency, this leads to a position ambiguity. The position ambiguity is solved by placing a fixed base station in the vicinity of the RTK GPS receiver. One centimetre accuracy is typical (Lekkerkerk, van der Velden et al. 2006).

4.1.2 Underwater positioning

Ultra Short Baseline positioning

Ship mounted USBL systems sends out an acoustic impulse (ping) which is received by the ROV transponder, see Figure 4.2. The ROV-transponder returns a ping to the transceiver. The range is computed from the time of flight of the ping. The bearing angles are calculated from phase measurements on the transducer elements on the returning ping. For USBL-systems ambient acoustic noise, acoustic noise from sources on the ROV-support vessel, speed of sound variations and multi-paths are the most important sources of error (Milne 1983).

Table 4.2 Operating frequency bands of common USBL systems

Manufacturer	Product name	Frequency	Frequency Band	Accuracy Range	Accuracy angular
Kongsberg Maritime	HiPAP 500	21 – 31 kHz	MF	0.1 m	0.12°
	HiPAP 100	10 – 15.5 kHz	LF	0.1 m	0.14°
Sonardyne ¹⁵	Scout	35 – 55 kHz	HF	0.5 % of range	
	Fusion	18 – 36 kHz 35 – 55 kHz	MF HF	0.2 % of range	
Link-Quest ¹⁶	Tracklink 1500	31 – 43.2 kHz	HF	0.2 m	3.0° - 0.25°
	Tracklink 5000	14.2 – 19.8 kHz	MF	0.3 m	3.0° - 0.15°
	Tracklink 10000	8.4 – 11.7 kHz	LF	0.4 m	3.0° - 0.25°
Applied acoustics ¹⁷	Easy Trak	17 – 32 kHz	MF	0.1 m	1.4°
IXSEA ¹⁸	Posidonia	8 – 18 kHz	LF	0.3 % of range	
	GAPS	20 – 30 kHz	MF	0.2 % of range	
ORE ¹⁹	Trackpoint 3	8 – 30 kHz	MF	0.5 % of range	

The numbers for accuracy in Table 4.2 should be treated critically. The numbers are taken from product specifications and the conditions for the performance may vary. In general lower frequency results in better range for the system, but poorer system accuracy.

¹⁵ Sonardyne, Hampshire, UK

¹⁶ Link Quest, San Diego, California, USA

¹⁷ Applied acoustics, Great Yarmouth UK

¹⁸ IXSEA, Marly-le-Roi, France

¹⁹ ORE, West Wareham, Massachusetts, USA

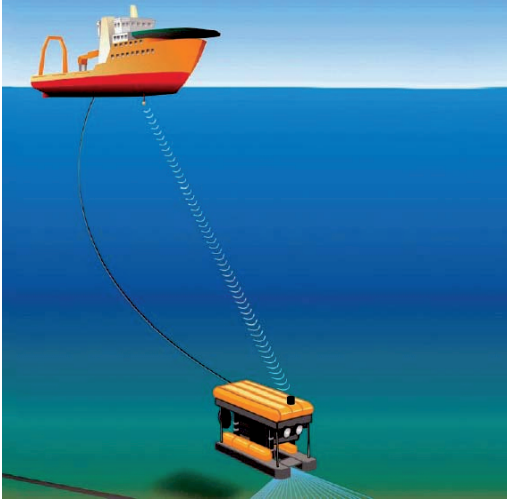


Figure 4.2 USBL positioning principle (Kongsberg 2004).

Propagated uncertainty estimation for USBL positioning

In a USBL setup the GPS, gyro and USBL system all contribute to the resulting global position accuracy. A basic approach to calculate the uncertainty of a complete navigation setup is to sum the statistical variances of the individual measurements as in eq. (4.1).

$$\sigma_{total} = \sqrt{Var_{GPS} + Var_{Gyro_position} + Var_{USBL_position}} \quad (4.1)$$

Since the gyro measurement accuracy is specified as standard deviation of the heading angle, the gyro error contribution to the xyz position estimate depends on the geometry between the ROV and the support vessel. The situation is the same for the USBL xyz-position error contribution from the depression and bearing angles. The horizontal distance from the vessel to the ROV acts as an arm in the calculation of the error contributions from the bearing angle measurements and the gyro measurements. Ideally the vessel should be placed directly above the ROV to reduce the error components from vessel mounted gyro and USBL bearing angle measurements.

Eq. (4.2) is set up to derive position standard deviation for the USBL position expressed in meters. ν denotes depression angle for the USBL system, while ω denotes the bearing angle. R denotes the range from transducer to transponder and $R_{horizontal}$ denotes R projected to the horizontal plane.

$$\begin{aligned} \sigma_{USBL_position} &= \sqrt{Var_R + Var_{\omega} + Var_{\nu}} \\ Var_{\omega_metric} &= R_{horizontal} \cdot (\sin(Var(\nu)) + \cos(Var(\nu))) \\ Var_{\nu_metric} &= R \cdot \cos(Var_{\nu}) \cdot (\cos(\omega) + \sin(\omega)) \end{aligned} \quad (4.2)$$

Table 4.3 Calculation of typical underwater position accuracy at 200 m range for the instruments installed onboard the RV Gunnerus.

	Instrument	Example values	Standard deviation	Standard deviation [m]
Range	USBL – HiPAP	200	0.1 [m]	0.10
Depression angle	USBL – HiPAP	70	0.12 [°]	0.39
Bearing angle	USBL – HiPAP	40	0.12 [°]	0.39
Heading	Gyro - Simrad GC-80-S	215	0.1 [°]	0.39
Position	GPS – Seatex DPS 116	-	0.5 [m]	0.50
Total standard deviation				0.85

Summing specific instrument variances from a set of common survey sensors including range, depression angle, bearing angle and heading, an example of propagated uncertainty is calculated in Table 4.3. By upgrading the GPS to a system with 0.20 m standard deviation the total standard deviation for the setup will decrease to 0.70 m.

It should however be emphasised that the uncertainties discussed above are white measurement noise. In practical implementation one can suffer from a variety of systematic errors. Efforts to observe and control potential systematic errors are discussed in section 4.5.

Long Baseline positioning

In LBL positioning the transceiver on the ROV triggers the seabed beacons, either all at the same time (in simultaneous mode) or one at the time (sequential mode) (Milne 1983). The distance to each beacon is calculated from time of flight measurements and the position of the ROV is triangulated from these ranges, see Figure 4.3.

Before the operation can begin, LBL requires installation of transponders on the seabed and positioning of the transponders. The LBL is often more accurate than USBL and the accuracy is not dependent on depth in the same way as for USBL since the transponders are situated on the seabed.

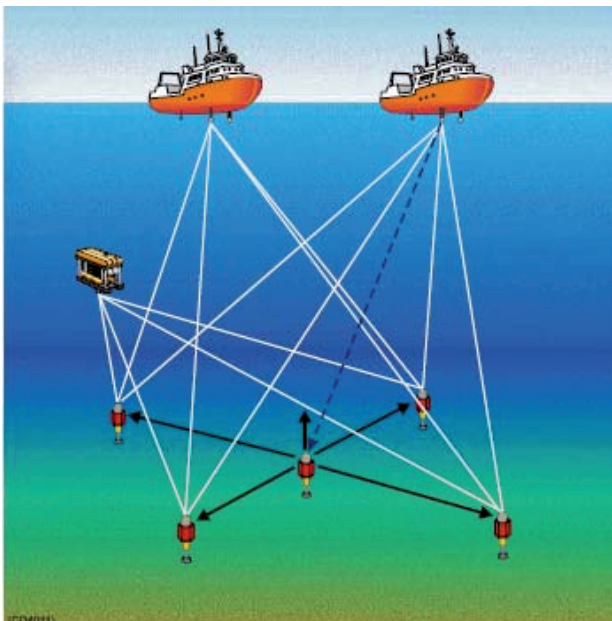


Figure 4.3 ROV and vessels performing LBL positioning (Kongsberg 2004).

For both USBL and LBL positioning the position update frequency is limited by the speed of sound. Position update rates depend of the distance between transducer and the transponder on the ROV.

The speed travels with approximately 1480 m/s in seawater. If the range is 500 meter and we are using USBL with a transponder, the acoustic signal has to travel 1000 m (back and forth from the ship to the ROV) which will be approximately 675 milliseconds. The systems also need some milliseconds for processing time, and the overall position measurement frequency is around 1 second. For longer distances the position update frequency will hence decrease. For long ranges the transponder on the ROV can be triggered electronically reducing the travel distance for the ping with 50 %.

4.1.3 Heading pitch and roll

There are two types of heading sensors that dominate for ROV-operations, the fluxgate compass and the gyroscope. The fluxgate compass is inexpensive, but has limited accuracy, typically standard deviation 5° . The dynamic performance is often insufficient for ROV applications (Vik 2000). In survey terminology the heading sensor is often called gyro whether it contains a gyroscope or not.

The gyro has direct impact on the result of an ROV-based surveys in general and bathymetric surveys in particular. Gyros measure heading to true north and provide good accuracy, often down to 0.5° standard deviation. There are many types of gyros available, but for ROV applications only strap-down technologies based on

quartz elements, RLG (Ring Laser Gyro) or FOG (Fibre Optical Gyro) are suited due to mechanical robustness and physical size.

A VRU (Vehicle Reference Unit) is used to measure roll, pitch and heave. Pitch and roll sensors are often termed IMU (Inertial Measurement Unit) in the hydrographic survey curriculum. It consists of three accelerometers and three angular rate sensors. By integrators and navigation equations orientation angles are calculated (Savage 1998). Typical performance for roll and pitch are 0.05° – 0.1° standard deviations and 5 cm or 5% for heave. Typical accuracy for roll/pitch sensors used in bathymetric surveys is 0.03° RMS (Kongsberg 2001). For bathymetry surveys the output rate must be high, typically higher than 20 Hz, to provide a sufficiently accurate orientation stamp on each data point.

4.1.4 Speed of sound

To accurately calculate the range between transponders from time-of-flight measurements, both LBL and USBL need precise information about the speed of sound in the seawater. If the speed of sound varies over the water column, the path of the sound will be curved, as seen in Figure 4.4. The path can be calculated according to Snell's law, see eq. (4.3), where Θ_1 is incident angle for the sound path and Θ_2 refraction angle. c_1 and c_2 represents the two levels for speed of sound.

$$\frac{\sin(\Theta_1)}{c_1} = \frac{\sin(\Theta_2)}{c_2} \quad (4.3)$$

The speed of sound can be measured directly, or calculated from CTD (Conductivity Temperature and Depth) data, see eq. (4.4). The speed of sound depends on temperature, salinity and depth with temperature as the most significant variable. The relation between temperature, salinity, depth and speed of sound is empirically decided and the formula by UNESCO (United Nations Educational Scientific and Cultural Organization) is the most commonly used (Fofonoff and Millard 1983).

$$c(S, T, P) = C_w(T, P) + A(T, P)S + B(T, P)S^2 + D(T, P)S^3 \quad (4.4)$$

Table 4.4 Symbols for equation (4.4).

Symbol	Variable
C	Speed of sound
S	Salinity
T	Temperature
P	Pressure
C_w, A, B, C, D	Empirical constants derived from polynomials

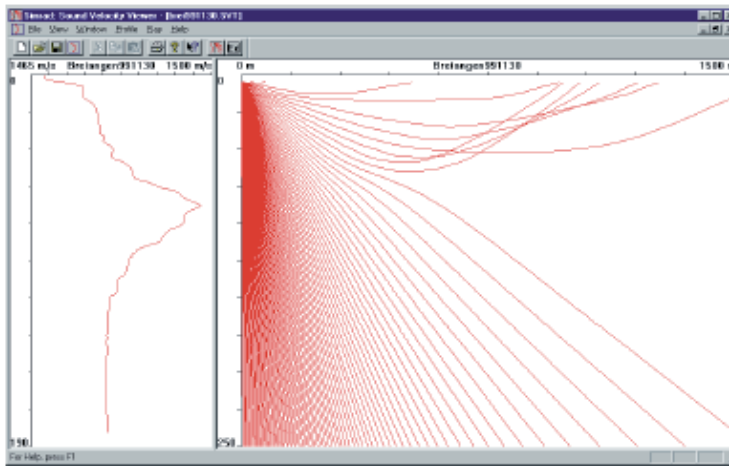


Figure 4.4 Speed of sound profile and ray bending patterns from a survey in the fjord of Trondheim in the autumn season. The depth is 250 meters and the speed of sound varies from 1465 m/s to 1500 m/s.

Figure 4.4 shows a typical speed of sound profile with examples of ray paths. The maxima of speed of sound found at approximately 100 meters depth is most likely a result of a thermocline. Such thermoclines are common in the Trondheim area at the fall season (Sakshaug and Sneli 2000). Speed of sound profiles must be measured and applied to correct ranges and to compensate for acoustic ray bending. During a survey, new speed of sound profiles should be collected every day and more often if the salinity and temperature conditions are unstable due to e.g. river plumes or tide currents. However for low precision surveys in shallow waters an assumption of constant speed of sound can be sufficient.

4.1.5 Depth

Depth is calculated from pressure measurements using eq. (4.5). The conversion from pressure to depth depends on the density of seawater, the local value of gravity, the atmospheric pressure and the surface and the compressibility of seawater. The atmospheric pressure is measured with a barometer on the surface.

$$d = \frac{P_t - P_a}{\rho \cdot g} \quad (4.5)$$

The density of seawater is calculated from salinity, temperature and pressure values measured by CTD (Conductivity Temperature and Depth sensor) according to (Fofonoff and Millard 1983), see the empirical expression in eq. (4.6). Salinity is the most significant variable for the density.

$$\rho(S, T, P) = \frac{\rho(S, T, 0)}{\left[\frac{1 - p}{K(S, T, P)} \right]} \quad (4.6)$$

The local gravity value depends on latitude and altitude, and in addition constant local variations up to 100 μg may occur. The gravity can be calculated according to eq. (4.7) (Britting 1971).

$$g = \frac{\mu_g}{|r|^2} \left[1 - \frac{3}{4} J (1 - 3 \cos 2\mu) \right] - |r| \omega_e^2 \cos^2 \mu \quad (4.7)$$

Table 4.5 Symbols for equation (4.5), (4.6) and (4.7).

Equation	Symbol	Variable
(4.5)	d	depth
	p_t	measured pressure
	p_a	atmospheric pressure on the surface
	ρ	Seawater density
(4.6)	$K(S,T,P)$	Secant modulus
(4.7)	g	Gravity
	μ_g	Gravitational constant equal to 398601×10^8
	J	Empirical constant 1.407645×10^{-6}
	μ	Latitude
	ω	Earth rotation
	r	Geocentric position vector

When the pressure is read and converted to depth using the measured values for atmospheric pressure, seawater density and gravity, the depth should be corrected for tide and the vertical datum should be applied. The most common vertical datums are mean sea level, LAT (Lowest Astronomical Tide), geoid height and ellipsoid height.

4.1.6 Combined navigation systems

To increase the position estimate accuracy the position measurements can be combined with dead-reckoning. Dead reckoning is a method for estimating the positioning where initial position, heading, time and velocity is used to calculate the position. Common sensors used for dead reckoning are gyro, DVL (Doppler Velocity Log), IMU and INS (Inertial Navigation System). Mathematically, speed and accelerations are integrated over time to establish position estimates.

When integrating speed or acceleration measurements the measurement errors are also integrated. The integration of acceleration and velocity error will cause the position error to grow with time and the position estimate will drift. The measurement noise of accelerations and velocities is however low. Acoustic baseline positioning and dead reckoning have opposite error characteristics, with high noise and no drift. Stochastic noise in the position measurements is among the most important errors for acoustic baseline positioning.

By combining dead reckoning and acoustic baseline position measurements it is possible to obtain position estimates with low levels of white noise and no drift. An error state Kalman-filter is used to estimate the error of the position measurement (Gelb 1974), (Larsen 2000), (Marthiniussen, Faugstadmo et al. 2004). The white

noise can be reduced with 60 – 70 % in a combined systems compared to conventional acoustic baseline positioning (Gade 2005).

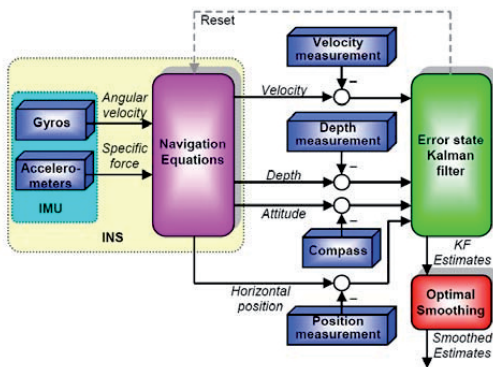


Figure 4.5 Example of instrument setup for position estimation using position, velocity and acceleration measurements combined using Kalman filter (Gade 2005).

4.1.7 Navigation from payload sensor data

It is possible to use sensor data to strengthen the quality of the position estimate. One approach is terrain navigation, where e.g. a bathymetric model is compared to the data from a multibeam echosounder. The measured data are then correlated to the reference model (Hagen and Stoerkersen 2006). An alternative solution is to form closed loops with the vehicle trajectory. By comparing data from different point of time from an operation possible time varyig position drift can be observable and can be adjusted (Roman and Singh 2007). Both approaches can be implemented both real time and for post processing. These approaches sorts under SLAM (Simultaneous Localisation and Mapping) which is an establish field under robotics.

4.2 Navigation setup specification

Both the sensor resolution and the planned usage of the data set should be considered when determining the navigation precision level for a survey. Over-specification of the survey requirements will cause unnecessary high cost and under-specification may leave the collected data useless. Navigation setup requirements for four categories of survey are discussed:

1. Video
2. Photo mosaic
3. Bathymetry sonar
4. Photogrammetry

Even though video-surveys in general provide data with higher resolution than sonar surveys, one usually settles for lower position accuracy for video surveys than for acoustic surveys like bathymetry sonars. The correlation between information

content and position estimate uncertainty is considerably stronger for bathymetry data than for video imagery. Video surveys can hence often be completed with less accurate geo-referencing than bathymetry surveys. Table 4.6 sums up the levels of accuracy for position measurements for survey techniques relevant for habitat mapping.

Table 4.6 Accuracy requirement for different types of surveys generalised.

	Video	Photo Mosaic	Bathymetry Survey	Photo-grammetry
Horizontal position	moderate	moderate	high	high
Depth	moderate	moderate	high	high
Altitude	low	moderate	no	high
Heading	moderate	Low	high	high
Roll/Pitch	no	no	high	high

4.2.1 Video surveys

For video surveys the most important navigation data are the horizontal position of the ROV. Heading and depth are also necessary, but the accuracy requirements are moderate. Some degrees deviation for heading measurements is acceptable. The accuracy requirements for x-y coordinates and depth depend on the type of the survey. The seabed altitude is useful during video survey to decide the scale of objects on the seabed, and to obtain constant altitude an altimeter is necessary. Ten centimetre standard deviation for seabed altitude is sufficient. Video imagery is used to recognise objects, and the exact observation angle (roll and pitch angles) is useful but seldom compulsory. The viewer can often estimate the observation angle of the seabed from the video images.

4.2.2 Photo mosaics

The processing of photo mosaics is based on image feature recognition (Pizzaro and Singh 2003), which means the photo mosaic can be created without navigation data. But the user needs the geo-localisation of the photo-mosaic images. The position and heading must therefore be measured. The heading measurements are only advisory and typical fluxgate compass accuracy is sufficient. The depth accuracy is not important. Altitude measurements can be used to scale the objects in the images. But with the present processing scheme altitude, roll and pitch measurements are only complimentary information to the user. The camera is mounted along the vertical axis of the ROV. The ROV is passively stable in roll and pitch and that is considered sufficient for photo mosaic applications.

4.2.3 Bathymetry sonars

Bathymetry sonars are normally hull mounted on surface vessels. In deeper water they can be mounted on underwater vehicles to reduce the slant range and increase the quality and data resolution. To realise this potential for detailed bathymetry data ROV-based bathymetry surveys require high position accuracy. The quality of the x-

y coordinates and the depth estimates should comply with “special order surveys” in the IHO (International Hydrographic Organization) 44 standard (IHO 2008). Bathymetry sonar measures the seabed altitude but an external altimeter is useful for QC (Quality Control), but not compulsory. To achieve the desired data precision the orientation angles of the ROV must be measured to better than half a degree accuracy.

Ideally there should be a position and orientation measurement of the ROV for each sonar ping. Modern bathymetry sonars have ping-rates up to 50 Hz (Kongsberg 2004), (Reson 2008). In the most common underwater positioning systems, the position update frequency is 1 Hz or lower, while orientation angles are measured at higher frequencies, from 25 – 400 Hz. Hence for position measurements one must rely on extrapolations. A common grid size for high resolution bathymetry data is 0.5 meter, which means the position accuracy ideally should be in the same order.

4.2.4 Photogrammetry

To construct a photogrammetric model, information of relative motion of the camera from one image to the next is important, i.e. position, depth, heading, altitude, roll and pitch are significant factors. Precision is vital and most acoustic baseline systems are insufficient. For the photogrammetry processing the relative position from one image to the next is essential, global position and orientation accuracy is less important. One can estimate the relative position from one image to the next by doing dead reckoning with inertial measurements and Doppler log velocity data. Due to the short time span the position drift will be acceptable. To be able to scale the photogrammetric model, high accuracy of the seabed-altitude is necessary.

4.3 Position accuracy standards

Research surveys are seldom bound by standards, but for conformity and repeatability it may be wise to comply with present standards. IHO released its 5th edition of their Standard for Hydrographic Surveys in February 2008 (IHO 2008). Bathymetric surveys are treated in general, ROV-based operations are not specifically discussed. The standard is often referred to as S-44 and operates with four orders (special order, order 1a, order 1b and order 2) of hydrographic surveys and describes accuracy requirements for bathymetry data in general, see Table 4.7. Because the main objective of S-44 is navigational safety of ships, the accuracy requirements are eased with increasing depths. For scientific surveys accuracy maintains its relevance independent of depth.

Table 4.7 Position requirements according to IHO S-44 (IHO 2008). a is the constant depth error, i.e. the sum of all errors, b denotes a factor dependent of depth and d is the depth.

S-44 PRECISION:	Special order	1 (a+b) order	2 order
Horizontal accuracy (95 % Confidence Level)	2 m	5 m + 5 % of depth	20 m + 5 % of depth
Depth Accuracy for Reduced Depths (95 % Confidence Level)	a = 0.25 m b = 0.0075	a = 0.5 m b = 0.013	a = 1.0 m b = 0.023

$$e = \pm\sqrt{a^2 + (b \cdot d)^2} \quad (4.8)$$

In eq. (4.8) e denotes the acceptable error (system propagated uncertainty), a is the acceptable constant error, while b represent the component proportional to depth, d . The standard was developed for bathymetric surveys for maritime ship security; hence the requirements for accuracy ease proportionally with depth.

4.4 Processing

There are three steps in the processing of the navigation data (Lekkerkerk, van der Velden et al. 2006):

1. Validation
2. Filtering
3. Corrections

4.4.1 Data validation

Navigation data are validated by checking the consensus between individual sensors. In the data validation the raw data from dGPS, USBL/LBL, gyro on ROV and vessel, VRU on ROV and vessel, DVL, pressure cell, and altimeter measurements are plotted along a common time axis. Typical error indicators seen with this check is zero readings, lack of sensor dynamics, implausible measurements, and large jumps in measurement like constant heading signals (“frozen signals”) or unphysical position jumps. These errors are typically caused by instruments temporarily halting sending data or faulty sensors. By comparing data latency and the sign convention, inconsistencies can be seen. If e.g. the ROV accelerates, it will be seen in the speed measurements from the Doppler log, and one will expect the ROV to pitch nose up due the cable drag. To complement the time plots the error estimate produced by instruments like USBL and dGPS should also be used in the validation process.

4.4.2 Data filtering

Remaining data outliers should be rejected by filtering. Outliers are data points which are self evidently erroneous, e.g. measurements indicating motion that is not physically possible. For position data the filter can e.g. calculate the ROV speed from positions and time-stamps, and remove data points associated to velocities

above a limit value. When outliers are removed the ROV-trajectory can be carefully filtered to reduce white noise with e.g. a low-pass Butterworth filter. Care should be taken with low-pass filters as they introduce phase-error. Kalman-filter is the superior method for filtering as it takes into account the statistical properties of all measurements and does not introduce phase-error (Gelb 1974). The application of Kalman-filter depends on good knowledge of the statistical error characteristics for the instruments. For combined navigation systems a smoothing filter is ran applying the Kalman-filter on the data set both forward and backwards along the time axis.

4.4.3 Data corrections

After the data validation and filtering, the corrections for datum, tide, density, speed of sound and heading deviation should be carried out. If it is necessary to transform the position coordinates to a different datum it should be done at this stage. The tide component is either calculated or measured before it is applied to the pressure depth readings. To further improve the accuracy of the depth calculated from the pressure readings the mean density of the seawater is calculated from a CTD-profile of the water column as described in section 4.1.5. If not applied in real-time, the speed of sound should be calculated and applied to the USBL/LBL data. The magnetic deviation of the heading reading of magnetic compasses should be compensated.

4.5 Quality assurance and control

The expression “quality assurance” covers the method to increase the probability for fulfilling the end-product requirements by examining the production process. Quality control is the practise of checking that the product has the expected characteristics. In marine operations, these terms are close and often treated together since quality assurance and quality control have overlapping definitions. In commercial offshore operations there is a strong tradition for QA/QC. The terms are more unfamiliar in academia, but the scientific criterions for accuracy and repeatability causes awareness of the quality of the product even though other terms are more common.

The QA/QC process must run in parallel with survey planning, data acquisition and data processing to assure the data produced comply with the requirements established before the survey starts. The first step in the QA/QC process is to evaluate the *survey plan*. Flaws in the survey plan will most likely result in a suboptimal operation and reduced data quality. The propagated error budget developed during the planning of the operation is an important part of the quality management.

During data acquisition quality assurance starts by controlling that all instruments are calibrated properly. When the survey is running the quality should be controlled as described in the section on online data processing. The quality assurance process continues into the data processing phase. The described data validation is essential to quality control. Elements like a separate stationary position transponder or a

survey cross line are elements that can strengthen the integrity of the collected data. Finally the data process pipeline is documented in the data assurance work.

4.5.1 Instrument offsets

For the vessel mounted GPS, USBL transceiver, VRU and gyro it is important that positions and angles according to the vessel axes system are correctly configured. Likewise for the ROV, the gyro, transponder, VRU and Doppler must be entered into the navigation system with correct positions and angles. Incorrect offset distances and angles will result in systematic errors.

4.5.2 Instrument calibration

The last valid calibration should be known for all navigation instruments. Depending on the precision requirement for the current survey, the demand for new calibrations should be sorted out. All calibrations must be thoroughly documented.

GPS

The survey GPS should be compared to the other GPS units onboard the vessel before start on all surveys to confirm their integrity and accuracy. By logging two or more GPS's while moored to the quay, the noise characteristics and offsets of the instruments will be observable. If doubt arise about the position of the antennas relative to the vessel's reference system a surveyor team must re-establish a valid position for the antenna.

VRU and gyro

Calibration of gyros, VRU's and INS's are often laboratory work to be left to professionals, but the gyro-, VRU- and INS-offsets for the vessel and the ROV can be measured by a surveyor-team when the vessel is quay-side. For the ROV one can get a measure for possible mounting angles by setting the ROV on the quay and read of roll and pitch. Then lift the ROV up and change the heading 180°, put it down and reread the roll and pitch angles. This will reveal if the quay is level and the relative angle between the ROV-coordinate axes and the sensor coordinate axes can be calculated.

USBL

The USBL positioning system is calibrated through a “box-in” procedure and a “spin” procedure (Lekkerkerk, van der Velden et al. 2006). To maximize the outcome of a USBL calibration the dGPS, gyro and must be calibrated individually before the USBL calibration can commence. It is also essential that the correct speed of sound profile is measured and applied for the calibration. The following possible error sources will affect in the result of an USBL calibration;

- Scaling error
- Velocity error
- Horizontal alignment of system reference frames
- Gyro error
- Transducer alignment
- Vertical alignment of system reference frames
- Pitch error
- Roll error

During a box-in calibration a stationary transponder is deployed on the seabed. The position of the transponder is measured from the ship at four different positions having the transponder aft, fore, starboard and portside of the vessel. The vessel heading should be constant. This procedure will reveal any angular offsets between the axis-system associated with the attitude sensor and the USBL transducer. The tolerances depend on the accuracy needed, but in general $\pm 0.5^\circ$ is acceptable (Kongsberg 2004).

In the spin-procedure the vessels is situated directly above the transponder and measures the position of the transponder from different headings. Then linear offsets between USBL reference point and dGPS reference point is revealed. Normally ± 10 cm tolerance is tolerable. It is sufficient if there is performed a calibration within the last 6 months. The calibration should be repeated when something is changed to the system e.g. if an antenna is moved.

DVL

To calibrate the DVL the scale and bias for the speed readings along with the mounting errors are established. During the calibration procedure the ROV is run along a line in both directions. To achieve enough data points the vehicle is running $\frac{1}{2}$ - 1 hour in each direction. By dead-reckoning positions from the Doppler log reading and comparing these with the positions measured with the baseline system (LBL or USBL), the mounting biases, scale factors and mounting angles can be calculated (Kongsberg 2005). Before a DVL calibration is performed, the USBL system must be calibrated to avoid USBL errors to propagate through the setup and possibly result in erroneous offset values for the DVL.

Recommendations for accuracies

IMCA (International Marine Contractors Association) has given the following recommendations for sensor calibration accuracy listed in Table 4.8 (Danson, McNiell et al. 2003). The guidelines also propose how often the calibration routines should be completed. The USBL-transducer can be calibrated to 0.5° accuracy, but it is more challenging to be able to mount the roll/pitch sensor with 0.1° accuracy on the ROV. The tolerances for GPS is stricter in these guidelines than what is proposed by Kongsberg Maritime, see the section on USBL calibration.

Table 4.8 IMCA recommendations for position setup calibrations.

Item	Minimum calibration frequency	Calibration procedure	Allowable tolerance
USBL transducer	Initial installation	Offsets	$< 0.5^\circ$
Gyro	Initial installation and at start of each project	Operator's gyro/heading sensor calibration procedures	$< 0.5^\circ$
Roll/pitch	Start of each project	Per manufacturer's procedures	$< 0.1^\circ$
GPS	Initial installation and checked at start of each project	Offsets	~ 2.5 cm
Sound velocity	As many as required to sustain necessary precision		$0.2 - 0.3$ m + 0.5% x water m/sec

4.5.3 Real time control

During operation it is necessary to monitor the online navigation quality. The DOP (Dilution Of Precision) for the GPS and the USBL system should be watched. The operators and survey managers should have an idea of what position values to expect. With this knowledge errors in mapping datum, projection zone, and other erroneous instrument settings can be revealed at an early stage.

For USBL positioning, a simple way to observe position integrity in real time is to put a stationary transponder on the seabed in the work area. By approaching the transponder with different vessel-headings, the operator will immediately get an indication on the precision of the sensor offsets. The position of the transponder should remain fixed; otherwise there is an error in the navigation setup. Possible errors in this situation are incorrect sound profile, faulty VRU, faulty gyro.

5 Video survey

5.1 Introduction

This chapter describes how the information value of video surveys is significantly increased by analyzing the information chain through survey design, ROV setup, data analysis and reporting procedures. Biological video surveys can by proper analysis provide information about distribution of substrates, bio-diversity (from species to habitat level), dominant taxa, and eco-physiology. A short description of the underwater imaging process is given. Then the survey design is described starting by defining the survey site and desired data quality. Knowing the requirements for data quality the hardware configuration can be compiled before the data acquisition strategy is designed. Finally the procedure for data processing and interpretation is worked out. Best practices and relevant standards are discussed.

Video surveys are among the most used ROV applications in the marine scientific communities (Myhrvold, Hovland et al. 2004), (Shucksmith, Hinz et al. 2006), (Pinkard, Kocak et al. 2005). In cold-water coral research they are performed for all four categories of survey operations established in section “2.2 Functional requirements for ROV-based habitat mapping”.

- Coral reef confirmation by ground-truthing sonar observations and confirm other coral reef reports
- Searching and mapping of coral reefs
- Condition and fauna documentation of the coral reef
- Development monitoring

The first task in ROV video surveys for cold water coral reefs is the detection of cold-water coral colonies. If no prior record exists for coral occurrence, the ROV and video can be used to search the area for corals. If prior coral indications are available, the ROV will be used to confirm the coral occurrence. When the coral presence is verified, the area needs to be mapped to find the dimensions of the habitat. To achieve more detailed information the following issues need to be investigated: physiological state (distribution of living- and dead corals), species distribution of hard- and soft corals, differences in ecotypes of a given species (phenotypic traits), other taxa of associated organisms, effects/coupling of key environmental variables to biodiversity (e.g. temperature, salinity, nutrients), coupling between biology and substrate (e.g. hard bottom versus soft bottom), identification if taxa zonation etc. (Hovland 2008), (Freiwald 2002). To further

increase the knowledge of a reef, it can be followed over time by frequent re-visits to investigate how the habitat develops.

5.2 The underwater imaging process

In the underwater imaging process artificial lighting is projected on the target at the seabed and the reflections are recorded by the camera. Photons are transmitted and attenuated through the water column before the reflected photons are registered by the camera, see illustration in Figure 5.1. The image is made from the registration of photons reflected from the seabed back to a image sensor. When photons travel through seawater the water itself attenuates some portion of the light. The spectral attenuation, illustrated by arrow *B* and *D* in Figure 5.1, of visible light (400 to 700 nm) is dependent of the coloured dissolved matter, suspended matter and plankton in the water. In addition to the components in the seawater, the water itself heavily attenuates the red part of the light spectrum (600 – 700 nm). There are usually high concentrations of dissolved and particulate matter in seawater and when a given photon hits a particle the direction of the photon is changed either back towards the camera or out of the camera field of view, illustrated by arrow *A*, *C* and *F* in Figure 5.1. This light-scattering reduces the amount of light that is forming the imagery. The backward scattered light reduces the quality of the image (blurring), by lowering the contrast in the image. When the photons reach the seabed they are scattered and absorbed by the seabed components. A fraction of the photons from the seabed are reflected back to the camera they are again subject to scattering and absorption by seawater and its constituents. Some reflected photons are scattered at small angle (small-angle forward scattering). These photons reach the camera and become recorded in the image, but since their trajectory from the seabed to the camera is not straight, they blur the image and reduce the resolution of the image. (Funk, Bryant et al. 1972), (Jaffe 1990).

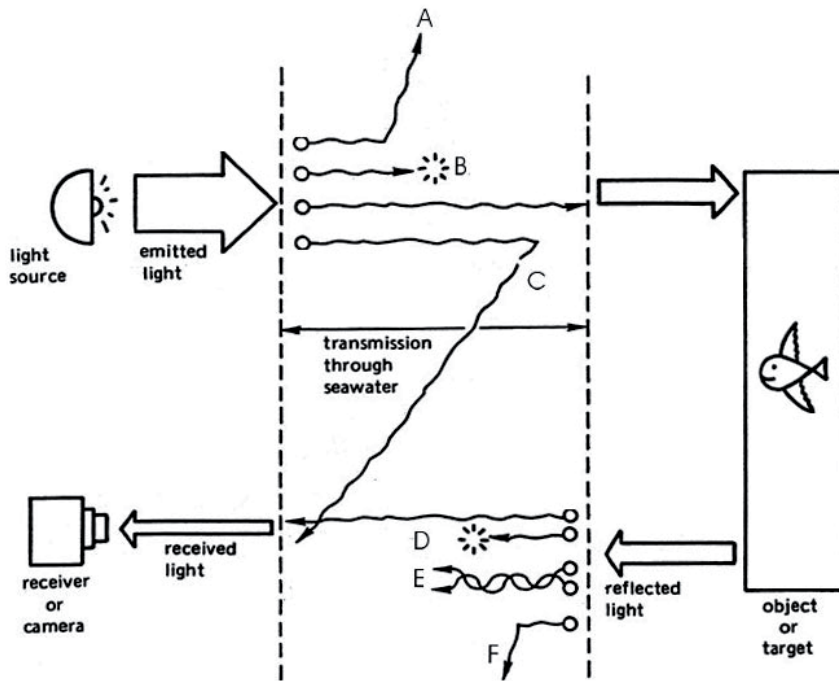


Figure 5.1 The underwater imaging process illustrating the losses of light to an image in an underwater imaging system (Funk, Bryant et al. 1972).

Figure 5.1 illustrates the mechanisms causing loss of light intensity underwater:

- A. projected light outward scattered
- B. projected light attenuated
- C. projected light backscattered
- D. reflected light attenuated
- E. reflected light small angle forward scattered
- F. reflected light outward scattered

5.3 Video survey design

The design process presented here follows the concepts of axiomatic design and is split into three sub design processes, see Table 5.1. The design described here starts by compiling the instrument suite and proceeds to the data acquisition plan based on both the chosen instruments and the operational parameters. The data processing pipeline phase depends on the instruments used and the data acquisition plan. “Processing pipeline” is a term for the sequence of steps performed refining raw data to usable end products. If the result fails to meet the initial survey requirements, the process has to be iterated. In the second design iteration the

survey requirements has to be reviewed. The functional requirements or design constraints can be altered to try to make it possible to reach the design goals. The design of instrument suite, acquisition plan and data processing pipeline is then repeated.

Table 5.1 Design relation between sensor suite, data acquisition and data processing illustrated.

FR \ DP	Image quality	Survey pattern	Procedures for video and geo-data
Image and light configuration	X		
Acquisition plan	X	X	
Processing pipeline	X	X	X

To ensure that the survey results in the expected data quality the objective of the survey should be identified early in the planning. It is necessary to decide which variables should be measured/mapped (e.g. taxa, sediments, abundance and biodiversity at different variables). A survey plan should be established where the objective of the survey is stated and the site is described together with the prior knowledge of the survey area. Operational factors like expected weather and current conditions should be explained. The survey plan should include a plan for vessel, vehicle, equipment, crew and required crew qualification for the operation.

Operational conditions and constraints should be identified in the planning phase. Factors like expected sea state, current, depth, ship traffic, etc. should be clarified. Marine operations are often resource-demanding and the availability of vessel, ROV, equipment and personnel demands are reasonable to clarify before commencing the survey design. If there are special motives for the survey like seabed classification, the ROV trajectory must be designed to contain sufficient data to allow statistical analysis. The trajectory containing the data sample must then be repeated at least three times.

5.3.1 Sensor suite

The most important components of the sensor suite for ROV-based video surveys are cameras and light sources. The system should provide clear images of both details and overview of the scene. The products generated from the sensors should match the scope of the survey and the best result is achieved when the illumination is optimized for sea conditions and the image sensor utilised. For biological surveys it is often necessary to have some possibility to measure scale in the image.

Cameras

The choice of camera will be a compromise since the perfect all-round camera does not exist. The camera characteristics determining the quality of the video imagery are: focus, contrast, light sensitivity, field of view and resolution. Most high resolution cameras with high colour rendition have low light sensitivity. Thus it is beneficial to have cameras suitable for different applications mounted on the ROV. The most basic needs are covered by two cameras, one low-light wide-angle camera for search, navigation and overview imagery and one low noise, high quality zoom camera to identify details. For the vehicle to comply with observation class ROV in U-102 (NORSOK 2003), it must be possible to observe at least two video lines simultaneously.

The focus capability of a camera is controlled by the quality of optical objectives, image processing hardware and software. The depth of field is determined by the camera aperture opening. Larger aperture means that the camera is catching more light, but the depth of field is reduced, narrowing the focus area. ROV cameras come with manual focus, auto-focus or fixed focus modes. Manual focus is used on advanced cameras and requires an operator to control the camera during filming, and have the best potential for sharp images. Using auto-focus the operator is unnecessary, but there is a risk that the camera is unable to find focus or focuses on the wrong targets. For plain wide-angle over view and navigation cameras fixed focus is sufficient.

The camera image contrast is controlled by the MTF (Modular Transfer Function) (Kongsberg 1993). MTF expresses the contrast measured in two nearby pixels. A camera with low MTF will have low contrast and often blurred images. The contrast level is not only dependent of the camera, but also the previously discussed backscatter resulting from optical properties of seawater and its optically active components.

In ROV applications, high light sensitivity is beneficial since it will give better viewing range. The light sensitivity of a camera is generally determined by the size of the image sensor and the image signal amplification. The image sensor is either a CCD-chip or in more recent systems a CMOS (Complimentary Metal-Oxide Semiconductor) sensor. A large image sensor usually results in better light sensitivity. High signal amplification results in better light sensitivity. In low light situations, the signal from the image sensor experience low signal, resulting in low signal to noise ration and noisy images. The demand for light sensitivity depends on the application of the video. For ROV navigation a camera with high light sensitivity is sought (e.g. 10^{-3} lux). The inherent reduced image quality can often be accepted. However for e.g. taxonomy applications the image quality cannot be compromised and one usually has to settle for a lower light sensitivity (e.g. 5 lux).

The field of view for an ROV camera can be divided into three levels; wide, medium and narrow. The field of view does not relate to the distance from camera to target, but the viewing angle controlled by the camera zoom. The wide angle is used to get an overview of the scene and in coral research provide an impression of the density

of the coral colony, the present morphological variants and the associated fauna. Medium field-of-view is used to observe the type of substrate the colony is based on and smaller taxa will be revealed. Narrow field-of-view and closed up images are produced by zoom cameras and are used to observe biological details (Etnoyer, Cairns et al. 2006).

The resolution of video imagery has been measured in lines, but the terminology from digital imagery using pixels is becoming common also for video. Commercial standard definition cameras have from 300 to 570 horizontal lines. They produce images for either the PAL (Phase Alternating Line) video standard (625 lines and 25 frames per second) or the NTSC (National Television Steering Committee) video standard (525 lines and 30 frames per second). In the last few years various HD (High Definition) formats have emerged. Due to the commercialisation of HDTV (High Definition Television), cameras and recorders with higher resolution have become more available. Various HD formats exist ranging from 720 lines to 1080 lines.

Light sources

For artificial light sources in an ROV scene there are three important variables: light intensity, spectral distribution, and light patterns produced by the reflector and lenses (Jaffe 1999). Three main groups of light sources available: incandescent (e.g. halogen), HID (High Intensity Discharge), and LED (Light Emitting Diode) lamps. The most common light source is the incandescent light bulb in which electric current is lead through a tungsten filament. The filament heats up and emits light when the electric current is applied. In halogen lights the light bulb is filled with an inert gas and a small amount of halogen. Incandescent light sources are usually robust and reliable. A 250 W halogen lamp is specified to put 4500 lumens in the water (DSPL 2002). In HID light an arc between tungsten electrodes is ignited inside a gas filled bulb. When the arc is lit it produces heat which vaporizes a mixture of salts forming plasma inside the bulb. The vaporized salts contribute significantly to the efficiency in the process. HID lights require a control system to ignite and maintain the arc during operation; this system is often called the ballast. A typical HID light source of 150 W is capable of producing 12000 Lumens of light (OSRAM 2008). Lately LED lights have entered underwater lighting. LED can only be produce in small units. To come around this limitation, LED lights for ROV have arrays of multiple diodes. LED has high efficiency, and a commercially available unit emits 2400 Lumens from only 44 W of electrical power (DSPL 2008).

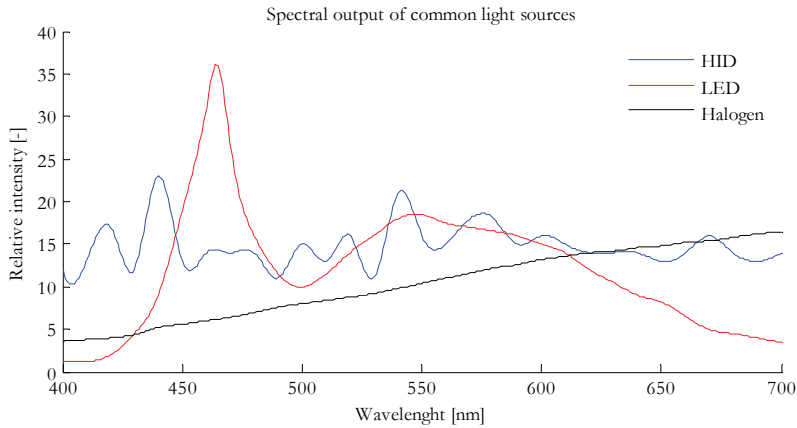


Figure 5.2 Comparison of light spectra for LED, HID and halogen light. Data are collected from (OSRAM 2008), (DSPL 2008) and (Gray 2004).

The spectral distribution of a light source is important due to the spectrally dependency of the light absorption properties of seawater, Figure 5.3. HID light sources are usually beneficial in underwater applications since they output more light in a spectral band where seawater normally have low absorption, Figure 5.2. Incandescent light sources like halogen emit more power in the red part of the spectrum where the seawater light attenuation is higher. Incandescent light sources have an unfortunate spectral distribution in seawater and are less efficient than HID and LED.

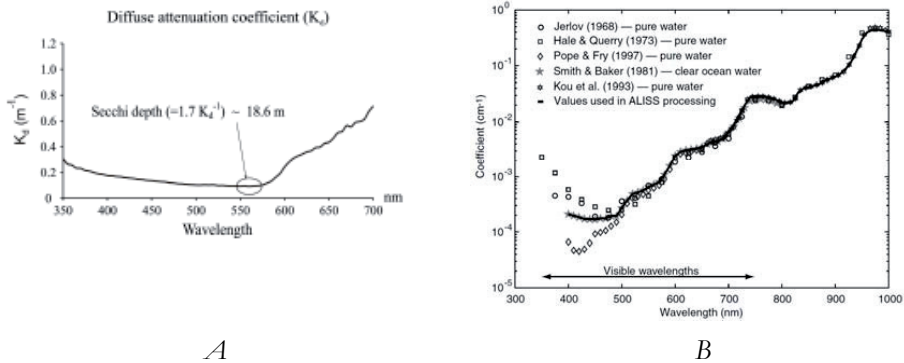


Figure 5.3 A) Diffuse spectral attenuation coefficient for Spitsbergen coastal seawater (400-700 nm m^{-1}) Ny-Ålesund, Svalbard in May 2004 (Volent, Johnsen et al. 2007). B) Spectral attenuation coefficient of pure water (White, Chave et al. 2002).

The light patterns in video imagery are directly dependent of the seabed altitude, positions of light sources and cameras, the seawater turbidity and light reflector and glasses. High seabed altitude enlarges the visible area but increases the potential for light attenuation and scattering and then reduces image quality. The contrast of the imagery will be reduced by high levels of backscattered light. In general the light

reflectors should be wide enough to illuminate the field of view for the camera. But wide light cones increases the common volume of the light sources and the camera and thus the backscattered light. An effective way to reduce the common volume of the light sources and the camera is to increase the separation between light and camera, see Figure 5.4. This separation can however be overdone. If the visibility is good the video images are less sensitive to camera and light geometry and common volumes of camera field of view and light cones. In high turbidity conditions minimization of the common volume is more essential, but one can use the backscatter effect to an advantage. Directing two narrow light beams just out the field of view light will be scattered out of the light cones and this scattered light will illuminate the scene (Kongsberg 1998).

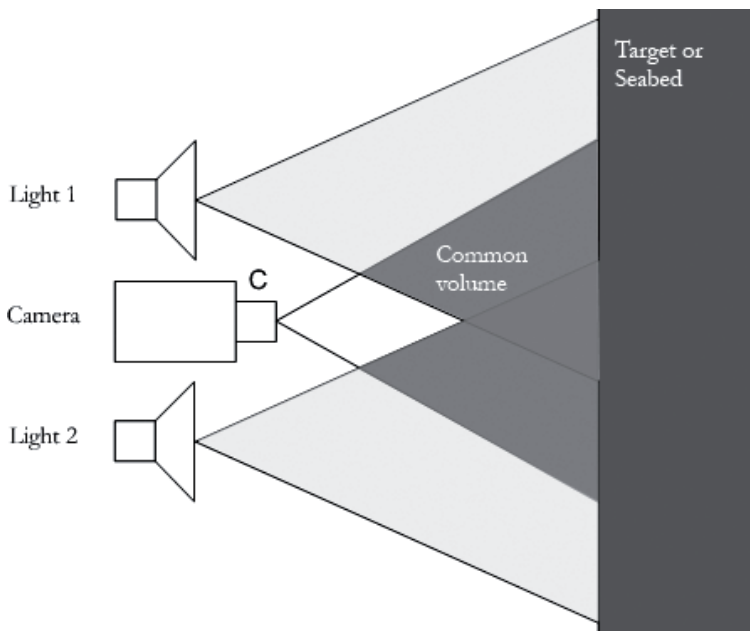


Figure 5.4 Illustration of common volumes for camera and lights sources (Jaffe 1990)

Scaling devices

To estimate the dimension of the objects seen on the video it is necessary to have some sort of size/distance measuring tool on the ROV since the video does not provide any depth vision. The simple variant is a meter scale placed in the picture close to the seabed or object of interest. A more convenient way to solve this issue is put two or more parallel lasers on the ROV making two dots with a known distance on the images. For orthogonally mounted cameras, the area covered can be calculated from field of view and measurements of the seabed altitude.

Recorders

The video signal is usually fed to a computer capture card, where it is digitized and stored on a hard disk. There is wide variety of formats available for digital video; the most common being avi and mpeg. It is important that the video is stored on a

format which can be played with generic video software and that the codecs (Coder/DECoder) applied are free and openly available. The resolution of the video should not be lower than that of the source signal, i.e. SD (Standard Definition) video should be recorded on 720 by 576 pixels. The data compression should be sufficient for efficient storage, but should not reduce quality and produce image artefacts. When choosing image resolution and compression parameters one should bear in mind that video clips can always be downgraded later for storage, but the opposite is impossible. A normal bit-stream for video with sufficient quality is 1 – 3 Mbps, which results in 450 - 1350 MB per hour. The recording system should also contain a system to associate metadata like time, position, ROV heading, and ROV depth with the video. The data can be edited and the overlay view can be switched on and off depending on the usage of the video. Examples of such systems are MAPIX²⁰ and Visual Soft²¹ (Riemersma 2004).

5.3.2 Data acquisition plan

When planning a survey track, the area coverage is derived from ROV survey speed, line spacing and survey pattern. The water quality, current speed, camera and light properties dictate the survey pattern. In eq. (5.1) A represents the area covered, v is the ROV velocity, t denotes time and the swath width is w .

$$A = v \cdot t \cdot w \quad (5.1)$$

The ROV speed is causing drag forces on the vehicle and the cable. The cable drag is proportional to the cable length (i.e. water depth), and hence limit the ROV velocity at large depth, see discussion in section “3.2 ROV Minerva”. For observation ROV’s survey velocities exceeding 1 knot are rare at depths where cold-water corals are found. For WROV’s the velocity can reach 3 knots. To ensure homogenous coverage of the area parallel lines are recommended for searching unknown areas, see Figure 5.5.a. The line spacing will represent the trade-off between area coverage and data resolution and must be adjusted considering the size of the colonies searched. If the seabed coverage shall be 100% and all individuals shall be mapped regardless of size the line spacing depends on the seawater conditions and the hardware used, still a line spacing of 3 meters is usually applied. If the search target is coral colonies larger than e.g. twenty meters, the line spacing is adjusted accordingly. The direction of the grid lines should be chosen parallel to the bathymetry contour lines if the terrain is rugged. Grid pattern have limited value in extreme topography like vertical drop offs.

If statistical analysis should be applied to the video, replicate survey lines may be necessary. When planning replicate survey lines, information of the planned processing is necessary. If one specific habitat, like stony corals, is the target for the

²⁰ MAPIX, Edinburgh, UK

²¹ Visaul Soft, Aberdeen, UK

analysis, one must ensure sufficient replicate survey lines within the coral reef. This naturally requires some prior knowledge of the site.

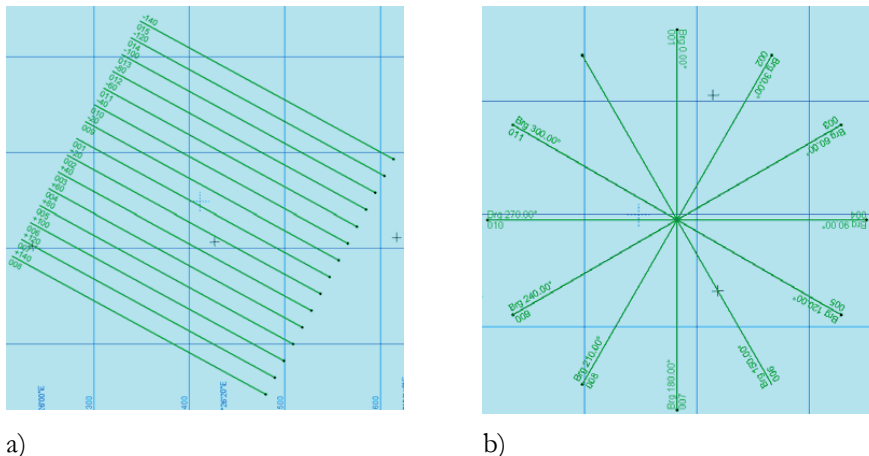


Figure 5.5 Examples of survey patterns. Grid lines and a star pattern are seen.

Situation 1 – grid lines – 3 meter line spacing

The seabed is searched with 100% coverage, three meter line spacing and surveying speed of one knot. The survey efficiency is 5600 m²h⁻¹. That corresponds to a square box approximately 75 by 75 meters per hour.

Situation 2 – grid lines – 20 meter line spacing

Searching the seabed with 3 meter swath width, 20 meter line spacing and surveying at 1 knot; survey efficiency is 37000 m²h⁻¹. The area coverage is then fifteen percent and approximately 190 by 190 meters are covered every hour. Theoretically all objects larger than seventeen meters are then found.

Situation 3 – star pattern

In situations where the coral colony is known and the aim of the survey is to document the zonation of the area, a star shaped survey pattern could be suitable (Lekkerkerk, van der Velden et al. 2006), see Figure 5.5.b. Since living corals often are surrounded by dead corals and coral rubble the star pattern is efficient if the centre of the pattern is located in the living part of the colony. If the search area is 200 meters in diameter and one line is placed for every 30° in the circle, the total line distance is 1460 meters. Using three meters swath width the area covered is 4400 m² of a total of 31000 m² which represents an area coverage of fourteen percent, comparable to the numbers found in example situation 2. There can however be operational challenges associated with star pattern surveys. At sea there is often a dominating direction of current and wind. Using grid lines, the direction of the lines can be adjusted according to the conditions, but for a star shaped survey pattern, the ROV and the vessel have to be able to manoeuvre in all directions.

5.3.3 Processing and interpretation

The design of the data processing pipeline depends on the instrument suite and the data acquisition plan and can only be completed subsequently to these. Cameras, lights sources, geo-referencing and video recorders form the instrument suite for video surveys. The processing pipeline contains online processing procedures, offline processing procedures, guidelines for data products, guidelines for data interpretation, strategy on data management, and a plan for reporting and quality control.

There are several software systems specially developed for handling underwater scientific underwater video. ADELIE is developed by IFRMER (IFREMER 2010). ADELIE can be used to geo-reference video imagery and for GIS analysis of video. With this functionality theme maps also including data like bathymetry can be produced. There is also a video-mosaic function in the ADELIE software package. OFOP (Ocean Floor Observation Protocol) is an alternative software package developed for biological application of ROV imagery (Huetten and Greinert 2008). This system can be used to process video and edit video, e.g. adjust time offsets, merge sensor- or navigation data into the video data, or to produce theme maps for easier interpretation. The main motivation for the OFOP was to enhance navigation and logging during scientific cruises. The system is now extended to also include tools for mission planning and data management.

Online

Online processing of the video is normally done by event marking of every interesting observation with time, position, observation category and comments. Typical events are observation of mega fauna, changes in sediments and occurrence of corals. Continuous control of data recorders and image quality is an obvious part on the online operations.

Offline

The time required to analyze the information from a video survey depends inherently of the goals for the survey, but a useful rule of thumb is that two or three times the duration of the raw video recording is necessary to process the video. For some projects the amount of video becomes too large and processing too time consuming. Then the video has to be sub sampled by choosing video sections either randomly or of particularly interesting areas or objects of interest. Some attempts of automated processing have emerged (Edgington, Cline et al. 2006), but taxonomy is complicated and automated video processing and biological classification will only be applicable to special surveys also for the foreseeable future. One variant of automated processing is the creation of video-mosaics (Vincent, Pessel et al. 2003). Video mosaics have many of the same advantages as photo-mosaics discussed in chapter 9.

Using digital video the geo-tags and other metadata can be post processed for e.g. datum, sensor offsets, etc, opposed to conventional video tapes where video overlay

systems burn the navigation information into the video image e.g. Vigra by Options²². The navigation data is common for all video channels and with the present digital video processing solutions it is convenient to search in the data set for all video channels simultaneously. The geo-tags can be processed as the described in the navigation section “4.4 Processing”.

Data interpretation

Events will be created according to an event scheme. One can use an existing set of events and event categories and register observations accordingly (top-bottom approach), or one can create the event list and event categories from the observations (bottom-top) (Davies, Baxter et al. 2001). The former is best suited when surveys should be compared, but requires specific characteristic species and key physical parameters. When an area is classified to a known classification scheme like the EUNIS-system (European Nature Information System) (Davies, Moss et al. 2004), a top-down approach analysing the events are necessary. When maximum information yield from a video survey is required the latter approach is best suited. With the bottom-top approach it is not necessary to ignore observations falling outside the event categories. To obtain quantitative information from a survey analysed by the bottom-up approach a large sample and statistical analysis is necessary.

Data products

Geo-referenced digital video is also easy to include in a GIS (Geographic Information System) database. For GIS analysis both video and events can be used to produce theme maps including data from previous surveys from the same area. A database of geo-reference video increases the usability of the video since the data can be effectively compared to other data of the area.

²² Options AS, Stavanger, Norway

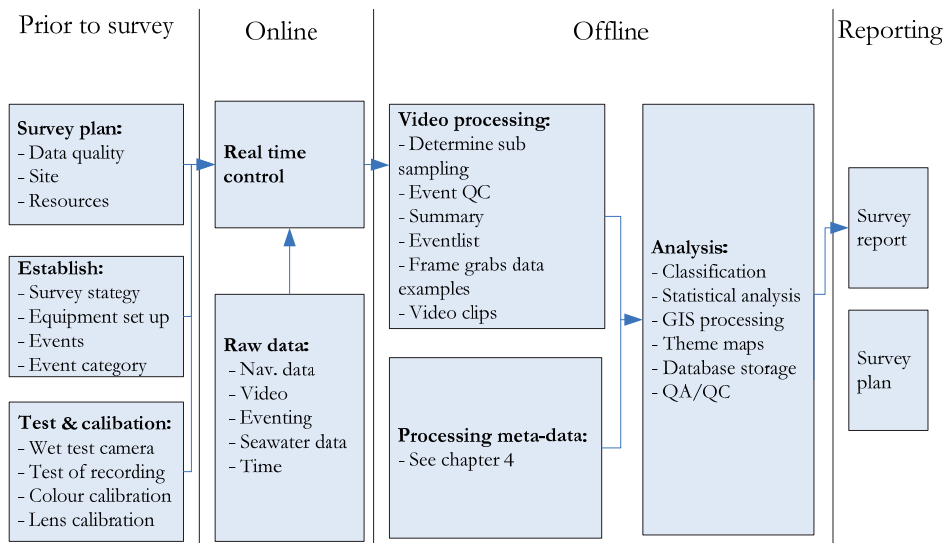


Figure 5.6 Video survey processing workflow from planning of an operation to the reporting of the findings.

5.3.4 Data management

When the images are produced on the ROV they need to be transferred to the surface where they are stored. Previously video storage was based on magnet tapes on formats like VHS (Video Home System), DV (Digital Video), DVCAM, Hi8, etc. These tape based systems are now being replaced by digital video on hard disk recording systems. The benefits of changing to digital recording and storage are significant: the storage cost is reduced, archiving is simpler, and the video can be copied without loss of quality. Digital video can easily be included in GIS and the video can be viewed together with other types of geo-referenced survey data to enhance interpretation. The processes controlling the quality of the digital video information apart from the raw video signal are: recording, processing and archiving (Riemersma 2004).

As Table 5.2 shows, the acquisition cost for video storage medium is insignificant. The total cost including acquisition, operation and data maintenance should be evaluated when deciding on video management for a project. CD (Compact Disc) and DVD (Digital Versatile Disc) storage is cheap but inconvenient because it is time consuming to make copies and back-up since it usually becomes a large number of units to handle. DLT-tapes (Digital Linear Tape) have larger storage capacity but the data access is inconvenient as the tape-drives are slow. Hard drives are convenient as they can store many hours per unit and they are easily searchable and accessible. To offer effective archiving the disks should be placed in a NAS (Network Attached Storage) which can handle many disks and provide back-up service to reduce the risk of data loss. A NAS can also be accessible from the

computer network enabling multiple users to easily access the data and allows the data to be included in a GIS database.

Table 5.2 Storage mediums and price efficiency for video records

Type	Storage (Gb)	Price (NOK/Gb) ²³
SVHS	3	7
CD	0.7	1.4
DVD	4.7	1.1
DLT	40	4.1
HD (Hard Drive)	500	1.5
NAS	2000	3.5

The media's sustainability to time should also be considered. CD and DVD storage last ten to twenty years before the information is degraded or lost. The time horizon for magnetic tapes (SVHS (Super-VHS) and DLT) and magnetic discs are in the same order. Therefore a procedure for backing up data and preserving them for the future should be established.

5.4 Video survey standards

Video surveys can be performed in many ways and the imagery is usually qualitative. To increase the value of video surveys and to work towards quantitative results several attempts have been made to normalize the survey parameters to make separate surveys comparable. This section gives a brief overview of three standards or guidelines for biological video surveys; a Norwegian national standard, a British guideline by JNCC and (Joint Nature Conservation Committee) an American guideline by NOAA (National Oceanic and Atmospheric Administration). The standards provide useful advices for planning, performing and analyzing video surveys.

5.4.1 Standards Norway

Standards Norway have developed a national standard for visual marine deepwater biology surveys (Standards-Norway 2009) for usage in marine resource management. The basis for the standard are situations where a specific area is investigated e.g. prior to subsea construction work. In such surveys one will under-sample, e.g. collect video from one transect and assume that the seabed observed is representative for the area. Researchers are usually not restricted to a confined area but many aspects of this standard regarding categorization of surveys, organization of survey, quality of position and imaging and data analysis are relevant not only in resource management but also in research. For positioning Standards Norway relies on S-44 (IHO 2008). Three types of surveys are defined in the standard by Standards Norway:

- 1) Informative investigations

²³ Prices pr 02-02-08

- 2) Biological surveys
- 3) Trend analyses

In the informative investigation the biology in terms of habitats, dominant species and type of substrate are recorded. This kind of survey is typically performed as initial and preliminary studies. The ROV should not run faster than 3 knots and not higher than 4 meters seabed altitude. The standard deviation for the position accuracy should not exceed 20 meters + 5% of depth.

For biological surveys the distribution of species is described and taxa should be identified and enumerated. The investigation should be performed with quantitative and semi-quantitative methods. The requirements for speed and seabed altitude are lowered to 1 knot and 3 meter. The allowed standard deviations for position measurements are 5 meters plus 5% of the depth.

To perform trend analysis the standard requires ability to relocate and revisit specific individuals. Trend analyses can be used e.g. close to industrial installations or in other areas where the conditions and the present fauna might change. At least three parallel transects should be run and they should be at least 200 meters long.

The Norwegian Standard sets few specific requirements for the video equipment. The seabed resolution shall be 5 cm² per pixel for informative investigations, and 0.5 cm² for biological surveys and trend analyses. An image of 480 by 600 pixel resolution can then cover no more than 24 by 30 meters of seabed for informative investigations and no more than 2.4 by 3 meters of seabed for biological surveys and trend analyses. To cover an area of 24 by 30 meters in one image frame is however not realistic with the present equipment due to the visibility in seawater.

5.4.2 Marine Monitoring Handbook

The Marine Monitoring handbook was developed during the EU-project “UK Marine Special Areas of Conservation” (Davies, Baxter et al. 2001). The project ran 1996 – 2001. The procedural guideline for ROV surveys is reproduced in “*Review of standards and protocols for seabed habitat mapping*” published by the EU-project MESH (Mapping European Seabed Habitats) starting 2004 (White, Mitchell et al. 2007).

The Marine Monitoring Handbook aims to provide recommendations for “Descriptive and quantitative surveys using remotely operated vehicles”. Two types of surveys are described; descriptive-, and quantitative ROV surveys. In the descriptive ROV surveys the species are recorded according to SACFOR (Super-abundant, Abundant, Common, Frequent, Occasional and Rare). Before the survey starts, a survey route and a list of habitats should be prepared. Preferably the survey should be part of a monitoring programme. For quantitative ROV survey the findings should be enumerated. The handbook suggests counting of species either along a predefined track, pr covered area or pr time. There are some challenges to counting along a track or pr area. Depending on the ROV and the survey conditions it can be challenging to keep constant velocity and seabed altitude. Constant seabed altitude is essential to provide image area coverage constant. The handbook

emphasise the importance of scaling devices and recording of pitch, roll and altitude information. It is suggested to use time-count if it is difficult to keep constant velocity and altitude. Another proposal is to put a line physically on the seabed and follow the line with the ROV and then count all specimens within a predetermined distance from the line.

5.4.3 MESH

MESH (Mapping European Seabed Habitats) is a habitat mapping method program. The publications on underwater video methodology are fairly general, but one must keep in mind the MESH objective considering the MESH guidelines and reviews.

Recommended Operation Guidelines (ROG) for underwater video and photographic imaging techniques

The MESH project has developed these guidelines to ensure that a consistent procedure is followed when collecting video and that the video is accompanied by relevant metadata including reliable geo-referencing, (Coggan, Mitchell et al. 2007). The ROG considers the practical side of video collection from sled, divers and ROVs.

A protocol for system test and verification which gives useful practical hints about video signal configuration, time synchronization, video overlay setup, and light mounting and alignment. The ROG's provide practical advices for field records, video overlay and operational procedures for deployments, video observations and recovery. For quality control it is recommended that the field record is confirmed, the integrity of the video records and the metadata files are checked. Cross checks for time stamps and geo-tags are also proposed. Two video recording platforms are recommended. A media log to catalogue video and metadata into a database is suggested. The MESH ROG's provide few advices on data processing and interpretation.

Review of standards and protocols

The MESH group has developed a review of standard and protocols relevant to habitat mapping in general. A chapter in the MESH review is dedicated to underwater video surveys. The review does not only provide a review but also many key points to video acquisition and interpretation. It is claimed that the main challenge at this point is to develop tools for analysis of video records integration of video records to other data types.

For video analysis MESH (White, Mitchell et al. 2007) suggests using the concepts qualitative, semi-quantitative and quantitative analysis. For qualitative analysis the present species are registered together with the present habitats and sediment types. It should be possible to classify habitats to level three or four in the EUNIS (European Nature Information System) system (Davies, Moss et al. 2004) by qualitative analysis according to this MESH review of standards and protocols (Coggan, Populus et al. 2007). When semi-quantitative analysis is performed the species density is registered according to the SACFOR notion (Davies, Baxter et al. 2001). The present biology can be registered as estimated average density, or by time

counts. EUNIS level five should be obtainable. For quantitative survey all specimen are directly counted before the observations are processed.

The MESH review of relevant standards and protocols mentions the following publications as interesting:

- ISO “Water quality – guidance for quantitative sampling and sample processing of marine soft bottom macro fauna” (ISO 2007)
- Marine monitoring handbook (Davies, Baxter et al. 2001)
- ICES BEWG guidelines (ICES 2004)

MESH Video working group report

A working group in the MESH system has published a report on collection, analysis and interpretation of video for habitat classification (White, Mitchell et al. 2007). The main body of the work presented concerns statistical analyses of video observations. Five variants of statistical analyses are described:

1. Descriptive analyses
2. Distribution / Goodness of fit
3. Hypothesis testing
4. Investigations of correlations
5. Multivariate analyses

First of all the variables to investigate must be determined. That can be variables like gorgonians per square meter. Applying descriptive analysis statistical values like mean, median, min/max values, percentiles and standard deviations are calculated for the investigated variable. To compute any statistical value there must be replicas of the observation. The report recommends three to five sample replicas. Sample replicas can be created by repeating a transect run or by sub sampling transects and treat every subsample as a replica. A distribution analysis can be applied to quantify the biological patchiness in the samples. Running hypothesis test the null hypothesis is compared to an alternative hypothesis. This can be used for comparison of means. Correlation investigations are typically used to investigate relations between species or relations between species and environmental variable. The outcome of the statistical analysis is often used to classify the seabed habitat, either to a recognized scheme like EUNIS or a user specified scheme.

5.4.4 Deep-sea Coral Collection Protocols

In 2006 NOAA developed a deep-sea coral collection protocol. This text also contains a guideline to video documentation of corals but does not intend to represent a standardization of video surveys for cold-water corals. Simple guidelines for equipments selection, data management and filming are provided. Vertical line transects are recommended for examination of large structures, while conventional survey grids with parallel lines are proposed for more systematic investigations. The

publication suggests radial or star shaped survey patterns for small features (Etnoyer, Cairns et al. 2006).

5.4.5 EUNIS

EUNIS is a database of European nature habitats (Davies, Moss et al. 2004). The system also contains an extensive system for classification of habitats. The habitats are arranged in a hierarchy. Parameters like altitude zone, depth zone, geomorphology, substrate and characteristic species are used when habitats are classified. Each habitat in the system has an established definition.

Table 5.3 The EUNIS habitat hierarchy path leading to Deep-sea communities of corals.

Level 1	Level 2 (Marine habitats)	Level 3 (Deep-sea bed)	Level 4 (Bioherms)
A. Marine habitats	A1. Littoral rock and other hard substrata	A.6.1 Rock and artificial substrata	A.6.6.1 Communities of deep-sea corals
B. Coastal habitats	A2. Littoral sediment	A.6.2 Mixed substrata	A.6.6.2 Deep-sea sponge aggregations
C. Inland surface waters	A3. Infralittoral rock and other hard substrata	A.6.3 Sand	
D. Mires, bogs and fens	A4. Circalittoral rock and other hard substrata	A.6.4 Muddy sand	
E. Grassland and lands dominated by forbs, mosses and lichens	A5. Sublittoral sediment	A.6.5 Muddy mud	
F. Heathland, scrubs and tundra	A6. Deep-sea bed	A.6.6 Bioherms	
G. Woodland, forest and other wooded land	A7. Pelagic water column	A.6.7 Raised features	
H. Inland unvegetated and sparsely vegetated habitats	A8. Ice associated marine habitats	A.6.8 Trenches, canyons and slumps of the continental slope	
I. Regularly or recently cultivated agricultural, horticultural and domestic habitats		A.6.9 Vents, seeps, hypoxic and anoxic habitats	
J. Constructed, industrial or other artificial habitats			

5.5 Quality assurance and control

The quality of a video survey should be controlled on all levels from design survey, to data acquisition, data processing and interpretation. For video cameras one should check that they are setup for the colour temperature corresponding to the light sources. If a laser scaling device is applied, the distance and angle of the laser beams should be controlled.

The findings in the video survey should be supported by samplings where that is possible. Some ROV's have samplers and can make samples of biota as an integral part of the survey (Shepherd and Juniper 1997), or grabbing and/or coring can be used to confirm the survey results. The event marking should be done by a person trained in taxonomy of the biota of interest. The observations shall be validated by a person with similar or higher competence. The processing procedure must be documented and included as part of the metadata for the video survey. If other data from the area exists (e.g. side scan sonar data) the findings from the video survey should be compared for confirmation of the results.

5.6 Reporting

The purpose of the report is to present the collected data and show that the predefined survey requirements are met. The report should give a precise description of the survey execution, the findings, processing and possible shortcomings. In addition to the already mentioned survey plan, there shall be produced a survey report after completion of the work. The survey report should be completed immediately after completion of the operation and be suitable to form the basis for further scientific publications. The outline of the report may vary with the application since research tasks are very diverse. In general the outline used in the offshore survey branch (Lekkerkerk, van der Velden et al. 2006) represents a useful framework for a technical report from a survey, also for scientific surveys.

Outline:

1. Introduction
2. Survey requirements
3. Summary of results
4. Detailed results
5. Conclusions

Appendix:

- Appendix A QA/QC
- Appendix B Calibration results
- Appendix C Personnel
- Appendix E Equipment
- Appendix F Methodology

The survey report should contain an introduction which includes the motivation for the survey and the data quality target. The method chapter in the survey report

should describe survey equipment like vessel, ROV, positioning setup, lights and camera. The strategy and the data processing should also be described in the method chapter. The results are summarized in the next chapter with navigation data, survey track, important data examples and a written summary of the survey. Theme maps produced during the GIS analysis should also be included in the result summary. Video frame grabs of observations fit in the detailed results section. These data should be further refined to maps coupling video observations together with positions and other data from the area (e.g. bathymetrical data or side scan images). If the video observations are statistically processed, they make an important part of the result. The data processing tube is illustrated in Figure 5.6.

6 Video survey for *Lophelia pertusa* at the Tautra ridge

6.1 Background

This chapter will present a video survey performed in the Trondheim Fjord in October 2006 using the ROV Minerva and RV Gunnerus. The planning, data acquisition, processing and results will be shown. The survey was conducted to prove or disprove *Lophelia pertusa* occurrence targeted in a side scan sonar data set. In addition to ground-truthing of sonar data all biology is registered qualitatively and compared with the sonar data set to reveal any biology – topography coupling.

6.1.1 The Tautra ridge

The site was the Tautra-ridge (63°35' N Latitude, 10°33' E Longitude) which is a threshold in the middle of Trondheim Fjord, see Figure 6.1. The Tautra ridge starts on the Tautra Island and spans the 6 kilometres across to the Fosen peninsula. The ridge divides two basins of the fjord that are more than 400 meters deep, but the ridge is only 40 meters deep at the shallowest. Towards north the edge is more distinct and there are several pinnacles five to fifteen metres high. The stony corals present here are the shallowest known occurrence of cold-water stony corals. Compared to most known cold-water coral occurrences the site is easy accessible at a distance only ~30 km from the Trondheim harbour. The area is renowned for strong currents and care must be taken to plan surveys to times with low difference between low and high tide.

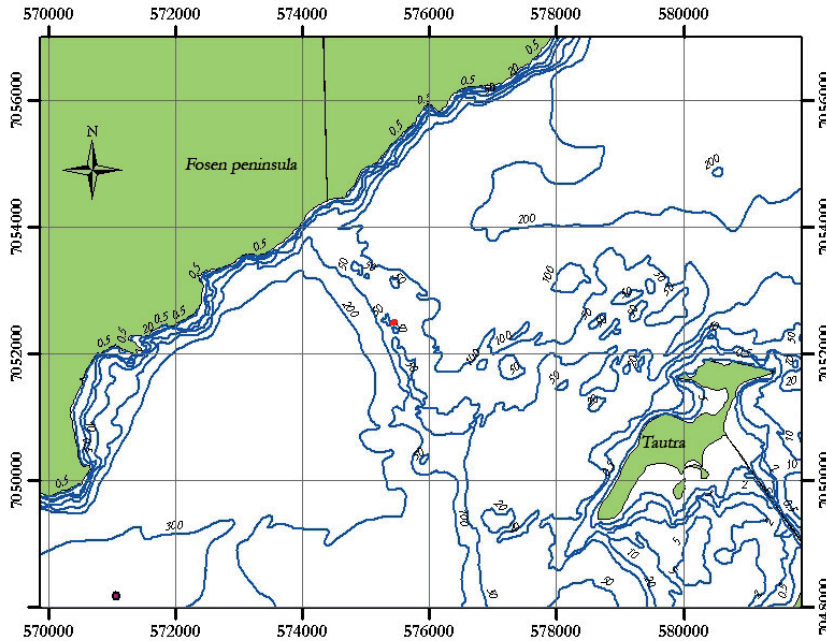


Figure 6.1 The Tautra ridge. Coordinates are UTM WGS84 zone 32N. The site of the video survey is marked with a red dot.

6.1.2 Sonar survey results summarized

The area was mapped with interferometric side scan sonar prior to the video survey. The sonar survey is presented in chapter 8. Six coral areas were observed seen as a rough pattern in Figure 6.2. The coral occurrences are marked Area 1 to Area 6 in the figure. In the northernmost area (Area 1) the sonar data indicated that seabed was covered with stony corals. Close to area 1 a low coral covered ridge in west to east direction is discovered (Area 2). Further south indications of small coral colonies are seen on two local tops on the ridge (Area 3 and Area 4). In the south-east corner of the sonar survey area two low east-to-west ridges are detected, apparently with corals (Area 5 and Area 6).

6.2 Method

6.2.1 Survey design

For the Tautra video survey, only a short time-slot was available and 900 meters of survey lines were planned. The survey line started in the north-west corner of the sonar survey area and went toward south-south-west. The seabed altitude was determined by the seawater visibility and camera-light setup and varied from 1 meter to 2 meters. Standard ROV cameras were sufficient as the stony coral is characteristic and uncomplicated to recognize. The survey velocity was limited by

the hydrodynamic drag force acting on the ROV and the umbilical, as discussed subsequently.

6.2.2 Hardware setup

During the video survey the vehicle was equipped with four 250 W halogen lights. The camera was wide angle, fixed focus and sensitive to low light. The video was recorded and geo-referenced on an RS100 digital video digital recorder by MAPIX. The ROV-position was also put on an overlay on the video. Navipac maritime survey software by EIVA was used to calculate global positions and to log navigation data from the instrument suite mentioned in section "3 Vessel and vehicle". The variations in speed of sound were compensated for by measuring the speed of sound profile. The profile was applied directly to the USBL system.

6.2.3 Processing

The navigation data was processed according to the procedures outlined in section "4.4 Processing". Data validation was performed and outliers removed. The navigation setup was calibrated prior to the bathymetry survey completed before the video survey.

The biological observations were performed in post process. Based on the observations made online, an event scheme was created, in a so called bottom-up approach. The event scheme is presented in Table 6.1. For hard corals events were created when the habitat changed e.g. from *Lophelia pertusa* to gravel and vice versa. Soft corals were recorded as points. Registration of mega fauna was limited to fish. The events and the geo-referenced video were combined with the bathymetry and sonar data in a GIS database to check the sonar observation against the video results, see Figure 6.2.

Table 6.1 Categories of video events

Category	Hard Coral	Soft Coral	Fish
<i>Sub categories</i>	Entering live <i>Lophelia pertusa</i> area	<i>Paramuricia placomus</i>	Cod <i>Gadus morhua</i>
	Entering dead <i>Lophelia pertusa</i> area	<i>Paragorgia arborea</i>	Pollock <i>Pollachius virens</i>
	Leaving live <i>Lophelia pertusa</i> area	<i>Primnoa resedaeformis</i>	Rockfish <i>Sebastes viviparus</i>
	Leaving dead <i>Lophelia pertusa</i> area	<i>Capnella glomerata</i>	Chimaera <i>Chimera montrosa</i>
	Yellow <i>Lophelia pertusa</i>		Shark <i>Etmopterus spinax</i> <i>Galeus Melastomus</i>
	<i>Lophelia pertusa</i> Lump		

6.3 Video results

The survey lasted for approximately 40 minutes. Approximately 300 meters of the survey line were covered with stony corals and 600 meters of the survey line went over gravel. From the video 77 events were created.

The first coral area observed (Area 1) in Figure 6.2 appears as a carpet of stony coral dominated by white, living *Lophelia pertusa* in the video imagery. But also the yellow morphological variant is seen side by side with the white variant in this area. The soft corals *Paragorgia arborea*, *Paramuricia placomus* and *Primnoa resedaeformis* are present, but the abundance is moderate. In this area Pollock and Rockfish is found in a moderate quantity. The second coral area (Area 2) is smaller and no macro fauna is recorded but white and yellow *Lophelia pertusa*. On the two small local tops (Area 3 and Area 4) on the edge only small lumps of white stony coral is found. In area 4 Rockfish is also observed. The fauna on the ridge visited last (Area 5) is very similar to the fauna found in the first coral area (Area 1) with white and yellow variances of *Lophelia pertusa*, together with species of soft coral and fish. On the gravel seabed separating the coral areas, Pollock (*Pollachius virens*) and small shark species (*Etmopterus spinax*, *Galeus melastomus*) were seen. There are also smaller lumps of living stony coral laying freely on the gravel seabed. These lumps are less than half a meter in diameter.

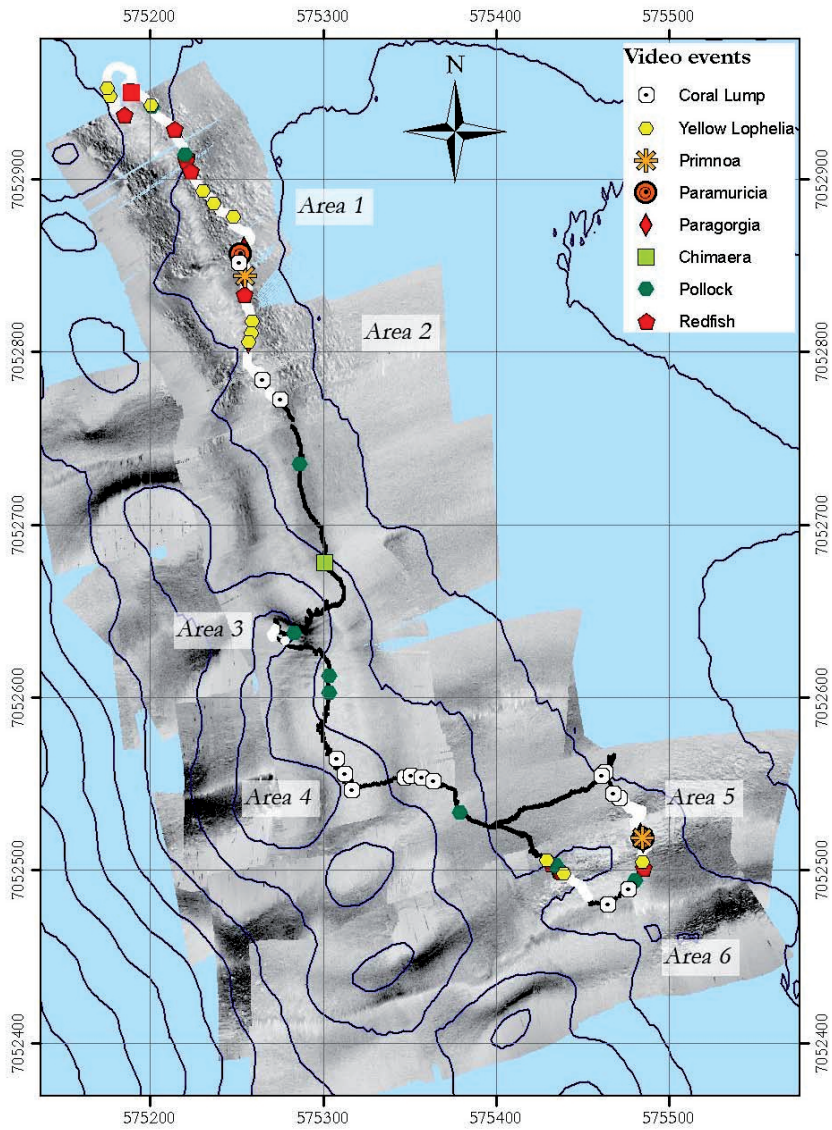


Figure 6.2 The ROV track plotted on top of side scan sonar data.

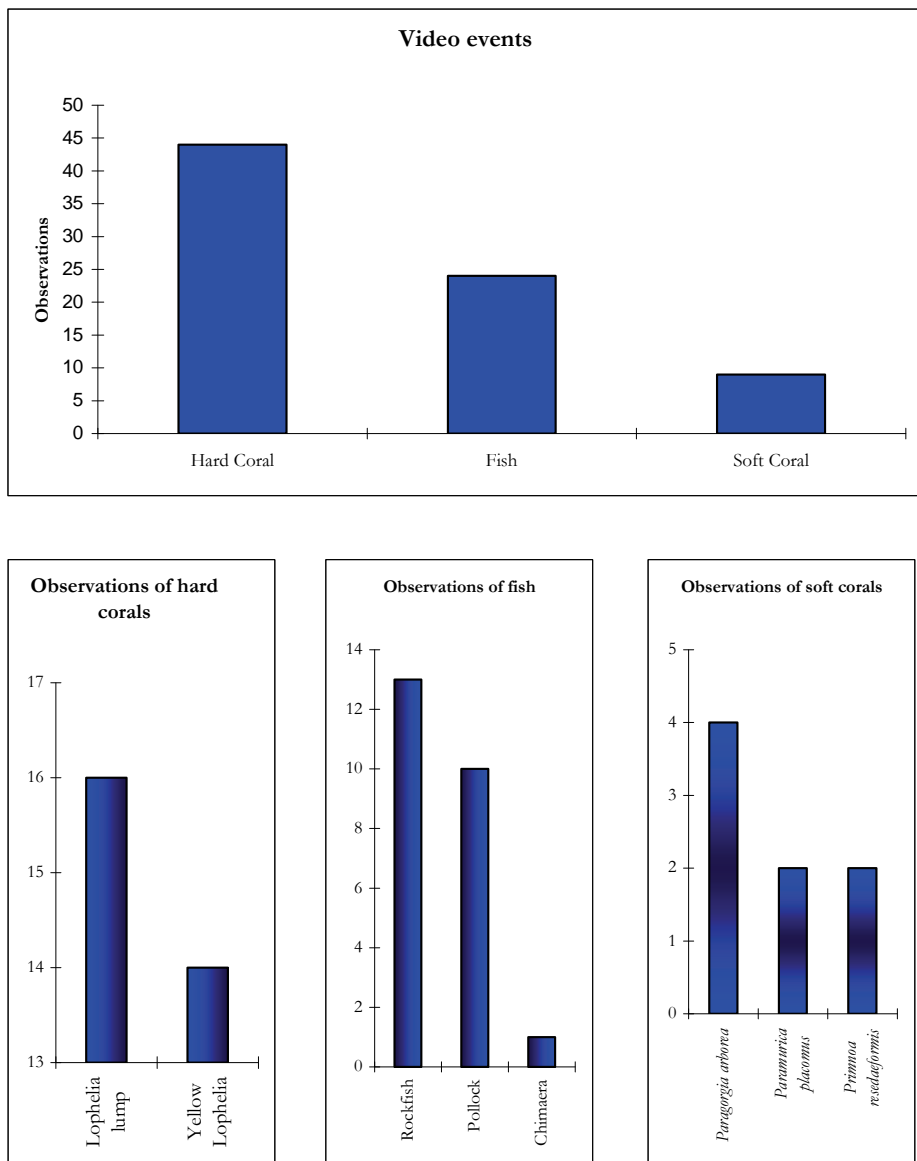


Figure 6.3 Histogram of the video event primary categories

To achieve some information on the geo-bio coupling the events are combined with sonar data and the theme map in Figure 6.2 is produced. The ROV track is plotted on top of sonar imagery acquired with a GeoSwath 500 interferometric side scan sonar mounted on a ROV. Based on the video observations, the ROV-track is plotted in white where the coral colony is covering the seabed. Comparing the white “coral-track” to the sonar imagery in the background we can see a clear correspondence. Frame grabs from the video can be seen in Figure 6.4.



A) *Lophelia pertusa* lump at shallow knoll.



B) School of Rockfish (*Sebastes viviparus*)

C) *Chimaera monstrosa*D) *Paragorgia arborea*

Figure 6.4 Frame grabs from the video showing characteristic species.

The images in Figure 6.4 should ideally be colour corrected. To do such a correction, information of spectral distribution of the light sources, spectral sensitivity of the camera and the spectral light absorption of the water must be known. As an approximation, the standard spectral distribution for halogen light could have been used. However, the spectral response for the camera was not

available. However, the colour rendition was sufficient to distinguish between white *Lophelia pertusa* and coloured *Lophelia pertusa*.

6.4 Discussion

To increase the information outcome of this survey, the observations could have been processed statistically to establish average area coverage for *Lophelia pertusa* and abundance of other taxa. To allow this processing the data body should have been larger. There should have been three duplicate survey lines to calculate maximum, minimum, average and standard deviations for variables like species densities. But in this area the patchiness of the stony coral could alter the statistical results. The patchiness can be dealt with in two ways; 1) large amounts of video can be collected and the calculated values for species densities can be calculated for the entire Tautra-ridge area, and thereby smoothing out the patchiness, or 2) the borders between the different habitat or seabed types can be established and values can be calculated for each seabed type. The latter solution would however provide the best information. To achieve quantitative measures of the distribution of white and yellow *Lophelia pertusa* the video should have been recorded having constant altitude and velocity.

With the present setup with an approximate distance from camera to object of interest of 3 meters, individuals with dimensions down to 5 cm can be identified. To be able to identify smaller specimen better image resolution and contrast are necessary. Resolution could be increased by upgrading the camera-system. HD-quality systems have become accessible the last few years. Light booms could have increased the separation of light and camera which would have reduced the backscattered light and increased image quality.

To further increase the image quality, HID-light could have replaced the halogen lights. HID-light would allow longer viewing range and thereby higher ROV seabed altitude and width of the field of view. To perform measurements of the dimensions of individual specimen parallel laser should have been applied.

The video results consent with the general opinion that stony coral thrive on edges and peaks. We would however expect to find more coral on the very edge of the Tautra ridge. On the more flat areas in the northern part of the survey area we are somewhat surprised to find these corals. Their carpet shape is seldom described in the literature.

For this survey the objective was to confirm targets established using bathymetry sonar and side scan sonar. The sonar observations were confirmed by the video results. No sampling was performed to verify or calibrate the video observations. However, the species recorded are rather characteristic and not easily mistaken in video imagery. According to the Norwegian standard for visual biological seabed investigations (Standards-Norway 2009) this survey would have been classified as an informative investigation. The hardware setup qualifies also for higher level investigations, but the extent of the survey is insufficient for biological surveys or trend analyses.

7 Bathymetry sonar survey

7.1 Introduction

In this section bathymetry sonar is used as a common term for multibeam echosounders and interferometric side scan sonars since both produce bathymetric data. A protocol for detailed seabed topology measurements using bathymetry sonar on ROV will be presented. Survey design, choice and setup of sensor suite, data processing and interpretation, data management, quality control and applicable standards are discussed.

A substantial part of the methodology is adopted from hydrography and offshore branches. In hydrography the primary concern is to create maps for navigational safety of ships. ROV-based bathymetry surveys are rather rare in conventional hydrography, but in commercial offshore operations ROV mounted bathymetry sonars are common practice. The setup is used on site- and route investigations prior to development of seabed installations and pipe laying (Lekkerkerk, van der Velden et al. 2006), (Hovland 2008). But in research the motivations for measuring bathymetry are more diverse. The survey motivation will affect the data quality requirements, the equipment selection, operating routines, processing routines and reporting. For scientific applications bathymetric sonars on underwater vehicles are used in deep waters (Jakuba, Yoerger et al. 2004), (Caress, Thomas et al. 2008). One well known application is the hot vents documented by WHOI (Roman and Singh 2007). Similar use of ROVs and bathymetry sonars has also been presented by IFREMER (Opderbecke, Simeoni et al. 2004).

7.2 The bathymetry survey process

Bathymetry survey systems are complex and consist even in its simplest form of: equipment (sonar, attitude sensors, positioning sensors and speed of sound sensors), data acquisition procedures, processing procedures, and personnel. The bathymetric sonar profiles the seabed by measuring range and angle for multiple points on a line perpendicular to the direction of motion for the sonar transducer, see Figure 7.1. By moving the vehicle and the transducer, a strip of the seabed is ensonified. These seabed points now have coordinates in the transducer-fixed reference. The transducer's global orientation and position is obtained as described in chapter "4 Underwater navigation" and is required to establish absolute coordinates for the seabed data. The level of uncertainty of the resulting bathymetry model is thus directly dependent on the accuracy of the navigation system on the underwater vehicle.

The xyz-points are processed to a surface replicating the seabed topography. In this application the sonar transducer is fitted to the ROV to reduce the operating slant range. The main objective of placing the bathymetric sonar on an ROV is to increase data resolution and precision.

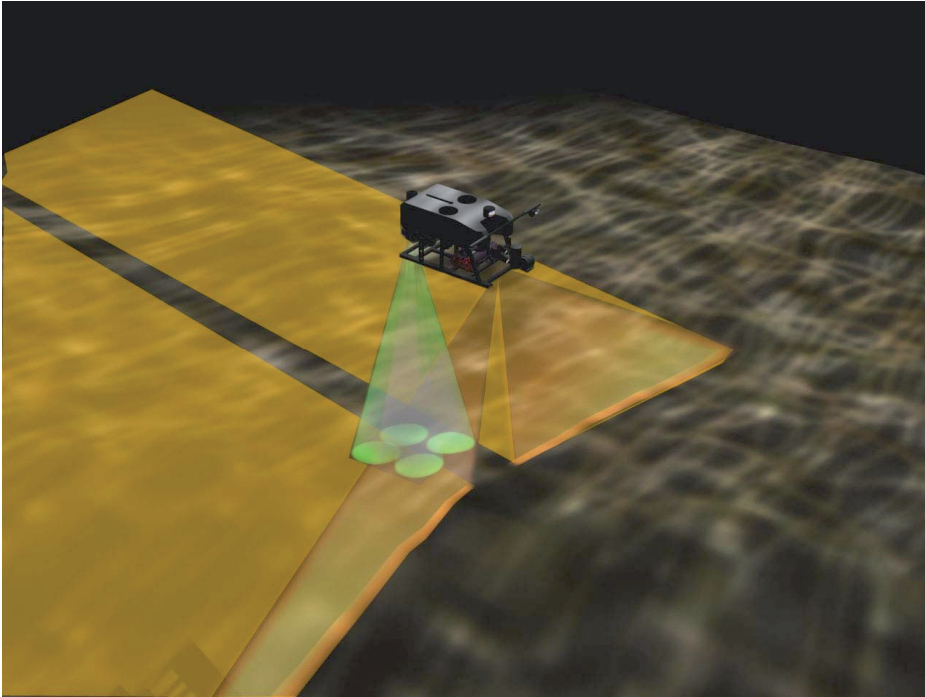


Figure 7.1 Interferometric side scan sonar ROV mounted. The ROV is also fitted with a DVL.

7.2.1 Multibeam echosounders (MBES)

Multibeam echosounders are occasionally termed beam formers to distinguish them from interferometric systems since they physically form acoustic beams, see Figure 7.2. The beams are produced by phase manipulation in transducers arrays, see (Urick 1983) and (Wilson 1988). MBES-systems suited for ROV applications have 200 to 500 discrete beams and produce a data point for each beam on each profile. The positions of the data points are determined by range measurements. The range measurements are determined by the time of flight of the acoustic ping. To identify the seabed in the incoming reflected impulse sonars apply detection algorithms based on amplitude or phase analysis. The angle is determined by the beam forming in the transducer.

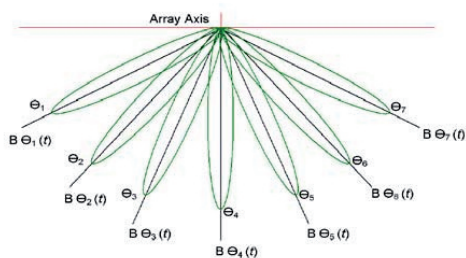


Figure 7.2 Illustration of beams for a beamforming multibeam (L-3-Communications 2000).

Some MBES systems also measure the intensity of the returning ping and store this information as backscatter data. An image somewhat similar to a side scan sonar image can be produced from the backscatter data. The resolution of the MBES backscatter intensity data is however coarser than a side scan sonar image. The returned echo intensity depends on the frequency of the system, the angle of incident and the type of seabed.

7.2.2 Interferometric side scan sonars

Interferometric side scan sonars use two or more receiving arrays for each side or channel. These systems calculate the range by time of flight measurements and determine the direction by phase measurements of the reflected acoustic signal. Existing systems can achieve 0.03° angular resolution (Hiller and Lewis 2004). The range resolution depends on the length of the ping like other sonars and is typically 0.06 m. This concept is not limited by physical beams and up to 40 soundings is achievable per meter slant range. The incoming reflection is continuous from the start to the end of the swath width and this induces noise on the phase angle measurements. The result is larger variation between data points compared to beam formers.

The swath width is larger for interferometric side scan sonar than for MBES. One disadvantage is that these systems like other side scan systems have poor coverage at nadir. Literature also reports limitations in complex structures (Bates and Byham 2001). But it is proven that interferometric systems are capable of detecting features 1 m^3 in dimension (Gostnell 2005) and hence satisfy the highest standards like the special order in S-44. It seems like the larger variation between single data points can be made up for by statistical analysis of the high number of soundings. A major advantage of interferometric side scan sonars is that side scan data are collected simultaneously. Synthetic aperture signal processing is a fledging new technology offering great prospective for data resolution and coverage (Hansen, Olsmo et al. 2005).

7.3 Survey design

The design of a bathymetry survey follows the design pattern established in the section on video surveys. When designing an ROV-based bathymetry survey we

want to plan the instrument suite, the data acquisition and the data processing. This process should result in a *survey plan*. Initially the design constraints like the survey area and the operational resource conditions must be clarified.

7.3.1 Instrument suite configuration

Initially the desired quality of the survey result should be formulated. Again, over-specification will lead to an unnecessarily expensive operation. The data quality prescription will be the background for the choice of instruments. One should bear in mind that it is the complete system consisting of positioning equipment, orientation and attitude sensor, sonar and processing system that should output data quality according to the quality level, not the sonar alone. It is common to establish a model for expected total uncertainty. This is termed propagated error budget and follows the same principles indicated in the error budget shown in the section on navigation (IHO 2008).

In addition to the sonar itself a navigation system is fundamental. Specifying navigation systems for bathymetric surveys are covered in section “4.2.3 Bathymetry sonars”. A speed of sound profiler is also necessary to produce bathymetric data of a certain quality. Navigation sensors are discussed in section 4.1 “Principles of ROV navigation”.

Bathymetric sonars

Finding a suitable instrument for a bathymetry project, the acoustic parameters like range, swath width and data resolution will give an indication whether the result will be satisfactory. Practical consideration like size of transducers, power requirements, data interface and cost will decide if the system can be mounted on an ROV. As a general guide to reading instrument specifications the most important functional requirements and design parameters are given in Table 7.1. There are however a limited number of instruments available. Their strengths and weaknesses make the instrument choices limited.

Table 7.1 Functional requirements and design parameters for bathymetric sonar system.

DP	Swath width	Number of beams	Transducer dimensions	Data and power interface	System Frequency and transducer design
Acquisition efficiency	X				
Data density and data resolution		X			
ROV mountable			X		
ROV operable				X	
Data accuracy					X

Bathymetric sonars suitable for ROV applications usually fall into the category shallow water bathymetry sonars because ROVs have low seabed altitude like a surface vessel on shallow water. Common sonars and some of their key features are listed in Table 7.2.

Table 7.2 Properties of common bathymetric sonars

DP FR	Swath width / footprint	Number of beams	Sonar head dimensions [mm]	Power requirement	Data requirements	Frequency	Range
Kongsberg Maritime EM3002	130°	254	332 x 190		Ethernet	~300 kHz	200 m
Reson ²⁴ Seabat 7125	128°	254	102 x 496 x 131	300 W	1 Gb/s Ethernet	200/400 kHz	
Imagenex Delta-T	120°	120 – 480	195 x 75 x 100	12 W	10 Mb/s Ethernet	260 kHz	100
GeoAcoustics GeoSwath 500	12 x seabed altitude		255 x 110 x 60	50 W	10 Mb/s Ethernet	500 kHz	50

System calibration

The orientation of the attitude sensors and the sonar transducer must be measured and applied in the data acquisition system. A priori offset of the navigation reference frame and the sonar reference frame must be established. Instrument offsets along x-, y- and z-axis can be measured sufficiently accurate with a meter. When these parameters are applied, there are four variables commonly calibrated for. These are:

1. Roll
2. Pitch
3. Heading
4. Latency

Some sonar systems and data acquisition packages have dedicated automatic or semi-automatic calibration procedures. The most common routine is called the patch test and requires a minimum of four lines to be run (Lekkerkerk, van der Velden et al. 2006). Roll calibration is performed running one line in both directions over a flat seabed. Coincident profiles are then compared and the roll offset is identified. To calibrate for pitch offsets the ROV is run in both directions along a line which is perpendicular to a slope. For the data collected on the two runs, the angle of the slope will vary proportionally to the error in pitch angle. To see the yaw error, two parallel lines are run uphill a slope and the error shows up as a

²⁴ Reson, Slangerup, Denmark

discontinuity in the slope. Latency errors occur when there are deviations in the time stamps for the sonar data and the position data. They can be revealed by running two parallel lines perpendicular to a slope. The speed should be different for the two runs, and the latency error will appear as a shift in the profile of the slope in the two runs.

7.3.2 Data acquisition plan

Survey pattern

The data acquisition parameters are planned after the instrument suite is compiled. The data acquisition process depends on the survey area, instrument suite, depth, current, time slot and the ROV velocity capacity which were identified and determined in the previous sequences. The plan shall contain descriptions of the survey lines, the direction of the survey lines, seabed altitude and the line spacing. These variables are adjusted to fulfil the requirements for seabed coverage, overlap and redundant data.

The data overlap between survey lines is important for the data quality control and is decided by swath width and line spacing. When determining seabed altitude, it is important to consider the desired data-density. With a swath angle of 120° and seabed altitude of 30 meters, the swath width is 104 meters. For 240 beams there will in average be a data point for every 0.4 m. Data density higher than 0.4 m is typically desired, since it is commonly used more than 4 data points for every grid point in the processed end product, see Table 7.3.

In commercial offshore surveys a grid size of 0.5 meters is common (Lekkerkerk, van der Velden et al. 2006), (IHO 2008), in scientific surveys one can adjust the grid size to the survey subject. For cold-water coral surveys 0.5 meters grid size is sufficient to show that dimensions and shape of the colony, but insufficient to completely resolve the cauliflower shape of the coral colony structure.

Table 7.3 Swath width, grid size and efficiency calculated for six seabed altitudes with swath angle 120° and 240 beams and survey speed of 0.75 m/s and no overlap.

Seabed altitude	Units	5	10	15	20	30	50
Swath width	m	17.3	34.6	52.0	69.3	103.9	173.2
Grid size	m	0.14	0.29	0.43	0.58	0.87	1.44
Pings in gridbox	-	6	12	17	23	35	58
Efficiency	m ² h ⁻¹	47000	98000	142000	190000	284000	474000

Normally a seabed altitude between 10 and 50 meters are chosen for ROV-based bathymetry surveys. The desired overlap depends on the terrain conditions and quality control requirements. 15 – 50 % overlap is usually a reasonable compromise between efficiency and redundancy. To further increase the quality control a survey line crossing the other lines can be added to the program.

Operational procedures and timeline estimations

A detailed timeline for the data acquisition reduces the project risk. The survey efficiency in area pr unit time can be calculated using eq. (7.1). Assuming the area is mapped flying the ROV in a lawn-mower patter with n lines and o overlap between lines, the coverage, S , in area pr time is given by:

$$S = \frac{(1+(n-1)(1-o)) \cdot 2a \sin(\alpha)v}{n(1+\cos(\alpha))} \tag{7.1}$$

where a denotes seabed altitude, α , denotes swath angle and v is the velocity of the ROV. The swap time for the ROV between survey lines is not included in eq. (7.1). The survey line pattern should preferably be turned along the direction of the current to increase the possibility to keep the ROV heading along the line.

To plan the survey line pattern, line spacing and seabed altitude please refer to section 5.3 “Video survey design” on video surveys and data acquisition planning. A constant seabed altitude results in constant sonar swath width and hence constant overlap between the lines. If the survey lines are turned perpendicular to the survey object, the errors are seen and the data integrity is high.

7.3.3 Processing pipeline

The design of the processing pipeline is presented in the following section. General guidelines for processing and reporting are found in the section on video survey.

Online

The data processing starts with the online data stream. Designing the online section of the processing pipeline, decisions on data storage, online data corrections and quality control routines are determined. The design sequence is indicated in Table 7.4.

Table 7.4 Design of online data processing.

Design Parameters Functional Requirements	Software and hardware configuration for data acquisition	Sensor setup and interface for metadata	Routines and procedures
Data encoding and storage	X		
Online data corrections	X	X	
Online QC	X		X

The DP “*software and hardware for data acquisition*” in Table 7.4 contains the software package for the project together the definition of data formats for processed data, raw sonar data, time tags and raw navigation data. It is also decided how data are stored and what back-up routines are necessary. Both raw data and corrected data should be stored. Corrected data are created for online quality control and raw data should be stored for subsequent offline data processing.

The DP “*Sensor setup and interfaces for metadata*” contains the setup for the data acquisition software package chosen in the previous step. The interfaces to metadata sensors for tide and speed of sound are considered.

Finally a strategy to monitor the data quality online is created in the step labelled “Online QC” in Table 7.4. For online quality control of bathymetry monitoring of data quality measures like GPS DOP values and observation of data is central. Acceptance values should be determined for the available quality measures. The bathymetry data are typically visualized online on so-called waterfall displays. Bathymetry surveys from underwater vehicles require complex instrument setups, and the result must be monitored online to early reveal what can turn out become costly blunders.

Offline data processing

Offline data processing consists of three steps, 1) data validation, 2) data filtering and 3) data correction. The offline data processing is illustrated in Figure 7.3.

Validation

Bathymetry data are validated by checking for unlikely seabed features and by comparing data from different survey lines. Features like slopes and large rocks are informative at this stage.

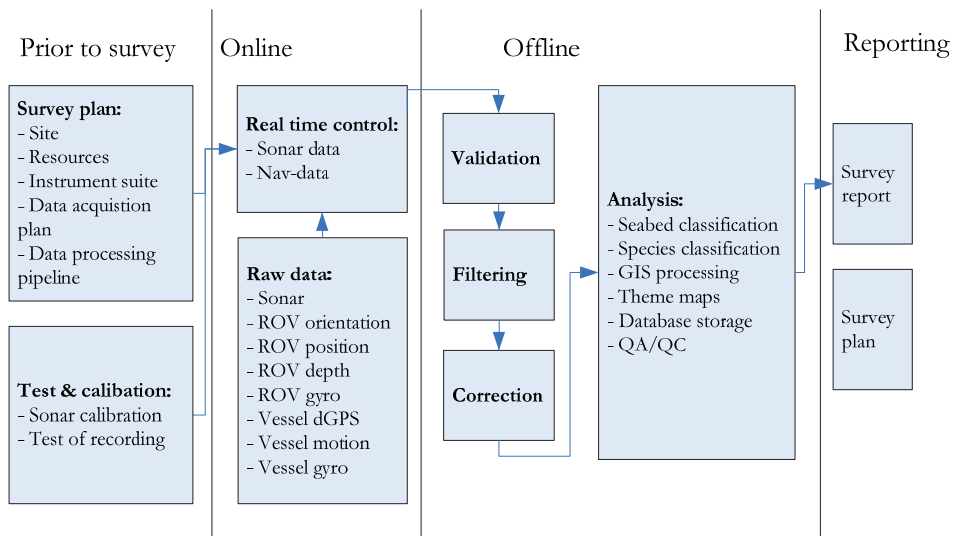


Figure 7.3 Data processing for ROV-based bathymetry sonar surveys.

Data filtering

Erroneous data should be removed in the data filtering. If the data are noisy smoothing filters can be applied. The navigation data and the sonar data should be processed individually before they are merged back together. Wild points must be detected both for navigation data and for sonar data. Outliers can be removed automatically or manually. Techniques for wild point removal in navigation data are described in the section on managing underwater navigation data “4.4.2 Data filtering”. Wild point detection and removal for sonar data can be done by a simple clip filter with a depth gate. The operator must also look through the data set and flag unlikely features. Sonar and software packages usually contain wild point removal tools.

Smoothing and filtering the data one risks removing features which are naturally present. Searching for cold-water coral colonies this is essential to remember as the structures of interest usually will stand out as a sonar anomaly and are subject to uncompromising filtering. It is therefore advantageous to compare the end product with the raw data. As a general rule, if in doubt whether a data point is noise or a feature, it will reappear in overlapping survey lines if they represent physical features.

Data correction

After the data measurements are filtered for outliers and other erroneous data points, the measurements should be corrected for known error sources. It is critical that the pressure depth is compensated for tide, seawater density and atmospheric pressure described in the navigation section. If not applied online, the correctly measured speed of sound profile must be applied both for the sonar itself and for the underwater positioning. The roll-, pitch- and heading angles must be corrected. Typical corrections are offset angles not previously known, or magnetic heading to true heading corrections. Finally the data should be converted into the desired datum.

Data interpretation

When bathymetry sonar is used to search for historic ship wrecks or coral reefs, it is important to have an idea of how these targets will appear in the data for the specific instrument used. A bathymetry survey produces large amounts of data which need to be visualized to be interpreted. A digital terrain model (DTM) is constructed and can be interpreted in software like Fledermaus²⁵ or Arcgis 3D Analyst²⁶. In this type of software the researcher can move around in a virtual landscape, zoom in and out, or change illumination to better understand the shapes on the seabed.

The *Lophelia pertusa* is the only cold-water coral in the North Atlantic which forms colonies large enough to be considered reefs. The *Lophelia pertusa* colonies can take

²⁵ IVS3D, Fredericton, New Brunswick, Canada

²⁶ ESRI, San Diego, California, USA

different forms on the seabed. They can make “towers” up to 35 meters high, they can make ridges or they can cover the seabed like a carpet (Hovland 2008). The coral grows and forms cauliflower-like structures which finally collapse under their own weight. In sonar bathymetry data, the surface of seabed covered with *Lophelia pertusa* corals can look rough and uneven, see Figure 7.4.

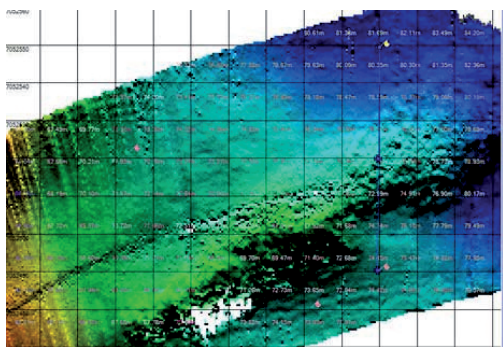


Figure 7.4 Bathymetric model of a small coral colony on the Tautra-ridge.

Software packages like the Kongsberg Triton²⁷ and the QTC by Quester Tangent²⁸ automatically classifies the seabed using statistical analysis of the backscatter data (Christensen 2006). The Geotexture software by GeoAcoustics uses pattern analysis together with statistical analysis for classification. The coverage of ROV-based bathymetry surveys is however usually limited and this type of processing has more potential for bathymetry survey collected with surface vessels. However, applying a recognised classification scheme the data can be used in comparative work. There are several classification schemes developed, like the EUNIS (<http://eunis.eea.europa.eu/>), Greene (Greene, Yoklavich et al. 1999) or Valentine (Valentine, Todd et al. 2002).

Map productions

The basic map is the contour map where the depths are indicated by contours. Colour and line styles can be shifted to distinguish major and minor contours, see Figure 7.5.A. Contour maps are compulsory when reporting bathymetry surveys. A variant of the contour map is the spot chart using colour to illustrate depth, see Figure 7.5.B, which may be more intuitive to conceive for the viewer. Shaded relief is an illustration where the surface is illuminated with an artificial light source and structures make shadows, see Figure 7.5.C. This is effective to reveal objects on a flat seabed. 3D views can be used to complement the basic maps and to help the reader comprehend the site investigated, see Figure 7.5.D. One should however note that 3D views do not contain quantitative information. For special objects identified, it can be informative to plot the depth profile along a line, as shown in

²⁷ Kongsberg Triton, Watsonville, California, USA

²⁸ Quester Tangent, Sidney, British Columbia, Canada

Figure 7.5.E. A common application of profiles is to measure the height of a ridge or a peak.

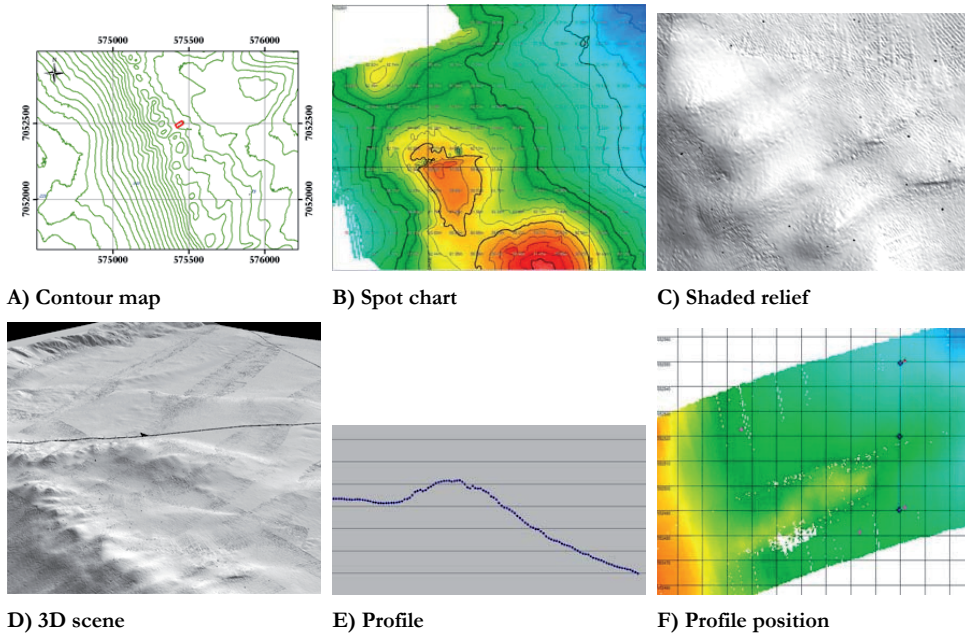


Figure 7.5 Typical map products. All examples are from the Tautra ridge area.

The number of maps and types of maps desirable to produce from a survey must be decided considering the motivation for the survey and the obtained results. Profiles should be created of interesting seabed features like coral reefs. When the data interpretation is complete theme maps showing e.g. coral abundance can be produced.

To identify possible coral occurrences, the bathymetry data can also be processed for slope, direction and rugosity. These parameters could also be compared. The coral colony seen in Figure 7.4 can also be seen in Figure 7.5 where the slope is processed and plotted. Together with seabed classification, such tools have the largest relevance for comprehensive data sets.

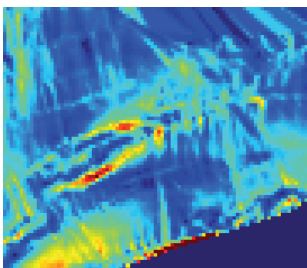


Figure 7.6 Bathymetry data set processed for slope. A red and yellow line indicate a boat shaped target. This is the same location seen in Figure 7.4. A faulty heave sensor have induced vertical lines to the data. These appear as straight lines in this data set.

7.4 Standards

7.4.1 IHO S-44

The S-44 standard (IHO 2008) on bathymetry is important for setting premises for hydrographic bathymetry services. The 5th edition of the Standard for Hydrographic Survey, Special Publication 44 (commonly referred to as S-44) is previously discussed in the section on underwater navigation but also contains requirements for bathymetry surveys. The four orders of hydrographic services are presented section “4.3 Position accuracy standards”.

In addition to the discussed requirements for total propagated uncertainty of data points described in Table 4.7, there are requirements for feature detection. For special order surveys, features of dimension 1 by 1 meter shall be detected. The requirement for order one is capability to detect 2 by 2 meter objects.

The S-44 standard also contains useful requirements for metadata. A data set should have digitally associated information about:

- Geodetic reference system (vertical and horizontal)
- Calibration procedures and results
- Speed of sound correction method
- Tidal datum and correction
- Uncertainties achieved and respective confidence levels
- Special or exceptional circumstances
- Rules and mechanisms for employed data thinning

For bathymetric models there shall be information about model resolution, computational method, underlying data density, uncertainty estimate for the model and a description of the underlying data set. The appendix of S-44 provides general guidelines for quality control. Issues of data storage, positioning, depth data integrity, error sources and propagation of uncertainties are discussed. General guidelines for data processing are also given in the appendix.

7.4.2 IMCA

IMCA has established guidelines for use of MBES in offshore surveys, either the transducer is hull-mounted or ROV-mounted (Danson, McNiell et al. 2003). Issues on navigation, sensor installation, transducer installation and test procedures are considered. In the section on calibration of multibeam echosounders, the theoretical foundation for the patch test is given. A reference surface for system verification is suggested. The reference surface is a well surveyed small flat area. By running four or five survey lines with high overlap in two perpendicular directions, the performance of the system will be highly observable. IMCA estimates 24 hours for the calibration of a multibeam echosounder system. Errors related to survey line directions are described along with survey planning.

Table 7.5 Error effects related to survey line directions

Error source	Across contours	Along contours
Beam-steering / small heading errors	Any errors will be adversely reflected in outer beams and results in staggered contours.	Any errors are less likely to corrupt outer beams.
Depth setting errors	System errors will propagate as a zigzag effect in contours.	Error is only detectable from beam overlap and could be overlooked.
Position offset errors	Any error will result in exaggerated contour offsets or zigzags.	Likely to be unnoticed in shallow water and flat topography. In deeper water or using towed systems, the effect will propagate as contour offsets.

7.4.3 MESH

MESH (Mapping European Seabed Habitats) does not offer a standard itself, but a review of general principles of operations, technical details of data acquisition, backscatter analysis and an evaluation of the usage of current bathymetric sonars for mapping of biological habitats (Coggan, Populus et al. 2007). Present sonar and software systems are discussed. Using acoustic back-scatter data, seabed topography and video ground-truthing habitat characterisation can be performed. Software both for seabed topography and acoustic backscatter analyses are discussed.

7.5 Quality assurance and control

The most important sources of error in a ROV-based bathymetry sonar surveys are listed in Table 7.6 along with suggested precautions. Twelve error sources to be kept under control to maintain knowledge of the overall system accuracy are listed. The table serves as a summary and practical checklist. The individual sensors and their associated calibration are discussed in the section on navigation and the section on survey design for bathymetry surveys.

Table 7.6 Error sources for bathymetry according to IHO (IHO 2008).

Source	Action
Positioning – both on the surface and subsea	Monitor performance and accuracy estimates (e.g. HDOP value)
Ray path model	Measure and apply frequent speed of sound profiles
Vehicle and vessel heading	Calibrate performance
Transducer misalignment	Calibrate setup
Sensor location – offset both on surface vessel and underwater vehicle	Measure setup. Control measurements
Time synchronization	Apply synchronizations of all sensors and computer frequently
Vertical datum error	Apply corrections. Control actions
Vertical position system error	Calibrate sensor
Tidal measurement error	Calibrate sensor. Compare to other measurements.
Instrument error	Check for consistency in data. Calibrate setup.
Sound speed error	Measure and apply frequent speed of sound profiles
Vessel motion error	Check for consistency in data. Calibrate setup.

The process to maintain quality of the survey is described in section on navigation. Issues as survey plan, budget of propagated error budget and online data control is essential also for bathymetry surveys.

7.6 Reporting and data products

The general survey report outline given in the section “5.6 Reporting” on video survey should also be applied for bathymetry surveys. The introduction should contain the background for the survey, the motivation, available equipment and a description of the application of the survey data. A written recapitulation presenting the main findings together with the most important figures like contour plots and spot charts belong in the chapter summarizing the results. Detailed results contain elements like target lists and presentation of the targets. Quality indicators are also plotted in the results chapter. Quality management including a propagated error budget, calibration reports, personnel listing, and description of the equipment setup and the methodology applied are contained in the appendices.

8 Bathymetry data from the Tautra ridge

8.1 Introduction

A bathymetry data set collected at the Tautra ridge in October 2006 is presented. NTNU was offered to test GeoAcoustics' newly developed subsea version of the GeoSwath 500+ interferometric side scan sonar. The sonar was mounted on the Minerva ROV, and RV Gunnerus was the base for the operation. The operation was completed on a low budget. GeoAcoustics provided an operator for the interferometric sonar, and the ROV was operated by NTNU personnel.

The Tautra ridge is a threshold dividing two basins in the Trondheim Fjord, described in section "6.1.1 The Tautra ridge". The Tautra area was chosen because data sets from Norwegian Mapping Authority²⁹ (Statens kartverk) were already available and could be used for comparison. Considering the practical limitations, logistics necessary to reach Tautra is limited compared to other reefs of similar dimensions.

For the survey depths in the Tautra area (40 – 80 meters) it could be questioned whether a hull-mounted sonar on a vessel would represent a less complicated and more efficient solution. But finding stony corals at this shallow depth is unique, stony corals are typically found substantially deeper. Tautra would be then only location where this sonar could be used for documentation of *Lophelia pertusa*. To survey larger depths, where cold-ware corals are commonly found, installation of sonar on an underwater vehicle will reduce the slant range and increase survey resolution.

The primary goal of the survey was to test the GeoSwath 500+ sonar ROV mounted for documentation of stony corals. The structures formed by *Lophelia pertusa* are sufficiently large to be observable in bathymetry data. Stony corals facilitate strong biological zonation and patchiness in diversity. Hence knowledge of the borders of stony coral reefs and distribution of dead and living coral is important to classify the fauna in the area. Such information can increase the understanding of the correlation between sediments, coral condition and the associated biota.

It is however usually necessary to ground-truth sonar data with video observations. Could the GeoSwath sonar mounted on ROV provide data sufficiently detailed to omit optical ground-truthing? Another important question is: Can the sonar data be

²⁹ Statens kartverk, Hønefoss, Norway

used to distinguish dead and living coral? To address such issues the seabed resolution need to be similar or better than the “special-order” found in S-44. Grid-size of half a meter or better should reveal the roughness of the seabed containing corals.

8.2 Method

8.2.1 Hardware setup

Sonar

The GeoSwath 500+ sonar appeared as promising to our cold-water coral research. The system can produce data according to the highest quality class in S-44. In published comparison tests the GeoSwath sonar show data quality comparable to the dominant MBES system Reson Seabat and Kongsberg Maritime EM 3002 (Gostnell 2005). According to GeoAcoustics specifications the maximum swath width is 190 meters or up to 12 times seabed altitude. The centre frequency of the system is 500 kHz. The physical transducer dimensions are 255 by 110 by 60 mm making the system convenient to implement on an observation class ROV. The power and data interface requiring 50 W DC and 10 Mb/s Ethernet is also suitable for most observation ROV's.

The capability of collecting side scan data was also considered advantageous for coral investigations. Reefs can be challenging to detect in bathymetry data sets. The structure of the coral is often smoothed out, and the result may look like any other seabed. The side scan data have higher resolution and indicates the seabed reflection intensity which increases the ability to identify the stony corals.

The GS 500+ sonar was mounted on the ROV as seen in Figure 8.2 with the sonar electronics housing was mounted on top. The transducers were placed on aluminium beams in front of the ROV with the port transducer facing starboard and vice versa. The sonar was controlled through a network connection to the top side GeoAcoustics computer, see Figure 8.1.

Attitude sensor

An MRU 6 was mounted on a frame in the front of the vehicle, see Figure 8.2. The unit was used for pitch, roll and heave measurements. The uncertainty of the measurements is specified by Kongsberg Seatex to 0.03° for roll and pitch and 5% or 5 cm for heave. Readings were sent directly to the top side GeoAcoustics computer.

The ROV's internal compass was used to supply the heading of the vehicle. The compass is a KVH³⁰ C100 and outputs data at 10Hz. KVH claims heading uncertainty of 0.5° for the instrument. There are various magnetic sources on the ROV that can increase the heading uncertainty. The dynamic response of this unit has however unfortunately proved to be limited.

³⁰ KVH, Middletown, Rhode Island, USA

Positioning

The ROV underwater position was measured by the HiPAP 500 USBL system onboard the RV Gunnerus. The RV Gunnerus was positioned by a DPS 116 dGPS with Starfix correction signals. The vessel gyro was a Simrad GC-80-S. Navipac survey software was used to create a global position for the ROV from dGPS, vessel gyro and the USBL measurements. The propagated error budget given in section “8.2.1 Hardware setup” is representative for this survey.

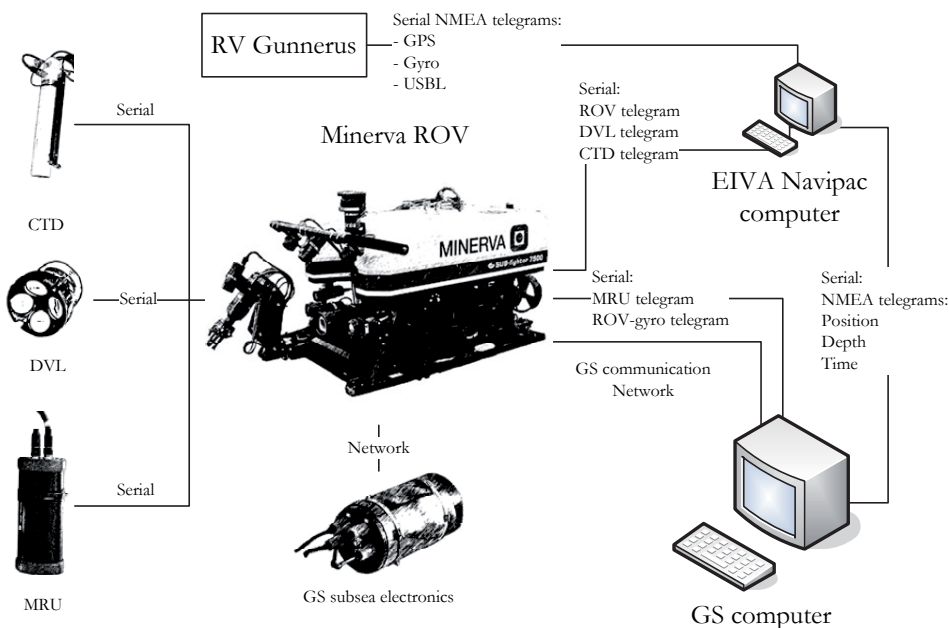


Figure 8.1 Signal flow for the survey – setup.

Speed of sound

A SAIV³¹ SD 204 CTD was fitted on the back of the ROV and used as pressure sensor. The unit corrects the pressure measurement for density variation using the measured salinity and temperature before outputting a depth value. The depth uncertainty is specified to 0.01%. The depth readings were fed directly to the top side GS computer at 1 Hz. The resolution of the data was 1 cm.

Altimeter

The GeoSwath 500+ does not have an integrated altimeter and the MS 1007³² altimeter on the ROV was used to keep a constant altitude during the data acquisition. Unfortunately the unit stopped functioning in the middle of the survey.

³¹ SAIV AS, Bergen, Norway

³² Kongsberg Mesotech, Port Coquitlam, British Columbia, Canada

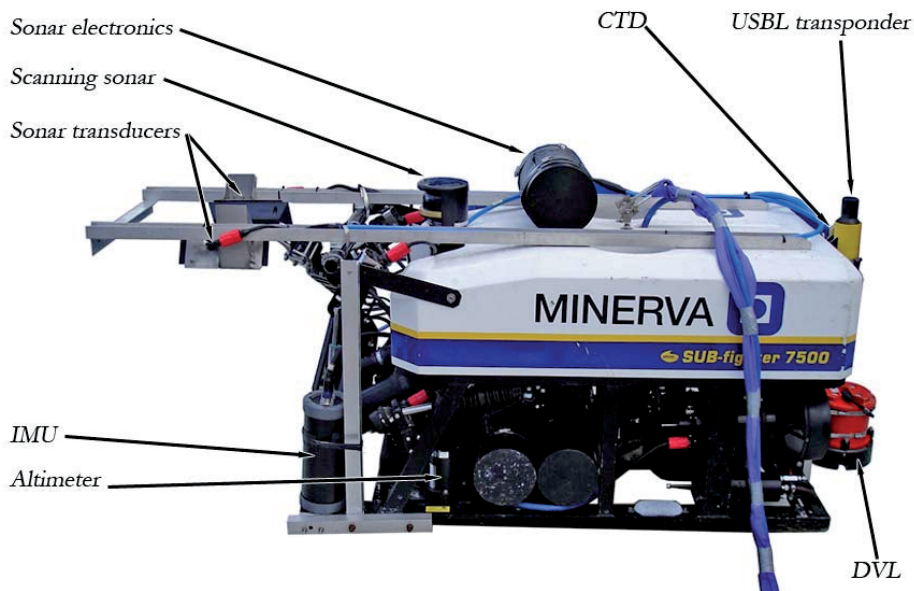


Figure 8.2 The installation of the GeoSwath sonar on the ROV.

Propagated error uncertainty estimation

The propagated error for the individual resulting data points for a bathymetric sonar can be calculated analogous to the propagated uncertainty estimations for the vehicle position using summation of variances eq. (8.1) and eq. (8.2):

$$\sigma_{xyz} = \sqrt{\text{var}_{\text{position}}^{\text{ROV}} + \text{var}_{\text{Gyro}}^{\text{ROV}} + \text{var}_{\text{Sonar}}^{\text{xyz}}} \quad (8.1)$$

$$\sigma_{\text{sonar}}^{\text{xyz}} = \sqrt{\text{var}_R + \text{var}_{\text{angle}}^{\text{phase}} + \text{var}_{\text{angle}}^{\text{roll}} + \text{var}_{\text{angle}}^{\text{pitch}}} \quad (8.2)$$

All standard deviations and variances must be given in meters. To transform the phase angle, roll angle and pitch angles to metric values it is necessary to apply a range values. A range of 50 meters is used. The variables are estimated in Table 8.1.

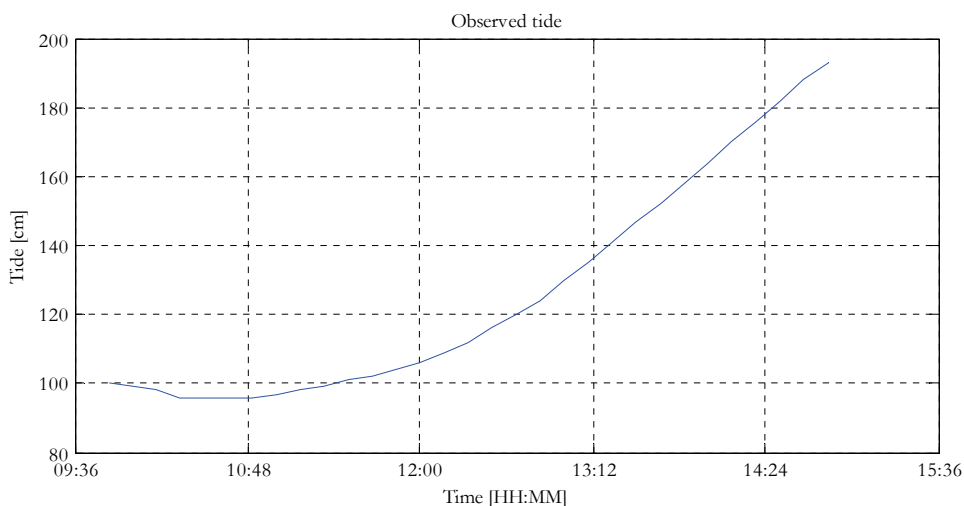
Table 8.1 Propagated error uncertainty estimation.

	Instrument	Standard deviation	Standard deviation [m]
Range	GS 500+	0.06 m	0.06
Phase angle	GS 500+	0.03°	0.03
Roll Angle	MRU 6	0.03°	0.03
Pitch angle	MRU 6	0.03°	0.03
ROV heading	KVH 100C	0.5°	0.44
ROV position	EIVA Navipac	0.85	0.85
Total Std			0.96

8.2.2 Data acquisition plan

Eight parallel 250 meters long survey lines were planned. Line spacing was proposed to 50 meters and a seabed altitude of 15 meters was decided. This would result in 75 – 100 m swath width. The line spacing would result 50 to 100% in overlap. A perpendicular cross line for quality control was added to the end of the survey scheme for quality control. The survey was planned to take three hours.

The survey area is exposed to tidal currents. The tide prediction tables were used to find a date for the survey with small differences between high and low tide to minimize the current, see Figure 8.3. When the tide turns from rising to falling or vice versa the current is at its calmest. The survey was performed in the calm period from 9.00 to 12.00.

Figure 8.3 Tide measured in Trondheim harbour 13th October 2006.

8.2.3 Processing

Online

The data was controlled online in a waterfall display. The integrity of the positioning and attitude was also watched continuously. The GeoSwath 500+ software have control functions to alert the operator if an instrument stops sending data, or the data are dubious, see “5.3.3 Processing and interpretation”.

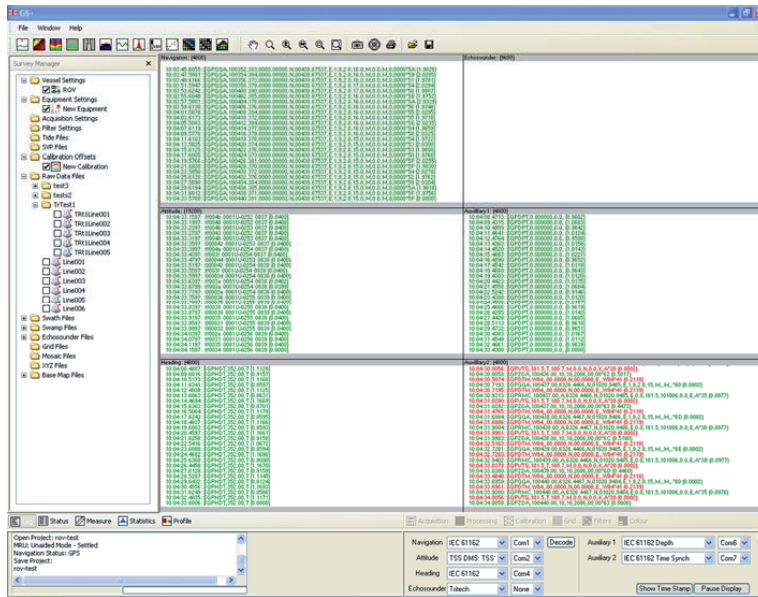


Figure 8.4 Operator screen for sonar operator indicating data quality. Green lines are accepted data telegrams, while red lines indicates rejected data.

Offline

In the GeoSwath software a cut-off filter is set to remove wild points in the online processing. This is a necessary feature for the GeoSwath system. The data were corrected for tide. Tidal data measured at Trondheim harbour were applied. All data were collected in the WGS84 datum.

The individual survey lines were immediately processed into a mosaic. The complete bathymetry model created from the data collected in this project was compared to data from the marine department of the Norwegian Mapping Authority. The integrity of the data was also confirmed in the mosaicing process. Speed of sound error, instrument mounting offset and measurement biases would appear as inconsistencies in the mosaic. There was an issue with the heave sensor in the MRU unit. This is seen in the data as lines perpendicular to the ROV direction of motion.

8.3 Results

Total of approximately 2.5 km of survey line was completed. The “main box” in the area covered is 250 by 400 meters. In this area we found five local peaks and two

smaller ridges, see Figure 8.7. These ridges were coral reefs. In the northern area the seabed was clothed with living stony coral.

8.3.1 Data examples

Even with the high resolution data collected at low seabed altitude it is difficult to confirm the presence of stony corals from bathymetry data alone. The bathymetry data suffered from artefacts originating from the heave sensor. But if the co-registered side scan data area consulted it is clear that the formation is coral, see Figure 8.5. These observations were also confirmed by video, see section “6.3 Video results”.

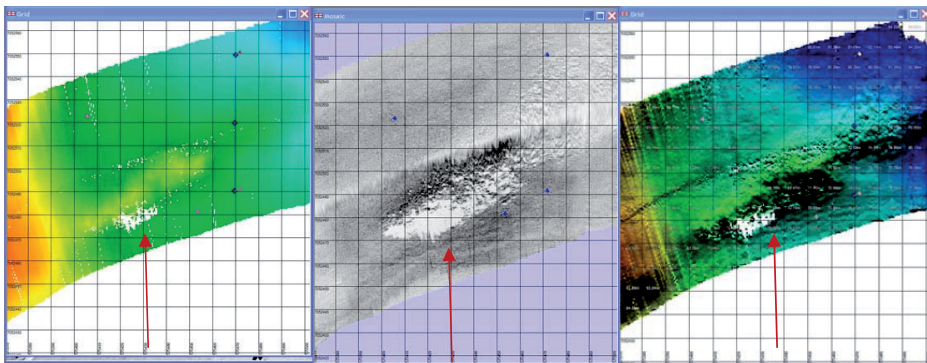


Figure 8.5 Coral ridge shown in; bathymetry spot chart, side scan data and bathymetry shaded relief. The elongated rough area on the seabed proved to be coral. The previously mentioned heave sensor issues are seen as lines perpendicular to the direction of travel (see red arrow). The presence of stony coral was verified by video.

8.3.2 Interpretations

In shaded reliefs of the bathymetry data, indications of stony corals can be seen in Figure 8.5. In the spot chart the corals cannot be positively identified, whereas both the side scan sonar plot and the shaded relief clearly shows the rough seabed surface typical for coral reefs. Combining these plots with knowledge of the local geology and biology, it can be stated that these features are likely to be coral reefs, but they can still not be positively distinguished from an aggregation of rocks. It is naturally not possible to state the state of the coral reef. The 3D model with side scan data overlaid is given in Figure 8.6. 3D models are however more informative sitting in front of a computer when the viewer can fly through the terrain.

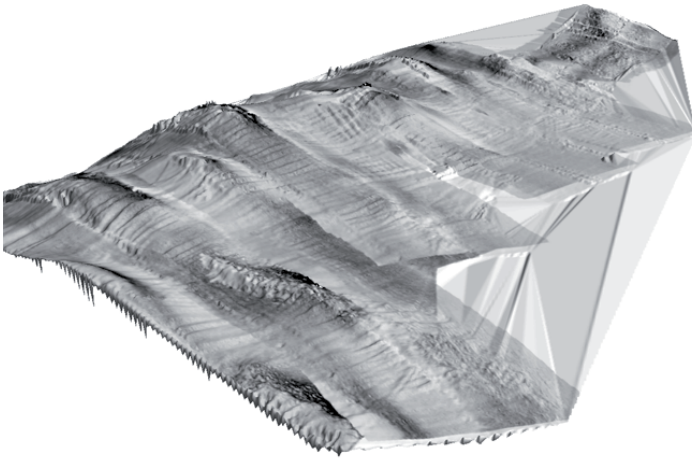


Figure 8.6 3D view of the constructed bathymetry model with side scan data overlaid. The mentioned heave issue is visible also in this figure.

8.4 Discussion

8.4.1 Biological

Living corals are found on all the local tops found in the bathymetry and on the two mentioned ridges. More surprisingly in the northern part of the survey area, the coral clothed the seabed in a carpet-like manner. It is not possible to observe other biological features than the calcium carbonate structure of the *Lophelia pertusa* in the bathymetry data.

8.4.2 Method

It looks like there are large areas with stony coral on the Tautra edge. It can be challenging to identify the corals from the bathymetry alone so the complement of side scan is useful. The side scan makes the GeoSwath 500+ suited for this type of operation. However these data can only say something about the geometrical shape of the coral colony, and it is not possible to extract information about the condition of the corals. Initially we asked if video ground-truthing could be made superfluous using this sonar. Identification of coral-like features seems possible with relatively high precision, but there is still no guarantee that corals are not interchanged with exposed coarse gravel or piles of rock. To obtain 100% confidence of the observations, video is still required. Using the sonar data, it was not possible to distinguish living coral and dead corals.

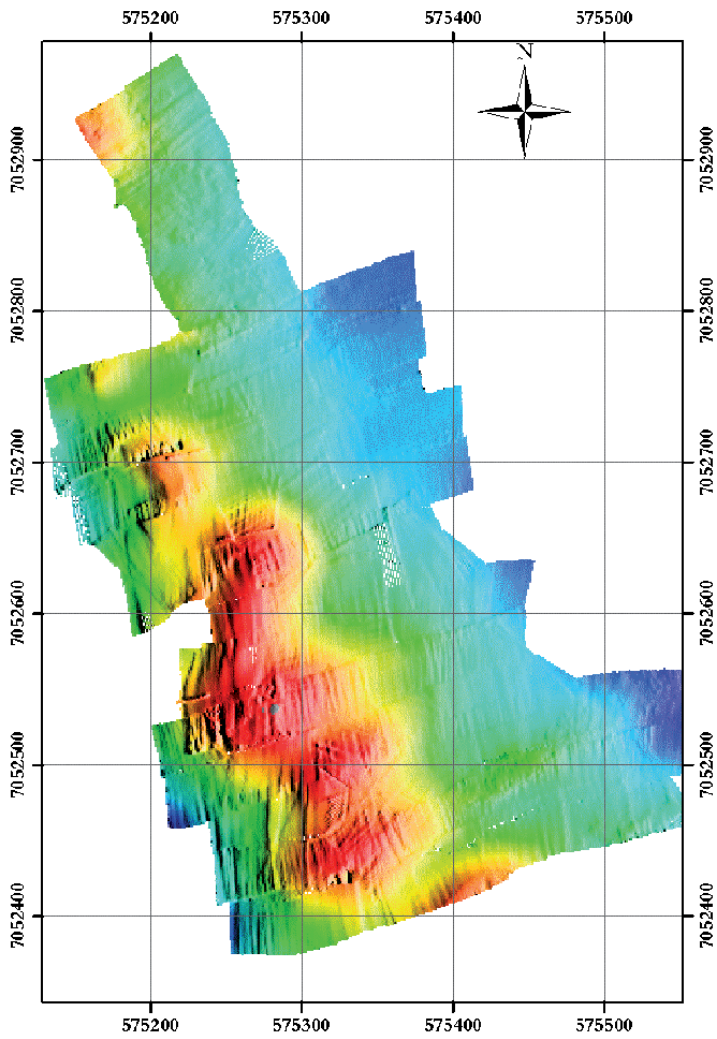


Figure 8.7 Bathymetry collected using the GeoSwath 500+ sonar. The systematic error seen is originating from the mentioned heave issue.

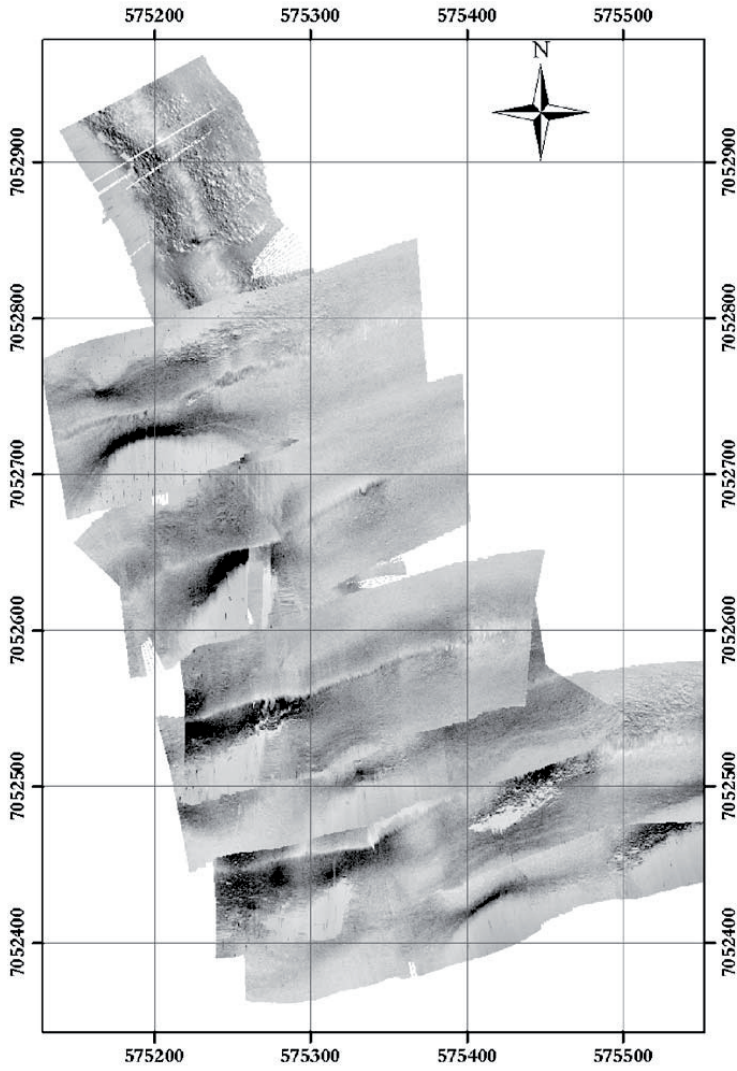


Figure 8.8 Side scan sonar mosaic.

9 Photo mosaic

9.1 Introduction

Serious attenuation and backscatter issues in seawater limit our field of view to a few square meters. To depict larger areas series of overlapping images can be compiled to a composite image with extended coverage. Photo mosaic is a tool for detailed documentation of a confined area, but the seabed coverage is modest. The desired information from photo mosaics is shape, colour, structure and texture of the seabed and the targets present. In the imaging process the 3D seabed is projected onto a 2D representation. The projection will induce inaccuracies to the resulting photo mosaic. An attempt to address this error source is found in (Johnson-Roberson, Pizarro et al. 2009). The result is a detailed imagery and in cold-water coral research photo mosaics can be used to document the physical state and species diversity of corals and the associated fauna. Biologists would typically want to extract information like seabed type and biotopes, taxa inventory and distribution (Jerosch, Ludtke et al. 2007), (Lirman, Gracias et al. 2007), (Ludvigsen, Sortland et al. 2007)).

9.1.1 Previous work

Photo mosaic has been applied in underwater applications for many years, but there is still limited usage. An early application of underwater photo mosaic was the depiction of the sunken submarine *Thresher* in the 1960's (Ballard 1975). Ballard had a large photo mosaic produced from the sunken ocean liner *Titanic* in 1987 (Ballard 1987). Before the 1990's photo mosaic was mainly an analogue technique, until it became digitized (Singh, Howland et al. 1998). In digital photo mosaic processing two directions emerged; feature based (Singh, Howland et al. 2004) and non-feature (Xu and Negahdaripour 1997) based. Computer vision and SLAM (Simultaneous Localization And Mapping) research have provided a substantial amount of the theory and techniques and formed the basement for modern photo mosaic work (Gracias and Santos-Victor 2001), (Eustice 2005).

Photo mosaic projects

IFREMER has developed an image mosaic solution based on video imagery called MATISSE (Mosaic Advanced Technologies integrated in a Single Software Environment) (Vincent, Pessel et al. 2003), (Allais, Sarradin et al. 2006), (Olu-Le Roy, Caprais et al. 2007). This system is video based and arranges the images using image feature detection, image flow and navigation data to create the mosaic. The research group of Underwater Vision and Imaging Lab at University of Miami have presented schemes for image mosaic both based on video and still images

(Negahdaripour and Madjidi 2003)). They have also showed applications in coral documentations (Lirman, Gracias et al. 2007).

9.2 The photo mosaic process

There is no “best practice” available and no industry standards or services recognized, like for bathymetry and video survey. The photo mosaic processing scheme described here is developed by a research group at WHOI and DSL lead by Hanumant Singh. The creation of seabed photo mosaics starts by collecting images in a structured way to depict the entire area of interest. These images are digitally corrected for light features and camera distortions before they are processed to one seamless image covering the whole area of interest. The process presented is based on still images and feature extraction.

9.2.1 Image capture

The image capture for photo mosaics shares the main concepts with the imaging described in section “5.2 The underwater imaging process”. The light reflected from the seabed is passing through an optic objective to a digital image sensor. The sensor is usually a CCD or CMOS chip and has millions of sensors in a matrix. When an image is shot the sensor is active for a preset period of time, typically 1/200 – 1/20 seconds. Each sensor outputs a signal for the light intensity sensed for one image pixel. This is put together to an image by a micro controller and later sent to storage. The image resolution is dependent of the number of elements in the image sensor, the MTF of the image sensor, and the precision of the lenses. The MTF-values of the image sensor should be high to produce sharp imagery. To generate sufficiently lit images from the deep water, the signal to noise ratio of the image sensor should be high. For colour imagery the colour definition is important in underwater applications since high colour definition allows for enhanced opportunities for image adjustments. For scenes with varying brightness, high colour definition enhances the ability to catch details in dark areas without over-exposing bright areas of the image.

Objectives consist of several lenses and are characterised by their aperture size, focal length and magnification or angular opening. The camera and objective’s ability to find focus is essential to create sharp images. A small optical aperture increases the chances of finding focus, but reduce the amount of light passed on to the image sensor. The optical aperture is quantified by an f-number. The mechanical precision of the lenses and the position of the lenses determine the distortions of the images taken using the optic objective.

9.2.2 Illumination

The light sources can be constant sources like LED, HID, and incandescent, or they can be strobe lights. Light pattern, intensity and colour temperature (spectral irradiance) are important parameters of an underwater light source. See the section “5.3.1 Sensor suite” on light sources for video survey for a discussion in light setup

and continuous light sources. However, in most cases strobe lights produces more light for still image capturing than its continuous counterparts.

Uniformly lit images are attractive for photo mosaic production since light intensity variations will make the mosaic look patchy. However the light intensity will in practice vary across the image frame to some level. During post processing the illumination component and reflectance component of the light captured by the image sensor is separated in the frequency domain. Illumination has low frequency while the reflectance is of higher frequency. Illumination is normalized and merged back with the reflectance (Singh, Roman et al. 2007) to create a uniformly lit image.

9.2.3 Photo mosaic construction

There are two basic steps in photo mosaic construction; topology estimation and image blending. The term topology is used to describe the images' internal position, rotation and scale. After topology estimation the images are moved, rotated, and scaled before they are connected. This process is called image registration. To remove the edges between the images and create a seamless image a method called image blending is applied. More details can be found in (Singh, Roman et al. 2007), (Pizzaro and Singh 2003), (Burt and Adelson 1983) and references therein.

Topology estimation

Initially the images are processed in pairs. Images are processed in the same temporal and spatial sequence they were captured. The relative position, scale and rotation are computed from the geometry of common image points. To establish common image points, interest points are created in both images using a technique proposed by Harris (Harris and Stephens 1988). When eq. (9.1) have two positive eigenvalues the point is a corner, one positive eigenvalue indicates an edge.

$$\mu(x, \sigma_i, \sigma_D) = \sigma_D^2 g(\sigma_i) * \begin{bmatrix} L_x^2(x; \sigma_D) & L_x L_y(x; \sigma_D) \\ L_x L_y(x; \sigma_D) & L_y^2(x; \sigma_D) \end{bmatrix} \quad (9.1)$$

In eq. (9.1) the interest point, μ , is a function of the derivation scale, σ_D , and the integration scale, σ_i . A more detailed description can be found in (Pizzaro and Singh 2003) or (Harris and Stephens 1988). Around each interest point a small image patch is selected. This image patch is given a unique identity using Zernike moments (Khotanzad and Hong 1990).

$$A_{nm} = \frac{n+1}{\pi} \sum_x \sum_y f[x, y] V_{nm}^*(x, y), x+y \leq 1 \quad (9.2)$$

The Zernike moments, eq. (9.2), consists of the image function, $f(x,y)$, and the Zernike polynomial, V_{nm} , where n denotes the polynomial order and m denotes the number of repetitions, summed over a circle. These Zernike moments are robust to variations in rotations. By comparing the Zernike moments, common points are recognized in the two overlapping images. There are typically established 200 – 1000 interest points created for each image. Using the image coordinates of common points, the relative position, rotation and scale of the images are determined. A least

median of squares method (LMS) is applied to remove outliers for the set of computed matching points. When all images are matched pair-wise the initial topology is iteratively used to check for further overlaps and connections across track and along track. Finally the topology is adjusted by minimizing a cost function for distance for point matches, image distortion and overall mosaic translation.

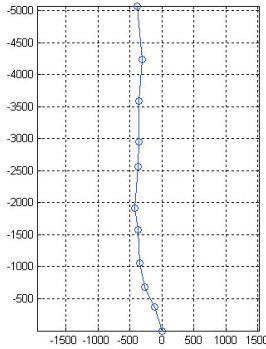


Figure 9.1 The position of the camera for each image is indicated by a circle in this topology plot from a photo mosaic. The units are image pixels.

Image blending

When all images are moved, scaled and moved to the correct position, the images are merged by image blending (Burt and Adelson 1983). All images are divided into frequency components by a series of band pass filters. Between two image frequency components (of the same frequency band) a centreline is defined. In a transition zone along this centre line the images are “mixed”. The image intensity of the pixels in the transition zone is calculated as an average of the overlaying pixels of the image frequency components. The average is weighted by the distance from the centre line to the pixel location. The width of the transition zone is different for each frequencies band. For low frequencies the width is larger, and for higher frequencies the width is smaller. This prevents broken edges for large features and double appearance for small items. When all image frequency components are connected and the image intensities in the transition zones are computed, all the frequency components are merged together again. The result is a photo mosaic with seamless image joints.

Camera calibration

Camera calibration is performed to compensate for camera optics imperfections and lens distortions in particular. The camera should be calibrated when the camera is mounted in the underwater housing. In this work a dedicated calibration routine proposed in (Heikkila and Silven 1997) is used. The physical camera parameters; principal point, focal length, radial distortions, tangential distortions and scale are calculated from a series of test images of a 3D object. An error function is derived from the theoretical camera model. The error function is then minimized in two steps, linear estimations and then non-linear estimations.

The refraction on air – glass and water – glass surfaces conflicts with the collinear assumption the pin hole camera model relies on. The result is an altered position for the principal point, but practice has shown that this still produces acceptable results.

9.3 Survey design

The survey design starts by establishing a survey plan as described in the video survey section “5.3.2 Data acquisition plan”. A typical basis for quality requirements for photo mosaic is ability to identify a certain type of seabed and interesting species. These requirements must be broken down to technical and operational requirements like e.g. seabed resolution (mm pr pixel), vehicle seabed altitude, or quantity of light. The next stage in the planning is to setup: 1) instrument suite, 2) data acquisition plan and 3) data processing pipeline.

9.3.1 Instrument suite

The instrument suite associated with photo mosaic consists of camera, objective, light sources and eventual positioning equipment. The photo mosaic system processing does not depend on navigation data, but the application of the photo mosaics relies on proper geo-referencing. To be able to maintain constant seabed altitude during data collection an altimeter should be used.

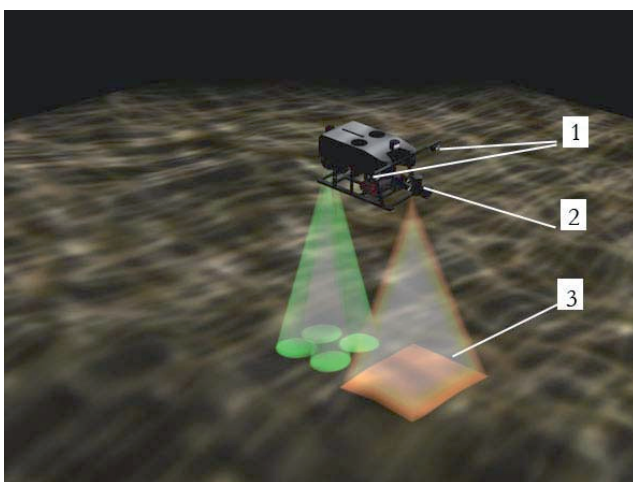


Figure 9.2 Rendering showing ROV collecting images for photo mosaic. 1) Light sources, 2) Camera, 3) Area of interest. The green area illustrates the seabed ensonification by the DVL used for navigation.

Camera

Choosing the camera it is important to have the purpose of the survey in mind. For underwater usage there are two types of camera dominating; 1) consumer cameras and 2) industrial block cameras. Consumer cameras are often easy to integrate with out-of-the-box software and remote control solutions running over a standard data protocol like USB (Universal Serial Bus) 2.0. They are however often bulky and cumbersome to place in underwater housings. The situation is opposite for

industrial block cameras, they are small and easy to mechanically adapt to the underwater environment, but more development is necessary to operate and interface the camera and optical objectives. Image resolution, light sensitivity, objectives, interface for strobe and image data transmission should be taken into consideration selecting camera.

Light source

Choosing light source for a photo mosaic survey light intensity, colour temperature and light pattern should be considered. The use of strobe has the advantage that the shutter speed can be set very fast on the camera, reducing the potential for motion blur in the imagery. On the negative side strobe lights have a recharge time limiting the frequency of the image acquisition. It is hardly ever too much light in underwater photography. TTL (Through The Lens metering) function for strobe lights is usually not necessary since the best practice would be to run the flashes at full power and adjust the camera according to the available light. If the imagery gets over-exposed, the diaphragm could be reduced with the positive side effect that the field-of-depth increases.

Optics

During image acquisition for photo mosaic the f-number, focus, zoom and distance from the camera to the image object should be constant. Motorized optic objectives allow changes to the aperture opening (f-number) and focus distance without opening the camera housing, but considering that all images in a photo mosaic data set should have equal settings, a manual objective could be preferable. The optic opening angle of the optic objective should not be to larger than 45° to avoid obliqueness of the imagery. Obliqueness will complicate the mosaic process and make the resulting photo mosaic harder to interpret.

9.3.2 Data acquisition plan

Photo mosaic surveys intend to cover the seabed 100%. When a data acquisition plan is made one is considering the area to cover and the necessary overlap. The data acquisition plan contains a description of ROV seabed altitude, vehicle velocity and line spacing for the survey lines.

The seabed altitude is determined from the optical opening angle of the objective together with the power level of the light sources and the light scattering and absorption levels of the seawater. The drag force and expected top speed of the ROV can be calculated to using the equations in section “3.2 ROV Minerva”.

The survey speed of the vehicle is limited by field of view, desired overlap, altitude and how often it is possible to take images. The image capture frequency can be limited by flash recharge time, or by data transmission capacity between the ROV and the surface. In eq. (9.3) v is the velocity of the ROV and f_i is the image frequency. o represents the overlap between each image.

$$v = (1 - o)l \cdot f_i \quad (9.3)$$

Calculating the dimension of the seabed patch depicted in each image and the overlap constraint, the line spacing can be calculated. The length of the area covered by each image, l , is directly dependent of the altitude of which the vehicle is flying. In eq. (9.4) h denotes the distance from camera to the seabed, and α is the camera-field-of-view.

$$l = 2 \cdot h \cdot \sin\left(\frac{\alpha}{2}\right) \quad (9.4)$$

In an example with altitude of 2 meters, the camera will cover an area 1.5 meter by 1.5 meters. To achieve the desired side lap (25 %), the line-spacing would have to be 1.1 meters. If the camera can capture an image every 4th second, the speed will be 0.2 m/s. The resulting survey efficiency will be 800 m² of seabed per hour. To pilot an ROV running lines with cross-track errors below 1 meter is challenging. This task is best solved using a closed loop control system (see section “3.2 ROV Minerva”) for the vehicle in combination with a high performance navigation system (Marthiniussen, Faugstadmo et al. 2004) as discussed in “3.2 ROV Minerva”.

Typical seabed altitude is 2 – 5 meters and typical velocity is 0.2 – 0.5 m/s. 50 % overlap can be used as a rule of thumb for a sensible compromise between efficiency and redundancy. Typical line spacing is 1 – 3 meters.

Capturing images for photo mosaic it is important that all images are taken perpendicular to the object. Deviation in angle will lead to distortions in the resulting photo mosaic. High camera altitude relative to the vertical extent of the image objects is beneficial, since all features should appear as similar as possible in the imagery.

9.3.3 Processing timeline and interpretation

Data validation

During the data acquisition the collected images should be controlled for overlap, exposure, field of depth and motion blur. Metadata like depth, position, time tag synchronisation, heading and roll/pitch should be controlled in real time.

Data correction

The images are corrected for light patterns and camera distortions. The first step is to correct for light patterns caused by uneven illumination from the light sources as previously described. This process is fully automatic and implemented as a batch process requiring minimum human interference. The camera correction is also an automatic process correction all the images in the data set without human intervention. However a camera calibration procedure is necessary to provide parameters for image correction. The navigation data should be processed according to section “4.4 Processing” on navigation.

Before the mosaic process can start, the images to be used are chosen. Duplicate images and images with obvious flaws should be removed from the list of images to

be processed. Then the topology estimation and image blending create the mosaic in automatic processes.

Geo-referencing

From matching time tags of the images and the positioning log of the underwater vehicle the position of each individual image are found. A selection of positions can be used to geo-reference the complete photo mosaic. The geo-referencing enables distance measurements and area calculations in the photo mosaic. The results must be used with care since photo mosaics can contain image distortions.

Data interpretation

In the case of cold-water coral investigations, the main goal is usually to identify taxa and their morphological variations. Seabed characteristics and distribution of seabed types and corals are important information that can be extracted from photo mosaics. The imagery can be used for seabed classification, see section “5.3.3 Processing and interpretation”.

9.4 Quality assurance and control

For photo mosaics a major quality indicator is geometrical distortions. Photo mosaics are conceptually prone to geometrical distortions which will appear as irregular shapes of features, inconsistent dimensioning or double appearances. A simple control of dimension consistency is to put an object with known dimensions in the image, e.g. a linear scale bar.

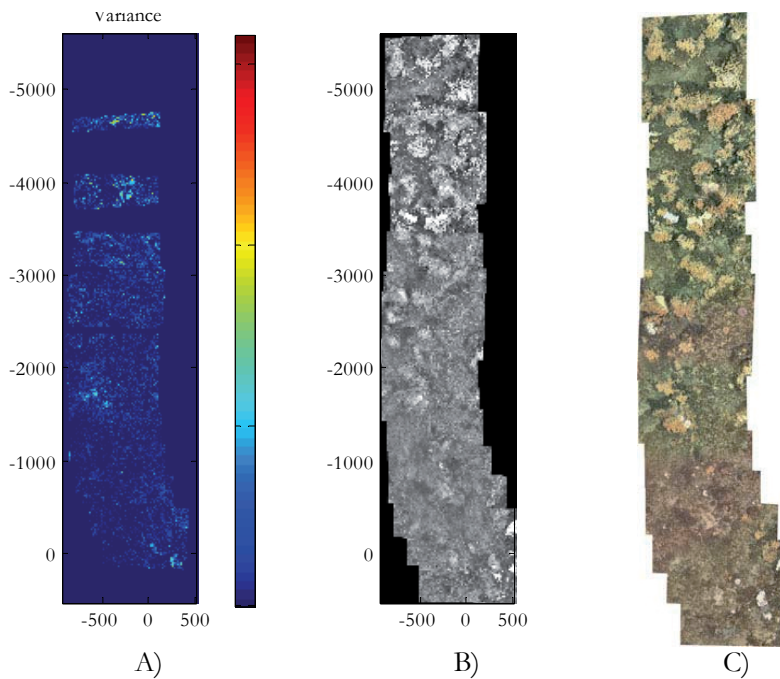


Figure 9.3 The axes in the figures are pixels. **A)** Variance of image intensity of overlapping pixels. **B)** Image registration prior to image blending. **C)** Resulting photo mosaic.

Calculating the topology it is also possible to calculate the precision process internally. In the topology estimation, an optimization technique is applied to find the best fit of position, scale and rotation for the images. This optimization procedure will calculate the distances between the positions of corresponding interest points after the topology is calculated. These distances can be used as a quality measure for the photo mosaic.

When the images are blended, intensity variations in overlapping pixels could be an indicator of inaccuracies as overlapping pixels should image the same object and hence have similar intensity, see Figure 9.3.A.

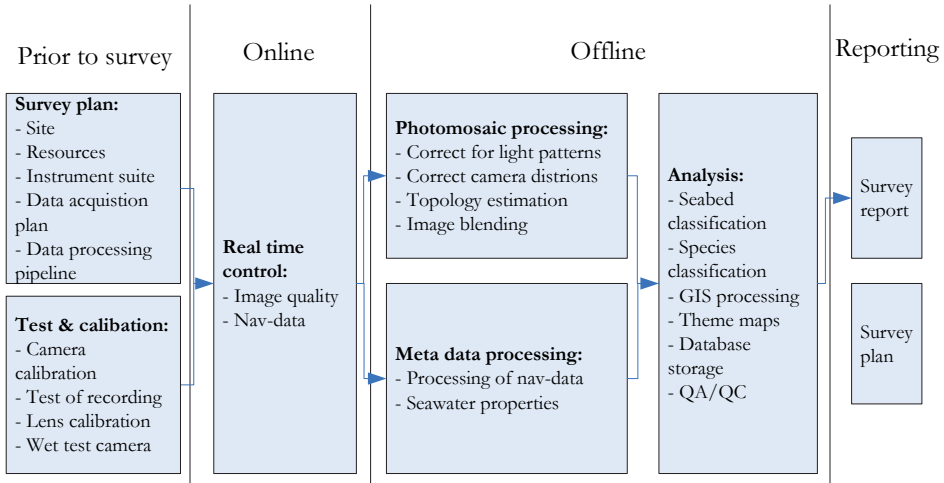


Figure 9.4 The process pipeline for photo mosaic production.

9.5 Reporting

For photo mosaic surveys the section on survey requirements should contain requirements from the client requirement level to performance requirements to camera, optics and light sources. The survey pattern, number of survey lines, line spacing, and seabed altitude should be described. The summary of results presented in chapter three includes a view of the photo mosaic together with indications of position, dimensions and orientation. The detailed results presented in chapter four section four the results of quality tests like the scaled bar, the topology variations and the deviations seen in the blending process are presented. Details of special interest are plotted in a larger scale together with an indication of the position. If there are done any analyses on seabed type coverage and distribution this should be included here. Strength and shortcomings of the data set should be pointed out, and if any processing steps are skipped this should be defended here.

10 Photo mosaic from the Tautra ridge

10.1 Survey motivation and site

A photo mosaic dataset was collected at the Tautra ridge in September 2007. The target area is illustrated by the box overlaid side scan imagery in Figure 10.1. The area was chosen based on observation made during the bathymetry survey and the video survey presented in previous sections. Further details about the location are found in section “8.3.1 Data examples” on bathymetry data examples and “6.3 Video results” on video data examples. To collect data for a more detailed documentation was the main objective of operation. The video, bathymetry and side scan imagery showed the presence of a cold-water coral reef. Information about distribution of seabed type, taxa, species, and morphological variants was desired.

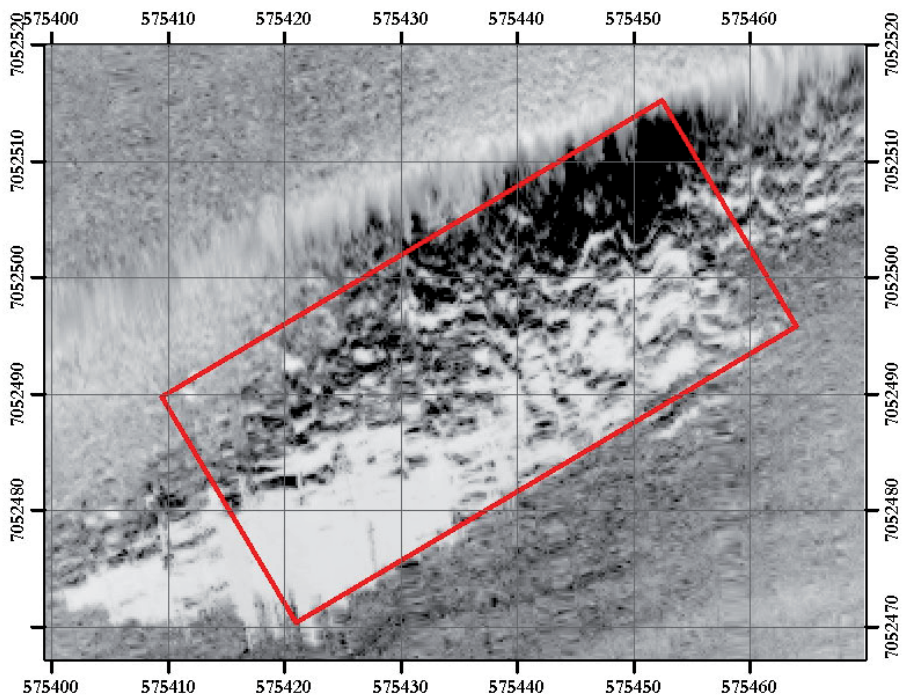


Figure 10.1 Map showing the area of interest overlaid side scan data. The units are UTM WGS84 zone 32N.

The Tautra ridge area is exposed to tidal currents because it forms a threshold between two of the main basins of the Trondheim Fjord see section “6.1.1 The Tautra ridge” for a description of the location. The date for the image acquisition was chosen based on the lunar cycles and the tide prediction table to minimize the effect of tidal current. For the data acquisition the Minerva ROV, see section “3.2 ROV Minerva”, was used in the data acquisition. The vessel used was RV Gunnerus which is rather robust for common fjord sea states. The depth in the area varied from 63 meters to 73 meters.

10.2 Method

10.2.1 Hardware setup

The ROV was fitted with two 400 W HMI (OSRAM 2008) lights mounted on light-booms. For image capture a digital camera from Uniq Vision (model 1830CL – 12-bit) was mounted with the image axis vertical facing downwards with zero roll and zero pitch for the ROV. The camera produces one mega pixel images with 12-bit colour definition. The imaging rate was limited by the camera and the communication link to one image every fourth second. The view opening is approximately 45°. At two meters altitude, the image will cover 1.5 by 1.5 meters of seabed. The seabed pixel size will be 2 by 2 millimetres. Using constant light sources we were forced to use rather long exposure times, up to 1/30 seconds.

The ROV was positioned with the HiPAP 500 USBL system mounted on RV Gunnerus. A CTD unit was placed on the seabed along with a transponder. The CTD was deployed to record the tide and speed of sound profiles for the USBL system and the transponder as a baseline for USBL position accuracy. The basic error budget shown in section “4.1.2 Underwater positioning” is representative for the setup used in this survey, and standard deviation between half a meter and one meter for the position estimates is anticipated depending on the geometry. EIVA Navipac maritime survey software was used for navigation computation and logging. It was also attempted to take advantage of HAIN (Hydroacoustic Aided Inertial Navigation) (Marthiniussen, Faugstadmo et al. 2004) inertial navigation system using an IMU, and a DVL together with the USBL system to increase to navigation accuracy. This could have reduced the standard deviation of the navigation estimates by 60 – 70%. Unfortunately a sensor fault prevented this increased navigation accuracy.

10.2.2 Survey design

The target area was 50 by 20 meters extension, see box in Figure 10.1. Line spacing was planned to one meter and the intended seabed altitude was 2 meters. The survey plan contained 20 survey lines, 50 meters long. Assuming 50 % overlap, the theoretical vehicle velocity is calculated to 0.25 m/s. The survey lines were laid in a north-east direction.

10.2.3 Processing

First the images were corrected for light pattern. The images were processed to photo mosaics (topology estimation, registration and blending) by the previously presented Matlab based software toolbox by WHOI. Using the time tags and the navigation log, positions were established for all individual images and photo mosaic patches. The geo-referenced results were loaded into a GIS base.

10.3 Results

The result of the survey was approximately 900 images. Due to restricted time available only thirteen of the planned twenty lines were ran. Light limitations distorted the colour balance and the red colour band was exaggerated. The images showed, as expected, occurrence of the stony coral *Lophelia pertusa* in both white and yellow variation, see Figure 10.3 and Figure 10.4. In the northern end the density of white living coral was high. In the southern area the colours were mixed and coral rubble was blended with lumps of living coral. The lowest density of stony coral was seen in the western corner of the area depicted.

10.3.1 Metadata

The position of the stationary test transponder is plotted in Figure 10.2. The plots indicate that the precision of the position estimates is higher than expected from the error budget given in section “4.1.2 Underwater positioning”. This type of plot will however not prove the absolute accuracy as certain systematic errors will not be revealed. As an example of systematic error, it can be shown that the error is correlated to the depression angle of the USBL measurements. This correlation can indicate inaccuracies to the speed of sound profile applied.

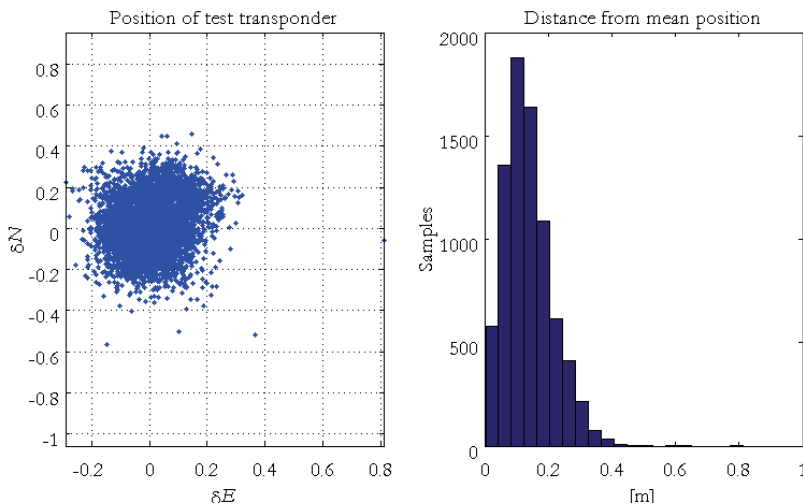


Figure 10.2 Position of stationary test transponder.

10.3.2 Data examples

In Figure 10.3 images from the western corner is compiled and five details are inserted to give an impression of the level of detail on the resulting imagery. Going through the imagery ten species of macro fauna is identified, see Table 10.1.

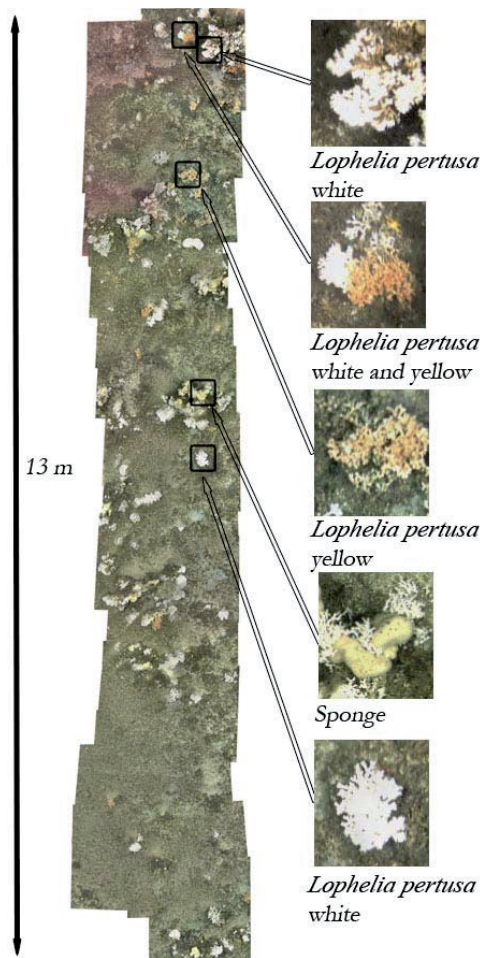


Figure 10.3 Part of photo mosaic over Tautra coral ridge.

Apart from the stony coral sponges and soft corals are observed in Figure 10.3. It is also apparent that the white and the yellow colour variant of *Lophelia pertusa* seem to be able to live practically on top of each other.

Table 10.1 Observed species

Species	
Stony coral	<i>Lophelia pertusa</i> (yellow/ white)
Sea tree	<i>Paragorgia arborea</i>
Lithodes	
Edible crab	
Sponges	<i>Geodia</i> sp.
Rockfish	<i>Sebastes viviparus</i>
Starfish	
Sea urchin	
Squat lobster	

It is common to define zones of fauna types on cold-water coral reefs. In Figure 10.4 three categories of seabed are defined; 1) More than 50% seabed coverage is dominantly yellow *Lophelia pertusa*, 2) More than 50% seabed coverage is dominantly white *Lophelia pertusa* and 3) Between 10% and 50% seabed coverage is *Lophelia pertusa* independent of colour. The uncategorized seabed contains less than 10% of *Lophelia pertusa*. The seabed coverage is determined by “the viewer’s best estimate” based on the imagery.

10.3.3 Quality assurance and control

To achieve a measure for the quality of this data set the stationary transponder was deployed. A linear meter, 5 meters long was dropped from the surface vessel. The intention was to capture the meter in the photo mosaic to measure image distortion of the resulting mosaic. Unfortunately the meter landed outside the coral area. Only sub patches were created using the Matlab based photo mosaic software and no map of pixel distortions was created. The photo mosaic was however compared to the side scan imagery and bathymetry of the area. The correspondence to the sonar data is positive. The western corner in Figure 10.4 contain low density of coral, and in the sonar data this area appear flat and with little reflectance. The eastern corner is elevated with high surface roughness in the sonar records. This corresponds well to the photo mosaic results.

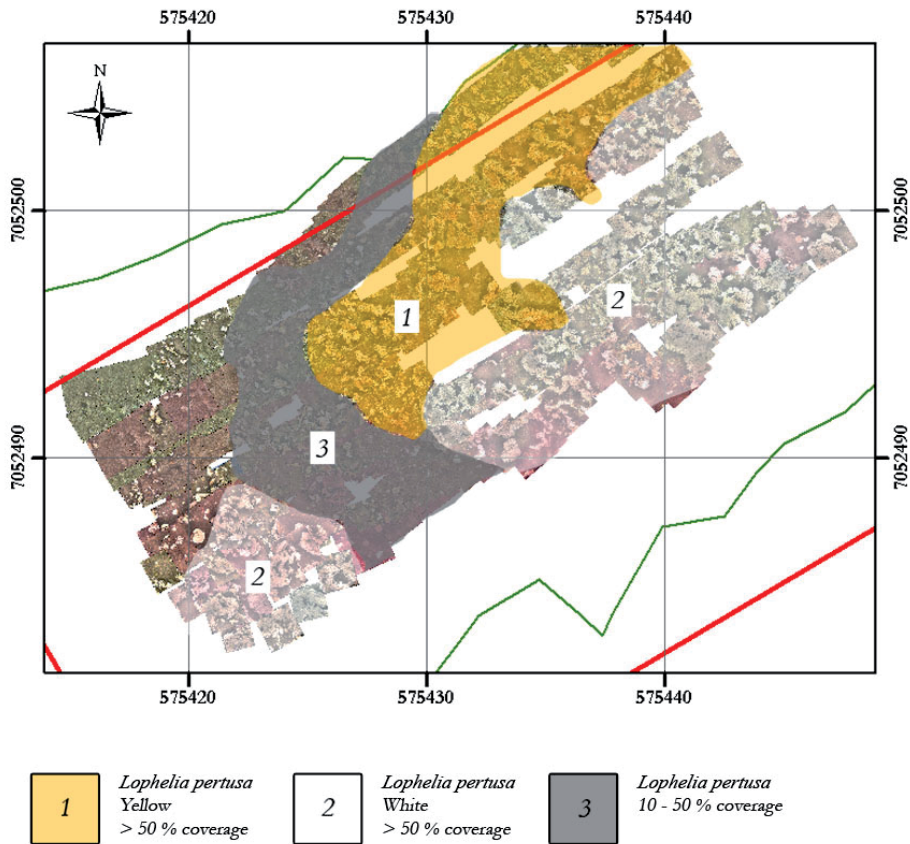


Figure 10.4 The area for the photo mosaic and the zonation of the reef. Light limitation has caused red sear in some of the images.

10.4 Discussion

10.4.1 Biological

This investigation has established a map of the distribution and density of *Lophelia pertusa* and its colour morphologies. The issues rose in the introduction concerning seabed type, taxa, species and morphological variants have been thoroughly addressed using photo mosaic. The documentation has been sufficiently detailed to identify species of macro fauna as described in Table 10.1. Individual specimen of macro fauna can be identified in the imagery. In Figure 10.4 it seems like the yellow stony coral is forming a band in the border area of the coral colony. Outside the area with more than 50% coverage of yellow *Lophelia pertusa* seen in Figure 10.4, the different colour morphologies seem to coexist.

The zonation and categories of seabed types could have been analysed further. The categories chosen here are established based on the findings. Some level of

standardized seabed categories would allow this study to be included in comparative studies. A numerical tool could have been created for the seabed characterisation. The potential of the Coral Point application (Kohler and Gill 2006) can be explored. General pattern recognition techniques can also be tested for determining the stony coral coverage.

10.4.2 Method

Due to the low seabed altitude the area coverage of each image was low. The intended line spacing was one meter. This put strict requirements to the ROV manoeuvring as mentioned in section “9.3.2 Data acquisition plan”.

To cope with accumulating geometrical distortions, patches of photo mosaic were created and geo-referenced. The error accumulation is then reset for every patch. The photo mosaic processing scheme would benefit from including the navigation data in the processing. Navigation is crucial for practically all underwater applications undermining the argumentation for keeping the processing scheme independent of navigation data.

An additional approach for reducing the accumulated geometrical errors of the photo mosaic is to calibrate the camera. Low overlap conditions the area close to the edge of the image is important for the mosaic, as it is more exposed to distortions than the centre of the image.

Strobes would probably have increased the level of light in the imagery and the image quality and hence improved the foundation for the photo mosaic. The camera shutter speed would also have been reduced decreasing the potential for motion blur in the imagery. Increased level of light would have allowed higher ROV seabed altitude. Because of the vertical extent of the corals, higher seabed altitude would have reduced the distortions to the imagery.

11 Photogrammetry

11.1 Introduction

Photogrammetry is used to create detailed 3D models of small sceneries. From overlapping imagery the xyz position of common image points are calculated. The laws of physics governing photogrammetry allow higher resolution results than the acoustic processes determining the resolution for sonar data. For maritime archaeological sites and marine biological observation stations the position, dimensions, colour, texture and shapes of objects are important records. An example of scientific application of underwater photogrammetry models is given in (Ludvigsen, Singh et al. 2006).

Underwater photogrammetry is exposed to specific challenges not found in terrestrial photogrammetry due to the attenuation of light in seawater. Hence the distance from the camera to the seabed is limited and usually below 5 meters. The vertical extent of the object is often large relative to the distance to the object. The vehicle carrying the camera must also hold the light source and this causes the illumination of the given objects to shift from image to image. Only small areas of the seabed can be covered in a single image and a photogrammetry model covering a site must be compiled from several two-view models. Photogrammetry relies on knowledge of the cameras position and orientation (pose) for each image. The navigation accuracy required for photogrammetric application is challenging to achieve with present underwater navigation systems. On the other hand, photogrammetry solutions can be used to reduce navigation uncertainties (Eustice, Pizarro et al. 2004).

11.1.1 Previous work

Underwater photogrammetry has been used for archaeology for some time (Rosenscrantz 1975) using manual extraction of common points (Green and Gainsford 2003). Biological applications of photogrammetry were early showed by Torlegar and Lundälv (Torlegard and Lundalv 1974) and more recently by Chong (Chong and Stratford 2002). An alternative approach based on automatic processing is given by Negahdaripour (Negahdaripour and Madjidi 2003). Negahdaripour applies a combination of optical flow and feature detection to establish 3D features from the image set. For terrestrial close range photogrammetry full models containing xyz-coordinates all pixels in the imagery have been demonstrated (Pollefeys, Koch et al. 2000).

Underwater photogrammetry is applied in a sub-discipline of offshore surveys called subsea metrology. In the 1990's stereo cameras were occasionally found on offshore ROV's. Photosea Systems Inc³³ produced of stereo cameras for the offshore branch. These cameras have lost popularity and stereo cameras are today only found in more specialized applications. Metrology is used for situations where high accuracy measurements are essential, like tie-in operations where oil and gas pipes are connected to templates and wellheads. Parker Maritime³⁴ has been in this market since 1999 and has currently developed propriotor photogrammetry software. Parker Maritime's method depends on markers placed on the object to be measured (Johannesen and Prytz 2005), (Parker 2009). Uncertainty is claimed to be a few millimetres, and a new system incorporating multiple camera as lasers for internal image reference is under development by Parker Maritime.

A promising photogrammetry system has been developed by the Australian Centre for Field Robotics, University of Sydney (Johnson-Roberson, Pizarro et al. 2009). This system is based on a two camera rig to ensure a constant baseline of image pairs. The seabed altitude provided by a DVL is used together with the navigation data to create a global model from a large set of image pairs.

11.2 The photogrammetry process

Photogrammetry survey execution holds many common characteristics to photo mosaic surveys like issues regarding camera and lights. But photogrammetry relies on accurate navigation and orientation data to be able to compute the position of the common data points. There are two ways to achieve the necessary knowledge of distance and orientation of the camera for the two images in an image pair. Two or more cameras can be mounted on a frame and with known relative positions and orientations can shoot simultaneously. If a single camera is applied, the position and orientation of the camera must be measured for all images. In this application the later approach is used. The position accuracy requirements exceed what most acoustic baseline systems can offer. Since it is the relative position and orientation of two subsequent images that is important, dead reckoning can be utilized. Doppler log or accelerometer data are then integrated over time to calculate the positions of the camera. Since the time span between two subsequent images is short the position drift will be correspondingly low. Heading, roll and pitch measurements are naturally important and can be recorded by an IMU. Measurements of seabed altitude are used in the model calculation.

Before the photogrammetry processing can start the images must be corrected for light artefacts. Camera calibration must be completed to obtain the intrinsic camera parameters. The first step in creating the photogrammetry model is to create a local model of the common points in an image pair. This is computed for all overlaps in the image set. The next step is to combine these local models into a global model.

³³ Photosea Systems Inc, San Diego, CA, USA

³⁴ Parker Maritime, Stavanger, Norway

The photogrammetry scheme presented here is a post processing scheme. It is however theoretically possible to develop this technique into an online processing and model construction tool.

11.2.1 Local models

When the images are captured, common interest points are identified and matched using the Harris detector and Zernike moments as described for photo mosaic (Eustice 2005). A SIFT (Scale Invariant Feature Transform) (Lowe 2004) operator is also used to establish and identify interest points. Navigation data is used to identify overlapping image patches before the search for interest points starts. When common points are found the essential matrix, E , is computed.

The fundamental matrix, F , in eq. (11.1) correlates two images as described in Hartley and Zisserman (Hartley and Zisserman 2003). The calibration matrix, K , is known from the camera calibration and contains the coordinates of the camera principal point u_0, v_0 , skew s and focal length α_x, α_y in eq. (11.2).

$$x'^T Fx = 0 \quad (11.1)$$

$$K = \begin{bmatrix} \alpha_x & s & u_0 \\ 0 & \alpha_y & v_0 \\ 0 & 0 & 1 \end{bmatrix} \quad (11.2)$$

The essential matrix is special a case of the fundamental matrix, F , incorporating the camera calibration parameters, see eq. (11.3).

$$E = K^T F K \quad (11.3)$$

$$x'^T E x = 0 \quad (11.4)$$

In eq. (11.4) x and x' represents the real-world coordinates of a common point represented in two image frames. The translation and rotation associated with the image pair is represented by t_x and R in the essential matrix in eq. (11.5). The calculation of the essential matrix involves estimation of the camera calibration parameters, 3 axis rotations, translation and seabed altitude. In eq. (11.8) \underline{u} and \underline{u}' represents the normalized coordinates of a common point in the two images in image coordinates, see eq. (11.7).

$$E = [t_x] R \quad (11.5)$$

$$\underline{u} = P \underline{X} \quad (11.6)$$

$$\underline{u} = \begin{bmatrix} u \\ 1 \end{bmatrix} \quad (11.7)$$

$$\underline{u}' = \frac{K R K^{-1} \underline{u} + K t / Z}{R_3^T K^{-1} \underline{u} + t_z / Z} \quad (11.8)$$

$$P = K \begin{bmatrix} {}^cR \\ {}_wR | {}^c t_{cw} \end{bmatrix} \quad (11.9)$$

P represents the projection matrix in eq. (11.9) and eq. (11.6) is used to perform the mapping from image coordinates to world coordinates. Using eq. (11.6) and epipolar geometry the positions of the interest points can now be calculated. There are uncertainties associated with the parameters used in these calculations, and statistical tools are applied to achieve an acceptable result. Using Horns relative orientation algorithm, the positions and orientations of the cameras are recalculated before a two-view bundle adjustment is applied to establish the final estimate for camera and positions and orientations. The positions of all common interest points are triangulated using two-view transfer model to form the local model (Eustice 2005).

11.2.2 Global models

The next step is to combine the local models to a global model. Initially the local models are related by navigation data. The relative scale, orientation and position of each local model must be determined. To determine scale when two local models are combined, pairs of common points are identified in both models. Then the internal distance for each pair of points are identified. Comparing this distance, d , for both local models, a measure for the scale is found. This is performed for all pairs of points, and each pair result in an estimate of scale. The standard deviation of the computed scale is then calculated, and values outside a cut off value are taken out. The final scale, S , value is then calculated as mean of the remaining selection, eq. (11.10).

$$S = \frac{1}{N} \sum_N \frac{d_{ig}(p_{s1}, p_{s2})}{d_{li}(p_{s1}, p_{s2})} \quad (11.10)$$

In eq. (11.10) N denotes the number of point-pairs considered while points p_{s1} and p_{s2} are randomly chosen points corresponding to the local and the global model. A similar procedure is performed to calculate rotations and translations, t , see eq. (11.11).

$$t = \frac{1}{N} \sum_N d(p_{ig}, p_{li}) \quad (11.11)$$

Most local models overlap with more than one local model. The scale, position and rotation are calculated for all overlaps. A common mean is then calculated for all overlapping values. In a lawn mower pattern this implies that the start of one line is connected to the end of the next survey line. This considerably limits the accumulation of error in the model. When all local models are scaled, rotated and translated into the global model, the global model is a point cloud representing the photogrammetry model.

Typically, 300 – 1000 data points are produced for each image pair (Ludvigsen, Singh et al. 2006). This is in the same range as the solution proposed by Johnson-

Roberson from University of Sydney (Johnson-Roberson, Pizarro et al. 2009). Johnson-Roberson demonstrates large area coverage capabilities and a streamlined software solution. The accuracy of the method presented in this thesis is unfortunately not controlled by calibration, but it can be expected that it is in the same range as Johnson-Roberson.

11.3 Survey design

A survey plan should be prepared before the project is executed also for photogrammetry surveys. The template for survey plans established for bathymetry surveys can be applied. The dimensions and uncertainties are however significantly different for photogrammetry surveys. The dimensions of the area of interest are reduced with more than a decade and the uncertainties of the resulting data are correspondingly lower. The data density is also increased compared to bathymetry sonar data sets.

11.3.1 Instruments

The requirements for precision are high and camera calibration is mandatory in photogrammetry as showed in the subsequent equations. Heading, roll and pitch sensor (IMU) are essential and the internal position of the camera and IMU must be measured and accounted for. Selection, installation and calibration of IMU are discussed in the sections for positioning and bathymetry surveys. The standards established for bathymetry can be applied selecting sensors for photogrammetry survey, see section “7.4 Standards”. DVL should also be installed on the ROV to strengthen the dead-reckoning solution used from one image frame to the next.

11.3.2 Data acquisition plan

The overlap must be above 50 % at all times since all areas of the seabed must be depicted at least twice. With 45° field of view and 3 meters seabed altitude, the line spacing must be less than 1.5 meters to ensure more than 50 % overlap on both sides. Assuming one meter line spacing the cross track error should be less than half a meter to ensure sufficient coverage. As mentioned in chapter 9 this is pushing the envelope in terms of positioning accuracy and manoeuvrability for common ROV's.

11.3.3 Data processing pipeline

Data validation

The data processing scheme is summarized in Figure 11.1. During the online data acquisition phase the collected images and navigation data should be monitored continuously to reveal eventual blunders as early as possible. Overlap, sharpness and exposure should be controlled closely during data collection. The time tag synchronization should be checked and the navigation data should be monitored. The position and orientation data should be assigned automatically online in real time for each image. Before the photogrammetry construction can start, the navigation data should be validated offline as discussed in section “4.4.1 Data validation”.

Data correction

The images must be corrected for lighting patterns before the photogrammetry construction can begin. These procedures are described in section “9.2.2 Illumination”. The necessary adjustments to the navigation data like horizontal or vertical datum transformations or compensation for known untreated sensor offsets is performed at this step.

Photogrammetry model construction

The 3D models of the site geometry is created applying images, camera calibration parameters and navigation data as described in section “11.2 The photogrammetry process”. When all xyz points are transferred to a common global model, the next step is to grid all the points in the global model into a data mesh. The mesh density is determined based on the data density. Typical values are 1 – 5 cm depending on the image quality and tuning of the processing setup. This mesh is the base for preparation of map products like contour plots, spot chart, shaded reliefs and 3D scenes.

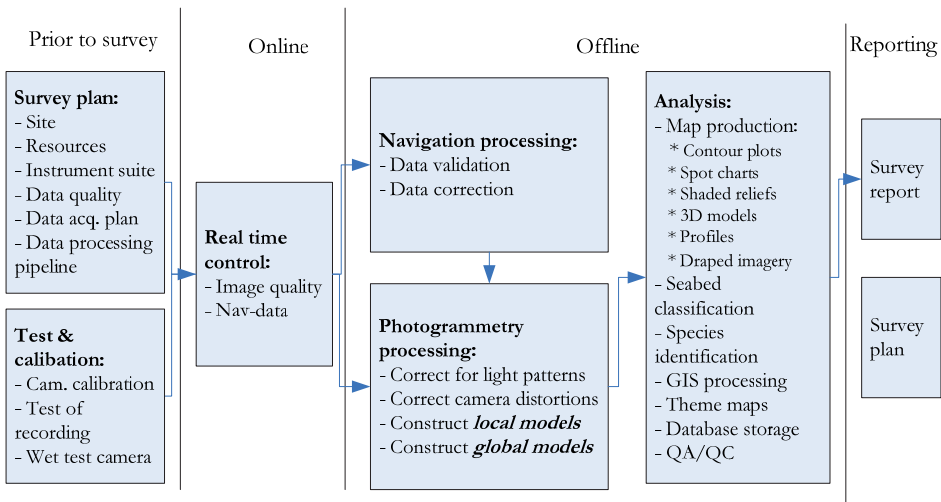


Figure 11.1 Data processing tube for photogrammetry.

11.3.4 Data analysis

The contour plot represents a quantitative measure of the results, see example in Figure 11.2. To achieve an understanding of the geometry of the site at a larger scale, a 3D scene can be constructed. This model can either be colour-coded for elevation, colour-coded for change in elevation, sun illuminated or draped with photo mosaic. 3D scenes are only qualitative, but efficient to increase the understanding to the site. Similar to bathymetry survey and photo mosaic surveys, the area of interest can be geologically or biologically classified according the present sediments and key species identified. The data analysis should advance into GIS processing and theme maps.

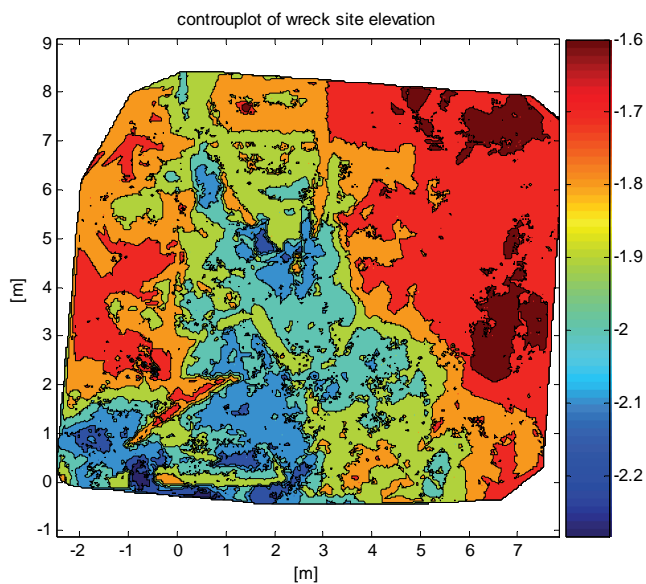


Figure 11.2 The elevation of an archaeological site measured using photogrammetry.

11.3.5 Data management

Raw data should be stored along with the survey plan and the survey report. Raw data includes navigation data like positions, orientation angles, seabed altitudes and qualities measures. Raw images and camera calibration data should be stored. A data processing description should be written and stored together with a metadata document for all raw data. Scripts of computer code applied in the processing must be saved together with the raw data.

When the data are ready to be imported to GIS depends on the GIS tools and the processing software. Metadata are mandatory also for data products like contour plots and 3D models. S-44 gives some advices of the content of metadata for topography models.

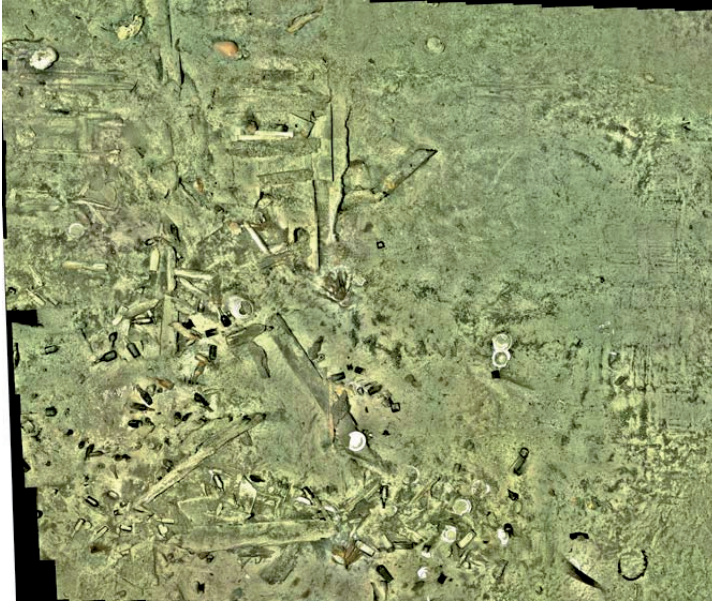


Figure 11.3 The area seen in Figure 11.2 documented using photo mosaic. The pit in the middle of the area seen in Figure 11.2 is also visible in the photo mosaic. Three wooden planks forming a triangle are also recognized.

11.4 Applicable standards

As there are no established best practises for underwater photogrammetry and there are no directly applicable standards. However, the S-44 can be applied for the geo-tagging of the photogrammetry model. The S-44 standard also contains descriptions of proper metadata of bathymetry data sets which can be used as a guideline for metadata of photogrammetry.

11.5 Quality assurance and control

As for photo mosaics, the most accurate proof of the model accuracy is to place an object with known shape and dimensions in the area of interest. Such an object can for example be a scale bar. The scale bar is a reliable proof of quality but not very useful if one is trying to tune the processing for improved accuracy. The statistical properties found when the local models are compiled to a global model are more informative about the weaknesses of the results in this respect. In addition to x-, y- and z-coordinates the data points will have deviations associated to them. The scale, rotations and translations are, as described, based on average calculations. Each point has a deviation from the average value. This deviation from average can be gridded and plotted as a spot chart analogous to seabed elevation illustrating the internal integrity of the global photogrammetry model.

11.6 Reporting

The report scheme should follow the template laid out in the section in section “5.6 Reporting”. The report should contain project motivation, description of the location, survey pattern, hardware description, digital processing description together with the results. At minimum, a contour map and a 3D scene with draped photo mosaic should be presented. Particularly interesting details can be pulled out and described and illustrated separately. Spot chart of photogrammetry model internal integrity should also be part of the results along with quality estimate of the geo-referencing. The report will should also include metadata for the data records and products.

12 Closure

This work intends to exploit the complementary properties of the methods presented. Video provides information about the substrate, macro fauna species and the condition of the specimen. Bathymetry data present information about the topography in the area of interest and creates a geological context for the research site. Depending on data quality and seabed type, possible coral areas can be extracted. For more detailed documentation and collection of data like seabed type, distribution of sediments, distribution of taxa and biological condition, photo mosaic are needed. For high resolution 3D measurements and analyses on an individual specimen level, photogrammetry is efficient. The supplementary properties of bathymetry, side scan, sub bottom profiles, photo mosaics and photogrammetry data for archaeological applications are discussed by the candidate (Ludvigsen and Soreide 2006).

12.1 Protocol template structure

Using a generic template, the survey protocols become more comprehensible. The generic survey template is seen Figure 12.1. In this thesis, the template is adapted to video survey, bathymetry survey, photo mosaic and photogrammetry. Some of the FR/DP are developed in sub-level matrixes. Table 7.1 and Table 12.2 show how the “data quality – instrument configuration” design process can be broken down. Likewise Figure 7.4 shows more details of the design of the processing pipeline.

Each of the 4 stages (prior to survey, online, offline and reporting) are analysed and advices and guidelines are developed. The survey design is performed prior to the survey and shall result in the survey plan. Using axiomatic design to formulate what we want from the survey plan, these FR’s are established:

Table 12.1 The top level of axiomatic design for survey plans for ROV-based surveys

FR \ DP	Instrument suite configuration	Operational parameters	Processing resources
Data quality	X		
Acquisition plan	X	X	
Processing pipeline	X	X	X

Table 12.1 is a general version of ref for video surveys. Based on the desired data quality instruments are chosen and configured. It is important to start here as these choices are controlling the design space for the acquisition plan and the processing pipeline.

Table 12.2 General presentation of the design parameter instrument suite configuration also seen in Table 7.1

	Seabed coverage	Instrument data resolution	Instrument dimensions	Data and power interface	System resolution and system design
Acquisition efficiency	X				
Data density and data resolution		X			
ROV mountable			X		
ROV operable				X	
Data accuracy					X

The common characteristics of various data sets and survey types are exploited in the structure and the knowledge compiled in this thesis more available to the reader. On the other hand, applying a common template will require adaptations for each application. An example from this work is the design of the data processing pipeline; video surveys without statistical analysis require only minor processing after the survey is complete. Protocol template points like data validation, data filtering and data corrections are hence cumbersome to apply for video surveys while for bathymetry surveys the processing is comprehensive.

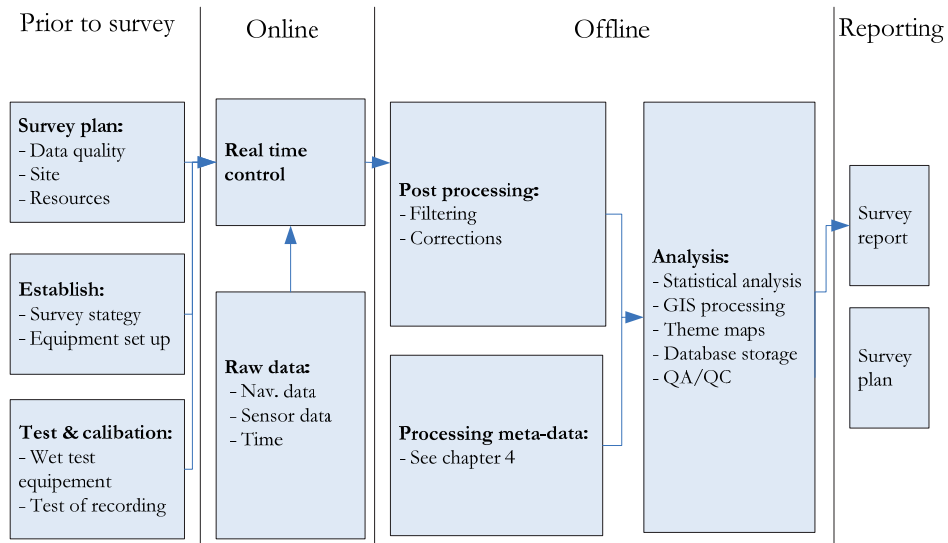


Figure 12.1 General processing tube for ROV surveys.

12.2 ROV survey strategy

12.2.1 Survey phases and sequence

Four categories of coral research were introduced in section 2.2 “Functional requirements for ROV-based habitat mapping”. The survey protocols does not address these survey categories individually, but can be applied to the various stages of documentation according to Figure 12.2. These categories of coral research are related to the investigation phases all depending on the subsequent survey steps.

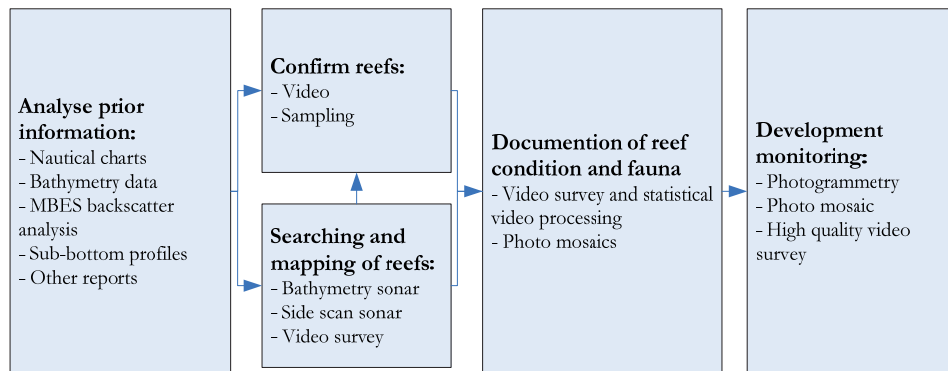


Figure 12.2 Data requirements for the different coral reef survey phases.

Analyse prior information

On an unknown site, the first investigation phase would be to pinpoint areas with increased potential for coral presence based on the available prior knowledge, like

nautical charts, existing bathymetry data, backscatter analysis of multibeam echosounder data, sub bottom profiles, or simply reports from local fishermen. The analysis of existing information can result in either search areas or distinct target locations.

Confirm reef presence

The core task of target confirmation is simple; provide imagery of the seabed to prove or disprove coral presence. For distinct target points it is sensible to establish a small grid of survey lines and make a small survey in case the observation is not immediately positive. The position uncertainty of the information used to establish the target points is often unpredictable. It can however be noted that for occasions where ROV has not been available, grabber or corer has been used for coral reef confirmation. Various drop cameras have also been used (Mortensen, Roberts et al. 2000), (Gordon, McKeown et al. 2007).

Searching and mapping of coral reefs

As pointed out already in chapter 2, sonar and video are effective tools in searching for corals and mapping coral occurrences. Table 12.3 summarises the arguments for each method. Practical constraints are however often decisive for the choice of technique.

Table 12.3 Evaluation of methods for coral reef search and mapping

Bathymetry and side scan sonar	Video
+ Large coverage	+ Inexpensive hardware
+ Provide geo-context of site	+ High availability (All ROVs have video cameras)
	+ 100% observation confidence
	+ Simple processing
- Observations require ground-truthing	- Low area coverage
- Complex hardware setup	- Discontinuous mapping
- Complex processing	- Qualitative data

When reefs are observed in sonar data, the operation proceeds to target confirmation. Coral observations in bathymetry or side scan data require visual confirmation to ensure 100% confidence since coral reefs can be mistaken for exposed gravel and piles of rocks in sonar records.

Documentation of condition and fauna

When a coral occurrence is confirmed and further information is sought, the next phase would be recording the situation at the site. Questions regarding extension, conditions and zonation are relevant. Video and photo mosaic are the main tools, see Table 12.4. Video surveys are uncomplicated to execute, but to proceed from qualitative data to quantitative data the scope of processing increases considerably.

Another effective tool for mapping a reef is photo mosaic. Photo mosaics are more detailed and more intuitive to interpret, but the efficiency is low. The documentation should be sufficiently detailed to apply a biological seabed classification scheme like EUNIS.

Table 12.4 12.5 Evaluation of methods for documentation of numerical coral reef condition and associated fauna.

Video	Photo mosaic
<ul style="list-style-type: none"> + Inexpensive hardware + High availability (All ROVs have video cameras) 	<ul style="list-style-type: none"> + Easy to understand the site + Larger structures can be depicted + Easier to estimate dimensions of larger structures and patterns
<ul style="list-style-type: none"> - Hard to understand a site - Labour intensive to extract numerical information - Statistical analysis requires strict planning of survey track 	<ul style="list-style-type: none"> - More complex setup of hardware and data processing - Higher requirements for data quality for mosaic processing - High requirements for survey execution to obtain full seabed coverage

Development monitoring

Development monitoring is the most detailed level of investigation and requires ability to revisit specific specimen and measure dimensions, colour, texture and shape of the specimen. Photo mosaic and photogrammetry can be used to document the status of the specimen. High quality video with laser scales can also be used for this purpose. Photogrammetry has an advantage over video since photogrammetry is inherently quantitative.

Table 12.6 Advantages and disadvantages of survey methods for development monitoring

Video	Photo mosaic	Photogrammetry
<ul style="list-style-type: none"> + Video is known to most researchers + Simple setup 	<ul style="list-style-type: none"> + Quantitative data 	<ul style="list-style-type: none"> + 3D data + Quantitative data
<ul style="list-style-type: none"> - Challenging to extract quantitative data 	<ul style="list-style-type: none"> - 2D data - Complex data processing 	<ul style="list-style-type: none"> - More complex hardware setup - More complex data processing

12.2.2 Survey resolution and efficiency

The fundamental trade-off when choosing survey tool is coverage and resolution. The survey method selection are previously elaborated, but Table 12.7 compares coverage and resolutions quantitatively.

Table 12.7 Typical survey efficiencies for the methods described

	Data resolution	Efficiency	Overlap	Swath width	Line spacing	Velocity
<i>Unit</i>	<i>[m]</i>	<i>[m²h⁻¹]</i>	<i>[%]</i>	<i>[m]</i>	<i>[m]</i>	<i>[ms⁻¹]</i>
Video	0.04	37000	-	3	20.0	0.5
Bathymetry	0.5	92600	60	80	50.0	0.5
Photo mosaic	0.02	1300	50	3	2.0	0.2
Photogrammetry	0.04	460	200	3	1.0	0.1

In Figure 12.3 a 3D scene of the Tautra ridge is shown to illustrate the coverage of acoustical surveys (side scan sonar) and optical surveys (photo mosaic). The sonar data set presented in chapter 8 and the photo mosaic discussed in chapter 10 are draped on high density data from the Norwegian Mapping Authority.

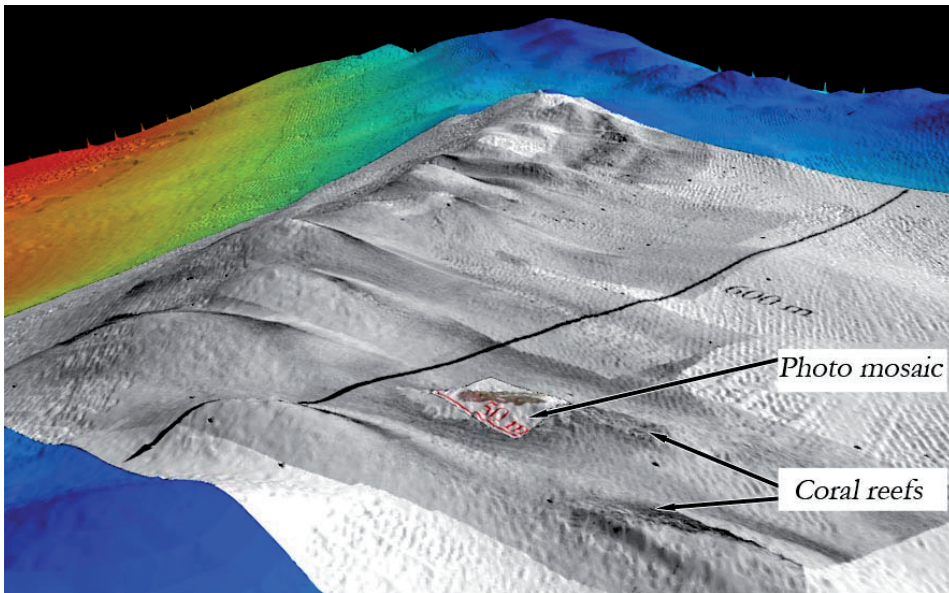


Figure 12.3 3D scene from the Tautra ridge illustrating the differences in scales area of interests for side scan sonar and photo mosaic

12.2.3 Data management

For data storage, interpretation, comparison, exchange, and creation of map products the data should be entered into a GIS database. Data from different survey campaigns can in a proper configured system be found intuitively. The database structure should enable easy searches based on either: time, location, project, data type, species and habitat type. This ability to uncomplicatedly find and hold together data sets strengthens the quality control and site understanding. Most available GIS software vendors have comprehensive generic analysis tools for statistical properties of data. A GIS database should be set up to allow fellow researchers to add, access and edit data. The storage system will hence facilitate increased usage and value of the survey data. To maximize data compatibility to other users and applications, the GIS database should be as general as possible and data entered into the database should be possible to re-export without loss of quality.

Raw data and metadata necessary to reproduce the results should hence be stored along with the processing procedure and necessary software. The storage facility must naturally have proper back up routines.

MinervaBase

All data presented in this project is compiled into a common GIS database called MinervaBase. The database is implemented using ArcGIS software by ESRI and allows data to be exported to fellow researchers with specific format requirements. The database contains:

Table 12.8 MinervaBase data types

Background data	ROV survey data
Terrestrial map	ROV tracks and navigation data
Nautical charts	Video and video event data
Hydrographic base data	Bathymetry data
	Side scan data
	Photo mosaics
	Still images

12.3 Design framework applied

In design theory it is common to start with the tasks to be solved and initially be free from connections to solutions. There are however examples that departing from technical concepts has been successful. The Norwegian Hugin AUV project started out “backwards”; the Norwegian Defence Research Establishment (FFI) had a salt water battery to which they sought an application (Hasvold, Johansen et al. 1999). To create an application for the battery, FFI built the first Hugin AUV. Later salt water batteries were abandoned for the Hugin vehicle, but the FFI AUV technology has grown to be world leading (Vestgaard 2007).

For our design task NTNU had the ROV and sought applications for it. But from that point on, the design had more freedom and could continue establishing functional requirements and searching for proper solutions. The axiomatic design was useful for organizing the design situation. Categorizing the variables and parameters controlling the outcome of a survey enhances the survey design process. Axiomatic design does however require some training to categorize parameters and variables. But the idea of independent and semi-independent design has made the survey protocols proposed more robust to adaptations. Individual variables can be changed without re-engineering the full protocol.

In this work the axiomatic design method is only used at a conceptual level. To take full advantage of the possibilities of the axiomatic design features, the development of sub-designs should have been symmetrical for all types of surveys and operations. Axiomatic design is not used for design choices that are trivial, as this would complicate the design process. The cost of completing axiomatic design formulation for all design solution is not proportional to the benefits in this case.

12.4 Future work:

There are three directions of departure continuing the work on this thesis for ROV-based seabed documentation: 1) Improving existing protocol entries, 2) Adding new protocol entries, and 3) developing new seabed documentation tools.

The video survey protocol would benefit from a case example for seabed classification applying a recognised seabed classification scheme on a larger data set. The seabed classification performed in the presented photo mosaic case example relies on subjective interpretation. For photo mosaics an automatic seabed classification system enable time series of a coral habitat to monitor changes. With the decreasing pH-levels in the ocean these time-series are ever more interesting. The photogrammetry protocol needs a case example to show biological interpretation and complement the archaeological example given in (Ludvigsen, Singh et al. 2006).

Side scan sonar, sub-bottom profiler and laser line scanners are seabed documentation sensors which all have a considerable potential for scientific ROV applications. Side scan sonar is briefly mentioned in the bathymetry sonar case example, but deserves a separate protocol entry. Side scan sonars are effective searching for objects on the seabed, and usually have better resolution than bathymetry sonars. For searching corals and mapping coral reef extension they are effective, as shown in the case example for bathymetry sonar. Sub-bottom profilers are frequently used on ROV's for surveys for the oil and gas industry. For coral research they provide information about the geology of the site. They can also collect information of the vertical extent of coral structures.

The need for a closed loop control system with auto-track and auto-positioning functionality have been called for in this thesis. Such a system would benefit the data acquisition and data quality of sonar-, photo mosaic- and photogrammetry surveys. Spectral processing of imagery for photo mosaic is an interesting path to

increase the information of photo mosaic surveys. Laser line scanner can possibly close parts of the gap between coverage and resolution for the instrument presented in this thesis. Some laser line scanners also provide information about the spectral distribution of the reflected light which can be used to identify matters found in the seabed substrates.

13 References

- Allais, A.-G., P. M. Sarradin, et al. (2006). Delievrable N 2D3 Report on image mosaic building. IFREMER, IFREMER: 16.
- Allmendinger, E. E. (1990). The Basic Design Process. Submersible vehicle systems design, Jersey City, N.J. : Society of Naval Architects and Marine Engineers: 1-48.
- Ballard, R. D. (1975). "Photography from a submersible during a famous project." Oceanus **18**(3): 40-43.
- Ballard, R. D. (1987). Discovering the Titanic. New York, NY: Warner/Madison Press.
- Ballard, R. D. (1993). "The MEDEA/JASON remotely operated vehicle system." Deep-Sea Research, Part I (Oceanographic Research Papers) **40**(8): 1673-87.
- Ballard, R. D., A. M. McCann, et al. (2000). "Discovery of ancient history in the deep sea using advanced deep submergence technology." Deep-Sea Research, Part 1: Oceanographic Research Papers **47**(9): 1591-1620.
- Bates, C. R. and P. Byham (2001). "Swath sounding techniques for nearshore surveying." Hydrographic Journal **100**: 13-18.
- Britting, K. R. (1971). Inertial Navigation System Analysis. Cambridge, Wiley Interscience.
- Brooke, S., J. Järnegren, et al. (2005). Reproduction of Lophelia pertusa from Norway and the Northern Gulf of Mexico. Third International Symposium on Deep-Sea Corals, Miami, Florida.
- Burdon-Jones, C. and H. Tambs-Lyche (1960). Observations on the fauna of the North Brattholmen stone-coral reef near Bergen. Bergen.
- Burt, P. J. and E. H. Adelson (1983). Multi-resolution splining using a pyramid image representation. Applications of Digital Image Processing, San Diego, CA, USA, SPIE.
- Caress, D. W., H. Thomas, et al. (2008). High-Resolution Multibeam, Sidescan, and Subbottom Surveys Using the MBARI AUV D. Allan B. Marine Habitat Mapping Technology. J. R. Reynolds and H. G. Greene, Alaska Sea Grant College Program: 47-69.
- Chautón, M. S. (2005). Nuclear magnetic resonance spectroscopy of marine microalgae: metabolic profiling and species discrimination from high-resolution magic angle spinning NMR analysis of whole-cell samples. Trondhjem biologiske stasjon, Department of Biology. [Trondheim], NTNU. **PhD**: 1 b. (flere pag.).

- Chong, A. K. and P. Stratford (2002). "Underwater Digital Stereo-Observation Technique for Red Hydrocal Study." Photogrammetric Engineering & Remote Sensing **68**(7): 745-751.
- Christensen, O. (2006). SUSHIMAP: survey strategy and methodology for marine habitat mapping. Department of Electronics and Telecommunications. Trondheim, NTNU. **PhD**: 210.
- Coggan, R., A. Mitchell, et al. (2007). Recommended operating guidelines (ROG) for underwater video and photographic imaging techniques. V. w. group, MESH: 32.
- Coggan, R., J. Populus, et al. (2007). Review of standards and Protocols for Seabed Mapping MESH. R. Coggan, J. Populus, K. Sheehan, F. Fitzpatrick and S. Piel, MESH: 210.
- Dalheim, U. (2008). Hevet fra 240 meters dyp. Adresseavisen. Trondheim.
- Danson, E., A. McNeill, et al. (2003). Guidelines on the use of multibeam echosounders for offshore surveys. IMCA, IMCA: 67.
- Davies, A. J., J. M. Roberts, et al. (2007). "Preserving deep-sea natural heritage: Emerging issues in offshore conservation and management." Biological Conservation **138**(3-4): 299-312.
- Davies, C. E., D. Moss, et al. (2004). EUNIS Habitat Classification revised 2004, European environment agency - European topic centre on nature protection and biodiversity: 310.
- Davies, J., J. Baxter, et al. (2001). Marine Monitoring Handbook. Peterborough, Joint Nature Conservation Committee.
- de L. Wenneck, T., T. Falkenhaus, et al. (2008). "Strategies, methods, and technologies adopted on the R.V. G.O. Sars MAR-ECO expedition to the Mid-Atlantic Ridge in 2004." Deep-Sea Research Part II: Topical Studies in Oceanography **55**(1-2): 6-28.
- DSPL (2002). Multi SeaLite Specification San Diego, Deep Sea Power and Light: 2.
- DSPL (2008). LED Multi SeaLite Matrix. San Diego, Deep Sea Power and Light: 2.
- Edgington, D. R., D. E. Cline, et al. (2006). Detecting, tracking and classifying animals in underwater video. OCEANS 2006, Boston, MA, USA, IEEE Computer Society.
- Etnoyer, P. J., S. D. Cairns, et al. (2006). Deep-sea Coral Collection Protocols, NOAA: 49.
- Eustice, R. (2005). Large Area Visually Augmented Navigation for Autonomous Underwater Vehicles. Applied Ocean Science and Engineering. Woods Hole, Massachusetts Institute of Technology/Woods Hole Oceanographic Institution joint program. **PhD**: 187.
- Eustice, R., O. Pizarro, et al. (2004). Visually Augmented Navigation in an Unstructured Environment Using a Delayed State History. International Conference on Robotics and Automation, New Orleans, LA, USA, IEEE.
- Fofonoff, N. P. and R. C. Millard (1983). Algorithms for computation of fundamental properties of seawater. Paris, Unesco.

- Fossa, J. H., B. Lindberg, et al. (2005). Mapping of Lophelia reefs in Norway; experiences and survey methods, Springer-Verlag Berlin Heidelberg, New York, NY, United States.
- Fossa, J. H., P. B. Mortensen, et al. (2002). "The deep-water coral *Lophelia pertusa* in Norwegian waters: Distribution and fishery impacts." Hydrobiologia **471**: 1-12.
- Freiwald, A. (1998). Geobiology of *Lophelia pertusa* (scleractinia) reefs in the north Atlantic. Fachbereich Geowissenschaften. Kiel, der Universität Bremen. **Habilitation**: 116.
- Freiwald, A. (2002). "The Sula Reef Complex, Norwegian Shelf." Facies **47**: 179-200.
- Funk, C. J., S. B. Bryant, et al. (1972). Handbook of underwater imaging system design (TP-303). San Diego, CA, USA, Ocean Technology Dept., Naval Undersea Center.
- Gade, K. (2005). "NavLab, a generic simulation and post-processing tool for navigation." Modeling, Identification and Control **26**(3): 135-50.
- Gelb, A. (1974). Applied optimal estimation. Cambridge, MA, USA, MIT Press.
- German, C. R. (2004). RV Atlantis voyage 7 leg XXX, 06 Mar - 12 Mar 2004. UK ROV Isis - Engineering trials - Cruise Report of the Southampton Oceanography Centre
Southampton, UK, Southampton Oceanography Centre: 6-17.
- Gjølmesli, K. and G. Koch (2007). "John Cassons Blackburn Skua funnet i Trondheimsfjorden." Norsk luftfartshistorisk magasin(2): 32.
- Gordon, Jr., D. L. McKeown, et al. (2007). "Canadian imaging and sampling technology for studying benthic habitat and biological communities." Special Paper - Geological Association of Canada(47): 29-37.
- Gostnell, C. (2005). "Efficacy of an Interferometric sonar for hydrographic surveying: Do interferometers warrant an in-depth examination?" Hydrographic Journal(118).
- Gracias, N. and J. Santos-Victor (2001). Underwater mosaicing and trajectory reconstruction using global alignment. OCEANS 2001, Honolulu, HI, USA, MTS/IEEE.
- Gray, R. (2004). "Light Sources, Lamps and Luminaries." Sea Technology: 39-43.
- Green, J. and M. Gainsford (2003). "Evaluation of underwater survey techniques." The International Journal of Nautical Archaeology **32**(2): 252-261.
- Greene, H. G., M. M. Yoklavich, et al. (1999). "A classification scheme for deep seafloor habitats." Oceanologica Acta **22**(6): 663-678.
- Guinotte, J. M., J. Orr, et al. (2006). "Will human-induced changes in seawater chemistry alter the distribution of deep-sea scleractinian corals?" Frontiers in Ecology and the Environment **4**(3): 141-146.
- Hagen, P. E. and N. J. Stoerkersen (2006). HUGIN AUV for Force Protection in the Littorals, Norway.
- Hansen, R. E., T. Olsmo, et al. (2005). Synthetic aperture sonar processing for the HUGIN AUV. Euro-OCEANS 2005, Brest, France, MTS/IEEE.

- Harris, C. and M. Stephens (1988). A combined corner and edge detector. 4th Alvey Vision Conference, Manchester, UK.
- Hartley, R. and A. Zisserman (2003). Multiple view geometry in computer vision. Cambridge, Cambridge University Press.
- Hasvold, O., K. H. Johansen, et al. (1999). "The alkaline aluminium/hydrogen peroxide power source in the Hugin II unmanned underwater vehicle." Journal of Power Sources **80**: 254-60.
- Heikkila, J. and O. Silven (1997). Four-step camera calibration procedure with implicit image correction. Computer society conference on computer vision and pattern recognition, San Juan, Puerto Rico, IEEE.
- Hiller, T. M. and K. Lewis (2004). Getting the most out of high resolution wide swath sonar data. Hydro 2004, Galway, UK, The Hydrographic Society.
- Hoerner, S. F. (1965). Fluid-dynamic drag: practical information on aerodynamic drag and hydrodynamic resistance. Midland Park, N.J., S.F. Hoerner.
- Hovland, M. (2008). Deep-water coral reefs: unique biodiversity hot-spots. Dordrecht, Springer.
- Hovland, M., P. B. Mortensen, et al. (1998). "Ahermatypic coral banks off mid-Norway; evidence for a link with seepage of light hydrocarbons." Palaios **13**(2): 189-200.
- Hovland, M. and M. Risk (2003). "Do Norwegian deep-water coral reefs rely on seeping fluids." Marine Geology **198**(1-2).
- Hovland, M., S. Vasshus, et al. (2002). "Mapping and imaging deep-sea coral reefs off Norway, 1982-2000." Hydrobiologia **471**: 13-17.
- Huetten, E. and J. Greinert (2008). "Software controlled guidance, recording and post-processing of seafloor observation by ROV and other towed devices: The software package OFOP." Geophysical Research Abstracts **10**.
- ICES (2004). Report of the Benthos Ecology Working Group (BEWG). San Sebastian, Spain, International Council for the Exploration of the Sea: 102.
- IFREMER. (2010). "ADELIE." Retrieved 24.03, 2010.
- IHO (2008). IHO Standards for Hydrographic Surveys Special publication No. 44 5th edition, International Hydrographic Organization: 36.
- ISO (2007). Water quality -- Guidance on marine biological surveys of hard-substrate communities, International Organization for Standardization.
- Jaffe, J. (1990). "Computer modeling and the design of optimal underwater systems." Journal Oceanic Engineering **15**: 101-111.
- Jakuba, M., D. Yoerger, et al. (2004). "Mapping hydrothermal plumes in their rising and neutrally buoyant regimes with an autonomous underwater vehicle." Eos, Transactions, American Geophysical Union **85**(47, Suppl.).
- Jerosch, K., A. Ludtke, et al. (2007). "Automatic content-based analysis of georeferenced image data: Detection of *Beggiatoa* mats in seafloor video mosaics from the HAKon Mosby Mud Volcano." Computers and Geosciences **33**(2): 202-218.

- Johannesen, R. and F. Prytz (2005). "Underwater Metrology - Exploiting old techniques for underwater surveying and metrology." Hydro International(12): 22-23.
- Johansen, V. (2007). Modelling of flexible slender systems for real-time simulation and control applications. Trondheim, Norwegian University of Science and Technology, Faculty of Engineering Science & Technology, Department of Marine Technology.
- Johnson-Roberson, M., O. Pizarro, et al. (2009). "Generation and visualization of large-scale three-dimensional reconstructions from underwater robotic surveys." Journal of Field Robotics 27(1): 21-51.
- Jonsson, L. G. and T. L. Lundalv (2005). Laboratory Studies of Lopheliha pertusa Poly Behaviour in Different Current Regimes. Third International Symposium on Deep-Sea Corals, Miami, Florida, USA.
- Khotanzad, A. and Y. H. Hong (1990). "Invariant image recognition by Zernike moments." IEEE Transactions on Pattern Analysis and Machine Intelligence 12(5): 489-497.
- Kirkwood, W. J. (2000). "Tiburon: MBARI's new ROV integrated to a SWATH R/V." Sea Technology 41(6): 51-55.
- Kohler, K. E. and S. M. Gill (2006). "Coral Point Count with Excel extensions (CPCe); a Visual BASIC program for the determination of coral and substrate coverage using random point count methodology." Computers & Geosciences 32(9): 1259-1269.
- Kongsberg, M. (2004). APOS Basic Operator Course. Horten, Kongsberg Maritime: 210.
- Kongsberg, M. (2004). EM3002 Multibeam echo sounder The new generation shallow water multibeam. Horten, Kongsberg Maritime: 4.
- Kongsberg, M. (2005). HAIN Instruction manual. Horten, Kongsberg Maritime: 122.
- Kongsberg, S. (1993). Underwater television sensor selection criteria, Kongsberg Simrad: 21.
- Kongsberg, S. (1998). TV camera lighting in turbid water conditions, Kongsberg Simrad: 9.
- Kongsberg, S. (2001). Seatex MRU 6 - The Ultimate Marine Motion Sensor. Trondheim, Kongsberg Seatex.
- L-3-Communications (2000). Multibeam sonar theory of operations, L-3 Communications Seabeam Instruments.
- Larsen, M. B. (2000). High performance Doppler-inertial navigation-experimental results. Oceans 2000, Providence, RI, USA, MTS/IEEE.
- Lekkerkerk, H.-J., R. van der Velden, et al. (2006). Handbook of Offshore Surveying. London, Clarkson Research Services Limited.
- Lirman, D., N. R. Gracias, et al. (2007). "Development and application of a video-mosaic survey technology to document the status of coral reef communities." Environmental Monitoring and Assessment 125(1-3): 59-73.

- Lowe, D. G. (2004). "Distinctive image features from scale-invariant keypoints." International journal of computer vision **60**(2): 91-110.
- Ludvigsen, M., H. Singh, et al. (2006). Photogrammetric models in marine archaeology. Oceans 2006, Boston, MA, USA, IEEE/MTS.
- Ludvigsen, M. and F. Soreide (2006). Data fusion on the Ormen Lange shipwreck project. Oceans 2006, Boston, MA, USA, MTS/IEEE.
- Ludvigsen, M., B. Sortland, et al. (2007). "Applications of Geo-Referenced Underwater Photo Mosaics in Marine Biology and Archaeology." Oceanography **20**(4): 140-149.
- Marthiniussen, R., J. E. Faugstadmo, et al. (2004). HAIN an integrated acoustic positioning and inertial navigation system. Oceans 2004, Kobe, Japan, Marine Technology Society Inc.
- Milne, P. H. (1983). Underwater acoustic positioning systems. Cambridge, Great Britain University Press.
- More, T. (2005). Medical Treasures Under The Sea. UK, Sky Channel.
- Mortensen, P. B. (2000). Lophelia pertusa in Norwegian waters. Distribution, growth, and associated fauna. Department of Fisheries and Marine Biology. Bergen, University of Bergen. **Dr.Scient**.
- Mortensen, P. B., L. B. Mortensen, et al. (2008). "Occurrence of deep-water corals on the Mid-Atlantic Ridge based on MAR-ECO data." Deep-Sea Research, Part II: Topical Studies in Oceanography **55**(1-2): 142-152.
- Mortensen, P. B., J. M. Roberts, et al. (2000). "Video-assisted grabbing: A minimally destructive method of sampling azooxanthellate coral banks." Journal of the Marine Biological Association of the United Kingdom **80**(2): 365-366.
- Myhrvold, A., M. Hovland, et al. (2004). Baseline and environmental monitoring in deep water - A new approach. SPE International conference on Health, Safety and Environment in Oil and Gas Production, Calgary, Canada, SPIE.
- Negahdaripour, S. and H. Madjidi (2003). "Stereo Imaging on Submersible Platforms for 3-D Mapping of Benthic Habitats and Sea-Floor Structures." Journal Oceanic Engineering **28**(4): 625-650.
- Neulinger, S. C., A. Gartner, et al. (2009). "Tissue-associated "Candidatus mycoplasma coralicola" and filamentous bacteria on the cold-water coral *Lophelia pertusa* (Scleractinia)." Applied and Environmental Microbiology **75**(5): 1437-1444.
- Neulinger, S. C., J. Jarnegren, et al. (2008). "Phenotype-specific bacterial communities in the cold-water coral *Lophelia pertusa* (Scleractinia) and their implications for the coral's nutrition, health, and distribution." Applied and Environmental Microbiology **74**(23): 7272-7285.
- Neyts, A. and L. M. Sunde (2007). DesignACT Deliverable 3: Site evaluation and assessment plan. Trondheim, NTNU/SINTEF: 53.
- NORSOK (2003). U-102 Remotely operated vehicle (ROV) services. U-102 Remotely operated vehicle (ROV) services, rev.1 Oslo, The, Competitive Standing of the Norwegian Offshore Sector (Standard Norway): 46.

- Odegaard, O. T., B. Sortland, et al. (2001). An interdisciplinary marine research programme. How to promote generative interaction between marine scientists, modellers and engineers. Oceans 2001, Washington, DC, USA, MTS/IEEE.
- Olu-Le Roy, K., J. C. Caprais, et al. (2007). "Cold-seep assemblages on a giant pockmark off West Africa: Spatial patterns and environmental control." Marine Ecology **28**(1): 115-130.
- Opderbecke, J., P. Simeoni, et al. (2004). High resolution swath bathymetric sea-bed mapping with the ROV Victor 6000. International Offshore and Polar Engineering Conference, Toulon, France, International Society of Offshore and Polar Engineers.
- Orejas, C., A. Gori, et al. (2008). "Growth rates of live *Lophelia pertusa* and *Madrepora oculata* from the Mediterranean Sea maintained in aquaria." Coral Reefs **27**(2): 255.
- OSRAM (2008). High Noon 24/7. Product specification HMI light sources, OSRAM: 4.
- Parker, M. (2009). Nøyaktig oppmåling under vann med fotogrammetri. Stikningskonferansen 2009.
- Pinkard, D. R., D. M. Kocak, et al. (2005). Use of a video and laser system to quantify transect area for remotely operated vehicle (ROV) rockfish and abalone surveys. Oceans 2005, Piscataway, NJ, USA, IEEE.
- Pizzaro, O. and H. Singh (2003). "Towards Large Area Mosaicing for Underwater Scientific Applications." IEEE Journal of oceanic engineering **28**(4): 651-672.
- Pollefeys, M., R. Koch, et al. (2000). "Automated reconstruction of 3D scenes from sequences of images." Isprs Journal of Photogrammetry and Remote Sensing **55**(4): 251-267.
- Rapp, H. T. and J.-A. Sneli (1999). Lophelia pertusa - myths and reality. 2nd Nordic Marine Science Meeting, Hirtshals, Denmark.
- Ratmeyer, V. and R. Gross (2003). "Scientific applications for the electric quest WROV." Sea Technology **44**(12): 29-33.
- Reson, A. S. (2008). Seabat 7125 Product specification High resolution multibeam echosounder system: 2.
- Riemersma, G. (2004). Digital Video and GIS - The management of digital video. ROV support for underwater construction, Zierikzee, Hydro International magazine.
- Rinderic, J. R. and N. P. Suh (1982). "Measures of Functional Coupling in Design." Journal of Engineering for Industry **104**: 383-388.
- Rinderle, J. R. (1982). Measures in functional coupling in design. Dept. of Mechanical Engineering. Boston, Massachusetts Institute of Technology. . **PhD**: 163.
- Roman, C. and H. Singh (2007). "A self-consistent bathymetric mapping algorithm." Journal of Field Robotics **24**(1-2): 23-50.
- Rosenscrantz, D. M. (1975). "Underwater photography and photogrammetry." Photography, Archaeology research.

- Sakshaug, E. (1991). Økosystemet Barentshavet (in norwegian). Økosystemet Barentshavet (in norwegian). Trondheim, NFR: 300.
- Sakshaug, E. and J.-A. Snøli (2000). Trondheimsfjorden (Norwegian). Trondheim, Tapir forlag.
- Sarradin, P. M., K. O. Leroy, et al. (2002). Evaluation of the first year of scientific use of the French ROV Victor 6000. Underwater Technology, 2002., Tokyo, Japan, IEEE.
- Savage, P. G. (1998). "Strapdown inertial navigation integration algorithm design. 1. Attitude algorithms." Journal of Guidance, Control, and Dynamics **21**(1): 19-28.
- SeeByte (2007). SeeTrack Offshore. Edinburgh.
- Shepherd, K. and S. K. Juniper (1997). "Creating a scientific tool from an industrial ROV." Marine Technology Society Journal **31**(3): 48-54.
- Shucksmith, R., H. Hinz, et al. (2006). "Evaluation of habitat use by adult plaice (*Pleuronectes platessa* L.) using underwater video survey techniques." Journal of Sea Research **56**(4): 317-328.
- Sinclair D.J., W. B., Risk M. (2006). "A biological oorigin for climate signals in corals - Trace element "vital effects" are ubiquitous in Scleractinan coral skeletons." Geophysical Research Letters **33**(17): L17707.
- Singh, H., J. Howland, et al. (2004). "Advances in Large-Area Photomosaicking Underwater." Journal Oceanic Engineering **29**(3): 872-886.
- Singh, H., J. Howland, et al. (1998). Quantitative photomosaicking of underwater imagery. Oceans 1998, New York, NY, USA, IEEE.
- Singh, H., C. Roman, et al. (2007). "Towards high-resolution imaging from underwater vehicles." International Journal of Robotics Research **26**(1): 55-74.
- Soltwedel, T., M. Klages, et al. (2000). "French ROV Victor 6000 first deployment from Polarstern." Sea Technology **41**(4): 51-53.
- Sortland, B. and K. Vartdal (1990). Optimization of ROV Pipeline Inspection Speed. Intervention 90, Vancouver.
- Standards-Norway (2009). NS 9435:2009 Water quality - Visual seabed surveys using remotely operated and towed observation gear for collection of environmental data. Oslo, Standards Norway: 18.
- Størseth, T. R. (2006). Chrysolaminarans from marine diatoms: structural characterization and potential as immunostimulan[t]s. Department of Chemistry. Trondheim, NTNU. **PhD**.
- Suh, N. P. (2001). Axiomatic Design. New York, Oxford University Press.
- Svendby, E. (2007). Adaptive control of ROV. Department of Engineering Cybernetics. Trondheim, NTNU. **MsC**: 87.
- Torlegard, A. K. and T. L. Lundalv (1974). "Underwater Analytical System." Photogrammetric engineering **40**(2): 287-293.
- Tvedten, H. M. (2008). Her er det siste Blackburn Skua-flyet i verden. Dagbladet. Oslo.
- Tønset, M. (2008). Jakter på dødsskipet fra Falstad. Adresseavisen. Trondheim.

- Urick, R. J. (1983). Principles of underwater sound 3rd edition. Los Altos, Peninsula Publishing.
- Valentine, P. C., B. J. Todd, et al. (2002). Regional habitat classification as applied to the marine sublittoral of northeastern North America. Effects of Fishing on Benthic Habitats Symposium; Linking Geology, Biology, Socioeconomics, and Management,, Tampa, Florida.
- Vestgaard, K. (2007). "Well-travelled AUV surveys the world." International Ocean Systems **11**(1): 14-15+17.
- Vik, B. (2000). Inertial navigation systems. Lecture notes. Trondheim, NTNU: 45-83.
- Vincent, A. G., N. Pessel, et al. (2003). Real-time geo-referenced video mosaicking with the MATTISSE system. Oceans 2003, San Diego, CA, USA, MTS/IEEE.
- Volent, Z., G. Johnsen, et al. (2007). "Kelp forest mapping by use of airborne hyperspectral imager." Journal of Applied Remote Sensing **1**(1).
- Whitcomb, L. L., J. C. Howland, et al. (2003). A new control system for the next generation of US and UK deep submergence oceanographic ROVs. 1st IFAC workshop on guidance and control of underwater vehicles, Newport, South Wales, UK, IFAC.
- White, J., A. Mitchell, et al. (2007). Seafloor Video Mapping - Collection, analysis and interpretation of seafloor video footage for the purpose of habitat classification and mapping, MESH: 87.
- White, S. N., A. D. Chave, et al. (2002). "Investigations of ambient light emission at deep-sea hydrothermal vents." Journal of Geophysical Research B: Solid Earth **107**(1): 1-1 - 1-13.
- Wilson, O. B. (1988). Introduction to theory and design of sonar transducers. Los Altos, Calif., Peninsula Publ.
- Xu, X. and S. Negahdaripour (1997). Vision-based motion sensing for underwater navigation and mosaicing of ocean floor images. Oceans 1997, Halifax, NS, Can, IEEE, Piscataway, NJ, USA.
- Yoerger, D. and J. C. Kinsey (2009). "Deep ocean surveying with autonomous vehicles." The Journal of Ocean Technology **4**(1): 15.

A Article 1

Ludvigsen, M., B. Sortland, et al. (2007). "Applications of Geo-Referenced Underwater Photo Mosaics in Marine Biology and Archaeology." *Oceanography* **20**(4): 140-149.

Applications of Geo-Referenced Underwater Photo Mosaics in Marine Biology and Archaeology



BY MARTIN LUDVIGSEN, BJØRN SORTLAND, GEIR JOHNSEN, AND HANUMANT SINGH

IN DEEP WATER, below the photic zone, still and video imaging of the seabed requires artificial lighting. Light absorption and backscatter caused by typical seawater components, such as dissolved organic matter, plankton, and inorganic particles, often limit the artificially lit area to a few square meters. To obtain high-resolution photographic data of larger seabed areas, a series of images can be compiled into a photo mosaic. Image mosaics are easier to interpret, communicate, and exhibit than video footage or a series of images, because the individual image frames in a photo mosaic are naturally represented in a spatial context.

The ideal photo mosaic should provide an overview of the area of interest and the distribution, size, position, and orientation of the objects found. The final result should include all the details captured in the initial images. Marine archaeologists and biologists are typical users of this technology. The information provided by a photo mosaic can help archaeologists reconstruct the sequence of events that formed the features in an underwater investigation site. In marine biology, photo mosaics can be used to document habitats by identifying morphological characteristics of present taxa (e.g., size and color), density, area coverage, substrate, and interactions between individuals.

Beginning in the 1960s, underwater photo mosaics were produced by physically stitching images together to create new images from the arrangements of individual picture frames. One of the first examples of underwater photo mosaics in the literature shows the sunken submarine *Thresher* (Ballard, 1975). The photo mosaic of the sunken passenger ship *Titanic* (Ballard, 1987) is among the most famous examples. As technology progressed, specialized hardware emerged, combining two images into a new image using slides and variable projection planes. Development of the computer and digital image processing gradually led to digital production of image mosaics in the 1990s. Then, the scientific discipline of computer vision emerged, focusing on automatic information extraction from imagery. Many of the most common image mosaicking schemes were developed in a subdiscipline of computer vision called SLAM (Simultaneous Localization And Mapping) (Xu and Negahdaripour, 1997; Gracias and Santos-Victor, 2001; Vincent et al., 2003; Eustice, 2005). Successful applications of photo mosaicking include archaeological imaging by Ballard et al. (2000) and Singh et al. (2004a) as well as marine biological photo mosaics for species inventory (Singh et al., 2004b) and spectral image analysis to map the abundance of bacterial mats (Jerosh et al., 2007).

Today, high-resolution data can be used to generate a complete overview of a seascape and details of organisms, substrate, and artifacts. Likewise, high-resolution images can be used to generate three-dimensional images of objects of interest. Geo-localized and high-resolution images are important for

revisits to a given site or object of interest and are very important for obtaining time series (e.g., for process-oriented and climate-related research in marine biology). We present two case examples to elucidate applications of photo mosaics in marine biology and marine archaeology. The marine biological example is part of a habitat mapping survey in the fjord of Trondheim at Stokkbergnset (63°28'N, 9°54'E), approximately 20 km west of the city of Trondheim, Norway. The site comprises a vertical rock wall rising from 530 m to 200 m depth. The objective of the survey was to map the characteristics of benthic filter feeder communities dominated by stony corals, horny corals, and bivalves attached to the vertical wall at 250–450 m depth.

The archaeological photo mosaic example was made during an investigation of the pipe line routes for the Ormen Lange gas field off Aukra (62°4'N, 6°54'E) in the Norwegian west coast. Norwegian cultural heritage authorities requested a marine archaeological survey

of the pipeline routes for the gas field, which led to the discovery of a historical shipwreck close to the pipeline route at 170 m depth. The field developer was ordered to conduct a detailed investigation of the site (Søreide and Jasinski, 2005). Two of the photo mosaics resulting from this detailed investigation are presented in this study. The first covers the whole wreck site, while the second shows a condensed area at the stern of the wreck where sediment was removed to uncover historical artifacts.

METHODS AND MATERIALS

Underwater Vehicles

The work at the marine biology site was carried out by an electric observation remotely operated vehicle (ROV; Sperr AS Sub-Fighter 7500; Figure 1). Its low, ~ 400-kg weight provided easy handling, and the ROV proved to have sufficient maneuvering and payload capacity to handle the currents on the site, despite drag on up to 650 m of cable. The 60-ft, twin-hull support vessel was positioned

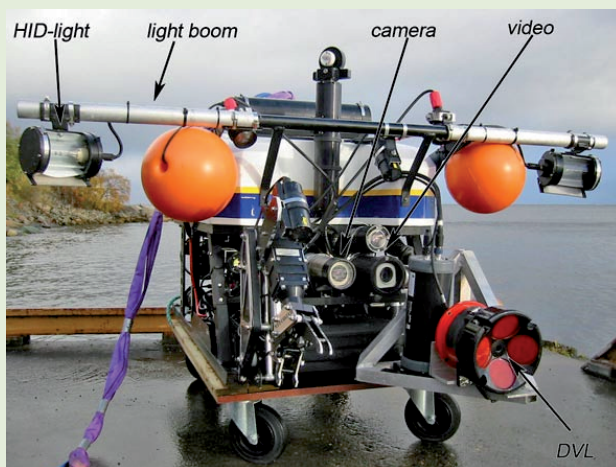


Figure 1. Configuration of the remotely operated vehicle *Minerva* used for image acquisition in a marine biology survey on the vertical rock wall of the fjord of Trondheim, Norway. The Doppler velocity log, high-intensity discharge lights, light booms, high dynamic range camera, and video cameras are all pointing forward.

using the Global Positioning System (GPS), and the location of the underwater vehicle relative to the surface vessel was measured by a super-short baseline acoustic system (Simrad HPR 300P). A Doppler velocity log (DVL; RDI Workhorse Navigator 600 kHz, Teledyne RD Instruments) was pointed forward.

At the marine archaeology site, an electric work-class ROV (WROV; Sperre AS Sub-Fighter 30k) was used. The WROV weighs about 1500 kg, has a large payload capacity, and thus was considered the best possible common platform for the variety of subtasks in the archaeology project. Because variations in camera angle during image acquisition can impose errors on the mosaic, a WROV is more favorable due to better stability in pitch and roll than a smaller vehicle. A closed-loop control system enabled the vehicle to follow the desired survey track automatically, resulting in more stable heading, speed, and seabed altitude than can be achieved by manual

control. The WROV was positioned by a long-baseline acoustical positioning system aided by a DVL (RDI Workhorse 1200 KHz, Teledyne RD Instruments).

An excavation support frame placed on the wreck site (Figure 2) enhanced the stability and maneuvering of the WROV during sediment excavation and image acquisition. The 10 x 10-m frame was leveled by ROV-operated jacks in all four corners. When the vehicle was docking into the support frame, it was kept rotationally and vertically steady. The WROV was moved in x and y directions by rack rails and gear motors, as described by Søreide and Jasinski (2005).

Camera and Light Configuration

In both surveys, constant lighting from two 400-W HID (High Intensity Discharge; OSRAM HMI) lights were used. One wide-beam light source was placed on either side of the camera to illuminate the image-frame area as evenly as possible. On the observation

ROV, the lights were mounted on booms to increase the lateral distance between light source and camera, with the aim of reducing backscatter light to the camera (see Figure 1). The lateral distance between the camera and light source was approximately 0.8 m. On the WROV, a lateral separation of light sources and camera of 0.7 m was obtained without light booms.

During the marine biological survey, the camera was mounted on the underwater vehicle with a horizontal image axis (i.e., aiming orthogonally at the rock wall). For the marine archaeological survey, the camera pointed downward, again imaging its target, the seabed, orthogonally. The camera used in both projects was a 12-bit dynamic range camera (Uniqvision) that captures one image every four seconds.

Survey Track Design

Optimal image overlap, sidelap, seabed resolution, and acquisition efficiency are essential to mosaic quality. They are achieved by carefully choosing proper altitude, line spacing, and velocity when planning the survey. The term “over-

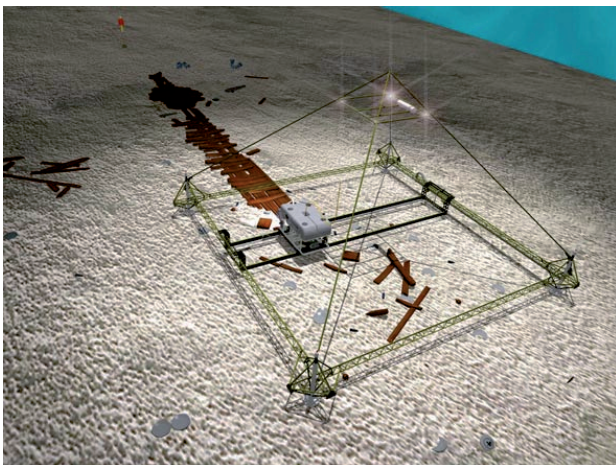


Figure 2. The excavation support frame placed over the aft part of a shipwreck during a marine archaeology survey in the Ormen Lange gas field off Aukra on the Norwegian west coast. The frame, leveled by jacks in each corner, is used to stabilize the work-class ROV during image acquisition. Figure provided by Fredrik Søreide

MARTIN LUDVIGSEN (*martinl@ntnu.no*) is Ph.D. candidate, Department of Marine Technology, Norwegian University of Science and Technology, Trondheim, Norway. BJØRN SORTLAND is Associate Professor, Department of Marine Technology, Norwegian University of Science and Technology, Trondheim, Norway. GEIR JOHNSEN is Professor, Department of Biology, Norwegian University of Science and Technology, Trondheim, Norway. HANUMANT SINGH is Associate Scientist, Applied Ocean Physics and Engineering Department, Woods Hole Oceanographic Institution, Woods Hole, MA, USA.

lap” is used for the common area in two images taken sequentially while the camera moves along a line, and “sidelap” denotes the common area of two images across track. The area covered by each image directly depends on the altitude of the vehicle and the camera’s field-of-view angle. A general recommendation for mosaics of aerial photography is to use 50% overlap and 25% sidelap. Practice has shown that this trade-off between redundant image points in image pairs and the need for effective data acquisition is also reasonable for underwater photo mosaics.

A 45° field of view was used in all data-acquisition operations described in this paper. This narrow field of view produces low obliqueness in images. Apart from the available propulsion power on the underwater vehicle, the survey speed is limited by the overlap constraint, covered area, and how often it is possible to take images during data acquisition. The potential for motion blur in the images captured was not considered when the theoretical speed was calculated.

Marine Biological Survey

During data acquisition for the marine biological study, the ROV followed horizontal paths along a vertical wall, with each path one meter shallower than the previous one, so that the rock wall was covered in a back-and-forth pattern similar to mowing a lawn. The ROV heading was kept constant so that the cameras always pointed toward the wall while the vehicle moved sideways.

The distance from the camera to the seafloor or wall target was approximately 2 m. This resulted in a coverage area of 2.3 m² for each image frame. The camera produced 1024 x 1024-pixel images, with each pixel covering 2.2 mm² of rock

wall. This resolution enables identification of specimens a few centimeters long, depending on the distinctness of their morphological characteristics.

In order to obtain a 50% overlap, we calculated that the velocity would theoretically be limited to 0.2 m s⁻¹. Heading

deviations resulted in overlap variations, and to compensate for this, the speed was lowered to 0.15 m s⁻¹. The vertical line spacing was one meter, providing a sidelap of 34%. The theoretical data collection efficiency was 800 m² h⁻¹ for this arrangement. The photo mosaic in

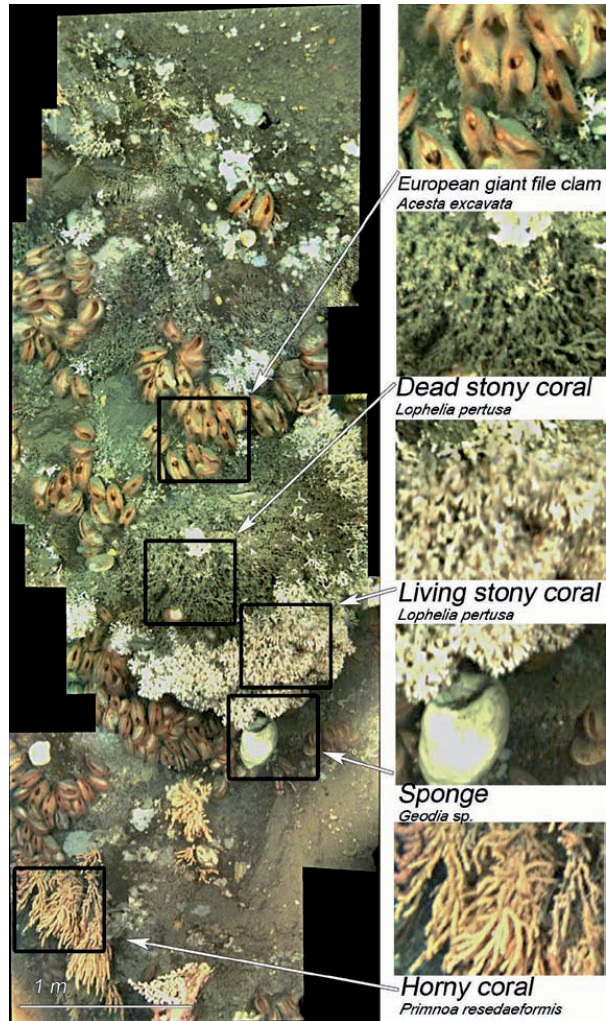


Figure 3. Photo mosaic with different taxa of benthic filter feeders growing on a vertical wall at 430 m depth in the fjord of Trondheim, Norway. Living stony corals appear white. Dead stony corals appear grey due to loss of antibacterial mucus production and consequent silt sedimentation. The area covered by the photo mosaic in the left image is approximately 2 m x 5 m.

Figure 3 is made from nine images, while the photo mosaic in Figure 4 is constructed from 73 images.

Marine Archaeological Survey

To cover the complete wreck site, the WROV was maneuvered along eleven 50-m-long survey lines in a lawn-mower pattern by the closed-loop control system. The camera altitude was approximately 1.9 m to ensure sufficient lighting and area coverage of 1.6 x 1.6 m. A line spacing of 1 m resulted in 36% sidelap. Approximately 550 images were used in the resulting photo mosaic shown in Figure 5. Due to varying current conditions at the site, it was difficult to keep the vehicle velocity constant and hence the velocity was kept lower than the theo-

retical 0.36 m s^{-1} to ensure overlap.

In the data set collected with the WROV installed in the excavation support frame (Figure 2), the vehicle was moved in a parallel or back-and-forth, lawn-mower pattern with 0.5 m line spacing. The distance between each image along track was also 0.5 m. The altitude varied from 1.5–1.7 m due to an excavated pit in the middle of the area. The resulting overlap and sidelap were close to 50%. The large sidelap enabled photogrammetry processing of the images. A total of 270 images were included in the photo mosaic in Figure 6.

Digital Image Processing

Image light-pattern corrections, topology estimation, and blending were

completed in automated Matlab-based software routines developed at Woods Hole Oceanographic Institution (Singh et al., 2007). Image topology estimation and image blending were performed by Intergraph software I/RAS C when manual intervention was necessary.

Light-Pattern Corrections

Even with proper light sources and camera setup, the image data set normally benefits from digital adjustments of light patterns. Light on an artificially lit underwater scene consists of an illumination component and a reflectance component. The illumination component is caused by the excitation of light on the area of interest. Illumination intensity usually varies gradually over

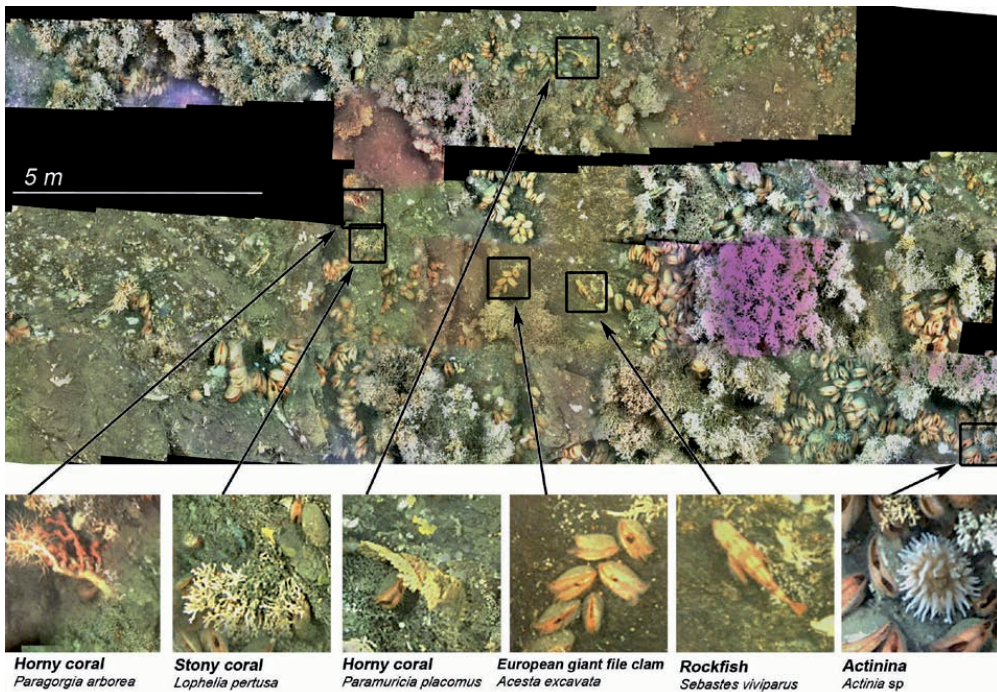


Figure 4. Photo mosaic of benthic filter feeders attached to the vertical rock wall in the fjord. This site is at 390-m depth and dominated by corals and bivalves. The area covered by the photo mosaic is approximately 8 m x 18 m and consists of 73 images.

the area captured by the camera because of the geometry of the reflector, characteristics of the light-source lenses, and the distance from the light source to the depicted seabed. The reflectance component consists of the light reflected by the different objects in the image and usually varies more strongly than the illumination. The reflectance naturally depends

on color, surface roughness, and inclination of the target of interest in the image. Hence, the illumination component and reflectance component of an image can be separated in the frequency domain. When the illumination component of the image is identified, it is modeled by surface fitting and corrected by enhancing dark areas and reducing bright areas

to ensure even illumination before illumination and reflectance are merged to form a uniformly lit image. More details and illustrated examples can be found in Singh et al. (2007).

Topology estimation

The topology of an image pair consists of their relative positions, orientations, and scales. In all the case examples, the topology estimation process was based on feature recognition. Features occurring in an image pair are identified and recognized in both images to calculate the topology.

The interest points are edges and corners detected by calculating the autocorrelation of the second moment matrix of small image patches according to the method described by Harris and Stephens (1988).

Once the interest points are established, a Zernike moment is calculated for each interest point to provide it with a unique identity or tag. The Zernike moment (A_{nm}) can be calculated according to the following equation:

$$A_{nm} = \frac{n+1}{\pi} \sum_x \sum_y f[x,y] V_{nm}^*(x,y), x^2 + y^2 \leq 1 \quad (1)$$

where $f[x,y]$ represents an image patch surrounding the interest point, V_{nm}^* represents the Zernike polynomial for the image patch, n is the order of the polynomial, and m is the number of repetitions for deriving the Zernike polynomial. The Zernike moment is a dependant of the image patch; hence, image patches showing the same feature will have similar Zernike moments. More details on Zernike moments can be found in Khotanzad and Hong (1990). By requiring the spatially coincident interest points to match, the relative position, rotation, and scale of an image

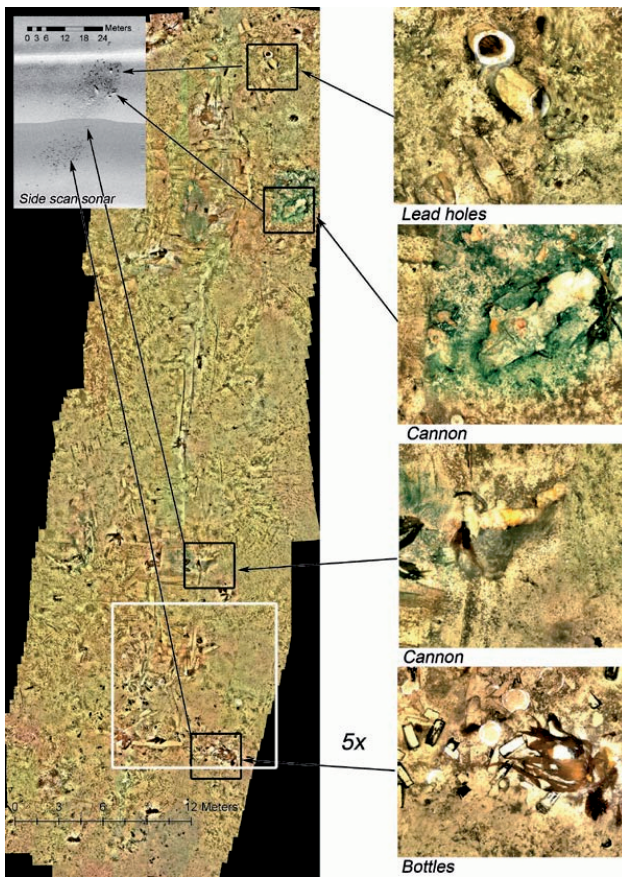


Figure 5. Shipwreck at 170 m-depth. The four squares are magnified five times to show the level of detail in the mosaic. The area covered by the photo mosaic is approximately 19 m x 37 m, and the photo mosaic is compiled from approximately 550 images. The white square indicates the approximate position of the excavation support frame in Figure 2, and the area within the square corresponds to the area in Figure 6. Note the kelp (*Laminaria* sp.) visible in the lower right image. Kelp does not live at this depth in these waters, so kelp seen at the wreck site must have been washed free from the substrate at shallower depth by heavy weather and transported by a current.

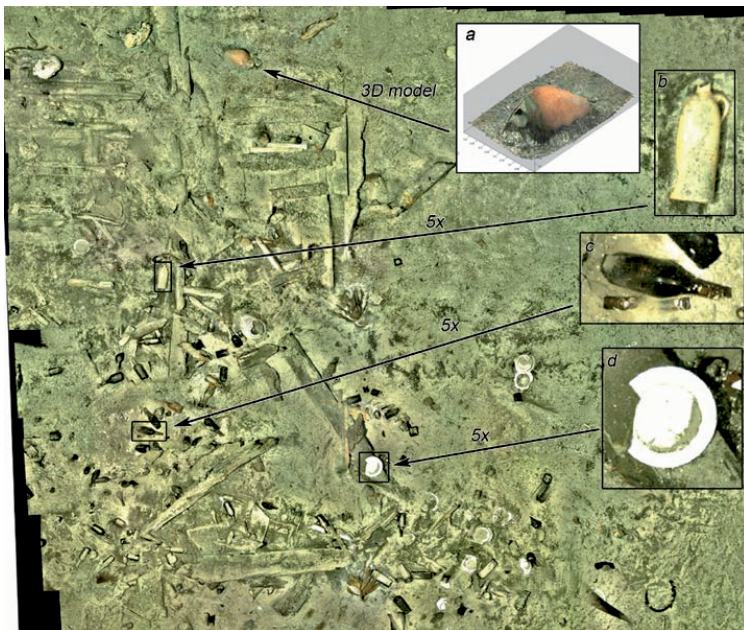


Figure 6. Detailed photo mosaic made inside the excavation support frame seen in Figure 2. Part (a) illustrates how the data set can be processed in three dimensions to measure the topography of the site. Insets (b), (c), and (d) demonstrate how the mosaic can be zoomed to reveal details of the artifacts observed. The photo mosaic is compiled from 270 images.

relative to the next image can be calculated (Pizarro, 2003).

For the data set acquired within the excavation support frame at the marine archaeology site, the processing was extended to include three-dimensional processing by means of navigation data. The three-dimensional positions of interest points were calculated to obtain a detailed bathymetrical model of the site. The method is described in Ludvigsen et al. (2006).

Image Blending

To make the mosaic appear seamless, it is necessary to avoid steps in image intensity on the borders between the images. After the topology has been estimated, intensity steps are reduced by merging the images in a process called blend-

ing (based on Burt and Adelson, 1983). In the first step of the blending process, the original images are decomposed in the frequency domain using band-pass filters to form several frequency component images. These images are then merged over transition zones within the overlay areas of the neighboring images. The center of this transition zone is a line in the middle between the centers of the images. The resulting pixel intensity in each frequency-component image in the transition zone is determined by applying a weighted average of the overlapping images. To remove the border between two images, the average is weighted by the distance to the center line of the transition zone.

A mosaic is built for each frequency component before they are joined in the

final step of the blending procedure. By choosing a narrow transition zone for the high-frequency components, and a wider transition zone for the lower-frequency components, double appearance of smaller objects is avoided, while the larger structures in the initial image set are merged smoothly; the resulting mosaic thus appears seamless.

RESULTS

Marine Biological Example

The area shown in Figure 3 is located at 430-m depth and is approximately 2-m wide and 5-m high. The temperature was 8.1°C and salinity was 35 psu at the site. It is exposed to the Norwegian coastal current (Sakshaug and Snøli, 2000), and high abundance of zooplankton was observed at the site. The photo mosaic shows a benthic filter-feeder community comprised of benthic cold-water corals, bivalves, sponges, and numerous other taxa. Abundant horny corals like the *Paragorgia arborea* and *Paramuricia placomus* are attached to the exposed rock wall. The dominant species are the stony coral *Lophelia pertusa* and the European giant file clam *Acesta excavata*. The bivalve appears in large numbers, found in high density on the rock wall beneath the hanging stony coral branches. Both living and dead stony corals are visible. Mucus containing antibiotic compounds, which also removes sediment and particles (Mortensen, 2000), makes living stony corals look “clean and white.” Dead stony coral, in which mucus production has ceased, is grey and brown due to sediment accumulation, microfauna attachment, and invasion by boring sponges.

The horizontal extent of the area shown in Figure 4 is approximately 18 m and the vertical extent is about 8 m. The

depth is about 390 m. At this site, horny corals, stony corals, bivalves, rockfish, and actinia are among the most detectable taxa. Large branches of stony corals are attached to the vertical wall, and again both dead and living corals are distinguishable. The bivalves reside in clusters both on exposed rock and at sites protected by stony coral branches.

The taxonomic diversity on the vertical rock wall appears to be remarkably high compared to other habitats at the same depth in the study region. Due to the near-vertical inclination, sediment does not accumulate on the rock wall, which can be advantageous for many filter feeders. A reduced risk of being buried by sediment or marine snow may be favorable for larval settlement and for slowly growing organisms. For the larger mobile biota, attached taxa, such as corals, represent shelter.

Marine Archaeological Example

The photo mosaic in Figure 5 shows a shipwreck at approximately 170-m depth. The area depicted was approximately 37-m long and 19-m wide. The wreck is eroded and most of the wood is decomposed, but the lower part of the wooden hull remains. The photo mosaic was produced for post-investigation documentation of the site before the investigation was closed. Two cannons, four lead cable holes, a large number of bottles, and the wooden remnants of the hull are the most distinct objects in the photo mosaic. The keel line is visible and indicates that the bow was probably located close to the leaden cable holes, while the stern was near the bottles. From observation of the wreck site and the artifacts recovered, archaeologists estimate that the wreck is most likely a merchant ship that

was involved in trade between Europe and Russia. It probably sank in the early 1800s (Søreide and Jasinski, 2005).

The Figure 6 photo mosaic illustrates the wreck site after 0–20 cm of sediment was removed by a suction unit mounted on the WROV. Inset (a) of Figure 6 shows a three-dimensional processed model of a mug in the site to elucidate how the geometry of objects can be reconstructed by photogrammetry. Insets (b), (c), and (d) illustrate how the photo mosaic can be magnified to reveal details of the site. The photo mosaic shows exposed wooden hull parts, bottles, bottle necks sticking out of the sand, dishes, mugs, and other artifacts from the ship. Bottle shapes include round and square; there are bottles made of glass, and bottles made of ceramic material. In the middle of the area, there are wooden planks remaining from the bottom and keel of the vessel.

DISCUSSION

Areas for Improvement

Two particular areas of photo mosaicking hold significant potential for improvement: image acquisition efficiency and geometrical distortions.

Image Acquisition Efficiency

Image acquisition efficiency associated with photo mosaics is low: only a few hundred square meters could be covered within the time available for the marine biological survey. More ROV time was available for the marine archaeological survey, resulting in a larger area covered.

To improve image acquisition efficiency, the images should cover a larger area of seabed or be taken at a higher frequency, or both. The area covered in each image can be extended by increasing the altitude of the camera above the sea-

bed. More powerful light sources would probably allow longer distances between camera and subjects, resulting in larger coverage. Increasing the light intensity on a scene will induce a higher degree of backscattered light from particles in the water, reducing the contrast in the resulting images. A trade-off between light and contrast must therefore be sought. Minimizing the common volume of the camera field of view and the light cones by using narrow-beam-pattern light sources and a large distance between light source and camera will also reduce the backscatter problem (Jaffe, 1990).

To further increase data-acquisition efficiency, the imaging frequency must be increased. The imaging frequency of the setup presented in the examples was limited by data-transfer capacity. This issue can be solved with proper systems engineering. If strobes are applied, their recharge time will limit the imaging frequency and thereby the vehicle speed during image acquisition. Using constant light, the next speed limitation during data acquisition is the amount of propulsion power installed to overcome the drag forces working on the vehicle and its tether.

By using light sources with spectral properties that fit the light absorption spectra of seawater, the altitude can probably be increased further. In the future, spectral analysis of both applied illumination and seabed reflectance can result in quantitative color analysis, which has great potential for identifying the present seabed compounds (Kirk, 1994).

Geometrical Distortions and Corrections

In the marine biological example, the extents of the subjects along the image axis were large. This causes geometrical

distortions when the three-dimensional topography is projected to two dimensions in the resulting photo mosaics. In Figures 3 and 4, the distortions can be seen as varying sizes of a feature, for example, the giant file clams. The low vertical relief in the marine archaeological example is beneficial, but some geometrical errors are nevertheless seen along the keel line of the shipwreck in Figure 5. The keel line is actually straight, though it appears slightly curved in the photo mosaic.

Camera calibration reduces distortions originating from imperfections in the camera and is the first step toward increasing geometrical consistency in photo mosaics. Calibration can be performed either automatically or through a designated calibration procedure (e.g., Heikkila and Silven, 1997; Zhang, 1999). To further enhance the geometrical consistency of photo mosaics, mosaic processing and image matching should be done in three dimensions so that a fully three-dimensional scene can be extracted (Pizarro, 2003). This will require instrumentation on the underwater vehicle to measure the position and orientation of the camera for each image. Three-dimensional processing can be used to document the bathymetry of the site in high resolution. But, to reduce the geometrical distortions of a two-dimensional photo mosaic, the three-dimensional scene could be used to reproject the images into a two-dimensional scene.

Quality Control

To increase the integrity of the information in photo mosaics, a procedure for quality control should be established. The simplest way to do this would be to physically place a linear scale bar

in the imaged area and compare the dimension and shape of the scale bar with the known values.

Measuring the quality of the topology estimate represents a more sophisticated quality control (Pizarro, 2003). The quality of the topology estimate can be quantified by determining the amount and precision of matching interest points used in the resulting topology. The topology estimate can also be controlled by closed loops if the survey track crossed itself and a part of the seabed is imaged by different sections of the survey track (Fitzgibbon and Zisserman, 1998).

Alternative Survey Methods

Other high-resolution documentation methods are available for biological and archaeological research surveys. Laser line scanners, available since the early 1970s (Funk et al., 1972), are effective and produce clear images, but the resulting imagery is monochrome and less detailed than images from optical cameras. Interesting for biologists, the laser line scanner can be used to record fluorescence to measure, for example, the presence of chlorophyll at a site (Jaffe et al., 2001). The most important disadvantages of laser line scanners are, however, complexity, availability, and price. Few models are designed, and few units have been produced.

High-frequency side-scan sonars or acoustical cameras can also perform comprehensive site documentation. In contrast to optical imagery, sonars are not dependent on seawater visibility. The resolution of sonar imagery is increasing as technology develops but is not yet comparable to optical imagery. However, there is information in an acoustical signal about the return intensity and phase, which provides information on targets'

hardness or surface roughness. Hence, sonars complement more than compete with optical image mosaicking. In Figure 5, a side-scan sonar image of the wreck site is inserted in the upper left-hand corner and can be directly compared to the photo mosaic to illustrate differences in coverage and details. The main characteristics of the site are recognized in both the Figure 5 sonogram and in the photo mosaic. More site details can be perceived from the photo mosaic than from the sonogram.


Video is the most likely alternative to photo mosaics. To cover an area larger than one video frame, the camera is moved and a virtual map is constructed in the mind of the viewer. The motion of the video camera can enhance understanding of a recorded object, as the object can be seen from different angles. But video is more complicated to communicate and present than a photo mosaic and the virtual map can vary between viewers.

CONCLUSION

Detailed site investigations may become more important in the future. Surveys like the biological example presented here can be useful for documenting damage caused by bottom trawling and other fishing methods (Fosså et al., 2002). Stony corals may become useful as climate markers because a climate-induced reduction of pH levels in the ocean is likely to degrade their aragonite skeletons (Sinclair et al., 2006). Photo-mosaic documentation and time-series analyses could thus be used to document changes in coral structures induced by the increased level of carbon dioxide in the atmosphere. Greater intensity in underwater construction work in the offshore petroleum industry, for example,

may induce a larger demand for photo mosaics for underwater archaeological investigations. Documentation of the extent and details of illegal dumping is another potential application.

Photo mosaicking is a useful tool for illustrating small- and medium-sized underwater scenes of known extent. With the present methodology, one can expect a single photo mosaic to cover up to a few thousand square meters of seabed. For larger areas, the disadvantages of geometrical distortions and low data-acquisition rate prevent geospatially correct images. Usually, it would be sensible to compromise resolution and obtain a coarser search with sonar.

To our knowledge, neither the filter-feeder communities documented in Figures 3 and 4 nor the wreck site shown in Figures 5 and 6 could have been documented to the same level of detail by other methods. In Figures 3 and 4, we can characterize the filter-feeder habitat by the most dominant taxa, the type of seabed, and the co-existence among species. The photo mosaics of the archaeological site reveal the condition, position, and orientation of a large number of historical artifacts that together outline the size, approximate age, and type of shipwreck. The characteristics of the wreck site can be perceived within a few seconds from the photo mosaics. It would take hours to obtain the same level of understanding and knowledge of a site by means of single images or video. 

REFERENCES

- Ballard, R.D. 1975. Photography from a submersible during project FAMOUS. *Oceanus* 18(3):40–43.
- Ballard, R.D. 1987. *The Discovery of the Titanic*. Warner/Madison Press, Toronto. 230 pp.
- Ballard, R.D., A.M. McCann, D. Yoerger, L.L. Whitcomb, D.A. Mindell, J. Oleson, H. Singh, B. Foley, J. Adams, and D. Piechota. 2000. Discovery of ancient history in the deep sea using advanced deep submergence technology. *Deep-Sea Research, Part 1* 47(9):1,591–1,620.
- Burt, P.J., and E.H. Adelson. 1983. Multi-resolution splining using a pyramid image representation. *ACM Transactions on Graphics* 2(4):217–236.
- Eustice, R. 2005. Large area visually augmented navigation for autonomous underwater vehicles. Ph.D. Dissertation, MIT/WHOI Joint Program in Oceanography/Applied Ocean Science and Engineering, Woods Hole, MA.
- Fitzgibbon, A.W., and A. Zisserman. 1998. Automatic camera recovery for closed or open image sequences. *Lecture Notes in Computer Science* 1,406:311.
- Fosså, J.H., P.B. Mortensen, and D.M. Furevik. 2002. The deep-water coral *Lophelia pertusa* in Norwegian waters: Distribution and fishery impacts. *Hydrobiologia* 471:1–12.
- Funk, C.J., S.B. Bryant, and P.J. Heckman. 1972. *Handbook of underwater imaging system design (TP-303)*. Ocean Technology Department. Naval Undersea Center, 92 pp.
- Gracias, N., and J. Santos-Victor. 2001. Underwater mosaicking and trajectory reconstruction using global alignment. Pp. 2,557–2,563 in *Proceedings of OCEANS 2001, Honolulu, Hawaii, November 5-8, 2001, Volume IV*, Marine Technology Society and Institute of Electrical and Electronics Engineers.
- Harris, C.G., and M. Stephens. 1988. A combined corner and edge detector. Pp. 147–151 in *Proceedings of The Fourth Alvey Vision Conference, August 31 – September 2, 1988*, Manchester.
- Heikkila, J., and O. Silven. 1997. Four-step camera calibration procedure with implicit image correction. Pp. 1,106–1,112 in *Proceedings of the 1997 IEEE Computer Society Conference on Computer Vision and Pattern Recognition, Jun 17-19 1997*, San Juan, PR, USA.
- Jaffe, J. 1990. Computer modeling and the design of optimal underwater systems. *IEEE Journal of Oceanic Engineering* 15(2):101–111.
- Jaffe, J., K.D. Moore, J. McLean, and M.P. Strand. 2001. Underwater optical imaging: Status and prospects. *Oceanography* 14(3):66–76.
- Jerosch, K., A. Ludtke, M. Schluter, and G.T. Ioannidis. 2007. Automatic content-based analysis of georeferenced image data: Detection of Beggiatoa mats in seafloor video mosaics from the Haakon Mosby Mud Volcano. *Computers and Geosciences* 33(2):202–218.
- Khotanzad, A., and Y.H. Hong. 1990. Invariant image recognition by Zernike moments. *IEEE Transactions on Pattern Analysis and Machine Intelligence* 12(5):489–497.
- Kirk, J.T.O. 1994. *Light and Photosynthesis in Aquatic Ecosystems*, 2nd ed. Cambridge University Press, Cambridge, 509 pp.
- Ludvigsen, M., H. Singh, and R. Eustice. 2006. Photogrammetric models in marine archaeology. In: *Proceedings of OCEANS 2006, Boston, Massachusetts, September 18-21, 2006*. Marine Technology Society and Institute of Electrical and Electronics Engineers.
- Mortensen, P.B. 2000. *Lophelia pertusa* in Norwegian waters: Distribution, growth, and associated fauna. Ph.D. Dissertation, Department of Fisheries and Marine Biology, University of Bergen, Norway.
- Pizarro, O. 2003. Large area underwater mosaicing for scientific applications. Ms.C. Dissertation, MIT/WHOI Joint Program in Oceanography/Applied Ocean Science and Engineering, Woods Hole, MA.
- Sakshaug, E., and J.O. Snøli, eds. 2000. *Trondheimsfjorden*. Tapir, Trondheim, Norway, 336 pp. [In Norwegian]
- Sinclair, D.J., B. Williams, and M. Risk. 2006. A biological origin for climate signals in corals: Trace element “vital effects” are ubiquitous in Scleractinian coral skeletons. *Geophysical Research Letters* 33(17): L17,707.
- Singh, H., J. Howland, and O. Pizarro. 2004a. Advances in large-area photomosaicing underwater. *Journal of Oceanic Engineering* 29(3):872–886.
- Singh, H., R. Armstrong, F. Gilbes, R. Eustice, C. Roman, O. Pizarro, and J. Torres. 2004b. Imaging coral habitats with the SeaBED AUV. *The Journal for Subsurface Sensing Technologies and Applications* 5(1):25–42.
- Singh, H., C. Roman, O. Pizarro, R. Eustice, and A. Can. 2007. Towards high-resolution imaging from underwater vehicles. *International Journal of Robotics Research* 26(1):55–74.
- Soreide, F., and M.E. Jasinski. 2005. Ormen Lange: Investigation and excavation of a shipwreck in 170-m depth. Pp. 2,334–2,338 in *Proceedings of OCEANS 2005, Washington DC, September 18–23, 2006, Volume III*. Marine Technology Society and Institute of Electrical and Electronics Engineers.
- Vincent, A.G., N. Pessel, M. Borgetto, J. Jouffroy, J. Opderbecke, and V. Rigaud. 2003. Real-time georeferenced video mosaicing with the MATISSE system. Pp. 2,319–2,324 in *Proceedings of OCEANS 2003, San Diego, California, September 22–26, 2006, Volume IV*. Marine Technology Society and Institute of Electrical and Electronics Engineers.
- Xu, X., and S. Negahdaripour. 1997. Vision-based motion sensing for underwater navigation and mosaicing of ocean floor images. Pp. 1,412–1,417 in *Proceedings of OCEANS 1997, Halifax, Nova Scotia Canada, October 6–9, 2006, Volume II*. Marine Technology Society and Institute of Electrical and Electronics Engineers.
- Zhang, Z. 1999. Flexible camera calibration by viewing a plane from unknown orientations. Pp. 666–679 in *Proceedings of the 1999 7th IEEE International Conference on Computer Vision (ICCV'99), September 20–September 27, 1999, Kerkyra, Greece*. Institute of Electrical and Electronics Engineers.

B Article 2

Ludvigsen, M., H. Singh, et al. (2006). Photogrammetric models in marine archaeology. Oceans 2006, Boston, MA, USA, IEEE/MTS.

Photogrammetric models for marine archaeology

Martin Ludvigsen

Norwegian University of Science and
Technology

Department of Marine Technology

7491 Trondheim, Norway

martin.ludvigsen@ntnu.no

Ryan Eustice

University of Michigan

Department of Naval Architecture and
Marine Engineering

Ann Arbor, Michigan 48109-2145

eustice@umich.edu

Hanumant Singh

Woods Hole Oceanographic Institution

Woods Hole, MA, 02543, USA

hsingh@whoi.edu

Abstract- The paper presents a method to create small scale topographic models of a deepwater archaeological site using photogrammetric methods. An example data set from a Norwegian archaeological investigation is discussed.

I. INTRODUCTION

This paper presents a method to create high resolution spatial models of underwater scenes from optical images. Optical imagery contains more detailed information than its acoustical counterpart, but how can this information be exploited to produce a spatial model? High resolution spatial models could benefit many users' underwater imagery, e.g. forensic investigators, marine biologists, marine geologists and archaeologists. This text will pursue the needs of the latter group.

Constructing photogrammetric models of underwater scenes differs from corresponding terrestrial techniques in several aspects. The vertical extent of features on the seabed is often large compared to the seabed-camera distance due to the limited range of optics underwater. Underwater light suffers from attenuation and backscattering causing challenges like low contrast and non-uniform lighting patterns [1], and [2]. The vehicle carrying the camera also usually holds the light source, making the shadow pattern shift around the depicted objects from image to image. To construct a photogrammetric model of a large area there is a navigation problem to solve because there is a disparity between the accuracy present navigational aids and the resolution offered by imaging sensors.

Archaeologists need information about dimensions, shape, material, structure of surfaces, colors, orientations and positions of objects on an excavation scene to be able to identify artifacts, reconstruct events and understand the scene in an underwater investigation [3]. The properties of light scattering and attenuation in seawater [2] prevent larger sites to be depicted within one frame. Thus, to cover a larger site, a large number of images have to be combined in a model. In underwater archaeology time is an expensive resource, implying that the data acquisition to be efficient. The method must be easy to implement on ROV's or AUV's of opportunity,

requiring the hardware requirements should be modest. The integrity of the measurements is crucial to give credibility to the results, and has to be verifiable.

The methods most commonly used to measure geometrical shape of a site in underwater archaeology are mapping by tape measure [4], photogrammetry by manual point matching [5], and acoustical measurements by single beam or multi beam sonars [6]. These techniques are often combined with optical imagery and preferably put together in a mosaic and in some cases a combined model is constructed [6]. These mapping approaches have major limitations. Using sonars, basic acoustics in terms of frequency, transducer geometry and noise suppression will limit precision and data resolution. The manual methods are too labor intensive to produce a sufficient amount of data points.

Photogrammetry has been used in underwater archaeology for some time [7]. A substantial advantage of the presented method is the automatic interest point identification and processing. Automatic interest point identification and processing is adapted from the science of computer vision [8], [9] and [10] the topics SLAM (Simultaneous Localization and Mapping) and SFM (Structure From Motion). An alternative approach which automatically can produce larger 3-d models underwater is presented by Negahdaripour [11]. On land close range photogrammetry models is an established tool for surveying and industry dimension documentation [12]. In the computer vision community, technology based on feature matching have only been used experimentally for underwater navigation, [13] and [14].

In this paper we will present an automated procedure to construct larger photogrammetric model from sets of still images. The process is automated in the sense that there is no human interaction in the photogrammetric interpretation of the images. The method produces a sparse spatial model and the archaeologist will still need to lean on the optical imagery to complete the historical information content. The presented method will meet the above laid out requirements to

operational efficiency. The reliability of the model is estimated during the construction of the model.

In section II this paper presents the framework and methodology for producing large scale underwater photogrammetric models. The requirements to the data-acquisition process of the images for the photogrammetry are laid out. Local models are constructed from image pairs before they are assimilated into a global model while computing the internal error. Section III describes the data acquisition, the data processing, and the resulting model for a dataset collected at an archaeology excavation at 170 meters depth. Section IV discusses the method and the performance on the data set used in section III.

II. METHODS

This section will describe how 3-d models can be made from a set of optical images. Requirements and guidelines to the image acquisition are offered, together with a description on how the images are put together and how the 3-d information is extracted.

A. Imaging

In order to make spatial models the images need to overlap. When covering a wreck-site it is recommended that $\sim 60\%$ of the image foot-print overlap. Likewise across-track there should be $\sim 25\%$ sidelay to be able to close loops in the vehicle trajectory, and to ensure consistency between lines in e.g. a lawn-mower pattern.

The lighting patterns within the images should be as uniform as possible. This is preferably provided by a well configured light(s)-to-camera geometry and sufficient amount of light power, see [2]. If this is not possible an option is to remove lighting patterns by software in post processing e.g. [15]. A high dynamic range camera is useful in this context because a wider color span increases the potential for color correction.

The presented methodology requires a prior pose estimate for all images as position and orientation stamps for all images are used in the model, both in the interest point matching and in the creation of the photogrammetric model.

To provide the necessary relative pose estimate between two images dead reckoning from doppler velocity or inertial measurements is recommended. Most acoustical baseline system do not have sufficient accuracy, while dead reckoning from one image to the next usually allows for high precision due to the short time span between images.

B. Local models

This section describes the image registration pipeline used for producing local models as described by Eustice et al in [8][9][10][18], which is briefly recapped here. The photogrammetric process starts by identifying interest points. The Harris corner detector is used to detect interest points [16] together with the SIFT (Scale Invariant Feature Transform) operator [17]. The Harris operator will detect corners and

edges, and is based on the curvature of the autocorrelation function in the neighborhood of each point. The Harris operator is invariant to rotations and robust to small variations in scale [10].

To match interest points the routine need descriptions of the points. The Zernike moment is used to encode the Harris interest points with a descriptor while the SIFT points are encoded by a SIFT descriptor. In underwater applications changing lighting patterns and rotations are often experienced but the Zernike moment is rotationally invariant and to some level robust to changes in scale.

Comparing the Zernike moments and SIFT operators attached to the Harris- and SIFT-points in both images in an overlapping pair, the interest points present in both images are identified and localized. To ease the requirements for the uniqueness of the interest point descriptors, the pose prior is used to derive regions that are common in both images and where corresponding points are sought. The routine then searches for common points along an area defined by epipolar lines. Outliers are rejected applying a least median of squares (LMedS) registration methodology. The essential matrix E used in the LMedS routine is derived by a six point algorithm [18].

When the essential matrix is defined, the relative pose is estimated using Horns relative orientation algorithm. After a two-view bundle-adjustment, the relative pose is finally estimated. The two-view local model is established by triangulation using a two-view point transfer model [8], and the x,y,z positions of the interest points are calculated.

C. Global registration

The first step in the global registration is to identify common points in the global model and the local models. The local models are related to each other position-wise by the navigation data.

To determine the scale between two local models a set of distances between points present in both models are calculated for both point clouds. The scale is determined as the ratio between the distances.

By monitoring the standard deviation of the scale estimates, an indication of the quality of the scale match is provided. Outliers of the point clouds are detected by comparing each scale to the mean of scales. The translation necessary to add a local model to the global model is determined in a comparable way.

The distance between the corresponding points in the local model and the global model is computed, and there are as many distances as there are pairs of corresponding points. The standard deviation of the distances is a check for overall quality of the translation and is used to detect outliers. The process of scaling and translating the local model is repeated

and outliers peeled off until an acceptable level of standard deviation is achieved.

A local point cloud will typically overlap the global model at different points or with part of the global model that origin from different local models. Thus there will be two estimates of scale and translation. The deviation between the two estimates will give an indication of the integrity of the model.

When a global point cloud is established, the data are gridded to a mesh and plotted.

III. EXPERIMENTAL DATA

A. Background

In the pipeline route for the Ormen Lange gas field outside the west coast of Norway *Museum of Natural History and Archaeology*, NTNU discovered a historic shipwreck at 170 meters depth [19]. The wreck was believed to originate from the beginning of the 19th century. This triggered a large ROV-based underwater investigation [20]. During the investigation several image sets were collected. It was decided to pursue the possibility of extracting 3-d geometrical information from these data sets.

B. Setup for data acquisition

A 10 x 10 meters excavation frame was purpose built for the project and placed over the stern of the wreck, see Figure 1 and Figure 3. Connected to this frame, the ROV moved along rack rails over the site without touching the wreck or the seabed. The orientation angles of the vehicle were fixed while docked to the frame. With the camera placed on the frame-driven ROV, two image series were taken from the excavation area, one before and one after the excavation. The first series contained 270 images and the second 252 images, both with the camera mounted 1.5 to 2.2 meters above the seabed. In both image sets the imagery was taken in a pattern consisting of 15 and 14 lines containing 18 images each. A high dynamic range camera and continuous light was used. The camera was calibrated in a tank.

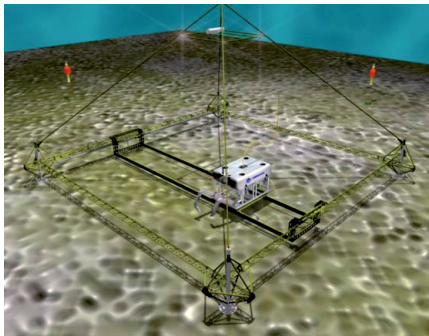


Figure 1 Artistic impression of the ROV in the support frame during excavation. LBL transponders are seen in the background. Image by Fredrik Soreide.

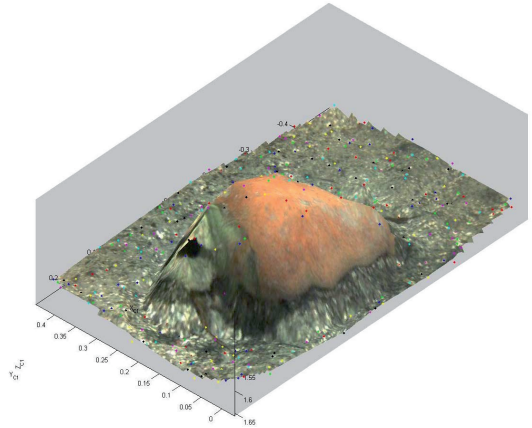


Figure 2 Local model of a large mug laying on the sandy seafloor. A surface was created from the xyz-points and one of the images draped over it. The data points are plotted on top.

C. Data processing

Overlapping imagery was identified from the position data associated with each picture. Applying the camera calibration parameters, the images were undistorted before they were used in the photogrammetrical model. The pose vector was used together with the images to make local models from all overlapping images. Each local model typically consisted of 300 to 1000 xyz points, see Figure 2.

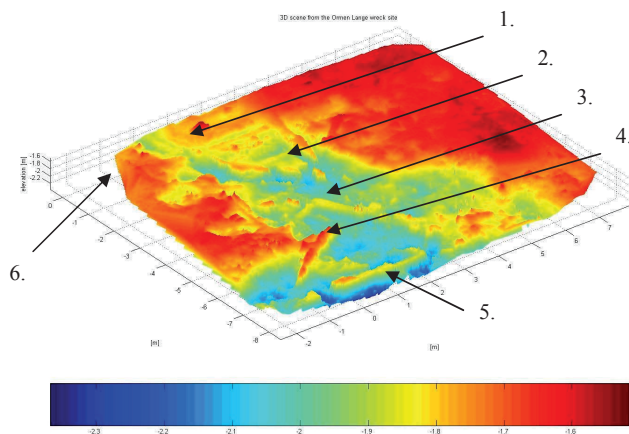
D. Resulting 3-d model

From the two data series more than 400 local models were produced and the local models were joined to two global models by adjusting the scale and translation as described in section II. The topographic model of the site is presented in Figure 4.A. The final model contained approximately 120,000 data points, but due to overlap most points had redundant point, so the actual information content was lower.



Figure 3 Picture of an ROV working on the investigation site. Image by Fredrik Soreide..

A:



1. Mug
2. Hull
3. Wooden plank1
4. Wooden plank 2
5. Wooden plank 3
6. Sponge

B:

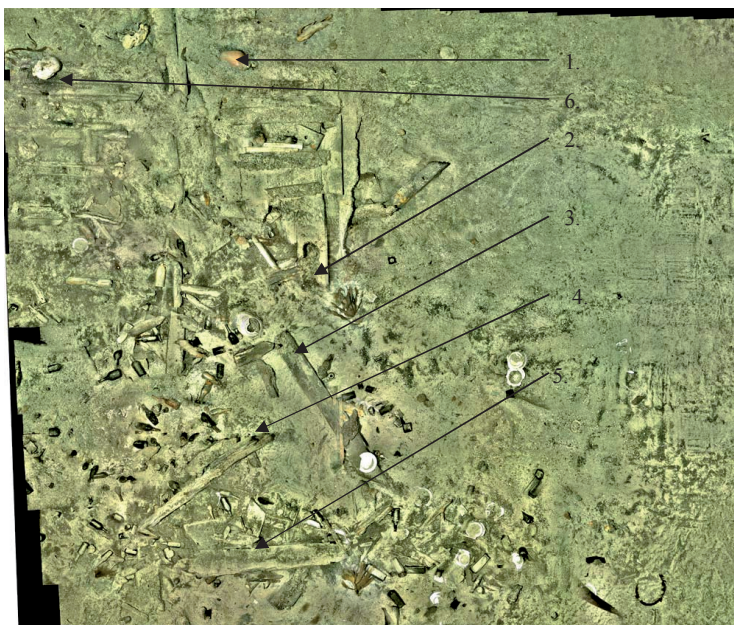


Figure 4.A: A 3-d model of the wreck site color-encoded for elevation. The elevation is local and derived from the camera centers. The grid size used in this mode is 25 mm.

Figure 4.B Shows a 2-d photomosaic made from the images used to construct the elevation model in 4.A. The mosaic is made from 252 images. Some characteristic features are pointed out in both figures.

The images used to construct the model in Figure 4 A are rendered to a photomosaic in Figure 4.B.

When Figure 4.A and Figure 4.B are compared some of the identifiable artifacts are a few wooden planks, an assembled part of wood appearing to be the bottom of the ship, a mug, and a sponge. A depression in the terrain in the middle of the scene is distinctive.

A model of the area before the excavation began was also constructed. When these two models are subtracted from each other, an estimate can be made of how much mass was physically removed during the excavation.

IV. DISCUSSION

At close range photogrammetrical methods have some advantages over corresponding acoustical methods. The method produces high density of data points due to the efficient interest point detector and matching routine. Photogrammetrical methods are not bound by the same limitations as acoustical methods, thus for close range the potential for accuracy are higher for photogrammetry underwater. The data density can be further by tuning the automatic point identification.

In the data set presented the camera-carrying vehicle was docked to a frame. The method presented should work well also with a free flying vehicle, as long as the attitude and position estimates are sufficiently accurate to form the pose prior vector data exist.

The global registration pattern applied here is basic, but during the registration of the example data sets it proved to perform satisfactorily. To add more robustness to the global registration, a more advanced approach will be considered in the future, e.g. a bundle adjustment procedure like the one described in [10].

To improve the scientific applicability, it should be attempted to proceed from the sparse photogrammetric model to a full photogrammetric model as Pollyfeys has discussed for terrestrial applications [21]. In the example data set it is hard to positively identify smaller objects like e.g. bottles merely from the shape of the model, but considering the 3-d model together with the images it is possible to identify dimensions and shape of the modeled objects down to bottle size.

The success of the local modeling depends on the image quality and the precision of the pose priors. In a lawn-mower pattern, some errors produced in the global registration are cancelled out and errors are not allowed to accumulate as local models are put together. The local models will in most cases be matched with models matched several steps back in the global registration process, limiting the aggregation of error.

V. CONCLUSION

We have presented a method to create small scale topographic models of a deepwater archaeological site, based on a SLAM algorithm previously developed by Eustice. We

have shown that the survey method is operational feasible, proved by processing an image set from a deepwater ship wreck.

ACKNOWLEDGMENT

The authors would like to thank Fredrik Søreide for providing the data set.

REFERENCES

1. Singh, H., Howland, J., Pizarro, O., Large Area Photomosaicking Underwater, *IEEE Journal of Oceanic Engineering*, pp. 872-886, vol 29, no 3, 2004.
2. Jaffe, J., *Computer modeling and the design of optimal underwater systems*. Journal Oceanic Engineering, 1990. **15**: p. 101-111.
3. Singh, H, Adams, J., Foley, B.P. Mindell, D., Imaging for Underwater Archaeology, *American Journal of Field Archaeology*, pp. 319-328, vol 27, no 3, Fall 2000.
4. Dean, M., *Archaeology underwater : the NAS guide to principles and practice*. 1992, [London]: Nautical Archaeology Society.
5. Green, J., S. Matthews, and T. Tufan, *Underwater archaeological surveying using PhotoModeler, Virtual Mapper: different applications for different problems*. The International Journal of Nautical Archaeology, 2002. **31**(2): p. 283-292.
6. Singh, H., et al., *Microbathymetric Mapping from Underwater Vehicles in the Deep Ocean*. Computer Vision and Image Understanding, 2000(79): p. 143-161.
7. Rosenscrantz, D.M., *Underwater photography and photogrammetry*. Photography, Archaeology research, 1975.
8. Eustice, R., *Large Area Visually Augmented Navigation for Autonomous Underwater Vehicles*. 2005, Massachusetts Institute of Technology/Woods Hole Oceanographic Institution joint program: PhD-thesis.
9. Eustice, R., H. Singh, and J.J. Leonard. *Exactly Sparse Delayed-State Filters*. in *International Conference on Robotics and Automation, IEEE*. 2005. Barcelona, Spain: IEEE.
10. Pizarro, O., *Large Scale Structure from Motion for Autonomous Underwater Vehicle Surveys*. 2004, Massachusetts Institute of Technology/Woods Hole Oceanographic Institution joint program: PhD-thesis.
11. Negahdaripour, S. and H. Madjidi, *Stereo Imaging on Submersible Platforms for 3-D Mapping of Benthic Habitats and Sea-Floor Structures*. Journal Oceanic Engineering, 2003. **28**(4): p. 625-650.

12. Mikhail, E.M., J.S. Bethel, and J.C. McGlone, *Introduction to modern photogrammetry*. 2001, New York: Wiley. IX, 479 s.
13. Gracias, N. and J. Santos-Victor. *Underwater mosaicing and trajectory reconstruction using global alignment*. in *OCEANS 2001*. 2001. Honolulu, Hawaii: MTS/IEEE.
14. Eustice, R., et al. *Visually Navigating the RMS Titanic with SLAM Information Filters*. in *Proceedings of Robotics Science and Systems*. 2005: MIT Press.
15. Zuiderveld, K., *Contrast limited adaptive histogram equalization*. Graphic Gems, 1994. **IV**: p. 474-485.
16. Chris Harris, M.S. *A combined corner and edge detector*. in *4th Alvey Vision Conference*. 1988. Manchester UK.
17. Lowe, D.G., *Distinctive image features from scale-invariant keypoints*. International journal of computer vision, 2004. **60**(2): p. 91-110.
18. Pizarro, O., R. Eustice, and H. Singh. *Relative Pose Estimation for Instrumented, Calibrated Imaging Platforms*. in *Digital Image Computing Techniques and Applications*. 2003. Sydney, Australia.
19. Jasinski, M. and F. Søreide. *The Ormen Lange marine archaeology project*. in *Oceans 2004*. 2004. Kobe, Japan: MTS/IEEE.
20. Søreide, F. *Ormen Lange: Investigation and excavation of a shipwreck in 170m depth*. in *Oceans 2005*. 2005: MTS/IEEE.
21. Pollefeys, M., et al., *Automated reconstruction of 3D scenes from sequences of images*. Isprs Journal of Photogrammetry and Remote Sensing, 2000. **55**(4): p. 251-267.

C Article 3

Ludvigsen, M. and F. Soreide (2006). Data fusion on the Ormen Lange shipwreck project. Oceans 2006, Boston, MA, USA, MTS/IEEE.

Data fusion on the Ormen Lange shipwreck project

MARTIN LUDVIGSEN

Norwegian University of Science and Technology
Department of Marine Technology
7491 Trondheim, Norway
martin.ludvigsen@ntnu.no

FREDRIK SØREIDE

Norwegian University of Science and Technology
Museum of Natural History and Archaeology
7491 Trondheim, Norway
fredrik.soreide@vm.ntnu.no

Abstract

An archaeologist's primary interest is to extract as much information as possible from a sunken ship. An archaeological investigation should therefore not rely on one single method but utilize sensor fusion as much as possible. Various survey equipment complement each other and by combining more than one tool the archaeologist's capability for interpretation is enhanced. This paper presents the use of sensor fusion on the Ormen Lange deepwater archaeology project, where a number of sensors were combined to document the site with improved precision and standards as a result.

I. INTRODUCTION

A. Background

The Ormen Lange field is located in the Norwegian Sea, 100 km north-west off the coast of Mid-Norway. It was proven through drilling by Norsk Hydro in 1997, and is Norway's largest gas field. The Ormen Lange gas will be piped directly to an onshore process and export plant.

In 2003 The Norwegian University of Science and Technology (NTNU) discovered a historic shipwreck close to one of the planned Ormen Lange pipeline routes [1]. The shipwreck is protected under the Law of Protection of Cultural Heritage and additional investigations of the wreck-site were necessary before the pipeline could be installed. Due to the substantial water depth of nearly 200 meters diving was not feasible. The use of remotely operated vehicles (ROVs) was required to conduct all mapping, surveying, sampling and excavation [2].

B. Scope

This paper will present the remote sensing survey methods and results of the Ormen Lange shipwreck project. The interpretation and fusion of the different sensors are discussed.

Experiences gained will be applicable to deepwater shipwrecks with low vertical signature.

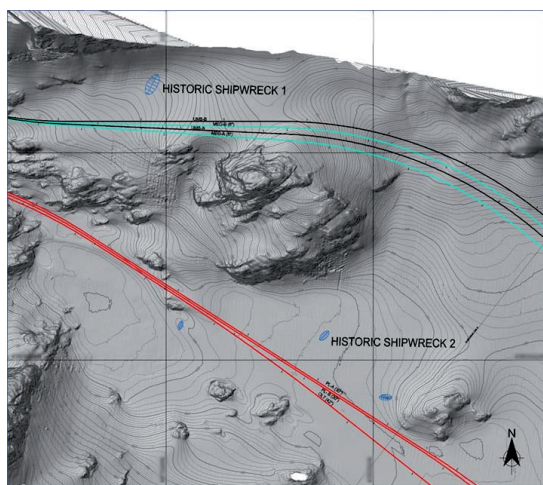


Figure 1 The shipwreck-site (1) and the pipeline routes.

C. Methods

A detailed investigation is necessary to extract information from deepwater shipwreck-sites. The data set presented here is among the most comprehensive data sets ever collected in connection with a deepwater archaeological investigation. Comparable large scale investigations have been performed in the Mediterranean and the Black Sea [3] [4] [5].

Side-scan sonar, multibeam echosounder, magnetometer and sub-bottom profilers were used to image the site, while photomosaics, micro bathymetry and photogrammetry models together with video and photo, were applied to document the site in even more detail.

It is clear that acoustic and optical methods complement each other in terms of coverage and resolution. To be able to obtain a detailed understanding of a wreck-site, it must be mapped at different scales employing both acoustic and optical imagery.

II. SURVEY METHODS

The shipwreck was first detected using an inspection ROV equipped with high resolution side-scan and scanning sonars. Once detected, the presence of the historical wreck was confirmed by video. The shipwreck was subsequently surveyed by ROV-mounted side-scan sonar, multibeam echosounder and sub-bottom profilers. Both the shipwreck itself and the area surrounding the wreck-site were mapped by this sensor suite. A magnetometer survey was also carried out with a proton magnetometer that was towed by the ROV. The topography of the wreck-site was measured in a micro bathymetry. Several photomosaics were constructed to record the site. During the project, the stern of the wreck was excavated and this process was documented by photogrammetry models.

A. Side-scan sonar

The presence of the site was originally confirmed by side-scan sonar. An area 40 meters long and 15 meters wide showed scattered returns. The scattered area had the shape of a ship, see Figure 2. Side-scan sonar was also employed to locate wreckage and archaeological targets on the seabed around the wreck.

Remains of historic shipwrecks are difficult to distinguish and the resolution of side-scan sonar is pushed to its limit when used to locate archaeological remains. Side-scan sonars are in addition prone to several acoustical problems; multi-path can cause "ghost objects" and variations in speed of sound can induce distortions in the imagery. Despite these limitations, side-scan sonar is probably among the most efficient tools to locate historical artifacts due to its coverage per time rate.

Recommendations for proper archaeological surveying with side-scan sonar include utilizing a modern high frequency (i.e. not less than 300 kHz) side-scan sonar with high-dynamic range. The system should be towed at an altitude no greater than 10 meters off the seafloor and be set to a range of no more than 100 meters to ensure detection of archaeological material.

B. Multibeam echosounder

Reson 8125 multibeam echosounder data was collected to locate archaeological remains and to form base maps to augment data for processing and interpretation. The shipwreck is visible in the topographical model as an elongated depression in the seafloor with three bulges, see Figure 3.

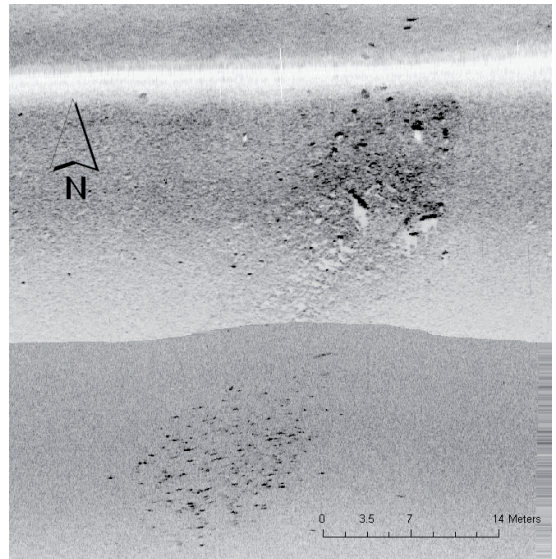


Figure 2 Side-scan mosaic detail of the wreck-site

The bathymetry data also provide useful information of the terrain surrounding the wreck and offer helpful information about the oceanographic and hydrographic context of the wreck-site. From the plot in Figure 4, we can see that the wreck is placed in a slope with increasing inclination to the north.

It is very difficult to detect small objects on the seabed from bathymetry data, as the resolution is coarse. In the dataset presented, the wreck could easily have been ignored, unless the multibeam echosounder data had been combined with other data.

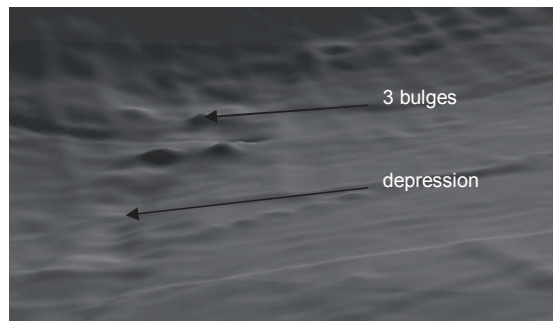


Figure 3 Multibeam data showing three bulges and a depression. The vertical dimension is exaggerated five times.

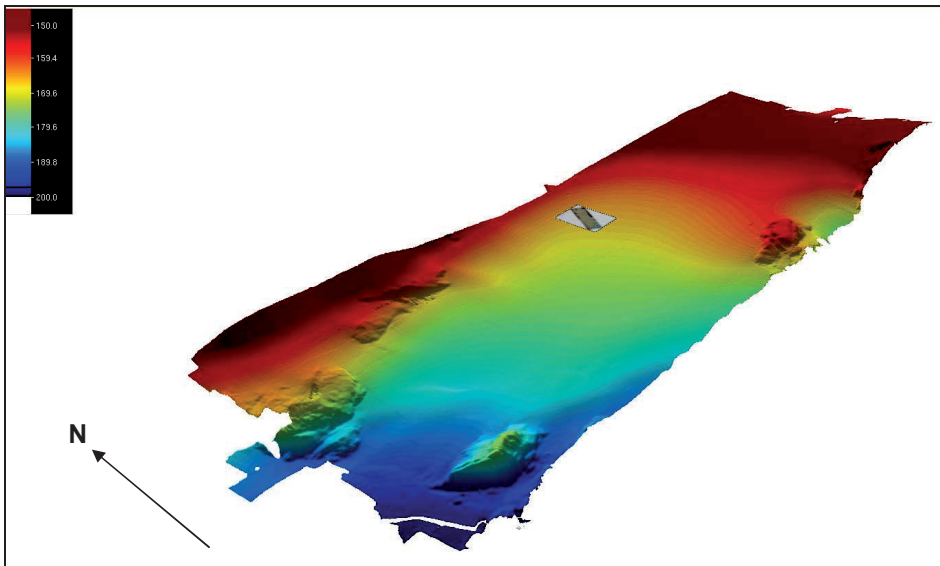


Figure 4 Bathymetry of the area surrounding the wreck. A photomosaic of the wreck is positioned in the terrain. The model extension is approximately 750 meters in the east-west direction and 250 meters in the north-south direction.

C. Sub-bottom profiler

The shipwreck-site was also imaged by three different sub-bottom profiling systems. The wreck showed a clear signature in the sub-bottom profiler results. A series of test pits were dug to correlate between the occurrence of targets in the sub-bottom profiler data and buried artifacts and/or sediment type. Within the site of the extant wreck, there was an apparent correlation between the higher density of localized higher amplitude reflectors and disturbed sub-seabed sediments which correlate with the location of the wreck. An extension of the main wreck-site were clearly demonstrated through the excavation as several meters of wooden construction were uncovered to the west, east and south of the visible structure.

D. Magnetometer

Geomagnetic data were collected with a Geometrics G822 Marine Magnetometer affixed to the survey ROV at the shipwreck-site and throughout the proposed pipeline routes. The magnetometer data were not detailed enough to identify individual artifacts. However, the general trend of the migration of artifacts and site taphonomy substantiated the data provided by the sub-bottom profilers.

E. Micro-bathymetry

Profiling sonar was applied to make a bathymetric model of the wreck-site itself. To be able to resolve a wreck of the type

located in this project, higher resolution than the collected multibeam data was required.

In order to successfully create a topography model from profiling sonar it is necessary to carefully measure position and orientation of the sonar-head [6]. The method is time consuming as the ping-rate is lower than for other bathymetry systems. The benefit is that the technology is cheap and available on most operative ROV's, and provides high resolution.

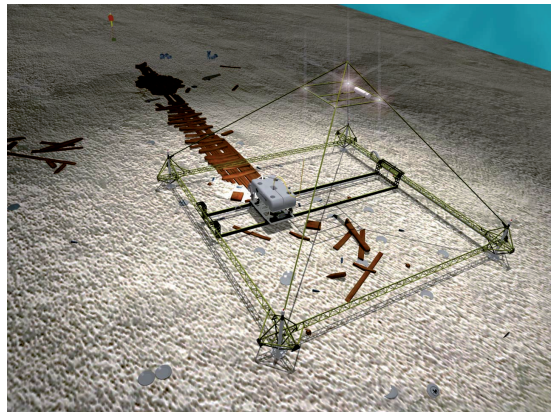


Figure 5 Illustration of the excavation support frame.

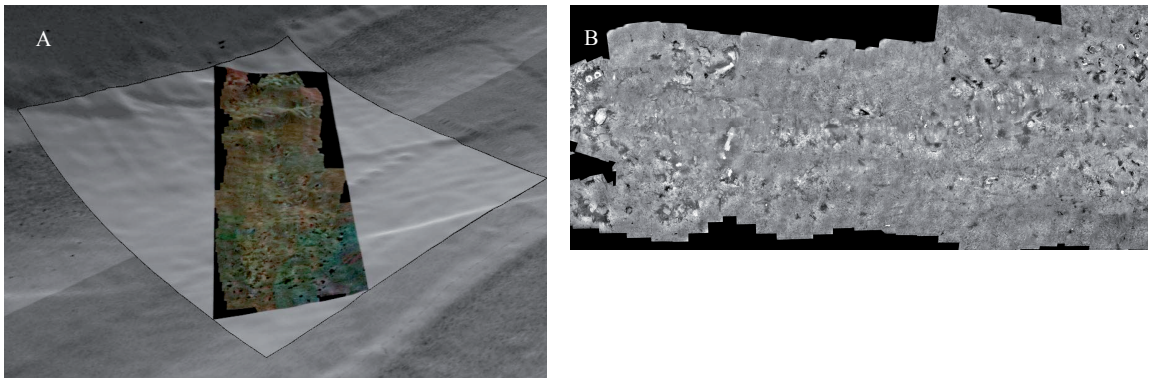


Figure 6 Photomosaic (B) and side-scan mosaic draped on top of the multibeam echosounder data (A).

The resulting microbathymetry model was able to resolve large artifacts, but did not provide more detail than the multibeam data, mainly due to the low expression and few distinguishing artifacts above the seafloor.

F. Photomosaics

The idea of making photomosaics is to provide a detailed overview of a wreck-site. The substantial size of the shipwreck-site and the turbidity of the water made it impossible to depict the area optically in one frame. A pre-disturbance photomosaic was created to provide preliminary information on how many objects were present, what was their condition and how they were located relative to each other.

Images were collected using a high dynamic range camera mounted on the ROV and the vehicle was flown in a lawn-mower pattern over the wreck. More than five hundred images were assembled into the pre-disturbance photomosaic which showed hundreds of bottles, pieces of wood and other artifacts spread over the seabed.

During the detailed investigations, a 10 x 10 meter excavation support frame was installed on the wreck-site to document and excavate the site with exceptional control, see Figure 5. While the ROV was mounted in this frame images for two photo-mosaics were collected, each set containing 250 images. One mosaic was made to document the site before the excavation and one to record the site when it was excavated, see Fig. 9.

Most photomosaics are subject to geometric distortions since they are constructed under the assumption of flat seabed and a reasonably constant altitude. The images are assembled based on recognizing features, thus geometrical errors accumulate when the mosaic grows [7]. Some parts of a mosaic may also

suffer from color distortion. This problem is caused by the color spectrum of the light source, the scattering of light in the water and the absorption spectrum of seawater [8].

The coverage efficiency of photomosaicing is low compared to acoustical methods and present methods are limited by time consuming data acquisition and processing.

However, when the error sources are under control, photomosaics provide more immediate and detailed documentation of the site.

G. Photogrammetry

A photogrammetry model was constructed to document the shape of the excavation area before and after sediment was removed.

With the vehicle mounted in the excavation support frame, the position and orientation of each image frame was sufficiently controlled to construct a photogrammetric model of the complete excavation area, see Figure 9.

Photogrammetry models experience similar problems as photomosaics, but they are more resistible to the geometric error sources than photomosaics. This type of modeling relies on accurate measurements of position and orientation of the camera for all images. Photogrammetric models are not limited by basic physics in the same way as geometrical measurements based on acoustics, and hence have a higher potential for accuracy.

Thus the photogrammetry models are of high resolution and provide detailed geometry information of the site not easily obtainable from other methods.

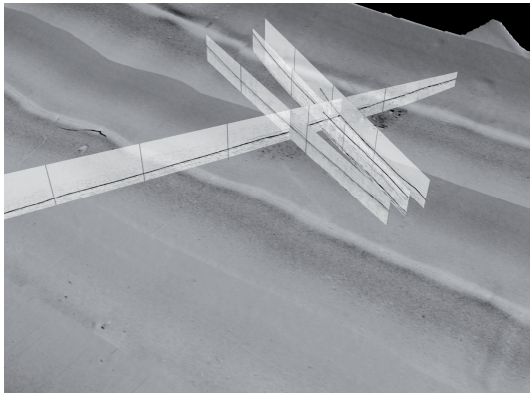


Figure 7 Bathymetric model of the wreck. Side-scan sonar mosaic of the shipwreck is draped on top. Sub-bottom profiler data is shown as curtains elevated 3 meters for visualization.

III. DISCUSSION

A. Compilation of results

Data was collected by various researchers in various phases of the project and much emphasis was placed on collecting data that could be compared.

In Figure 7 side-scan sonar data have been draped on top of the digital terrain model (DTM) derived from the multibeam echosounder data, and sub-bottom profiler data are presented as curtains in a 3D software environment.

The three bumps in the DTM correspond to three larger objects in the side-scan sonar mosaic. In the photomosaic these can be identified as a cannon, a large stone and a large unidentified piece of the ship, probably part of the rigging. The elongated depression in the DTM was parallel to the wood in the photomosaic. The target indications in the sub-bottom profiler data correspond to the extension of the wreck observed in the photomosaics and the side-scan mosaic. This clearly shows that the various data sets complement each other.

The appearance of the large unidentified piece of the ship, probably part of the rigging in sub-bottom profiler data, side-scan data, photomosaic and multibeam echosounder is shown in Figure 8.

B. Complementary properties

The complementary properties of the total data set have been utilized to match information types and error characteristics. The data can complement each other in (at least) two ways; data can be compared to increase accuracy in the data set(s) and they can complement each other by having different information types.

Photomosaics in this project are subject to geometrical distortions. By combining side-scan sonar imagery and photomosaics, distortions can be checked and controlled. Side-scan data can also be distorted, but due to different distortion patterns and mechanisms, matching is useful.

By interpreting multibeam echosounder data alone, it cannot be determined whether the detected small features are archaeological features, geological feature, modern remains or simply acoustic noise. Consulting the side-scan sonar data and sub-bottom profiles, the acoustic noise can be ruled out, even though most archaeological sites must usually be confirmed by visual methods.

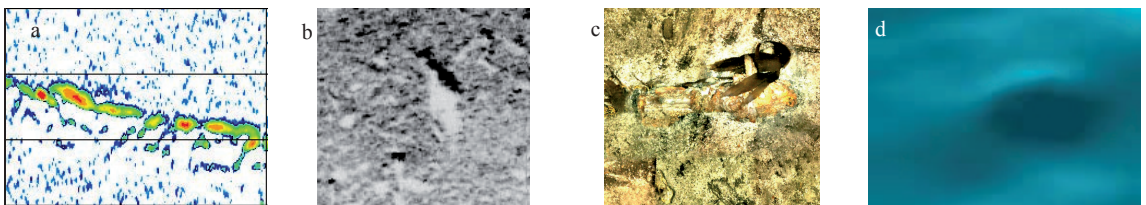


Figure 8 One of the large unidentified piece of the ship, probably part of the rigging seen on a) SBP-data, b) side-scan data, c) photomosaic and d) in the multibeam echosounder data

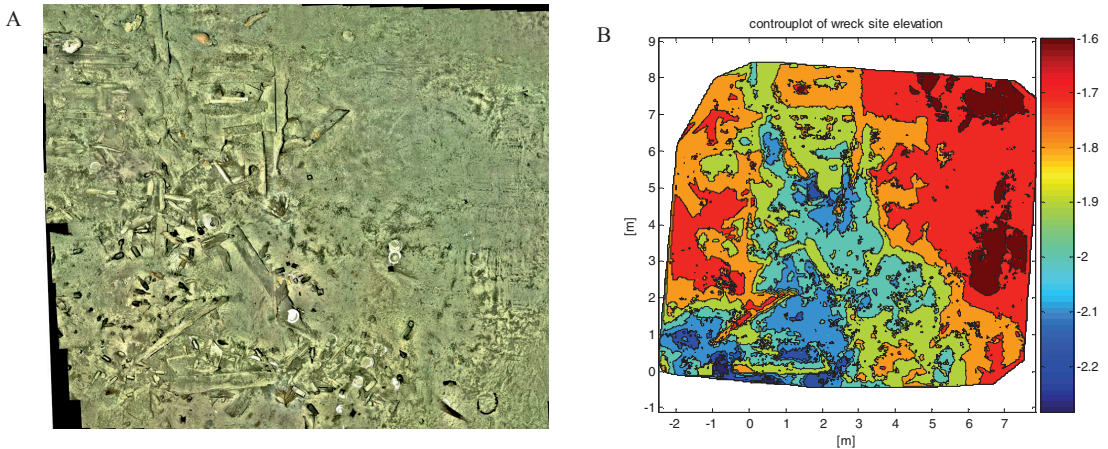


Figure 9 The most detailed results were created by the ROV within the excavation support frame. A photomosaic is shown in A, and results from the photogrammetry is shown in B.

Using multibeam echosounders and side-scan sonars large areas can be surveyed effectively. It is not possible to cover large areas with photomosaics. However, multibeam and side-scan sonar, if used appropriately, are usually sufficient to point out potential sites and once detected and confirmed, photomosaics and photogrammetry are better tools for precise documentation.

IV. Conclusion

An archaeologist's primary interest is to extract as much information as possible from a sunken ship. Important questions are: age of the wreck, origin of the wreck, what cargo did it carry, construction details etc. To document a wreck-site at a level of detail where it is possible to answer such questions photomosaics provide much more detail than its acoustical counterparts. In this project we gained a resolution of 1 - 5 mm in the different photomosaics, which is sufficient to recognize very small objects. The state of the entire wreck-site is clearly recognizable.

Overall, it is clear that archaeological investigations in the deep sea should not rely on one single method but utilize sensor fusion as much as possible. The survey methods complement each other and by combining more than one survey tool the archaeologist's capability for interpretation is clearly enhanced.

The Ormen Lange shipwreck was the first deepwater site that was documented and excavated with the same precision and standards as on land. This was partly made possible because photomosaics, photogrammetry, microbathymetry and

detailed visual inspections were combined with results from side-scan sonar, multibeam echosounder, sub-bottom profiler and magnetometer surveys.

REFERENCES

1. Jasinski, M.E. and F. Søreide. *The Ormen Lange marine archaeology project*. in *Oceans 2004*. 2004. Kobe, Japan: MTS/IEEE.
2. Søreide, F. and M.E. Jasinski. *Ormen Lange: Investigation and excavation of a shipwreck in 170m depth*. in *Oceans 2005*. 2005. MTS/IEEE.
3. Ballard R.D, McCann A.M, Yoerger D, Whitcomb L, Mindell D, Oleson J, Singh H, Foley B, Adams J, & Picheota D, 2000, *The Discovery of Ancient History in the Deep Sea Using Advanced Deep Submergence Technology*, Deep-Sea Research I Volume 47 No. 9 (September 2000): 1591-1620.
4. Ballard R.D, Stager L.E, Mater D, Yoerger D, Mindell D, Whitcomb L.L, Singh H and Pichota D, 2002, *Iron age shipwrecks in deep water off Ashkelon, Israel*, American Journal of Archaeology, Vol 16, No 2: 151-168.
5. Ballard, R.D, Hiebert F.T, Coleman D.F, Ward C, Smith J, Willis K, Foley B, Croff K.L, Major C. & Torre F. 2001. *Deepwater Archaeology of the Black Sea: The 2000 Season at Sinop, Turkey*. American Journal of Archaeology. 105.4: 607-623.
6. Singh, H., et al., *Microbathymetric Mapping from Underwater Vehicles in the Deep Ocean*. Computer Vision and Image Understanding, 2000(79): p. 143-161.
7. Pizzaro, O. and H. Singh, *Towards Large Area Mosaicing for Underwater Scientific Applications*. IEEE Journal of oceanic engineering, 2003. 28(4): p. 651-672.
8. Jaffe, J., *Computer modeling and the design of optimal underwater systems*. Journal Oceanic Engineering, 1990. 15: p. 101-111.
9. Ludvigsen, M., H. Singh, and R. Eustice. *Photogrammetric models in marine archaeology*, in *Oceans 2006*. 2006. Boston: IEEE/MTS.

R A P P O R T E R
U T G I T T V E D
INSTITUTT FOR MARIN TEKNIKK
(tidligere: FAKULTET FOR MARIN TEKNIKK)
NORGES TEKNISK-NATURVITENSKAPELIGE UNIVERSITET

Report No.	Author	Title
	Kavlie, Dag	Optimization of Plane Elastic Grillages, 1967
	Hansen, Hans R.	Man-Machine Communication and Data-Storage Methods in Ship Structural Design, 1971
	Gisvold, Kaare M.	A Method for non-linear mixed -integer programming and its Application to Design Problems, 1971
	Lund, Sverre	Tanker Frame Optimalization by means of SUMT-Transformation and Behaviour Models, 1971
	Vinje, Tor	On Vibration of Spherical Shells Interacting with Fluid, 1972
	Lorentz, Jan D.	Tank Arrangement for Crude Oil Carriers in Accordance with the new Anti-Pollution Regulations, 1975
	Carlsen, Carl A.	Computer-Aided Design of Tanker Structures, 1975
	Larsen, Carl M.	Static and Dynamic Analysis of Offshore Pipelines during Installation, 1976
UR-79-01	Bright Hatlestad, MK	The finite element method used in a fatigue evaluation of fixed offshore platforms. (Dr.Ing. Thesis)
UR-79-02	Erik Pettersen, MK	Analysis and design of cellular structures. (Dr.Ing. Thesis)
UR-79-03	Sverre Valsgård, MK	Finite difference and finite element methods applied to nonlinear analysis of plated structures. (Dr.Ing. Thesis)
UR-79-04	Nils T. Nordsve, MK	Finite element collapse analysis of structural members considering imperfections and stresses due to fabrication. (Dr.Ing. Thesis)
UR-79-05	Ivar J. Fylling, MK	Analysis of towline forces in ocean towing systems. (Dr.Ing. Thesis)
UR-80-06	Nils Sandsmark, MM	Analysis of Stationary and Transient Heat Conduction by the Use of the Finite Element Method. (Dr.Ing. Thesis)
UR-80-09	Sverre Haver, MK	Analysis of uncertainties related to the stochastic modeling of ocean waves. (Dr.Ing. Thesis)
UR-81-15	Odland, Jonas	On the Strength of welded Ring stiffened cylindrical Shells primarily subjected to axial Compression

UR-82-17	Engesvik, Knut	Analysis of Uncertainties in the fatigue Capacity of Welded Joints
UR-82-18	Rye, Henrik	Ocean wave groups
UR-83-30	Eide, Oddvar Inge	On Cumulative Fatigue Damage in Steel Welded Joints
UR-83-33	Mo, Olav	Stochastic Time Domain Analysis of Slender Offshore Structures
UR-83-34	Amdahl, Jørgen	Energy absorption in Ship-platform impacts
UR-84-37	Mørch, Morten	Motions and mooring forces of semi submersibles as determined by full-scale measurements and theoretical analysis
UR-84-38	Soares, C. Guedes	Probabilistic models for load effects in ship structures
UR-84-39	Aarsnes, Jan V.	Current forces on ships
UR-84-40	Czujko, Jerzy	Collapse Analysis of Plates subjected to Biaxial Compression and Lateral Load
UR-85-46	Alf G. Engseth, MK	Finite element collapse analysis of tubular steel offshore structures. (Dr.Ing. Thesis)
UR-86-47	Dengody Sheshappa, MP	A Computer Design Model for Optimizing Fishing Vessel Designs Based on Techno-Economic Analysis. (Dr.Ing. Thesis)
UR-86-48	Vidar Aanesland, MH	A Theoretical and Numerical Study of Ship Wave Resistance. (Dr.Ing. Thesis)
UR-86-49	Heinz-Joachim Wessel, MK	Fracture Mechanics Analysis of Crack Growth in Plate Girders. (Dr.Ing. Thesis)
UR-86-50	Jon Taby, MK	Ultimate and Post-ultimate Strength of Dented Tubular Members. (Dr.Ing. Thesis)
UR-86-51	Walter Lian, MH	A Numerical Study of Two-Dimensional Separated Flow Past Bluff Bodies at Moderate KC-Numbers. (Dr.Ing. Thesis)
UR-86-52	Bjørn Sortland, MH	Force Measurements in Oscillating Flow on Ship Sections and Circular Cylinders in a U-Tube Water Tank. (Dr.Ing. Thesis)
UR-86-53	Kurt Strand, MM	A System Dynamic Approach to One-dimensional Fluid Flow. (Dr.Ing. Thesis)
UR-86-54	Arne Edvin Løken, MH	Three Dimensional Second Order Hydrodynamic Effects on Ocean Structures in Waves. (Dr.Ing. Thesis)
UR-86-55	Sigurd Falch, MH	A Numerical Study of Slamming of Two-Dimensional Bodies. (Dr.Ing. Thesis)
UR-87-56	Arne Braathen, MH	Application of a Vortex Tracking Method to the Prediction of Roll Damping of a Two-Dimension

		Floating Body. (Dr.Ing. Thesis)
UR-87-57	Bernt Leira, MK	Gaussian Vector Processes for Reliability Analysis involving Wave-Induced Load Effects. (Dr.Ing. Thesis)
UR-87-58	Magnus Småvik, MM	Thermal Load and Process Characteristics in a Two-Stroke Diesel Engine with Thermal Barriers (in Norwegian). (Dr.Ing. Thesis)
MTA-88-59	Bernt Arild Bremdal, MP	An Investigation of Marine Installation Processes – A Knowledge - Based Planning Approach. (Dr.Ing. Thesis)
MTA-88-60	Xu Jun, MK	Non-linear Dynamic Analysis of Space-framed Offshore Structures. (Dr.Ing. Thesis)
MTA-89-61	Gang Miao, MH	Hydrodynamic Forces and Dynamic Responses of Circular Cylinders in Wave Zones. (Dr.Ing. Thesis)
MTA-89-62	Martin Greenhow, MH	Linear and Non-Linear Studies of Waves and Floating Bodies. Part I and Part II. (Dr.Techn. Thesis)
MTA-89-63	Chang Li, MH	Force Coefficients of Spheres and Cubes in Oscillatory Flow with and without Current. (Dr.Ing. Thesis)
MTA-89-64	Hu Ying, MP	A Study of Marketing and Design in Development of Marine Transport Systems. (Dr.Ing. Thesis)
MTA-89-65	Arild Jæger, MH	Seakeeping, Dynamic Stability and Performance of a Wedge Shaped Planing Hull. (Dr.Ing. Thesis)
MTA-89-66	Chan Siu Hung, MM	The dynamic characteristics of tilting-pad bearings
MTA-89-67	Kim Wikstrøm, MP	Analysis av projekteringen for ett offshore projekt. (Licenciat-avhandling)
MTA-89-68	Jiao Guoyang, MK	Reliability Analysis of Crack Growth under Random Loading, considering Model Updating. (Dr.Ing. Thesis)
MTA-89-69	Arnt Olufsen, MK	Uncertainty and Reliability Analysis of Fixed Offshore Structures. (Dr.Ing. Thesis)
MTA-89-70	Wu Yu-Lin, MR	System Reliability Analyses of Offshore Structures using improved Truss and Beam Models. (Dr.Ing. Thesis)
MTA-90-71	Jan Roger Hoff, MH	Three-dimensional Green function of a vessel with forward speed in waves. (Dr.Ing. Thesis)
MTA-90-72	Rong Zhao, MH	Slow-Drift Motions of a Moored Two-Dimensional Body in Irregular Waves. (Dr.Ing. Thesis)
MTA-90-73	Atle Minsaas, MP	Economical Risk Analysis. (Dr.Ing. Thesis)
MTA-90-74	Knut-Arild Farnes, MK	Long-term Statistics of Response in Non-linear Marine Structures. (Dr.Ing. Thesis)
MTA-90-	Torbjørn Sotberg, MK	Application of Reliability Methods for Safety

75		Assessment of Submarine Pipelines. (Dr.Ing. Thesis)
MTA-90-76	Zeuthen, Steffen, MP	SEAMAID. A computational model of the design process in a constraint-based logic programming environment. An example from the offshore domain. (Dr.Ing. Thesis)
MTA-91-77	Haagensen, Sven, MM	Fuel Dependant Cyclic Variability in a Spark Ignition Engine - An Optical Approach. (Dr.Ing. Thesis)
MTA-91-78	Løland, Geir, MH	Current forces on and flow through fish farms. (Dr.Ing. Thesis)
MTA-91-79	Hoen, Christopher, MK	System Identification of Structures Excited by Stochastic Load Processes. (Dr.Ing. Thesis)
MTA-91-80	Haugen, Stein, MK	Probabilistic Evaluation of Frequency of Collision between Ships and Offshore Platforms. (Dr.Ing. Thesis)
MTA-91-81	Sødahl, Nils, MK	Methods for Design and Analysis of Flexible Risers. (Dr.Ing. Thesis)
MTA-91-82	Ormberg, Harald, MK	Non-linear Response Analysis of Floating Fish Farm Systems. (Dr.Ing. Thesis)
MTA-91-83	Marley, Mark J., MK	Time Variant Reliability under Fatigue Degradation. (Dr.Ing. Thesis)
MTA-91-84	Krokstad, Jørgen R., MH	Second-order Loads in Multidirectional Seas. (Dr.Ing. Thesis)
MTA-91-85	Molteberg, Gunnar A., MM	The Application of System Identification Techniques to Performance Monitoring of Four Stroke Turbocharged Diesel Engines. (Dr.Ing. Thesis)
MTA-92-86	Mørch, Hans Jørgen Bjelke, MH	Aspects of Hydrofoil Design: with Emphasis on Hydrofoil Interaction in Calm Water. (Dr.Ing. Thesis)
MTA-92-87	Chan Siu Hung, MM	Nonlinear Analysis of Rotordynamic Instabilities in Highspeed Turbomachinery. (Dr.Ing. Thesis)
MTA-92-88	Bessason, Bjarni, MK	Assessment of Earthquake Loading and Response of Seismically Isolated Bridges. (Dr.Ing. Thesis)
MTA-92-89	Langli, Geir, MP	Improving Operational Safety through exploitation of Design Knowledge - an investigation of offshore platform safety. (Dr.Ing. Thesis)
MTA-92-90	Sævik, Svein, MK	On Stresses and Fatigue in Flexible Pipes. (Dr.Ing. Thesis)
MTA-92-91	Ask, Tor Ø., MM	Ignition and Flame Growth in Lean Gas-Air Mixtures. An Experimental Study with a Schlieren System. (Dr.Ing. Thesis)
MTA-86-92	Hessen, Gunnar, MK	Fracture Mechanics Analysis of Stiffened Tubular

Members. (Dr.Ing. Thesis)

MTA-93-93	Steinebach, Christian, MM	Knowledge Based Systems for Diagnosis of Rotating Machinery. (Dr.Ing. Thesis)
MTA-93-94	Dalane, Jan Inge, MK	System Reliability in Design and Maintenance of Fixed Offshore Structures. (Dr.Ing. Thesis)
MTA-93-95	Steen, Sverre, MH	Cobblestone Effect on SES. (Dr.Ing. Thesis)
MTA-93-96	Karunakaran, Daniel, MK	Nonlinear Dynamic Response and Reliability Analysis of Drag-dominated Offshore Platforms. (Dr.Ing. Thesis)
MTA-93-97	Hagen, Amulf, MP	The Framework of a Design Process Language. (Dr.Ing. Thesis)
MTA-93-98	Nordrik, Rune, MM	Investigation of Spark Ignition and Autoignition in Methane and Air Using Computational Fluid Dynamics and Chemical Reaction Kinetics. A Numerical Study of Ignition Processes in Internal Combustion Engines. (Dr.Ing. Thesis)
MTA-94-99	Passano, Elizabeth, MK	Efficient Analysis of Nonlinear Slender Marine Structures. (Dr.Ing. Thesis)
MTA-94-100	Kvålsvold, Jan, MH	Hydroelastic Modelling of Wetdeck Slamming on Multihull Vessels. (Dr.Ing. Thesis)
MTA-94-102	Bech, Sidsel M., MK	Experimental and Numerical Determination of Stiffness and Strength of GRP/PVC Sandwich Structures. (Dr.Ing. Thesis)
MTA-95-103	Paulsen, Hallvard, MM	A Study of Transient Jet and Spray using a Schlieren Method and Digital Image Processing. (Dr.Ing. Thesis)
MTA-95-104	Hovde, Geir Olav, MK	Fatigue and Overload Reliability of Offshore Structural Systems, Considering the Effect of Inspection and Repair. (Dr.Ing. Thesis)
MTA-95-105	Wang, Xiaozhi, MK	Reliability Analysis of Production Ships with Emphasis on Load Combination and Ultimate Strength. (Dr.Ing. Thesis)
MTA-95-106	Ulstein, Tore, MH	Nonlinear Effects of a Flexible Stern Seal Bag on Cobblestone Oscillations of an SES. (Dr.Ing. Thesis)
MTA-95-107	Solaas, Frøydis, MH	Analytical and Numerical Studies of Sloshing in Tanks. (Dr.Ing. Thesis)
MTA-95-108	Hellan, Øyvind, MK	Nonlinear Pushover and Cyclic Analyses in Ultimate Limit State Design and Reassessment of Tubular Steel Offshore Structures. (Dr.Ing. Thesis)
MTA-95-109	Hermundstad, Ole A., MK	Theoretical and Experimental Hydroelastic Analysis of High Speed Vessels. (Dr.Ing. Thesis)
MTA-96-110	Bratland, Anne K., MH	Wave-Current Interaction Effects on Large-Volume Bodies in Water of Finite Depth. (Dr.Ing. Thesis)

MTA-96-111	Herfjord, Kjell, MH	A Study of Two-dimensional Separated Flow by a Combination of the Finite Element Method and Navier-Stokes Equations. (Dr.Ing. Thesis)
MTA-96-112	Æsøy, Vilmar, MM	Hot Surface Assisted Compression Ignition in a Direct Injection Natural Gas Engine. (Dr.Ing. Thesis)
MTA-96-113	Eknes, Monika L., MK	Escalation Scenarios Initiated by Gas Explosions on Offshore Installations. (Dr.Ing. Thesis)
MTA-96-114	Erikstad, Stein O., MP	A Decision Support Model for Preliminary Ship Design. (Dr.Ing. Thesis)
MTA-96-115	Pedersen, Egil, MH	A Nautical Study of Towed Marine Seismic Streamer Cable Configurations. (Dr.Ing. Thesis)
MTA-97-116	Moksnes, Paul O., MM	Modelling Two-Phase Thermo-Fluid Systems Using Bond Graphs. (Dr.Ing. Thesis)
MTA-97-117	Halse, Karl H., MK	On Vortex Shedding and Prediction of Vortex-Induced Vibrations of Circular Cylinders. (Dr.Ing. Thesis)
MTA-97-118	Igland, Ragnar T., MK	Reliability Analysis of Pipelines during Laying, considering Ultimate Strength under Combined Loads. (Dr.Ing. Thesis)
MTA-97-119	Pedersen, Hans-P., MP	Levendefiskteknologi for fiskefartøy. (Dr.Ing. Thesis)
MTA-98-120	Vikestad, Kyrre, MK	Multi-Frequency Response of a Cylinder Subjected to Vortex Shedding and Support Motions. (Dr.Ing. Thesis)
MTA-98-121	Azadi, Mohammad R. E., MK	Analysis of Static and Dynamic Pile-Soil-Jacket Behaviour. (Dr.Ing. Thesis)
MTA-98-122	Ulltang, Terje, MP	A Communication Model for Product Information. (Dr.Ing. Thesis)
MTA-98-123	Torbergsen, Erik, MM	Impeller/Diffuser Interaction Forces in Centrifugal Pumps. (Dr.Ing. Thesis)
MTA-98-124	Hansen, Edmond, MH	A Discrete Element Model to Study Marginal Ice Zone Dynamics and the Behaviour of Vessels Moored in Broken Ice. (Dr.Ing. Thesis)
MTA-98-125	Videiro, Paulo M., MK	Reliability Based Design of Marine Structures. (Dr.Ing. Thesis)
MTA-99-126	Mainçon, Philippe, MK	Fatigue Reliability of Long Welds Application to Titanium Risers. (Dr.Ing. Thesis)
MTA-99-127	Haugen, Elin M., MH	Hydroelastic Analysis of Slamming on Stiffened Plates with Application to Catamaran Wetdecks. (Dr.Ing. Thesis)
MTA-99-128	Langhelle, Nina K., MK	Experimental Validation and Calibration of Nonlinear Finite Element Models for Use in Design of Aluminium Structures Exposed to Fire. (Dr.Ing. Thesis)

		Thesis)
MTA-99-129	Berstad, Are J., MK	Calculation of Fatigue Damage in Ship Structures. (Dr.Ing. Thesis)
MTA-99-130	Andersen, Trond M., MM	Short Term Maintenance Planning. (Dr.Ing. Thesis)
MTA-99-131	Tveiten, Bård Wathne, MK	Fatigue Assessment of Welded Aluminium Ship Details. (Dr.Ing. Thesis)
MTA-99-132	Søreide, Fredrik, MP	Applications of underwater technology in deep water archaeology. Principles and practice. (Dr.Ing. Thesis)
MTA-99-133	Tønnessen, Rune, MH	A Finite Element Method Applied to Unsteady Viscous Flow Around 2D Blunt Bodies With Sharp Corners. (Dr.Ing. Thesis)
MTA-99-134	Elvekrok, Dag R., MP	Engineering Integration in Field Development Projects in the Norwegian Oil and Gas Industry. The Supplier Management of Norne. (Dr.Ing. Thesis)
MTA-99-135	Fagerholt, Kjetil, MP	Optimeringsbaserte Metoder for Ruteplanlegging innen skipsfart. (Dr.Ing. Thesis)
MTA-99-136	Bysveen, Marie, MM	Visualization in Two Directions on a Dynamic Combustion Rig for Studies of Fuel Quality. (Dr.Ing. Thesis)
MTA-2000-137	Storteig, Eskild, MM	Dynamic characteristics and leakage performance of liquid annular seals in centrifugal pumps. (Dr.Ing. Thesis)
MTA-2000-138	Sagli, Gro, MK	Model uncertainty and simplified estimates of long term extremes of hull girder loads in ships. (Dr.Ing. Thesis)
MTA-2000-139	Tronstad, Harald, MK	Nonlinear analysis and design of cable net structures like fishing gear based on the finite element method. (Dr.Ing. Thesis)
MTA-2000-140	Kroneberg, André, MP	Innovation in shipping by using scenarios. (Dr.Ing. Thesis)
MTA-2000-141	Haslum, Herbjørn Alf, MH	Simplified methods applied to nonlinear motion of spar platforms. (Dr.Ing. Thesis)
MTA-2001-142	Samdal, Ole Johan, MM	Modelling of Degradation Mechanisms and Stressor Interaction on Static Mechanical Equipment Residual Lifetime. (Dr.Ing. Thesis)
MTA-2001-143	Baarholm, Rolf Jarle, MH	Theoretical and experimental studies of wave impact underneath decks of offshore platforms. (Dr.Ing. Thesis)
MTA-2001-144	Wang, Lihua, MK	Probabilistic Analysis of Nonlinear Wave-induced Loads on Ships. (Dr.Ing. Thesis)
MTA-2001-145	Kristensen, Odd H. Holt, MK	Ultimate Capacity of Aluminium Plates under Multiple Loads, Considering HAZ Properties. (Dr.Ing. Thesis)

MTA-2001-146	Greco, Marilena, MH	A Two-Dimensional Study of Green-Water Loading. (Dr.Ing. Thesis)
MTA-2001-147	Heggelund, Svein E., MK	Calculation of Global Design Loads and Load Effects in Large High Speed Catamarans. (Dr.Ing. Thesis)
MTA-2001-148	Babalola, Olusegun T., MK	Fatigue Strength of Titanium Risers – Defect Sensitivity. (Dr.Ing. Thesis)
MTA-2001-149	Mohammed, Abuu K., MK	Nonlinear Shell Finite Elements for Ultimate Strength and Collapse Analysis of Ship Structures. (Dr.Ing. Thesis)
MTA-2002-150	Holmedal, Lars E., MH	Wave-current interactions in the vicinity of the sea bed. (Dr.Ing. Thesis)
MTA-2002-151	Rognebakke, Olav F., MH	Sloshing in rectangular tanks and interaction with ship motions. (Dr.Ing. Thesis)
MTA-2002-152	Lader, Pål Furset, MH	Geometry and Kinematics of Breaking Waves. (Dr.Ing. Thesis)
MTA-2002-153	Yang, Qinzhen, MH	Wash and wave resistance of ships in finite water depth. (Dr.Ing. Thesis)
MTA-2002-154	Melhus, Øyvinn, MM	Utilization of VOC in Diesel Engines. Ignition and combustion of VOC released by crude oil tankers. (Dr.Ing. Thesis)
MTA-2002-155	Ronæss, Marit, MH	Wave Induced Motions of Two Ships Advancing on Parallel Course. (Dr.Ing. Thesis)
MTA-2002-156	Økland, Ole D., MK	Numerical and experimental investigation of whipping in twin hull vessels exposed to severe wet deck slamming. (Dr.Ing. Thesis)
MTA-2002-157	Ge, Chunhua, MK	Global Hydroelastic Response of Catamarans due to Wet Deck Slamming. (Dr.Ing. Thesis)
MTA-2002-158	Byklum, Eirik, MK	Nonlinear Shell Finite Elements for Ultimate Strength and Collapse Analysis of Ship Structures. (Dr.Ing. Thesis)
IMT-2003-1	Chen, Haibo, MK	Probabilistic Evaluation of FPSO-Tanker Collision in Tandem Offloading Operation. (Dr.Ing. Thesis)
IMT-2003-2	Skaugset, Kjetil Bjørn, MK	On the Suppression of Vortex Induced Vibrations of Circular Cylinders by Radial Water Jets. (Dr.Ing. Thesis)
IMT-2003-3	Chezhan, Muthu	Three-Dimensional Analysis of Slamming. (Dr.Ing. Thesis)
IMT-2003-4	Buhaug, Øyvind	Deposit Formation on Cylinder Liner Surfaces in Medium Speed Engines. (Dr.Ing. Thesis)
IMT-2003-5	Tregde, Vidar	Aspects of Ship Design: Optimization of Aft Hull with Inverse Geometry Design. (Dr.Ing. Thesis)
IMT-2003-6	Wist, Hanne Therese	Statistical Properties of Successive Ocean Wave

Parameters. (Dr.Ing. Thesis)

IMT-2004-7	Ransau, Samuel	Numerical Methods for Flows with Evolving Interfaces. (Dr.Ing. Thesis)
IMT-2004-8	Soma, Torkel	Blue-Chip or Sub-Standard. A data interrogation approach of identity safety characteristics of shipping organization. (Dr.Ing. Thesis)
IMT-2004-9	Ersdal, Svein	An experimental study of hydrodynamic forces on cylinders and cables in near axial flow. (Dr.Ing. Thesis)
IMT-2005-10	Brodtkorb, Per Andreas	The Probability of Occurrence of Dangerous Wave Situations at Sea. (Dr.Ing. Thesis)
IMT-2005-11	Yttervik, Rune	Ocean current variability in relation to offshore engineering. (Dr.Ing. Thesis)
IMT-2005-12	Fredheim, Arne	Current Forces on Net-Structures. (Dr.Ing. Thesis)
IMT-2005-13	Heggernes, Kjetil	Flow around marine structures. (Dr.Ing. Thesis)
IMT-2005-14	Fouques, Sebastien	Lagrangian Modelling of Ocean Surface Waves and Synthetic Aperture Radar Wave Measurements. (Dr.Ing. Thesis)
IMT-2006-15	Holm, Håvard	Numerical calculation of viscous free surface flow around marine structures. (Dr.Ing. Thesis)
IMT-2006-16	Bjørheim, Lars G.	Failure Assessment of Long Through Thickness Fatigue Cracks in Ship Hulls. (Dr.Ing. Thesis)
IMT-2006-17	Hansson, Lisbeth	Safety Management for Prevention of Occupational Accidents. (Dr.Ing. Thesis)
IMT-2006-18	Zhu, Xinying	Application of the CIP Method to Strongly Nonlinear Wave-Body Interaction Problems. (Dr.Ing. Thesis)
IMT-2006-19	Reite, Karl Johan	Modelling and Control of Trawl Systems. (Dr.Ing. Thesis)
IMT-2006-20	Smogeli, Øyvind Notland	Control of Marine Propellers. From Normal to Extreme Conditions. (Dr.Ing. Thesis)
IMT-2007-21	Storhaug, Gaute	Experimental Investigation of Wave Induced Vibrations and Their Effect on the Fatigue Loading of Ships. (Dr.Ing. Thesis)
IMT-2007-22	Sun, Hui	A Boundary Element Method Applied to Strongly Nonlinear Wave-Body Interaction Problems. (PhD Thesis, CeSOS)
IMT-2007-23	Rustad, Anne Marthine	Modelling and Control of Top Tensioned Risers. (PhD Thesis, CeSOS)
IMT-2007-24	Johansen, Vegar	Modelling flexible slender system for real-time simulations and control applications
IMT-2007-25	Wroldsen, Anders Sunde	Modelling and control of tensegrity structures. (PhD)

Thesis, CeSOS)

IMT-2007-26	Aronsen, Kristoffer Høy	An experimental investigation of in-line and combined inline and cross flow vortex induced vibrations. (Dr. avhandling, IMT)
IMT-2007-27	Gao, Zhen	Stochastic Response Analysis of Mooring Systems with Emphasis on Frequency-domain Analysis of Fatigue due to Wide-band Response Processes (PhD Thesis, CeSOS)
IMT-2007-28	Thorstensen, Tom Anders	Lifetime Profit Modelling of Ageing Systems Utilizing Information about Technical Condition. (Dr.ing. thesis, IMT)
IMT-2008-29	Bermtsen, Per Ivar B.	Structural Reliability Based Position Mooring. (PhD-Thesis, IMT)
IMT-2008-30	Ye, Naiquan	Fatigue Assessment of Aluminium Welded Box-stiffener Joints in Ships (Dr.ing. thesis, IMT)
IMT-2008-31	Radan, Damir	Integrated Control of Marine Electrical Power Systems. (PhD-Thesis, IMT)
IMT-2008-32	Thomassen, Paul	Methods for Dynamic Response Analysis and Fatigue Life Estimation of Floating Fish Cages. (Dr.ing. thesis, IMT)
IMT-2008-33	Pákozdi, Csaba	A Smoothed Particle Hydrodynamics Study of Two-dimensional Nonlinear Sloshing in Rectangular Tanks. (Dr.ing.thesis, IMT)
IMT-2007-34	Grytøyr, Guttorm	A Higher-Order Boundary Element Method and Applications to Marine Hydrodynamics. (Dr.ing.thesis, IMT)
IMT-2008-35	Drummen, Ingo	Experimental and Numerical Investigation of Nonlinear Wave-Induced Load Effects in Containerships considering Hydroelasticity. (PhD thesis, CeSOS)
IMT-2008-36	Skejic, Renato	Maneuvering and Seakeeping of a Singel Ship and of Two Ships in Interaction. (PhD-Thesis, CeSOS)
IMT-2008-37	Harlem, Alf	An Age-Based Replacement Model for Repairable Systems with Attention to High-Speed Marine Diesel Engines. (PhD-Thesis, IMT)
IMT-2008-38	Alsos, Hagbart S.	Ship Grounding. Analysis of Ductile Fracture, Bottom Damage and Hull Girder Response. (PhD-thesis, IMT)
IMT-2008-39	Graczyk, Mateusz	Experimental Investigation of Sloshing Loading and Load Effects in Membrane LNG Tanks Subjected to Random Excitation. (PhD-thesis, CeSOS)
IMT-2008-40	Taghipour, Reza	Efficient Prediction of Dynamic Response for Flexible and Multi-body Marine Structures. (PhD-thesis, CeSOS)
IMT-2008-41	Ruth, Eivind	Propulsion control and thrust allocation on marine vessels. (PhD thesis, CeSOS)

IMT-2008-42	Nystad, Bent Helge	Technical Condition Indexes and Remaining Useful Life of Aggregated Systems. PhD thesis, IMT
IMT-2008-43	Soni, Prashant Kumar	Hydrodynamic Coefficients for Vortex Induced Vibrations of Flexible Beams, PhD thesis, CeSOS
IMT-2009-43	Amlashi, Hadi K.K.	Ultimate Strength and Reliability-based Design of Ship Hulls with Emphasis on Combined Global and Local Loads. PhD Thesis, IMT
IMT-2009-44	Pedersen, Tom Arne	Bond Graph Modelling of Marine Power Systems. PhD Thesis, IMT
IMT-2009-45	Kristiansen, Trygve	Two-Dimensional Numerical and Experimental Studies of Piston-Mode Resonance. PhD-Thesis, CeSOS
IMT-2009-46	Ong, Muk Chen	Applications of a Standard High Reynolds Number Model and a Stochastic Scour Prediction Model for Marine Structures. PhD-thesis, IMT
IMT-2009-47	Hong, Lin	Simplified Analysis and Design of Ships subjected to Collision and Grounding. PhD-thesis, IMT
IMT-2009-48	Koushan, Kamran	Vortex Induced Vibrations of Free Span Pipelines, PhD thesis, IMT
IMT-2009-49	Korsvik, Jarl Eirik	Heuristic Methods for Ship Routing and Scheduling. PhD-thesis, IMT
IMT-2009-50	Lee, Jihoon	Experimental Investigation and Numerical in Analyzing the Ocean Current Displacement of Longlines. Ph.d.-Thesis, IMT.
IMT-2009-51	Vestbøstad, Tone Gran	A Numerical Study of Wave-in-Deck Impact using a Two-Dimensional Constrained Interpolation Profile Method, Ph.d.thesis, CeSOS.
IMT-2009-52	Bruun, Kristine	Bond Graph Modelling of Fuel Cells for Marine Power Plants. Ph.d.-thesis, IMT
IMT 2009-53	Holstad, Anders	Numerical Investigation of Turbulence in a Skewed Three-Dimensional Channel Flow, Ph.d.-thesis, IMT.
IMT 2009-54	Ayala-Uraga, Efen	Reliability-Based Assessment of Deteriorating Ship-shaped Offshore Structures, Ph.d.-thesis, IMT
IMT 2009-55	Kong, Xiangjun	A Numerical Study of a Damaged Ship in Beam Sea Waves. Ph.d.-thesis, IMT/CeSOS.
IMT 2010-56	Kristiansen, David	Wave Induced Effects on Floaters of Aquaculture Plants, Ph.d.-thesis, IMT/CeSOS.